Void-Free Flame Retardant Phenolic Networks: Properties and Processability

Christy Sensenich Tyberg

Dissertation submitted to the Faculty of the Virginia Polytechnic Institute and State University in partial fulfillment of the requirements for the degree of

Doctor of Philosophy
in
Chemistry

Judy S. Riffle, Chair

James E. McGrath

John J. Lesko

Thomas C. Ward

Jeffrey C. Hedrick

March 22, 2000

Blacksburg, Virginia

Keywords: Phenolic, epoxy, flame-retardant, composite, latent initiator

Void-Free Flame Retardant Phenolic Networks: Properties and Processability

Christy Sensenich Tyberg

Abstract

Phenolic resins are important components of the composite industry because of their excellent flame retardance and cost effectiveness. However, the common procedure for curing phenolic novolac resins uses hexamethylenetetramine (HMTA) and releases volatiles during the cure, which produce networks with numerous voids. This results in materials that lack the toughness necessary for structural applications. An alternative to curing with HMTA is to crosslink the pendant phenolic groups in the novolac resin with epoxy reagents. This reaction proceeds by nucleophilic addition without the release of any volatiles, thereby creating a void-free network. Flame retardance can be achieved by using an excess of the phenolic component. Network densities can also be controlled to maximize both toughness and stiffness by tailoring the stoichiometry of the reagents.

Structure-property relationships of phenolic/epoxy networks have been investigated. Glass transitions decreased, and toughness increased, as the phenolic content in the network was increased. Both results could be correlated to the decrease in network densities along this series, which was investigated by measuring the rubbery moduli well above T_g. Fracture toughness of phenolic/epoxy networks measured by K_{1c} reached 1.03 MPa-$m^{1/2}$, compared with an epoxy control with K_{1c} = 0.62 MPa-$m^{1/2}$ and phenolic control with K_{1c} = 0.16 MPa-$m^{1/2}$. In addition, an increase in novolac content improves flame retardance rather dramatically. The peak heat release rate (PHRR) dropped from 1230 kW/m^2 for the epoxy control to 260 kW/m^2 for the phenolic/epoxy networks, which approached that of a phenolic resol (PHRR = 116 kW/m^2). Phenolic/epoxy composite flame retardance also showed significant improvement when compared to epoxy composites.

Melt processability of phenolic/epoxy composites has been achieved through the use of latent nucleophilic initiators. Kinetics of the phenolic/epoxy cure reactions with latent initiators demonstrated that monomeric phosphine initiators yielded faster cure reactions as compared to polymeric initiators. These latent initiators allow composite melt processing, such as prepregging or pultrusion, without premature curing. In addition, cure cycles can be reduced from 4 hours to less than 30 minutes. Composites prepared using these latent initiators had toughness exceeding that of epoxy composites and fatigue limits significantly higher than those of vinyl ester composites.

Acknowledgements

I would like to extend thanks to the people whose contributions helped make this dissertation possible. In particular, I would like to thank my advisor, Dr. Judy S. Riffle, for igniting my interest in the field of polymer chemistry. Her inspiring ideas, encouragement and confidence in me have helped me develop personally and professionally. I would also like to thank Dr. J. E. McGrath, Dr. T. C Ward, Dr. J. J. Lesko, and Dr. J. C. Hedrick for serving on my committee and for being there to answer any questions that I had throughout my time at Virginia Tech. I am sincerely thankful for their valuable time and assistance.

I would like to thank all the members of my research group that I worked closely with. They have always been there to answer questions or give advice when I came to a stumbling block in my research. I would also like to thank Angie Flynn for always being available to answer questions.

Special gratitude goes to my family for their support of my schooling and their commitment to help me succeed. I thank my father for teaching me to think analytically, and I thank my mother for instilling in me a drive to succeed. I am immensely grateful to my husband, Justin, for his encouragement and unending support in everything I do. Finally, I must thank my Lord Jesus Christ for giving me strength and guiding me in the right direction.

Contents

List of Figures

List of Tables

1 Introduction

Lightweight, stiff polymer matrix composites may be effective alternatives to steel and concrete in many civil structures. It is anticipated that polymer matrix composites' superior oxidative resistance relative to steel and better freeze-thaw durability relative to concrete could lead to structural components with the needed improved environmental resistance. However, one major obstacle limiting the use of organic materials in construction is their high combustibility.

Phenolic resins, both Novolacs and Resols, are widely used commercially due to their excellent flame retardance and low cost.[1,2] There has also been significant academic interest in understanding the mechanisms of curing and decomposition of the phenolics in order to understand the reasons for their excellent flame retardance.[3] As a result of the low smoke generation of phenolic resins they are being used in the interiors of planes such as the DC-10 and Boeing 777.[4] Phenolics have a broad range of applications varying from construction to electronics and aerospace.

Commercial phenolic Novolac resins are commonly cured with hexamethylenetetramine (HMTA) which yields networks with relatively high crosslink densities. Curing with HMTA produces volatile by-products such as water, formaldehyde, and ammonia, which lead to voids in the materials.[1] This has been a negative feature in phenolic matrix composites because the high void content leads to brittle components. Therefore, current commercial Novolacs are limited to applications where high strength is not a requirement. On the other hand, epoxy resins are used for applications where high strength and toughness are needed, although they are highly combustible materials. The flame retardance of epoxy resins can be improved by incorporating bromine into the structure; however, bromine also increases the toxic smoke emission.[5]

Phenolics have been used as curing agents for epoxy resins where the epoxy is the major component.[6] In many cases, these systems make up the base resins for semiconductor packaging due to their improved hydrophobicity relative to amine-cured epoxies and their low cost. Effects of crosslink densities on the physical properties of the

networks have been studied.[7] Unfortunately, these systems do not have good flame retardance because of the high content of combustible epoxy resin.

This research focuses on curing phenolic resins with epoxies, as opposed to HMTA (Figure 1.1). The cure reaction produces no volatiles and therefore can produce tough, void-free networks. Network density can be at least somewhat controlled by the stoichiometric offset between phenol and epoxy groups. The approach is to utilize networks high in phenolic content (up to ~ 80 wt. %) so that the flame retardant properties of the phenolic material are retained while tailoring mechanical properties via crosslink densities and molecular structure. In addition, these systems should be much tougher than the phenolic Novolac resins cured with HMTA as a result of the lack of voids in the networks. The intent is to prepare materials as strong as epoxy networks which retain the flame retardance of phenolic resins.

This work has been divided into two main sections to achieve the goals of developing a flame retardant, tough, processable matrix material for composite applications. The first section focuses on structure-property relationships of the neat networks in order to determine the factors that influence flame retardance and mechanical properties. The second section discusses methods of processing these matrix materials by melt processing. Several types of latent initiators were investigated to allow melt processing of composites. In addition, the mechanical properties of composites prepared by melt prepregging were investigated in detail.

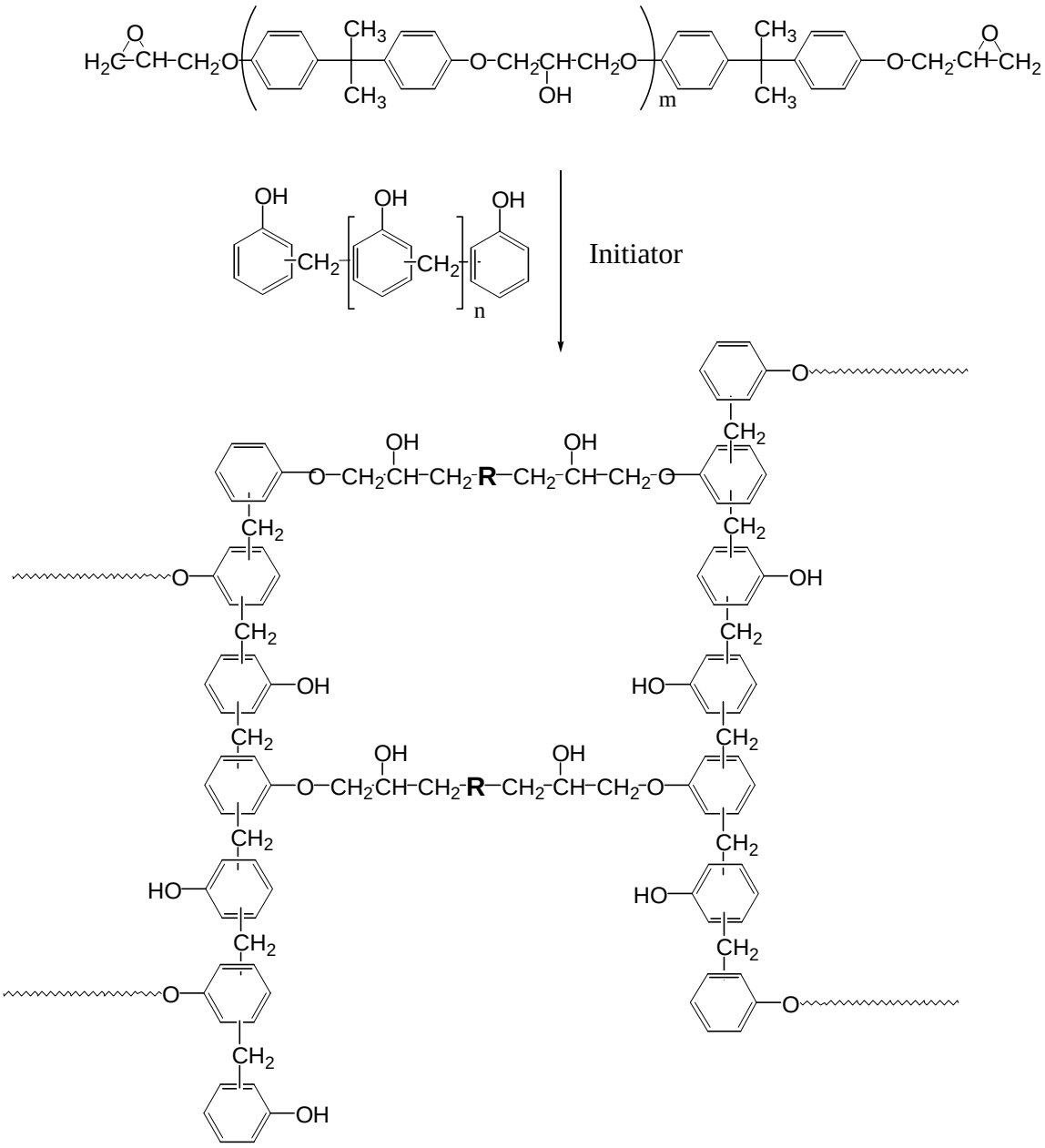

Figure 1.1: Network formation of phenolic novolacs cured with epoxies.

2 Literature Review

2.1 Phenolic Resin Chemistry

2.1.1 Introduction

Phenolic materials have extensive industrial importance due to their high flame retardance and low cost. Applications range from construction to electronics and aerospace. The two most common types of phenolic resins (resols and novolacs) are derived from the reaction of phenol with formaldehyde. The reaction mechanism to form the prepolymers is controlled by the pH and the reactant ratio of phenol to formaldehyde. In strongly acidic conditions with an excess of phenol, novolacs are formed; whereas, in basic conditions with an excess of formaldehyde, resols are formed. Novolacs are soluble and fusible, and require an external curing agent, such as HMTA, to form the phenolic network. On the other hand, resols will crosslink with heat to form insoluble, infusible networks. The specifics of these two reactions will be discussed in the following sections.[1]

2.1.2 Resol Chemistry

Resols are prepared under alkaline conditions with an excess of formaldehyde. The ratio of phenol to formaldehyde ranges from 1:1 to 1:3.[1] The mechanism of the phenol formaldehyde reaction is a base catalyzed electrophilic aromatic substitution to form a combination of the mono, di and trihydroxymethylphenols (Figure 2.1). These hydroxymethylphenols are then reacted to form the prepolymers. There are two distinct pathways of prepolymer formation that depend on pH and temperature (Figure 2.2). The first pathway, which leads to dihydroxydibenzyl ether, is more predominant under neutral to weakly acidic conditions and at temperatures less than 130°C. At higher temperatures dihydroxydibenzyl ether will eliminate formaldehyde to produce dihydroxydiphenylmethane. The second pathway, which leads to dihydroxydiphenylmethane, is predominant under alkaline conditions and temperatures

between 130 and 150°C. At temperatures greater than 150°C many other side reactions are present.[1,8]

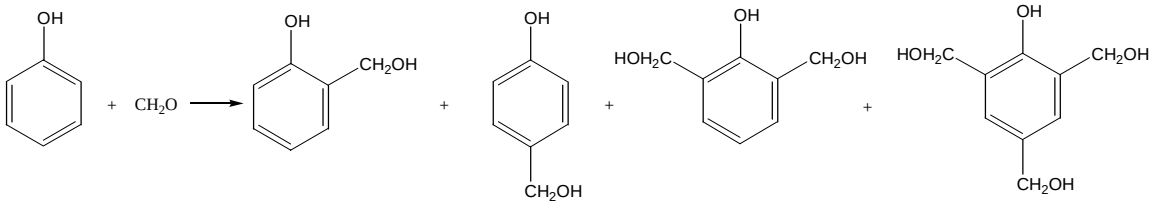

Figure 2.1: Base catalyzed reaction of phenol with formaldehyde[1]

Once the prepolymers are formed the resol resin can be crosslinked with heat. Usually a pH of 9 or greater and temperatures between 130 and 180°C are used. In order to prevent premature curing the resins should be stored under cool conditions. The prepolymers are heated to promote crosslinking of the resin by further reaction of hydroxymethylphenols. Water and formaldehyde are produced and volatilize during curing (Figure 2.2). This release of volatiles results in networks with a significant amount of voids that detract from the mechanical properties.[1, 8]

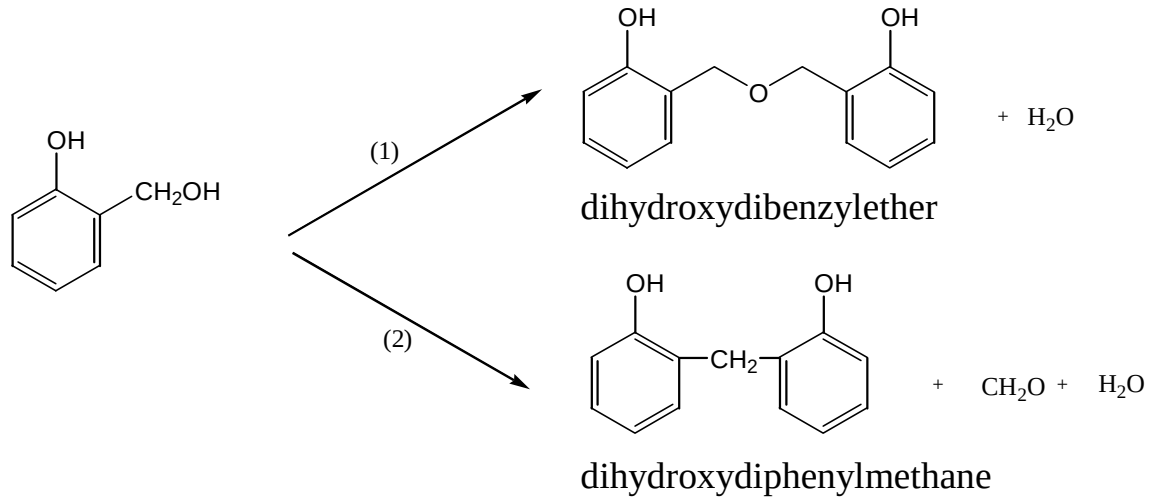

Figure 2.2: Resol prepolymer formation[1]

2.1.3 Novolac Chemistry

Novolacs are prepared under acidic conditions with an excess of phenol. This procedure produces relatively linear chains with molecular weights typically between 500

and 1000 g/mol. The initial reaction of phenol with formaldehyde, under acidic conditions, is an electrophilic substitution on the phenol (Figure 2.3a). Further reaction of the methylol-substituted phenol with another phenol molecule produces dihydroxydiphenylmethane (Figure 2.3b). Novolac oligomers, once formed, are stable and require an external crosslinking reagent to produce networks.[1, 8]

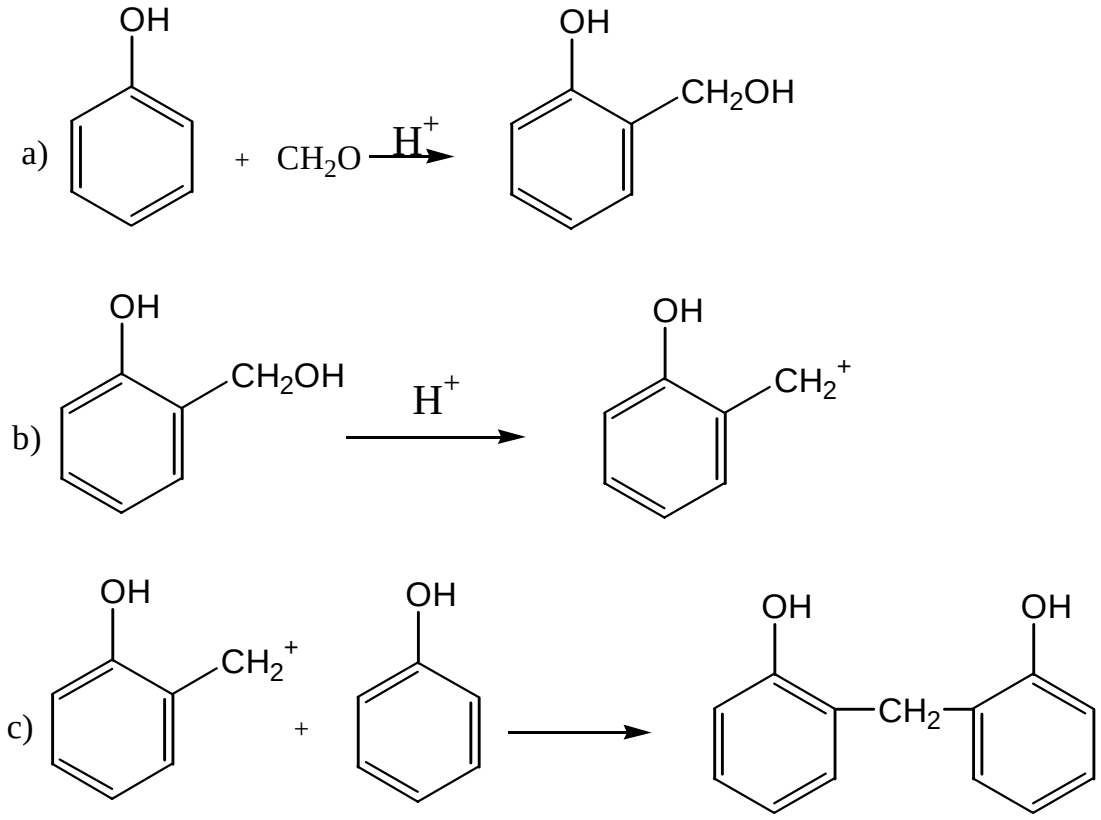

Figure 2.3: Novolac prepolymer formation[1]

Under weakly acidic conditions with a large excess of phenol and the use of divalent salts such as Mg or Zn, the reaction can be somewhat controlled to give preferentially ortho substitution.[1] Boric acid has also been used to achieve preferentially ortho addition. The proposed mechanism for the preferentially ortho addition is the "formation of chelates as transient intermediates" (Figure 2.4).[1,8]

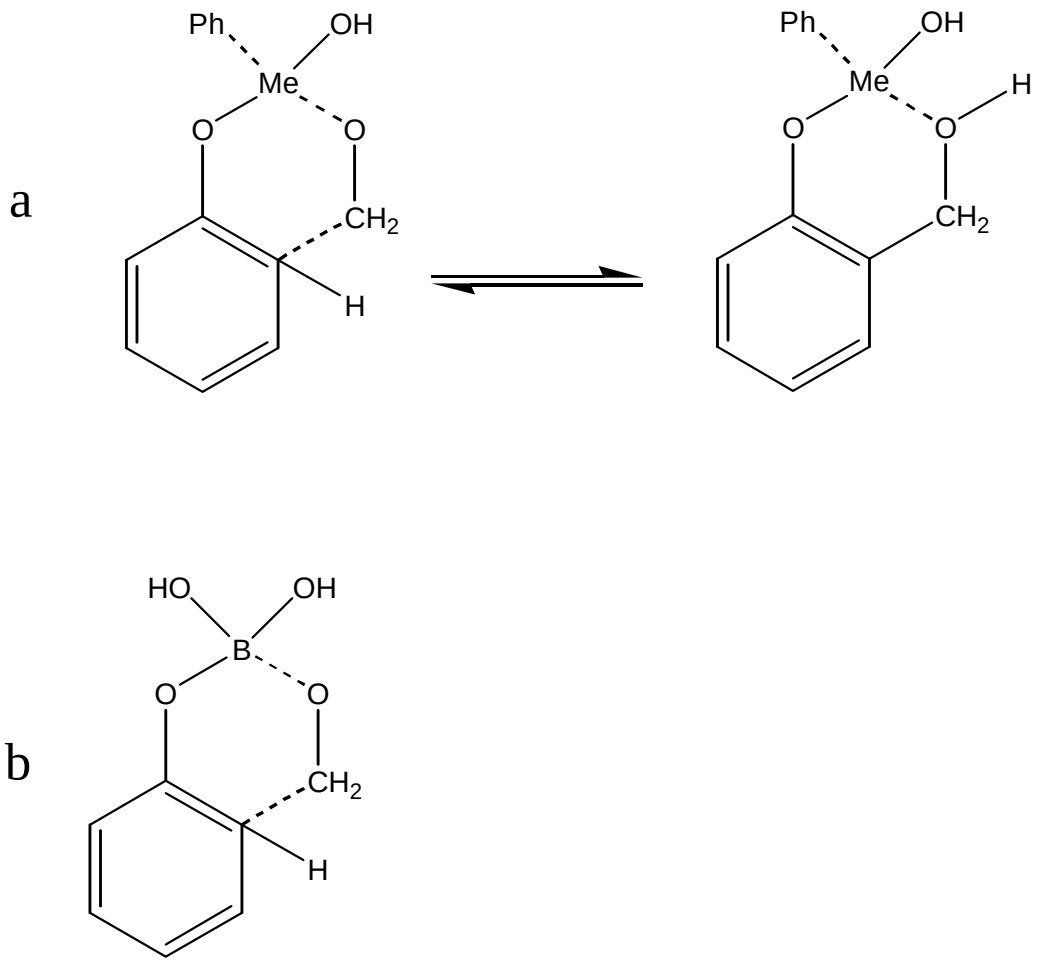

Figure 2.4: **Transition intermediates in the formation of highly ortho-linked novolacs (a) using divalent metal catalysts(Me = Mg or Zn) and (b) boric acid.[1]**

The most common crosslinking reagent for novolacs is hexamethylenetetramine (HMTA). Typically between 5 and 15 wt % HMTA is used to produce the nitrogen containing crosslinked network. With this process a significant amount of gas is produced during the crosslinking reaction which contains at least 95 % ammonia, and the cured resin may contain up to about 6 % bound nitrogen. Therefore, about 75 % of the nitrogen from HMTA becomes chemically bound in the network. The volatiles released during the cure can create voids in the network, just as with the resols. An alternative to the HMTA, to avoid the production of volatiles during the cure reaction, is to convert the novolac to an alternative type of epoxy resin that can be cured with and amine. In this process the novolac oligomers can be reacted with epichlorohydrin to form epoxidized

novolacs (Figure 2.5). The epoxidized novolacs are then co-cured with amine curing agents. This type of cure produces materials with excellent strength, adhesion, dielectric properties, and oxidation resistance, although the thermal resistance is somewhat reduced due to the addition of the epoxy component.[1, 8]

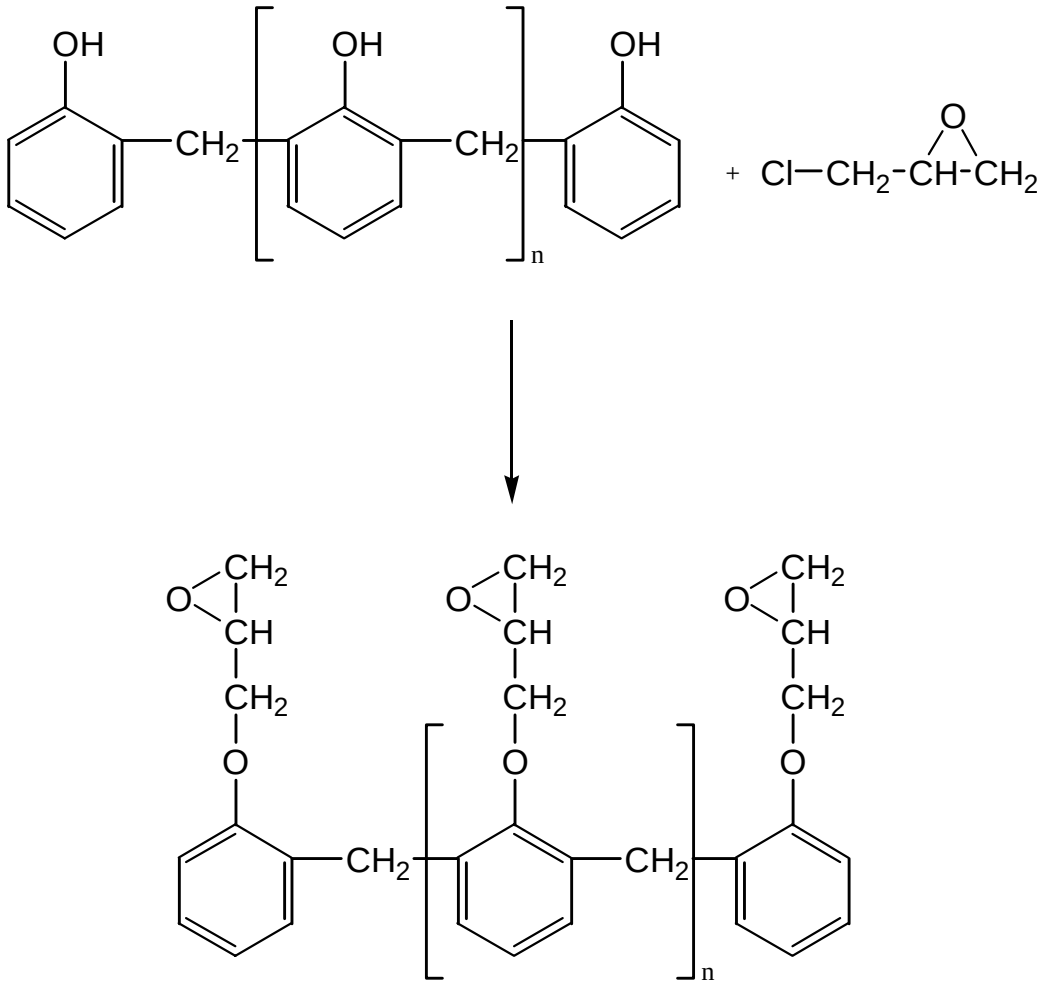

Figure 2.5: Epoxidized novolacs[1]

2.1.4 Phenolic Degradation and Flame Retardance

Phenolic networks have been shown to possess moderate non-flammability and low smoke generation with a self-ignition temperature of 482°C.[3] They are currently used in the interiors of airplanes such as the DC-10 because of their excellent flame retardance and low smoke emission. Their excellent flame retardance promoted interest in understanding the mechanisms behind the degradation of phenolics. To understand the

flame retardance of phenolics it is important to consider the degradation pathways in both oxygen (oxidative degradation) and in an inert atmosphere (thermal degradation).

Madorsky and Straus[9] studied the mechanisms and kinetics of the thermal degradation (without oxygen) of cured phenolic resols. In this study the phenolic materials were pyrolized in a vacuum at several different temperatures ranging from 355°C to 1200°C to analyze the mechanisms of degradation as a function of temperature. The apparatus used in the test was capable of collecting the volatiles given off during pyrolysis in three separate fractions: (1) material volatile at the pyrolysis temperature but not at room temperature, (2) material volatile at room temperature, and (3) material volatile at -190°C. Each fraction as well as the char were analyzed to help understand the mechanisms of thermal degradation. At lower temperatures the main products of degradation were propanols, acetone, propylene, butanols and only a small amount of carbon dioxide. However, at higher temperatures (800 and 1200°C) significant amounts of carbon monoxide as well as methane were produced. These products could be formed from a complete breakdown of the benzene ring occurring at high temperature. It was hypothesized that such a degradation pathway could lead to free radicals capable of stripping the residue of hydrogen and oxygen leading to a more carbonized char. This proposed mechanism was consistent with the analysis of the char, which contained 99.2 % carbon after pyrolysis at 1200°C. Molecular weight analysis of the fraction volatile at the pyrolysis temperature but solid at room temperature (fraction 1) indicated crosslinked phenolic fragments with an average of three to four benzene rings per chain.[9] Based on the results of pyrolysis, Madorsky suggested that the primary mechanism for thermal degradation of phenolics is thermal scission at the bond between the methylene and the phenolic ring.[9]

In addition to thermal degradation, oxidative degradation is important to understand the mechanisms of flame retardance of phenolics. Conley and Bieron[10] investigated the low temperature (100-200°C) oxidative degradation of phenolics using infrared spectroscopy. They observed no changes in the infrared spectra with heating fully cured phenolic resin in either nitrogen or vacuum up to 200°C for 50 hours, suggesting no degradation. However at the same temperatures in air several changes in the infrared spectra were observed. Therefore, Conley and Bieron concluded that "the initial

degradation is dependent on the presence of oxygen and that the products of degradation are oxygenated species."[10] In the temperature range investigated (100-200°C) the rate of oxidation increased with increasing temperature, however the mechanism was unchanged. In addition, no differences were observed between the infrared spectra of the degradation of resols compared with that of novolacs. This similarity between the resol and novolac degradation pathways was also shown to be true for the high temperature degradation of phenolics.[11] Conley and Bieron went on to show that the oxidation observed at these temperatures was a surface phenomenon. After a detailed analysis of the changes in functional groups in the IR along with some chemical analyses, a mechanism for the low temperature thermal degradation of phenolics was proposed (Figure 2.6).[10]

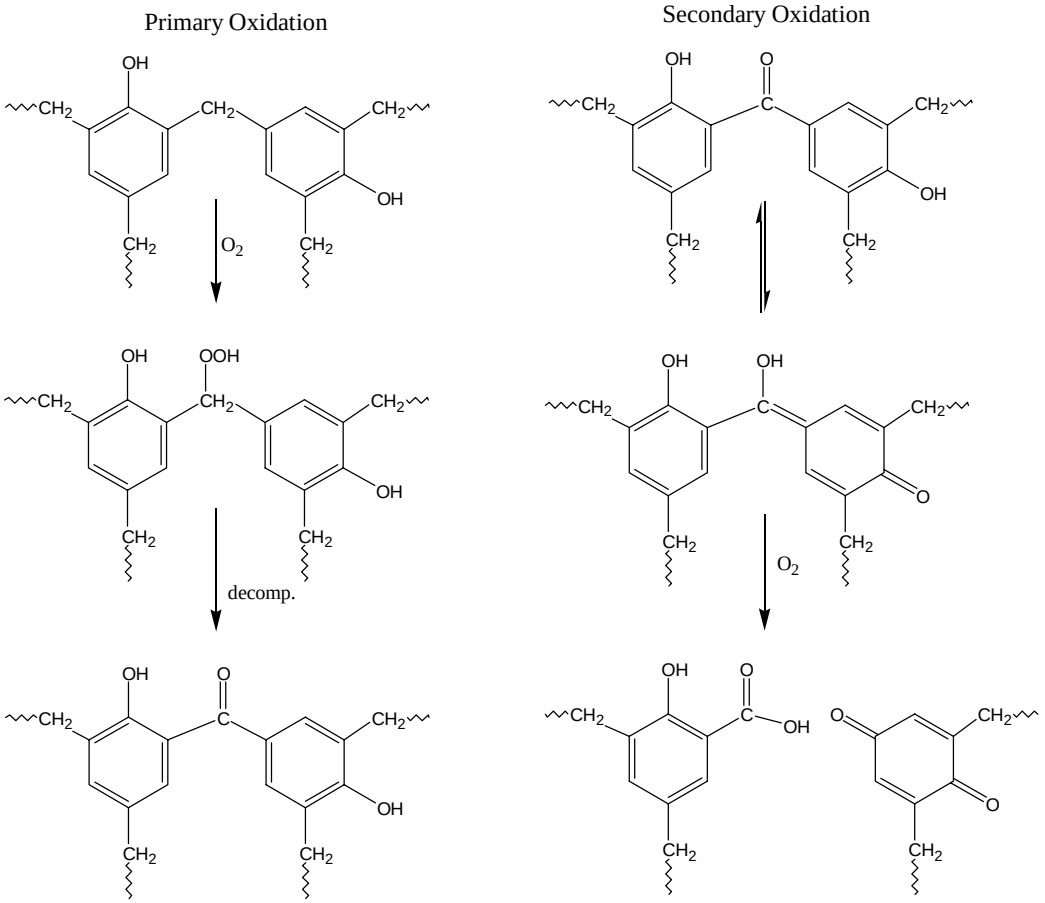

Figure 2.6: Low temperature oxidative degradation of phenolics.[10]

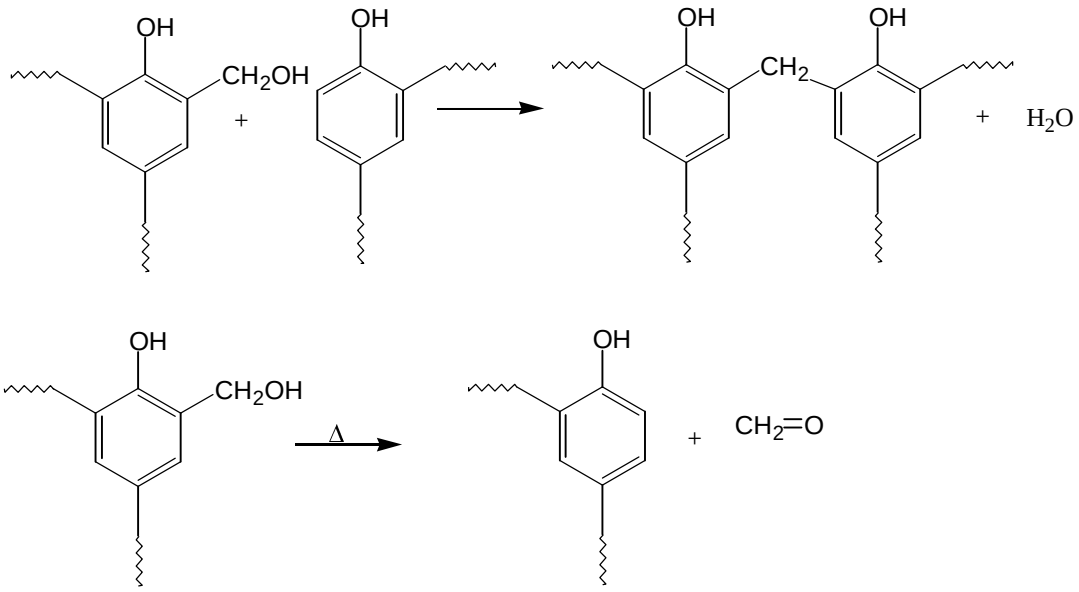

Figure 2.7: Possible loss of methylol groups during high temperature degradation.[12]

Jackson and Conley[12] investigated the high temperature (greater than 200°C) oxidative degradation of phenolics using infrared spectroscopy, vapor phase chromatography, as well as thermogravimetric and X-ray analysis. The major volatile products of extended oxidation of the resin were carbon dioxide and carbon monoxide. However, water, paraformaldehyde, methane, and aromatic products were also produced. Water and paraformaldehyde were major products at temperatures up to 400°C, which suggests a high temperature post-curing reaction. These products could be the result of the loss of methylol groups as shown in figure 2.7. However, this reaction should be minor for fully crosslinked resins. This high temperature post curing reaction imparts improved oxidative stability and resistance to thermal pyrolysis due to the complete crosslinking of the resin. Jackson and Conley proposed three types of degradation mechanisms (oxidative degradation, fragmentation, and formation of benzoid species) to account for all the observed products produced during high temperature oxidative degradation (Figure 2.8).[12] Route A describes the oxidative degradation of phenolics in generalized form, which accounts for the production of carbon monoxide and carbon dioxide. Route B accounts for the formation of methane, phenol, cresol and other methyl substituted species by radical bond rupture during thermal pyrolysis. Route C accounts

for the formation of benzene, toluene, benzaldehyde, and methane as a result of loss of the hydroxyl from the phenolic species generated in Routes A and B. Although products from both oxidation and thermal pyrolysis (fragmentation) were observed at high temperatures, oxidative degradation is the predominant mechanism for the degradation of phenolics.[3,12] Lochte et al. suggested that "the resin itself can act as an oxygen source for the oxidative process."[11] The hydroxyl radical produced in route C can act as the source of oxygen for further oxidation.

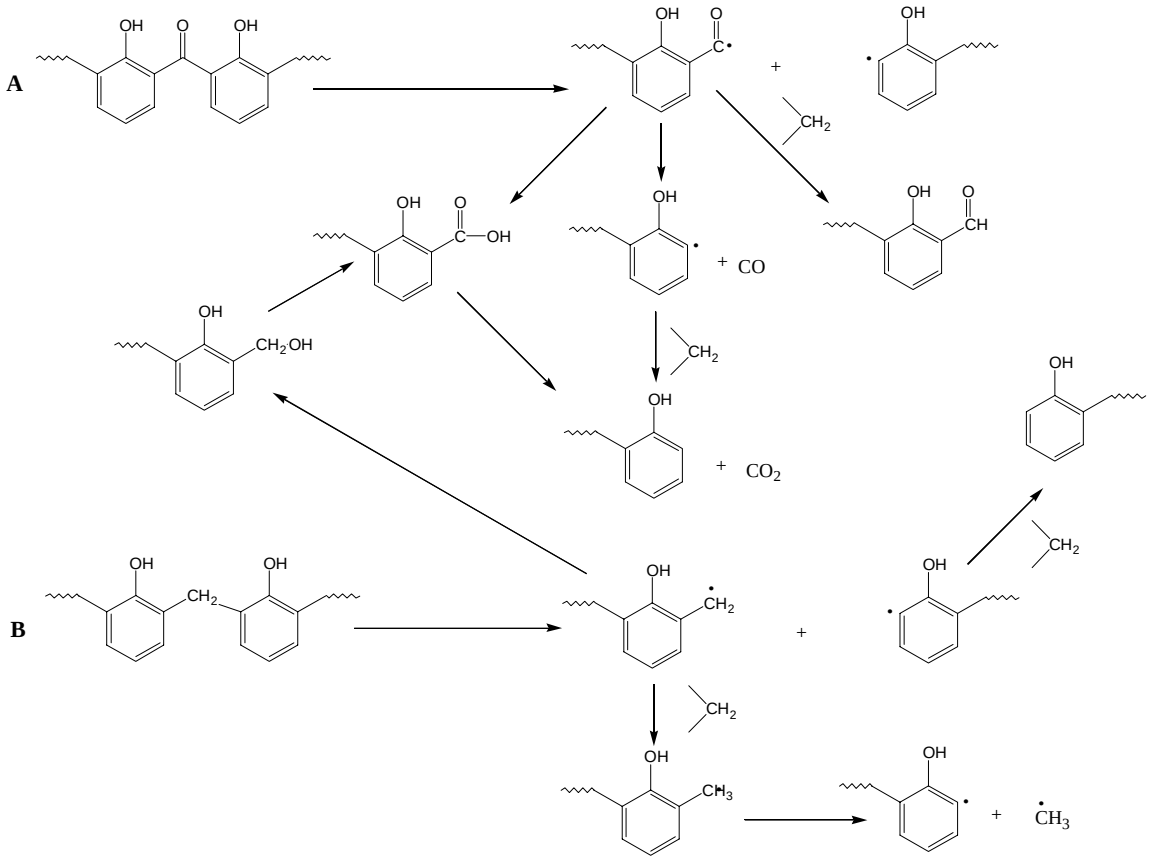

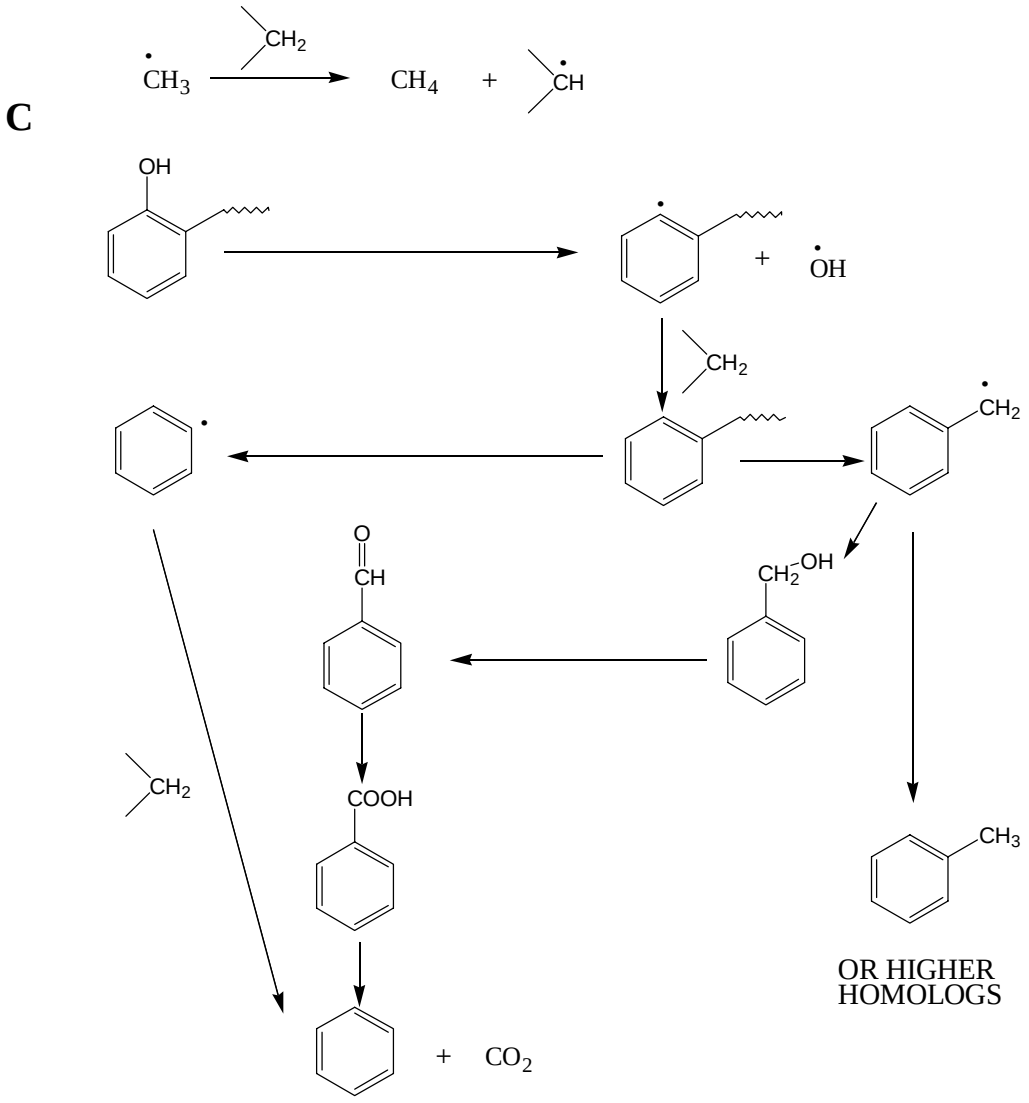

Figure 2.8: **High temperature oxidative degradation pathways for phenolic materials.[3]**

Jackson and Conley went on to explain the mechanisms of char formation based on the degradation mechanisms and infrared analysis of the char (Figure 2.9). Infrared analysis of the char indicated the appearance of hydroxyl and carbonyl groups at 700°C. In addition, gas chromatograms of the volatile components indicated that carbon monoxide is produced only at elevated temperatures and is produced simultaneously with the formation of graphite like char. Infrared analyses indicated that the char formation reactions proceed through the initial formation of quinone-type species (Figure 2.9).

Elemental analysis indicated a drastic loss of oxygen from the char at temperatures above 450°C, confirming the production of carbon monoxide during char formation.[11] The proposed mechanism of char formation is consistent with the appearance of hydroxyl and carbonyl groups at 700°C as well as the production of carbon monoxide at higher temperatures. Based on these degradation studies Lochte et al. suggested that "the elevated temperature degradation is fundamentally associated with the chemical stability of the dihydroxydiphenylmethane unit."[11]

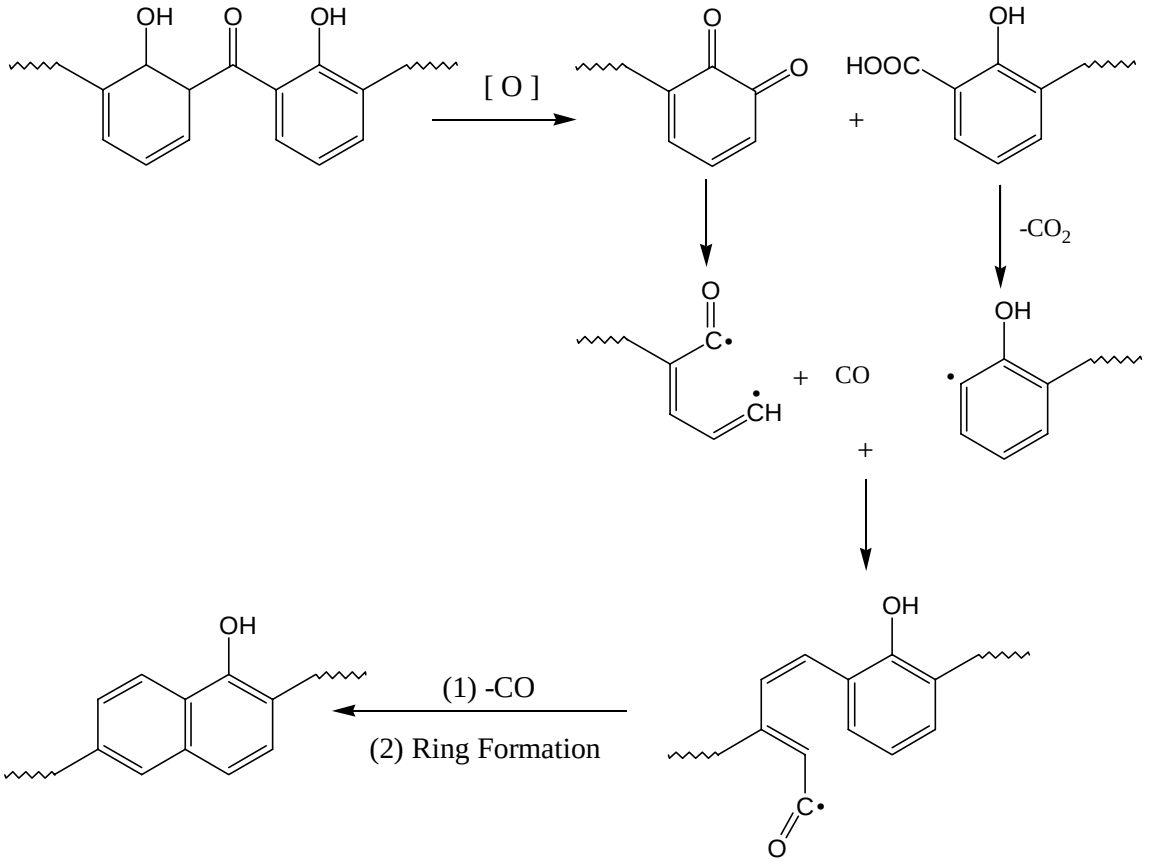

Figure 2.9: Mechanisms of char formation in phenolic resins.[3]

Although phenolic resins possess good flame retardance and low smoke generation addition of fire retardants can improve the flame retardance even further. Incorporation of only 6 % by weight of elemental phosphorus (Figure 2.10) or a combination of 2 % nitrogen and 2% phosphorus, renders phenolic resins self-extinguishing. Addition of

boron can result in non-flammable phenolic compounds. Addition of halogens can increase the flame retardance of phenolics, but in many cases the halogens result in an increase in smoke emission.[3]

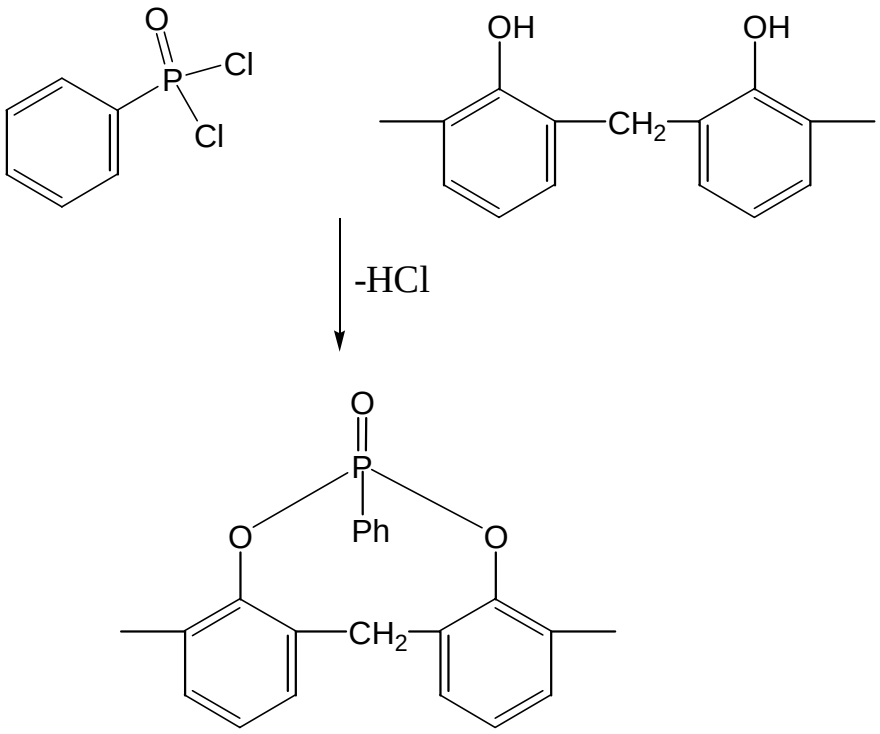

Figure 2.10: Incorporation of phosphorus into phenolic resins to improve flame retardance.[3]

The flame retardance of phenolics is directly related to their structure and thermal degradation mechanisms. The production of a structural char, as explained above, results in remarkably low flame spread rates. In addition, they have low smoke production and low toxicity of the smoke produced due to the low carbon monoxide production during degradation. They have significantly less carbon monoxide, hydrogen chloride, and hydrogen bromide production than flame retardant polyester resins.[13]

2.2 Phenolic-Epoxy Chemistry

2.2.1 Phenolic-Epoxy Mechanisms

The reaction of an epoxy with a phenol has been studied extensively in the literature. This reaction has some importance in the epoxy industry in the preparation of high molecular weight epoxy resins and polyhydroxyethers, as well as for the crosslinking of epoxy resins with phenolic novolacs for microelectronics packaging applications. The reaction mechanism and extent of side reactions are highly dependent on the reaction conditions and the type of catalyst used.[14]

There are two main reactions possible when a phenol is reacted with an epoxy. The primary reaction is the addition of phenol to epoxy (Figure 2.11A). After this reaction occurs, the secondary hydroxyl generated from the phenol epoxy reaction can react with another epoxy to give a branching reaction (Figure 2.11B). The ratio of these two reactions is dependent on catalyst structure, catalyst concentration, reaction temperature, and stoichiometry.[14]

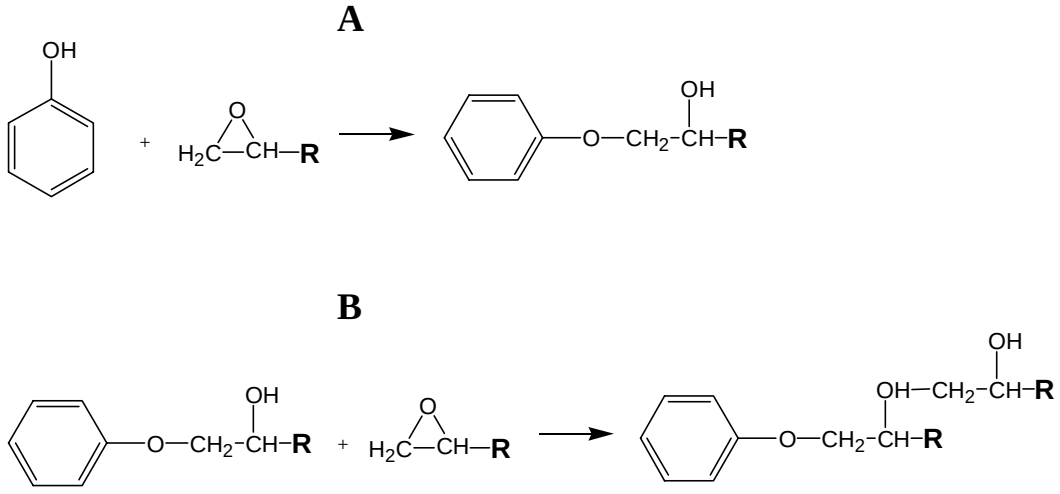

Figure 2.11: Phenolic-epoxy reactions[14]

Shechter and Wynstra have investigated the uncatalyzed reaction between epoxy and phenol. In reacting equimolar quantities of phenolic hydroxyl with a low molecular weight epoxy, no reaction was evident when held at 100°C. However, at 200°C the

epoxy was consumed at a much faster rate than the phenol, indicating that both reactions were taking place (epoxy with phenol, and epoxy with secondary hydroxyl)[14]. The reaction of the secondary hydroxyl with the epoxy group is undesirable in the synthesis of high molecular weight polyhydroxyethers because it leads to branching. Banthia and McGrath have suggested the use of sterically hindered catalysts to prevent this secondary reaction.[15] Due to their low basicity and steric hindrance, triaryl or trialkyl nucleophiles of Group Va elements catalyzed the 1:1 phenolic-epoxy reaction with reduced probability of side reactions in dilute solution at low temperatures.

Following these initial studies, the mechanism of the epoxy-phenol reaction in the melt with tertiary amine and phosphine catalysts was investigated. In 1981 Romanchick et al. proposed a mechanism for the triphenylphosphine catalyzed epoxy-phenol reaction (Figure 2.12)[16]. In this mechanism the triphenylphosphine ring opens the epoxide producing a zwitterion, followed by rapid proton transfer from the phenol to form a phenoxide anion. The phenoxide anion then reacts with the electrophilic carbon attached to the phosphorus regenerating the triphenylphosphine.[16] It is likely that in addition to this reaction, the phenoxide anion could ring open an epoxy followed by proton transfer from another phenol to regenerate the phenoxide anion. In 1985, Gagnebien et al. proposed a mechanism for the epoxy phenol reaction in the melt catalyzed by a series of tertiary amines (Figure 2.13).[17] Gagnebien proposed that the trialkylamine abstracts a proton from the phenolic hydroxyl to form an ion pair complex. The ion pair then forms a complex with the epoxy ring, which dissociates to form a β-hydroxyether and the amine (Figure 2.13).

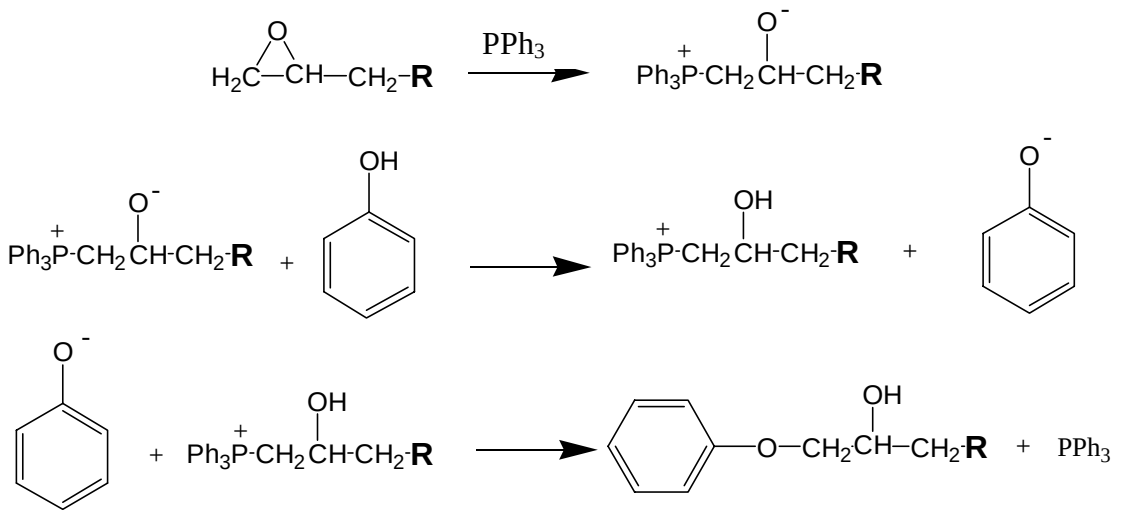

Figure 2.12: Mechanism for a triphenylphosphine catalyzed epoxy-phenol reaction.[16]

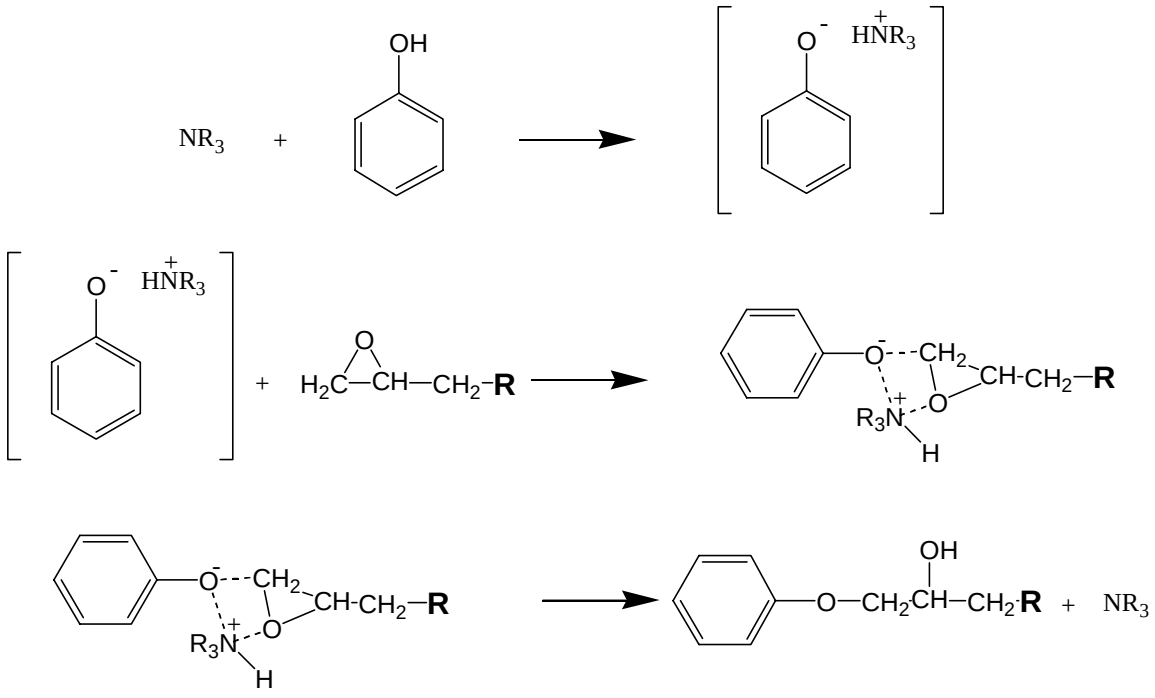

Figure 2.13: Proposed mechanism for the epoxy-phenol reaction catalyzed by tertiary amines.[17]

Three side reactions have been proposed in addition to the main epoxy phenol reaction described above, including epoxy homopolymerization, a branching reaction through the secondary hydroxyl, and a zwitterion catalyzed branching through the secondary hydroxyl. Of these side reactions, the branching reactions have been shown to be the only significant side reactions in the melt.[14] In addition, the extent of these side reactions should decrease as the ratio of epoxy to phenol decreases. With an excess of epoxy the side reactions would be expected once all the phenols had been reacted.

2.2.2 Kinetics of Phenolic/Epoxy Reaction

The reaction of phenolic hydroxyl groups with epoxies became important commercially in the curing of epoxy resins for microelectronics packaging. Their low coefficients of thermal expansion and low mold shrinkage reduced thermal stresses in the packaging leading to reduced stress cracking. The high T_g's of these materials are also important to withstand the temperature requirements of the applications.[14]

A detailed understanding of the kinetics of the phenolic-epoxy reaction and the effects of the catalyst on the mechanisms is important in developing processing conditions to suit the applications. In a comprehensive review by Biernath and Soane, the kinetics of the epoxy/phenolic reaction was studied in detail. The materials used were an epoxidized cresolic novolac cured with a phenolic novolac and catalyzed by triphenylphosphine(TPP). Both isothermal and ramp cures in the DSC were used to investigate the cure kinetics. The area of the exotherm was integrated and scaled to the ideal heat of reaction for an epoxy with a hydroxyl which was determined by Hale to be 85.8 kJ/mole of epoxy.[14]

Soane showed that at a ratio of 1 epoxy to 1 phenol the uncatalyzed reaction and epoxy homopolymerization were significantly slow compared to the epoxy-phenol reaction catalyzed with 0.5 phr triphenylphosphine. The uncatalyzed reaction reached 90 % conversion in 12 hours at 200°C. Therefore, Biernath and Soane concluded that these side reactions are negligible in the catalyzed epoxy phenol reaction. However, another side reaction between the epoxy and secondary hydroxyl generated from the reaction of the epoxy with phenol needs to be considered. To investigate the extent of this secondary reaction, kinetics of the epoxy phenol reaction with a ratio of 2 epoxies to 1 phenol and

catalyst concentrations ranging from 0.5 to 8.0 phr were studied. With this ratio of epoxy to phenol, 50 % conversion of the epoxy would be expected if no side reactions were present. With less than 1 phr TPP a ramp cure in the DSC resulted in the expected 50 % conversion of epoxy, suggesting the presence of only the primary epoxy phenol reaction. However, with higher catalyst concentrations (2 to 8 phr TPP) the epoxy conversion was greater than 50 % indicating some reaction between epoxy and 2° hydroxyl in addition to the primary epoxy phenol reaction. These samples cured with 2.0 phr TPP or greater also had a higher T_g, indicative of increased crosslink density, confirming the presence of the secondary reaction. However with lower ratios of epoxy to phenol, less than 1.3:1, there was no evidence of any secondary reaction, even with the higher catalyst concentrations. Biernath and Soane suggested that with the 2:1 epoxy/phenol ratio there is a threshold catalyst concentration between 1 and 2 phr at which the secondary reaction becomes significant. It was also shown that with very high catalyst concentrations (greater than 4 phr) there was significant reaction at room temperature during solvent mixing in acetone.[14]

In a study of the epoxy reaction rate versus time, both the ratio of epoxy to phenol and the catalyst concentration were varied. An initiation period, where the reaction rate was accelerating, was noted. This initiation period was most apparent with the higher ratios of epoxy to phenol, and was nonexistent with higher concentrations of phenol (0.5 epoxy to 1 phenol) (Figure 2.14). Therefore, Biernath and Soane concluded that the catalyst undergoes a reaction to form an activated catalytic complex, which involves both the catalyst and the phenol.[14] This conclusion was drawn from the fact that the initiation period was most pronounced with higher ratio's of epoxy to phenol. Therefore with less phenol present this complex would form slower. However, they did not propose any structures for the proposed complex. It is likely that these results could be explained by the initiation period being the time required for the triphenylphosphine to ring-open the epoxy followed by proton transfer from the phenol to the alkoxide. With a higher concentration of phenol there should be more phenolic hydroxyls near the zwitterion allowing for more rapid proton transfer. The suggested "complex" may be the interaction of the phenolate anion with the phosphonium cation.

First order rate constants were determined from plots of reaction rate versus fraction of epoxy reacted. In all cases except the 2:1 epoxy/phenol stoichiometry there was a linear relationship at higher conversions, after the initiation period. Soane suggested that the deviation from linearity for the 2:1 stoichiometry may be a result of reaction of the secondary hydroxyl with epoxy. The rate constants were determined from the linear regions at four temperatures ranging from 130 to 200°C for each of the stoichiometries (Figure 2.15). Activation energies were calculated from an Arrhenius analysis of the rate constants (Figure 2.16). The activation energies were similar for the different stoichiometries with an average of 64.7 +/- 2.4 kJ/mol. From the results of the Arrhenius analyses, Soane concluded that diffusion limitations were insignificant for the majority of the reaction. In addition, the linearity of the Arrhenius plots indicated that either the reaction mechanism did not change over the temperature range studied, or that competing mechanisms had the same activation energies and could not be distinguished.[14]

Reaction termination can occur as a result of depletion of limiting reagent, steric limitations, or diffusion limitations. Soane suggested that in most cases the reaction was terminated by the depletion of the limiting reagent. However, with 1:1 stoichiometry steric effects become important and prevented greater than 94% conversion. Diffusional limitations were only evident at the lower cure temperatures of 130-150°C, where the T_g of the material may reach the cure temperature preventing further reaction.[14]

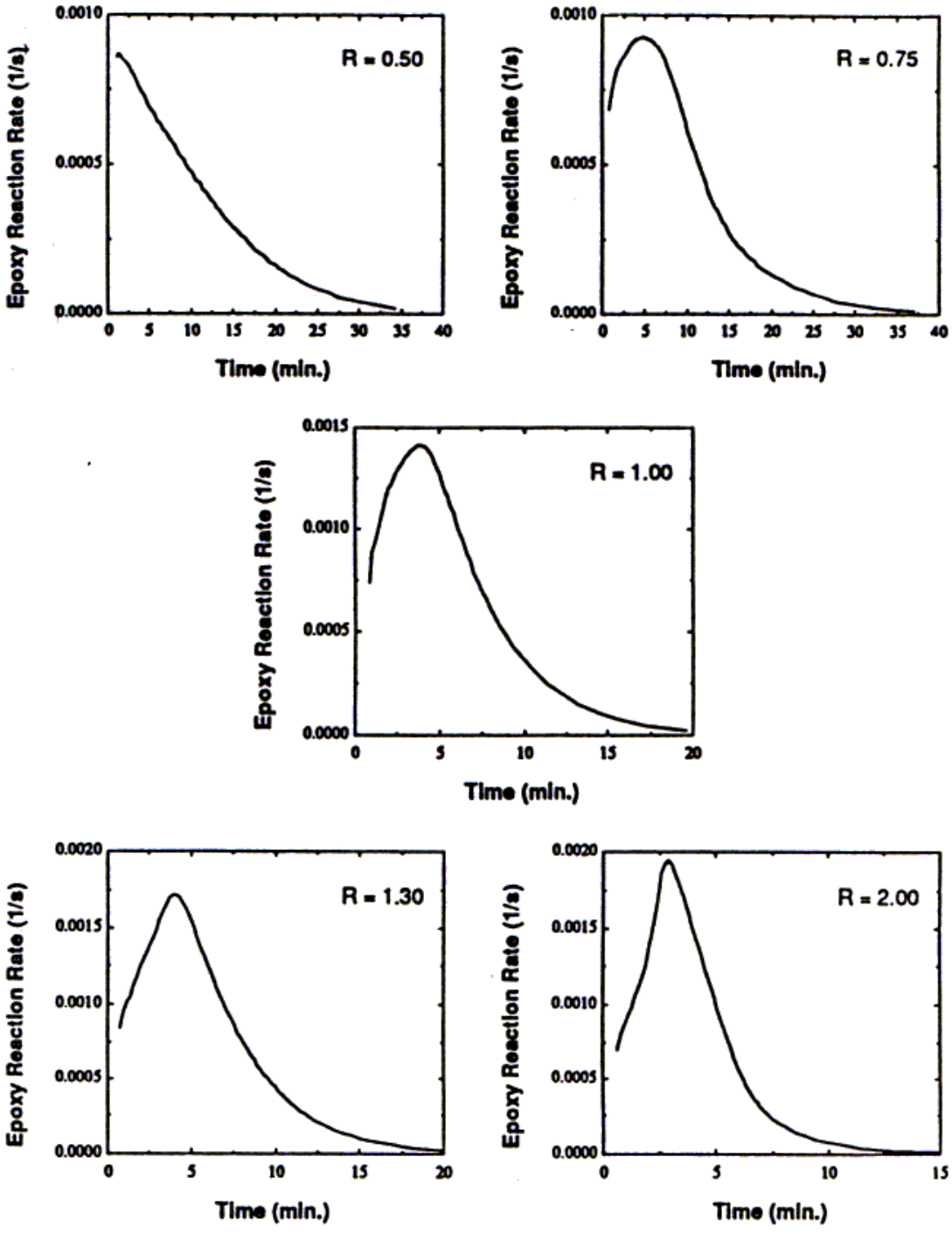

Figure 2.14: **Phenolic epoxy kinetics - reaction rate versus time where R is the ratio of epoxy to phenol.[14]**

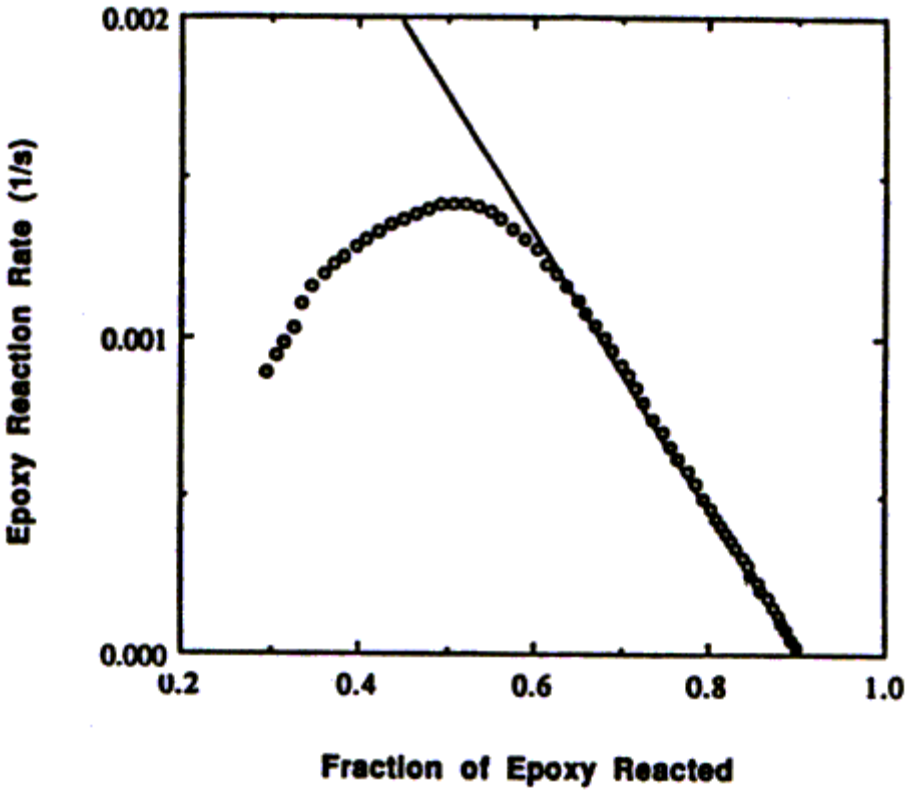

Figure 2.15: **Phenolic-epoxy kinetics - determination of first order rate constants from the slope of the linear region.**[14]

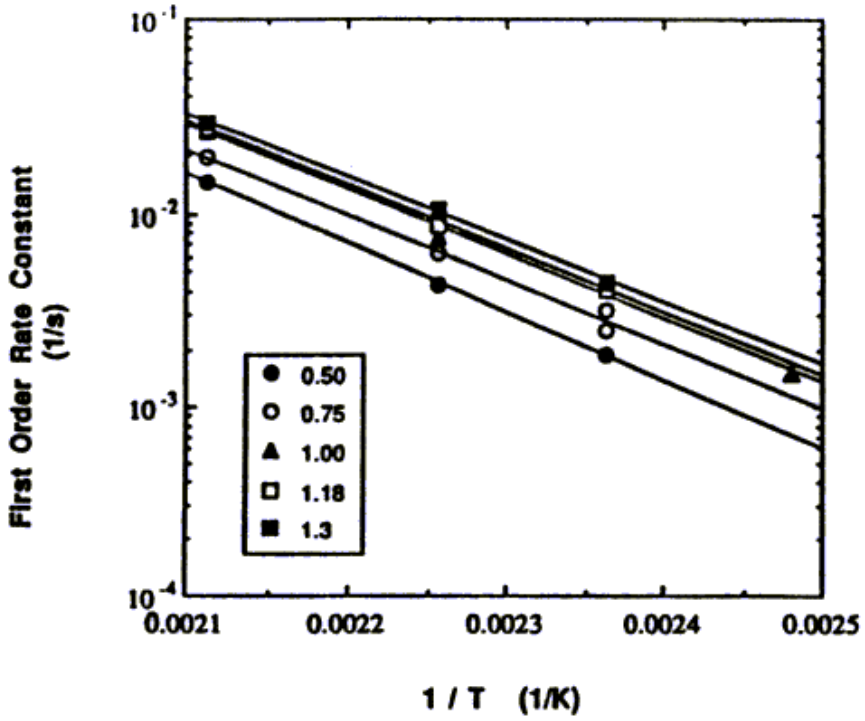

Figure 2.16: Phenolic-epoxy kinetics - Arrhenius plot of the first-order rate constant, k_1, for various stoichiometries.[14]

In addition to the work by Biernath and Soane, Han and coworkers have published several articles on the kinetics of curing biphenyl epoxy resins with phenolic "hardeners". They investigated the kinetics of the biphenyl epoxy with (1) a dicyclopentadiene type phenolic hardener varying the catalyst type (Figure 2.17), (2) different types of phenolic hardeners catalyzed by TPP (Figure 2.18), and (3) a phenolic novolac hardener with different concentrations of the TPP catalyst. For system (1) the kinetics of dicyclopentadiene-type phenolic resin (DCPDP) with five different types of catalysts: Triphenylphosphine (TPP), 1-Benzyl-2-methylimidazole (1B2MI), Tris(4-methoxyphenyl)phosphine (TPAP), Diazabicycloundecene (DBU), and Tetraphenyl phosphonium tetraphenyl borate (TPP-TPB) (Figure 2.17) were investigated.[18] In all cases a 1:1 ratio of epoxy to phenol with 1.5 phr catalyst was used. The peak in the reaction exotherm was determined from dynamic DSC cures from 10-300°C at 5°C/min. The peak in the reaction exotherms of the reactions catalyzed by TPP, 1B2MI, and DBU were close to 135°C, whereas, the peaks for the reactions catalyzed by TPAP and TPP-

TPB were significantly higher (170-176°C) indicating a "latent acceleration of the cure reaction."[18] However, in comparing the peaks in the reaction exotherms for different types of catalyst it would be more accurate if the catalysts were compared on an equal mole basis. This would give a more accurate comparison of the catalytic activity of the different types of catalysts.

Table I Description of Raw Materials Used in This Study

Materials	Structure
Biphenyl epoxy resin (YX-4000H)	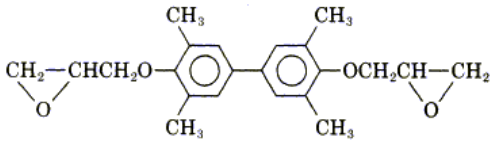
Dicyclopentadiene-type phenolic resin (DCPDP)	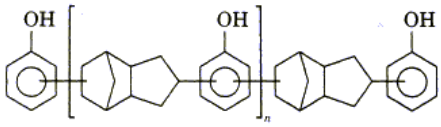
Triphenylphosphine (TPP)	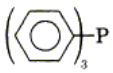
1-Benzyl-2-methylimidazole (1B2MI)	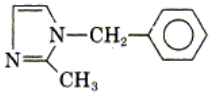
Tris(4-methoxyphenyl)phosphine (TPAP)	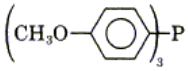
Diazabicycloundecene (DBU)	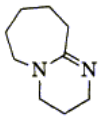
Tetraphenyl phosphonium tetraphenyl borate (TPP–TPB)	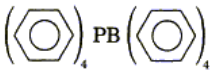

Figure 2.17: Phenolic-epoxy kinetics - description of materials used.[18]

Table I. Description of Raw Materials Used in This Study

Materials	Structure	Epoxy/Hydroxy Equivalent (g/eq)	Maker
Biphenyl Epoxy Resin	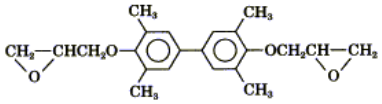	193	Yuka Shell Epoxy Co.
Phenol Novolac	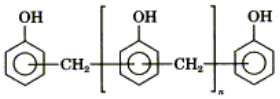	106	Meiwa Kasei Co.
Xylok	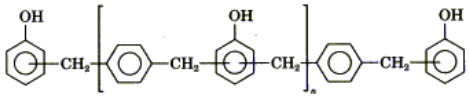	178	Mitsui Toatsu Chemicals
Dicyclopentadiene Type Phenolic Resin (DCPDP)	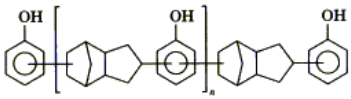	170	Nippon Petrochemicals Co.
Triphenylphosphine (TPP)		—	BASF AG.

Figure 2.18: Phenolic epoxy kinetics - Phenolic materials investigated.[19]

Another difference noted between catalysts was evident from the plots of conversion rate versus time. For the reactions catalyzed by TPP, 1B2MI, and TPAP, Han and coworkers suggested that the maximum reaction rate was at time zero, and the reactions followed first-order kinetics according to equation 2.1:

$$d\alpha/dt = k(1-\alpha)^n \qquad (2.1)$$

where n was the reaction order and k was the rate constant. Deviations from the first order rate law at conversions greater than 80 % were attributed to diffusion limitations due to gellation of the networks. The reactions catalyzed by DBU, and TPP-TPB showed peaks in the conversion rate versus time plots that increased and shifted to shorter times with higher temperatures. Han and coworkers suggested that this initiation period was an indication of an autocatalytic kinetic mechanism (Figure 2.19).[18] They described the isothermal reaction rate of an autocatalytic curing reaction by the following equation:

$$d\alpha/dt = (k_1 + k_2\alpha^m)(1-\alpha)^n \qquad (2.2)$$

where m and n were the reaction order and k_1 and k_2 were the kinetic rate constants.[18] In the case of the TPP-TPB as catalyst, the initial reaction rate was close to zero so k_1 was assumed to be zero. For the reaction catalyzed by DBU, k_1 was determined from the conversion rate versus time plots at zero time. With all catalysts investigated the experimental data fit well with the kinetic models.[18]

In addition to the effects of the catalyst on the reaction kinetics, Han and coworkers have investigated the effects of the type of phenolic hardener on the reaction kinetics.[19] The phenolic materials investigated were a phenolic novolac, Xylok™, and a dicyclopentadiene type phenolic resin (DCPDP) (Figure 2.18). Plots of conversion rate versus time for the biphenyl epoxy with each of the three phenolic materials were investigated at four temperatures, ranging from 120°C to 150°C. The results indicated an initiation period (where the maximum conversion rate was not at zero time) for the compositions with phenolic novolacs as the hardener, and no initiation period with the other phenolic materials. Therefore, Han and coworkers suggested that the reaction of biphenyl epoxy with phenolic novolac catalyzed by TPP followed an autocatalytic kinetic mechanism according to equation 2.2. They suggested that the other types of phenolic hardeners (Xylok and DCPDP) promoted a first order kinetic mechanism (equation 2.1).[19]

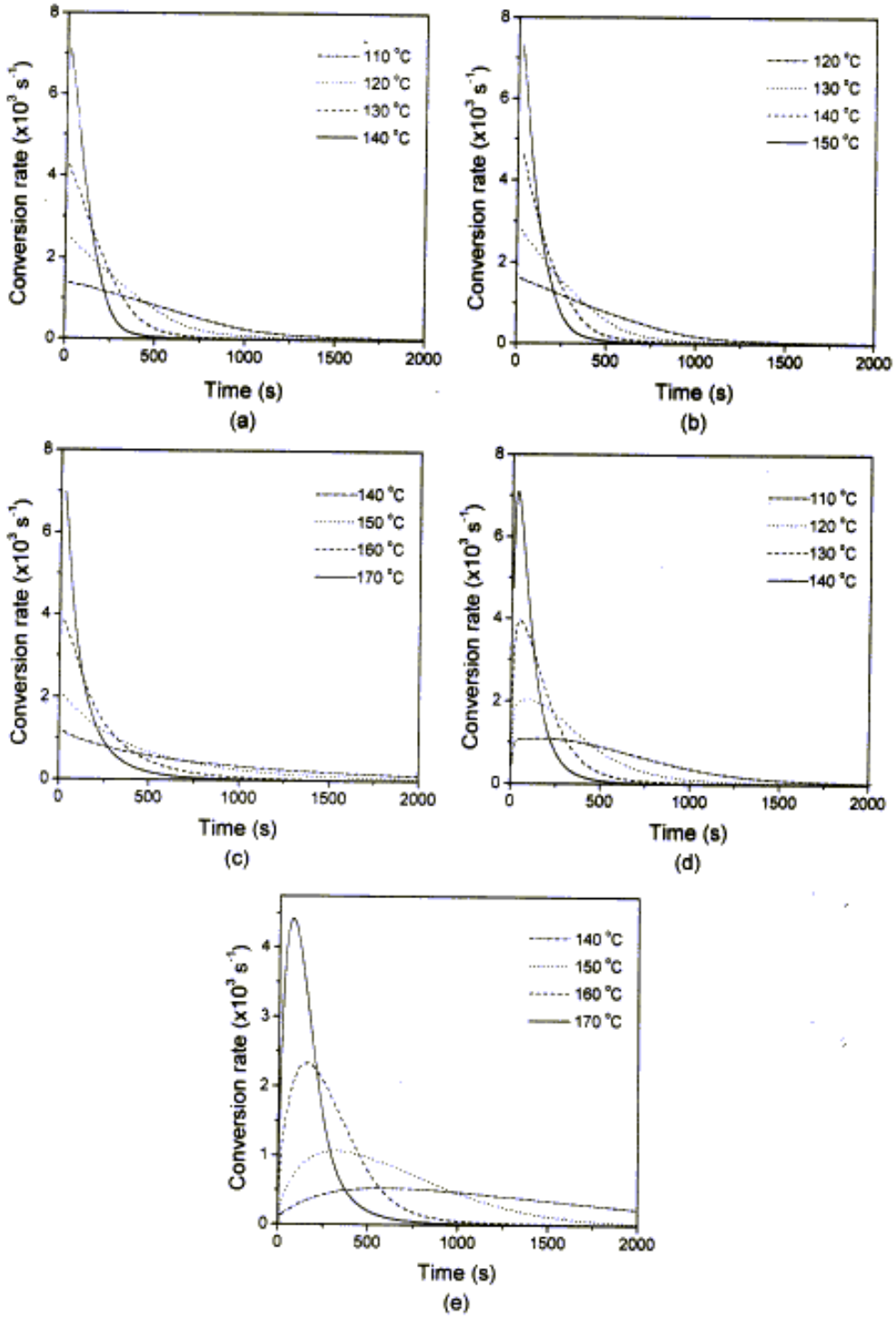

Figure 2.19: **Phenolic - epoxy kinetics - conversion rate as a function of time at several isothermal temperatures of biphenyl epoxy resin compositions with (a) TPP, (b) 1B2MI, (c) TPAP, (d) DBU, and (e) TPP-TPB.[18]**

The composition with biphenyl epoxy cured with phenolic novolac catalyzed by triphenylphosphine was studied in great detail to determine the effect of catalyst concentration on the cure kinetics. Han and coworkers suggested that the reaction proceeded through an autocatalytic kinetic mechanism for all catalyst concentrations (an initiation period was observed) (equation 2.2). As the catalyst concentration was increased, the kinetic constants k_1 and k_2 increased, but the reaction orders, m and n, only slightly increased. Based on the kinetic analyses and the relationships between T_g and conversion, Han and coworkers suggested that TPP promoted only the rate of the cure reaction without altering the network density.[20]

Throughout their work, Han and coworkers suggested that epoxy-phenol reactions followed autocatalytic or first order kinetics depending on the catalyst structure and the structure of the phenolic component. The bases for the difference in the kinetic mechanism were isothermal DSC scans indicating an initiation period for some compositions and no initiation period for others. The observed initiation period is most likely due to the build-up of active chains in the reaction. It is reasonable that the rate of initiation would be dependent on the type of catalyst used to generate the phenolate anion. However, one would expect at least some initiation period for all the resin compositions. One question that was not answered in the papers was how they determined zero time in the conversion rate versus time curves. In isothermal DSC it takes some period of time to reach the isothermal temperature. In the cases where no initiation period was observed it is possible that the initiation occurred during this heating stage or during mixing of the catalyst with the resin. Therefore, these authors have successfully modeled the kinetic behavior with equations. However, it is likely that the differences they observed in the autocatalytic versus first order kinetics was a result of the inability to mix the accelerator into the resin and heat to the isothermal cure temperature without promoting some initiation or cure. In the reactions that they label first order the initiation period has probably occurred during mixing and heating to the isothermal temperature.

2.2.3 Latent Catalysts for Epoxy and Epoxy-Phenolic Reactions

There has been significant interest in the development of latent catalysts in the curing of networks to allow long shelf lives and/or a long processing window followed by rapid cure at elevated temperatures. Smith[21] has described a “perfect latent catalyst” for epoxy resins as one having the following properties:

(1) "It should give rapid cure of epoxy resins at moderately elevated temperatures (e.g., < 60 min at 135-180°C).

(2) It should be completely miscible with the resins at all temperatures. This is particularly true of impregnating resins.

(3) The storage life of the catalyzed resin should be indefinite. In practice, the viscosity of the resin should not change appreciably at room temperature after periods of several months to years.

(4) It should not adversely affect the properties of the cured resin. In particular, the electrical and mechanical properties of the resin should not be affected by the catalyst."[21]

These desired properties would vary with different resin compositions, depending on viscosity and cure rates. The desired cure temperature is highly dependent on the viscosity of the resin. A cure temperature of 130°C would be optimum for an epoxy which is low viscosity at room temperature; however, the temperature would need to be significantly higher if the resin required high temperatures to achieve low viscosity necessary for processing.

Several different types of latent catalysts for epoxy curing have been investigated. One of the most successful of these is the boron trifluoride monoethylamine complex (BF_3•MEA or BF_3•400).[21] BF_3 complexes were initially investigated by Landua in 1964.[22] The rate of polymerization of phenyl glycidyl ether with ethyl alcohol using a BF_3-etherate complex was investigated. A significant reaction rate was observed at 15 °C ($k = 6.14 \times 10^3$ sec^{-1}). However the BF_3 complexes with amines showed no detectable reaction over a period of 3 to 4 days at 15°C. Landua suggested that "these strong complexes dissociate to BF_3 and amine only at much higher temperatures," due to the

basicity of the amine. Landua proposes that once dissociated BF_3 can complex with epoxy to catalyze the epoxy polymerization (Figure 2.20).[22] The high temperature required for dissociation of the BF_3-amine complex enables use of these complexes as thermally latent catalysts for epoxy curing reactions. The disadvantage of using BF_3-amine complexes as latent catalysts for epoxy curing is that the networks have poor electrical properties at elevated temperatures.[21]

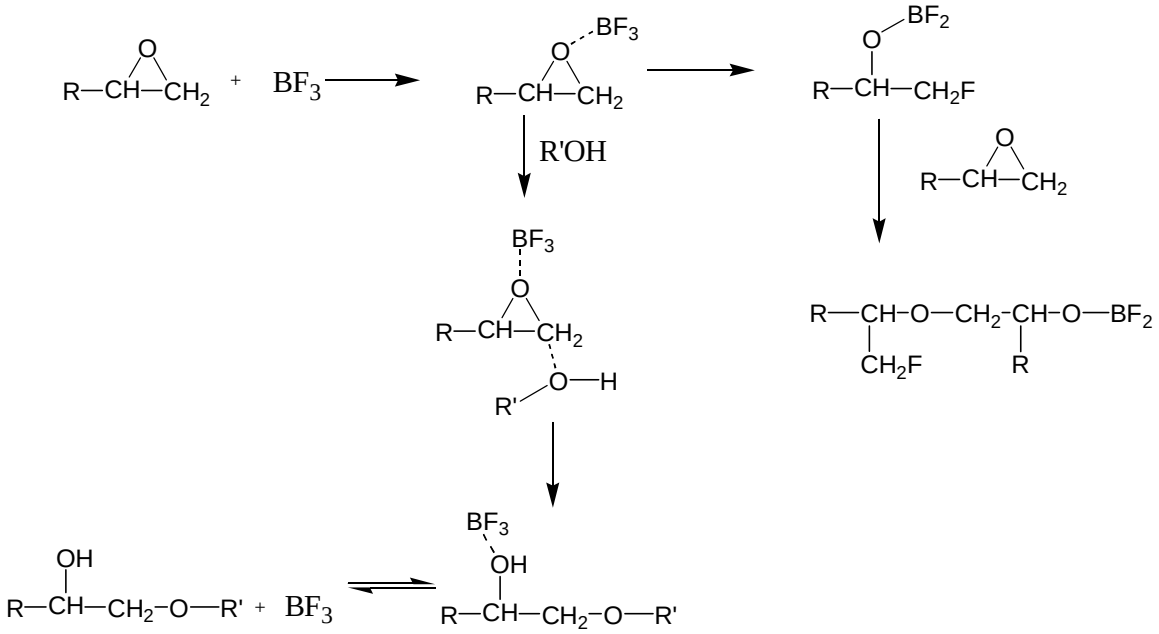

Figure 2.20: Proposed mechanism of BF_3 catalyzed epoxy polymerization. [22]

Smith[21] investigated metal acetylacetonates as latent catalysts for anhydride cured epoxy resins. The metal acetylacetonates that exhibited the best properties were those of titanium (IV), chromium (III), cobalt (III), cobalt (II), zirconium (IV), aluminum (III), and manganese (III). These catalysts exhibited good latency, fast gel times, and good electrical properties. Smith suggested that the method of cure may be thermal degradation of the catalyst to produce active species for initiation of epoxy-anhydride polymerization. The evidence for this type of reaction was the fact that the most effective latent accelerators were the ones that showed significant thermal degradation between 95 and 170°C determined from particulate analysis. In addition, based on the thermal degradation studies he suggested that the active species may be a degradation product

such as a metal cation, metal oxide, or other ionic fragment.[21] Smith suggested one of these species may interact with the anhydride to open the ring. Later Smith determined chromium (III) to be one of the best metal acetylacetonates due to it's storage stability, fast gel times, and good electrical and tensile properties.[23] In addition to chromium acetylacetonates, chromium hexacarbonyl, chromium trifluoro-acetylacetonate, and chromium acetate showed similar advantageous properties. Smith suggested that these unique characteristics of the chromium compounds were a result of the thermal dissociation of the chromium compounds to form an "epoxy-reactive cationic carboxylic anhydride species and the reduction of chromium (III) ion to chromium (II) ion"(Figure 2.21).[23] He suggests that this carboxylic cationic species (Figure 2.21) could initiate polymerization of both the anhydride and epoxy molecules resulting in a rapid cure reaction. The evidence for this mechanism was a color change of the material suggesting the reduction of chromium(III) to chromium (II).[23] Smith also investigated organotin-amine molecular complexes as latent accelerators for epoxy-anhydride blends.[24] The premises behind using organotin-amine complexes as latent catalyst for the epoxy-anhydride resins was that at high temperatures the complex should dissociate into separate organotin and amine components. Smith suggested that once dissociated, both the organotin and amine components had the ability to catalyze the epoxy resin. However, there was no evidence given to confirm this conclusion. These latent catalysts produce fast gel times at 150-175°C with good storage stability at room temperature and low power factors in cured networks.[24] Although the storage stability at room temperature using these complexes was good, there was no data to indicate at what temperature these catalyst become active. If they remained latent until close to 150°C where they promote rapid cure, they may be of interest for other higher viscosity melts.

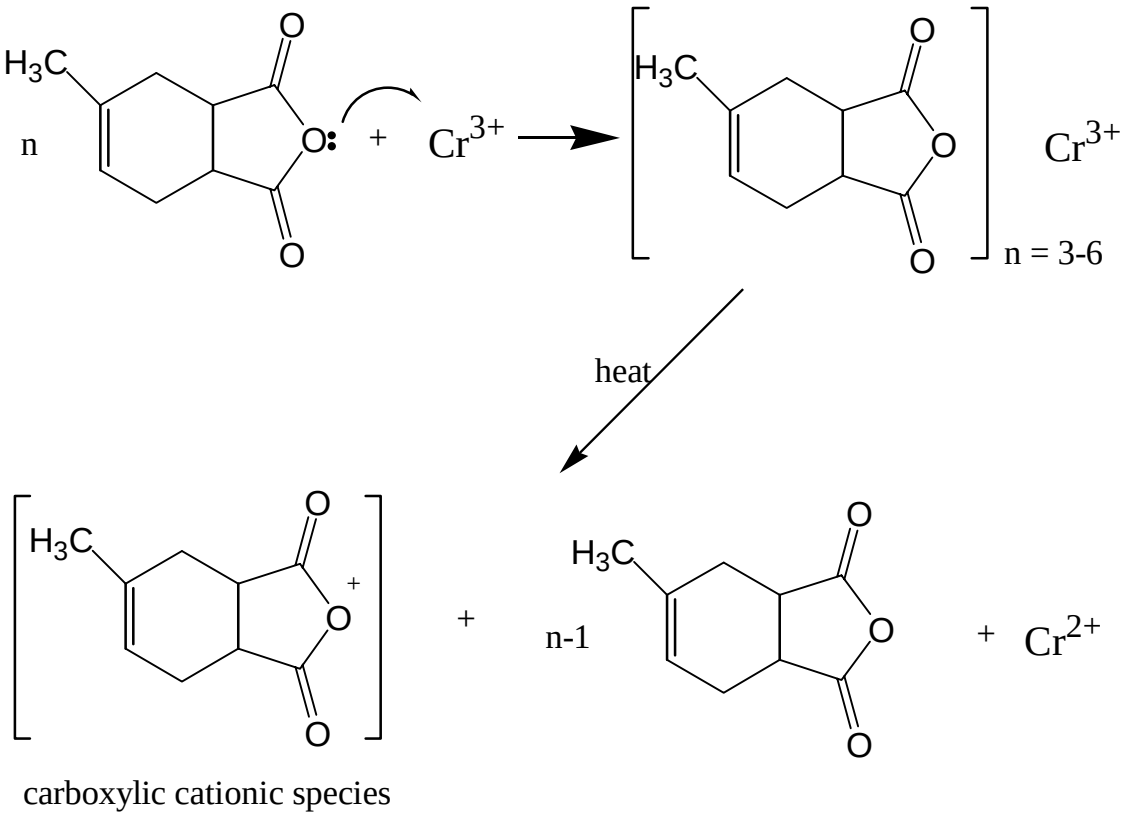

Figure 2.21: Generation of an epoxy-reactive anhydride species with the reduction of chromium (III) to chromium (II).[23]

Another method to achieve storage stability of the epoxy along with rapid cure at elevated temperatures is to use dicyandiamide as the curing agent. There is no cure at low temperatures due to the insolubility of dicyandiamide in epoxy resins. To achieve a rapid cure the epoxy must be heated above ~175°C. Phosphine catalysts can be used to reduce the cure temperature while maintaining the storage stability at room temperature, therefore acting as latent initiators for curing epoxy dicyandiamide compositions.[25] Other such latent catalysts investigated were adducts formed from the association of tertiary amines with haloboranes or pseudohaloboranes (BX_3) (X = Cl or NCS (isothiocyanato)).[26] These initiators act as latent sources of amine produced from the decomposition of the adducts. Reaction initiation appears around 100°C in the presence of these latent accelerators. Depending on the choice of X, the epoxy homopolymerization or the epoxy-dicyandiamide copolymerization can be favored.[26]

Pappas et al. investigated latent amine catalysts for the reaction of epoxy with carboxylic acid functional polyesters as hybrid powder coatings.[27] For these applications the particles must be able to coalesce and form a film prior to the crosslinking reaction. Therefore, it was important that the cure reaction was delayed during storage, processing, and film formation stages followed by crosslinking at only moderately high temperatures. The method to obtain the desired properties was to use amic acids that existed in the zwitterionic form in which the tertiary amine was protonated (Figure 2.22).[27] The amic acids in the zwitterionic form have minimized catalytic ability because the tertiary amine is protonated and they have low solubility in the powder coatings. Once the amic acids are imidized, the tertiary amine is capable of catalyzing the carboxylic acid-epoxy reaction (Figure 2.22). Pappas et al. suggests that these latent catalysts would also catalyze the reactions of epoxies with anhydrides, phenols, and thiols.[27]

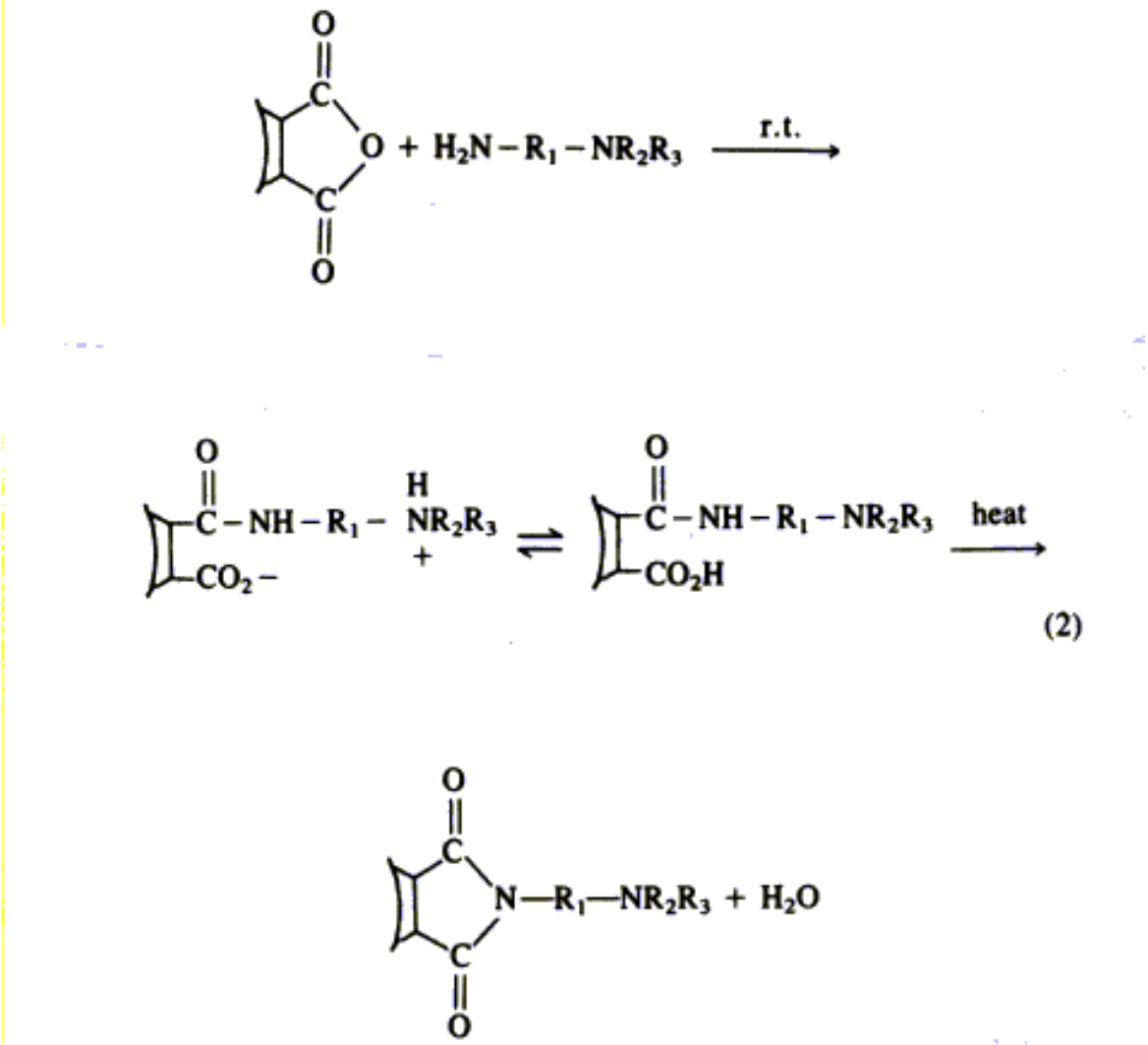

Figure 2.22: Latent catalyst for the epoxy-carboxylic acid reaction[27]

Recently, Kobayashi et al. have investigated phosphonium ylides as latent catalysts for the epoxy-phenol reaction (Figure 2.23).[28] Using these phosphonium ylides no epoxy conversion was observed below 90°C, but significant conversion in the presence of the catalysts was observed above 90°C indicating the thermally latent catalytic ability of these phosphonium ylides. Kobayashi et al. found the catalytic ability of the phosphonium ylides to increase with the electron-accepting character of the acyl group.

Therefore, several different types of latent catalysts for epoxy curing have been developed. Selection of the appropriate catalyst depends on the type of curing agent for the epoxy. Most of the latent catalysts have been tailored toward resins that are liquid at room temperature. Therefore, the goal of these latent catalysts has been to prevent cure during storage to increase storage stability. However, there is a need for a latent catalyst that would remain latent even at higher temperature to allow processing of high viscosity melts. This creates a challenge because the catalyst must be latent at the processing temperature but active at a cure temperature somewhat higher. The phosphonium ylide catalyst is the only catalyst that shows no catalytic activity up to a temperature of 90°C. This catalyst may be important for materials that require processing temperatures above room temperature but below 90°C. However, there is still a need for catalyst that remains latent at higher temperatures (up to 150°C), then promotes rapid cure at temperatures around 200°C.

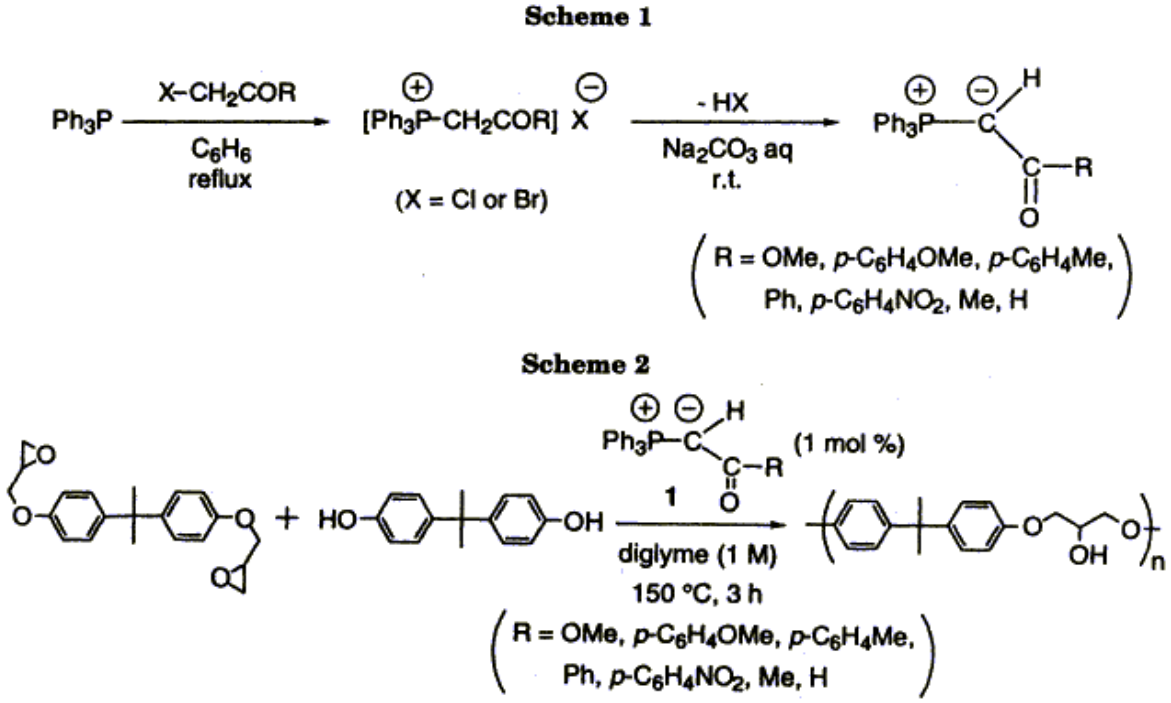

Figure 2.23: Phosphonium ylide latent catalysts[28]

2.3 Polymer networks and Analysis

2.3.1 Crosslink Density

An understanding of network density is essential in developing an understanding of the thermal and mechanical properties of crosslinked polymers. Network density can be quantified by determining the molecular weight between crosslinks (M_c). In some networks the molecular weight between crosslinks can be accurately predicted by the molecular weights of the oligomers assuming complete conversion. However, in many networks the molecular weight between crosslinks is difficult to predict due to incomplete conversion or random crosslinking along the polymer chain, such as in rubber vulcanization. In these cases, it is necessary to measure the molecular weight between crosslinks from physical tests. One method for determining the molecular weight between crosslinks is through swelling experiments (equation 2.3), where V_1 is the molar volume of the solvent, ρ is the density of the polymer, ϕ is the volume fraction of the polymer in the swollen state, and χ is the Flory Huggins interaction parameter.

$$M_c = -V_1\rho_p[\phi^{1/3} - \phi/2]/[\ln(1-\phi) + \phi + \chi_1\phi^2] \quad (2.3)$$

This equation assumes a perfect network with no elastically inactive chains or dangling ends. Dividing M_c by a correction factor $(1-2M_c/M_n)$ accounts for these elastically inactive chains in the networks, where M_c is the molecular weight between crosslinks and M_n is the molecular weight of the polymer before crosslinking. This method is most accurate for typical vulcanized rubbers with M_c's around 5000. However, for highly crosslinked networks with lower M_c's this equation is not quantitatively accurate, although the general trend of increasing M_c with increasing swelling still holds.[29]

The most common method of determining the molecular weight between crosslinks of highly crosslinked networks is with mechanical tests to determine the moduli in the rubbery region. According to the theory of rubber elasticity the modulus in the rubbery region is proportional to network density (or $1/M_c$) (Equation 2.4).

$$G = (\langle r^2\rangle/\langle r_o^2\rangle)\rho RT/M_c\,(1 - 2M_c/M_n) \quad (2.4)$$

In this equation the term ($<r^2>/<r_o^2>$) is often neglected because this ratio is usually about 1.0. The term ($1 - 2M_c/M_n$) is a correction factor to account for "polymer chain ends not effectively tied into the network," and is sometimes ignored. In the development of the statistical theory of rubber elasticity four assumptions were made which are clearly stated by Aklonis and MacKnight:

1. "The internal energy of the system is independent of the conformations of the individual chains.
2. An individual network chain is freely jointed and volumeless, that is, it obeys Gaussian statistics
3. The total number of conformations of an isotropic network of such Gaussian chains is the product of the number of conformations of the individual network chains.
4. Crosslink junctions in the network are fixed at their mean positions. Upon deformation, these junctions transform affinely, that is, in the same ratio as the macroscopic deformation ratio of the rubber sample."[30]

These assumptions must be taken into account in the determination of molecular weight between crosslinks from the rubbery moduli. Nielsen suggests that at high degrees of crosslinking the assumptions are not valid. However, he states that "the elastic moduli at high temperatures are still a good empirical method of characterizing cross-linked materials."[29] Lemay et al.[31] indicated that although densely crosslinked epoxy networks should contradict the assumptions of Gaussian statistics and negligible internal energy changes, their experimental results suggest that the theory is applicable for these networks. Therefore, it has been shown that determination of M_c from rubbery moduli in highly crosslinked networks is valid, in spite of the assumptions.

The glass transition temperatures of crosslinked networks are dependent on the degree of crosslinking. For lightly crosslinked networks there is less dependence of T_g on M_c. However for highly crosslinked networks the dependence is much stronger. At high crosslink densities very small changes in M_c result in large changes in T_g. Some work has been done to quantitatively predict the molecular weight between crosslinks based on the shift in T_g, but there is debate on the validity of the equations. It is difficult

to make a direct correlation between M_c and T_g, because as the molecular weight between crosslinks changes the chemical composition of the network also changes. This is known as the copolymer effect. Therefore, there are two independent factors affecting the T_g when the network density is varied, the degree of cross-linking ($1/M_c$) and the copolymer effect.[29]

Bos and Nusselder[32] investigated the effect of network density on the toughness in the glassy state using polyurethane networks from a triisocyanate and well defined polymeric diols of controlled molecular weights. They calculated the theoretical molecular weights between crosslinks both from assuming full conversion and based on the measured percent conversions, which ranged from 97 to 99 percent. This theoretical calculation assumed that there were no physical crosslinks. They compared these theoretical M_c's to M_c's determined experimentally from the equilibrium rubbery moduli, according to the theory of rubber elasticity. Based on the agreement of the theoretical and experimental M_c's, Bos and Nusselder suggested that the networks were ideal, "with no additional physical crosslinks."[32] The results showed a decrease in the T_g with decreasing crosslink density but no significant change in the glassy moduli. In addition the critical stress intensity factor, K_{1c}, was directly proportional to the molecular weight between crosslinks, indicating an increase in toughness with decreasing crosslink density. The toughness (K_{1c}) was measured using the single edge notched bend geometry on samples prenotched by tapping with a razor blade, according to the protocol for K_{1c}/G_{1c} testing, prepared by ESIS. Bos and Nusselder also suggested "that the yield stress, as well as the plastic zone size, increased with decreasing crosslink density."[32] Nusselder and Bos investigated the effects of network defects such as bimodality, dangling chain ends, and high sol fractions on the critical stress intensity factor, K_{1c}.[33] Surprisingly, they found little to no effect on the toughness with the introduction of defects into the network structure.

There has also been a significant amount of work on the effect of the crosslink densities of epoxies on their mechanical properties. Espuche et al.[34] investigated the effects of crosslink density on the glass transition temperature, fracture toughness, yield stress, and cooperativity of a diglycidyl ether of bisphenol A (DGEBA) cured with 4,4'-diamino-3,3'dimethyldicyclohexylmethane (3DCM). In this study, the crosslink density

was varied by adding different amounts of a difunctional amine chain extender (methylcyclohexylamine MCHA). Molecular weights between crosslinks were calculated from the rubbery storage moduli, based on the theory of rubber elasticity. The results indicated that as the molecular weight between crosslinks increased, the T_g and yield stress decreased, the fracture toughness increased, and the degree of cooperativity decreased.[32]

Lemay et al.[31] also investigated the effect of molecular weight between crosslinks on fracture toughness. They varied the crosslink density by two methods, first by controlling the stoichiometry of epoxy to amine and secondly by varying the molecular weights of the epoxy oligomer. They found the second method to be a more precise method of changing M_c while holding other variables constant. Altering the stoichiometric ratio of epoxy to curing agent leads to increased dangling chain ends and sol fractions. The molecular weights between crosslinks were calculated from the equilibrium rubbery moduli at Tg + 40°C based on the theory of rubbery elasticity (equation 2.4). Lemay et al. suggested that the theory of rubber elasticity is effective in predicting the molecular weights between crosslinks in spite of the assumptions of the theory. These M_c's provided a measure of the crosslink density of the samples being tested. In comparing the glassy fracture energy, the samples with stoichiometric epoxy/DDS ratios followed the expected trend of increasing fracture energy with increasing M_c. However, in the series with the offset stoichiometries, the network with the highest M_c had the lowest fracture energy. Therefore, Lemay et al. suggested that the large soluble fraction in the networks with the offset stoichiometry had an effect on the fracture energy. Additionally, for the series with the stoichiometric epoxy/DDS ratios, the fracture energy appeared to be proportional to $M_c^{1/2}$.[31]

Bell[35] investigated the effects of molecular weights between crosslinks on the mechanical properties of networks prepared from a bisphenol-A based epoxy (Epon 828) cured with 4,4'-diaminodiphenylmethane (MDA). The network density was varied by varying the ratio of epoxy to amine. For this system there was no effect of changing the molecular weights between crosslinks on the ultimate tensile strength, ultimate elongation, or initial modulus. However, a strong dependence of impact strength on M_c was observed. The impact strength increased with increasing M_c up to a maximum at an

M_c of about 1100, followed by a significant drop in the impact strength at higher M_c's. Bell suggested that the drop in impact strength at high M_c's may be "due to structural weakness associated with the small amounts of unreacted amine remaining at the high M_c values." The amount of unreacted amine ranged from 0 to .35 meq/g (up to .07 eq of unreacted amine per mole of epoxy), with the highest amounts of unreacted amine for the materials with M_c's greater that 1000. In all cases the unreacted epoxy concentration was less than 0.07 meq/g. It is not clear whether they accounted for linear segments from the reaction of 2 amine functional groups.[35]

The importance of network density and molecular weight between crosslinks on thermal and mechanical properties has been shown extensively. Increasing the molecular weight between crosslinks results in a decrease in the glass transition temperature and an increase in toughness for networks without numerous defects. Therfore an understanding of the network structure and the molecular weight between crosslinks is crucial in the optimization of thermal and mechanical properties of networks.

2.3.2 Phenolic/Epoxy Crosslink Density – Effects on Physical Properties

Ogata and coworkers[7] give an excellent description of the effects of crosslinking on the physical properties of novolac cured epoxy resins, including effects on the glass transition temperatures, coefficients of thermal expansion, glassy moduli, specific volumes, water absorptivity and relaxation behavior. In this work, 1:1 equivalence ratios of phenol to epoxy were used, and the crosslink density was varied by two methods. First, they used different accelerators, which they suggested promoted changes in the reaction mechanism. The primary reaction mechanism was the reaction of the phenolic hydroxyl with the epoxy group. However, there were some possible side reactions such as the reaction of a secondary hydroxyl group generated in the phenolic epoxy reaction with an epoxy. This side reaction would offset the stoichiometry by consuming the epoxy groups, leaving some unreacted phenolic groups. Therefore networks were formed with the same composition and different crosslink densities. The change in mechanism may also affect the polarity of the network by changing the concentration of unreacted phenolic hydroxyl groups, because for every aliphatic hydroxyl lost one phenol would remain. Changes in crosslink density were observed when using the different initiators.

However, there was no quantitative analysis to determine the extent of side reaction compared to the main reaction of epoxy with phenol. Infrared analysis to quantify the residual functional groups was unsuccessful. There was no significant difference in the infrared spectra between samples with different crosslink densities cured with different accelerators. Therefore, networks with the crosslink density varied in this manner remain somewhat undefined.

The second method of varying the crosslink densities of the cured networks was by changing the molecular weight of the epoxy, while maintaining the same equivalent weight. This was achieved by varying the functionality of the epoxidized novolac being incorporated. Therefore, this increase in functionality should cause an increase in the crosslink density of the networks without changing the mechanism of the reaction or the composition of the networks. This method appears to be a better way of varying the crosslink density. However, both methods of varying the crosslink densities in these systems showed consistent results. In addition, the variation in polarity between the samples was small. Therefore, differences due to polarity were assumed negligible. Crosslink densities for both systems were determined based on the kinetic theory of rubber elasticity (equation 2.5), from the storage moduli at 40°C above the peak in the tan delta curves, and assuming a density(ϕ) of 1.0 for the networks.[7]

$$\rho(E') = E'/3\phi RT \qquad (2.5)$$

Ogata and coworkers found that the glass transition temperatures increased with an increase in the crosslink density, and followed the equation $Tg = K_1 \log K_2 \rho$ where K_1 = 111 and K_2 = 3.9, and ρ is the crosslink density. K_1 represents a measure of the influence of the crosslink points on molecular chain motion, and K_2 is a constant that depends on interactions and rigidity of the main chain.[7] The values of K_1 and K_2 are similar to those for epoxies cured with anhydrides, diamines, or imidazoles, which have been shown to have K_1 = 50-110 and K_2 = 3.7-5.9. The high value of K_1 for these networks indicates that the crosslink points have a strong influence on chain mobility.

Ogata also showed that the linear coefficients of thermal expansion in the rubbery region decreased with increased crosslink density as would be expected. However, the coefficients of thermal expansion in the glassy region increased with crosslink density.

Similarly, the glassy moduli (at Tg – 60°C) decreased with an increase in crosslink density, and the specific volume increased. Therefore, it appears that the effects of the crosslink points in the glassy region may be opposite those of the rubbery region. Ogata and coworkers suggested that these seemingly backwards results in the glassy region could be explained by fractional free volume, and that for networks with high crosslink densities, the molecules were loosely packed in the glassy region.[7] They suggested that the crosslinking points prevented close packing of the chains in the glassy state. Ogata and coworkers attempted to explain this increase in the specific volume with increased crosslink density using a schematic of the specific volume change with temperature Figure 2.24). The schematic was based on results of the temperature dependence of the specific volume of networks with varied crosslink densities. Resin I represents a network with a higher crosslink density, and Resin II results in a material with a lower crosslink density. At high temperatures Resin I, with the higher crosslink density, had a lower specific volume but "the molecular motion was frozen at a relatively large specific volume due to a strutting of the crosslink points."[7] This results in a higher specific volume in the glassy state, when compared to materials with lower crosslink densities. In contrast, the specific volume of the material with the lower crosslink density (Resin II) decreased significantly before the molecular motion was frozen at the Tg. It would be interesting to investigate the effects of hydrogen bonding on free volume and packing in the glassy state using similar methods.

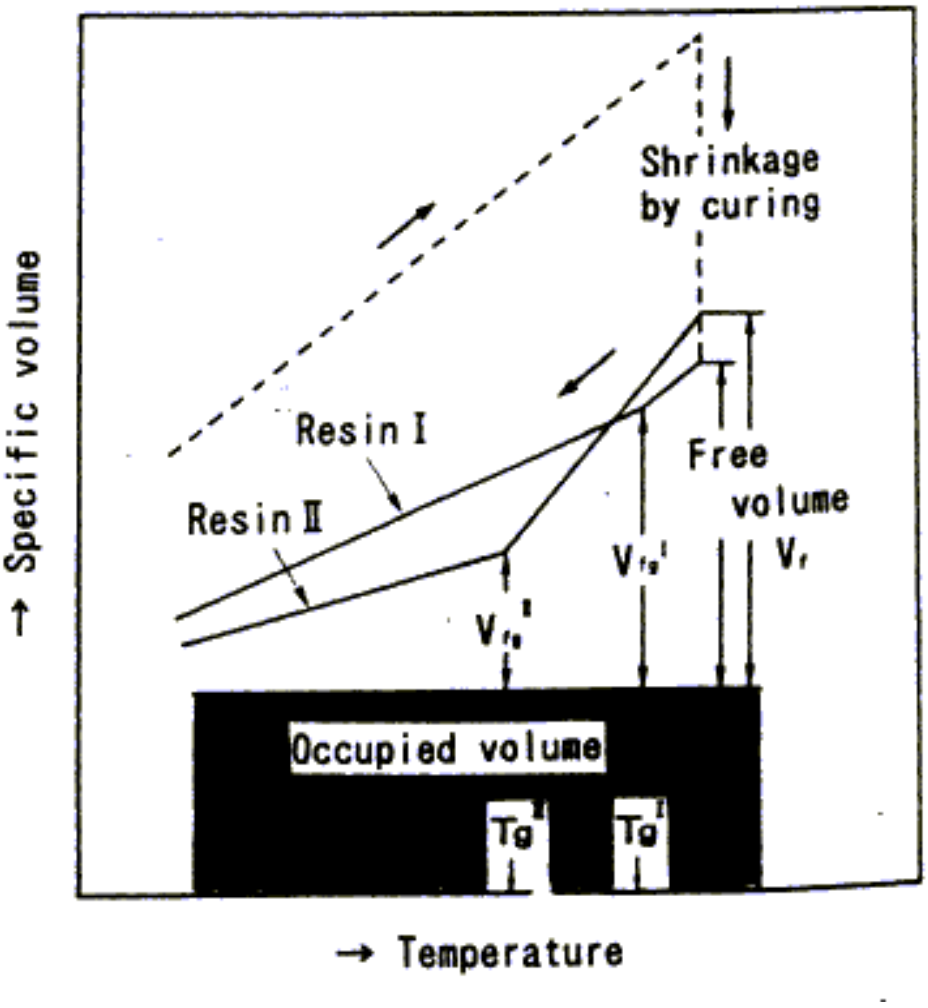

Figure 2.24: **Schematic representation of specific volume changes with temperature for materials with different crosslink densities.**[7]

Investigation of the effect of crosslink density on moisture absorption showed an increase in the saturation water uptake, diffusion coefficient and permeability of the phenolic-epoxy networks with an increase in the crosslink density. This increase in moisture uptake with increased crosslink density is consistent with the fact that the specific volume in the glassy region increases with increased crosslink density due to the loose packing of chains in the glassy state. Since several factors influence the moisture uptake, such as the free volume and packing state, as well as the concentration of polar groups in the cured network, a definite interpretation of these results is difficult. The

polarity of the networks is dependent on the concentrations of the unreacted phenolic and aliphatic hydroxyl groups remaining after cure.[7]

Investigations of the relaxation behavior of these materials indicated that the temperature and frequency dependence of the relaxation decreased with increased crosslink density. This means that the materials with the higher crosslink densities have broader relaxations (relaxations over a long time scale). This conclusion could be analyzed further by a study of the cooperativity of these materials.

2.3.3 Cooperativity

An understanding of the intermolecular cooperativity of polymeric materials is important in understanding the temperature dependence of the transition region as well as developing an understanding of the non-equilibrium glassy state. Many authors have studied both the non-linearity and non-exponentiality of segmental relaxations in the transition regions. Polymers with small flexible repeat units tend to have Debye type (exponential) relaxations that are near Arrhenius.[36] Therefore, as these materials are cooled from the glassy state the temperature dependence of relaxation times follows Arrhenius behavior, and there is not a broad distribution of relaxation times. Exponential (Debye) relaxations have only a single relaxation time that governs relaxation behavior. Materials with Debye type relaxations that are near Arrhenius have very low cooperativity. However, polymers with large sterically hindered monomer segments tend to show broad asymmetric distributions of relaxation times at a given temperature, and relaxation times with non-Arrhenius temperature dependencies.[36] It has been suggested that this behavior results from intermolecular cooperativity with neighboring non-bonded segments.[36]

Matsuoka and coworkers related cooperative motion to a mesh of gears. In order for one gear to move several adjacent gears must also move.[37,38] A gear represented the smallest segmental unit of rotation, which for polymers was called a segment. In order for one segment to move, some if its neighbors must also move with cooperative motion. Therefore, the movement of one segment is dependent on other segments in order to relax. The number of segments required to move together was represented by z. This

concept was illustrated with a two dimensional cooperative domain with 6 conformers per domain (z = 6) (Figure 2.25). [37,38] The cooperative domain size (z) at a particular temperature is dependent on free volume (packing) and intermolecular attraction between neighboring domains.[39] Hodge illustrated that the number of segments in a cooperative domain increases with a decrease in temperature near the transition region.[40] In addition, the activation energy of relaxation is the product of the number of segments in a domain (z) and the activation energy for the relaxation of a single segment. Therefore the activation energy has a temperature dependence based on the temperature dependence of the cooperative domain size.

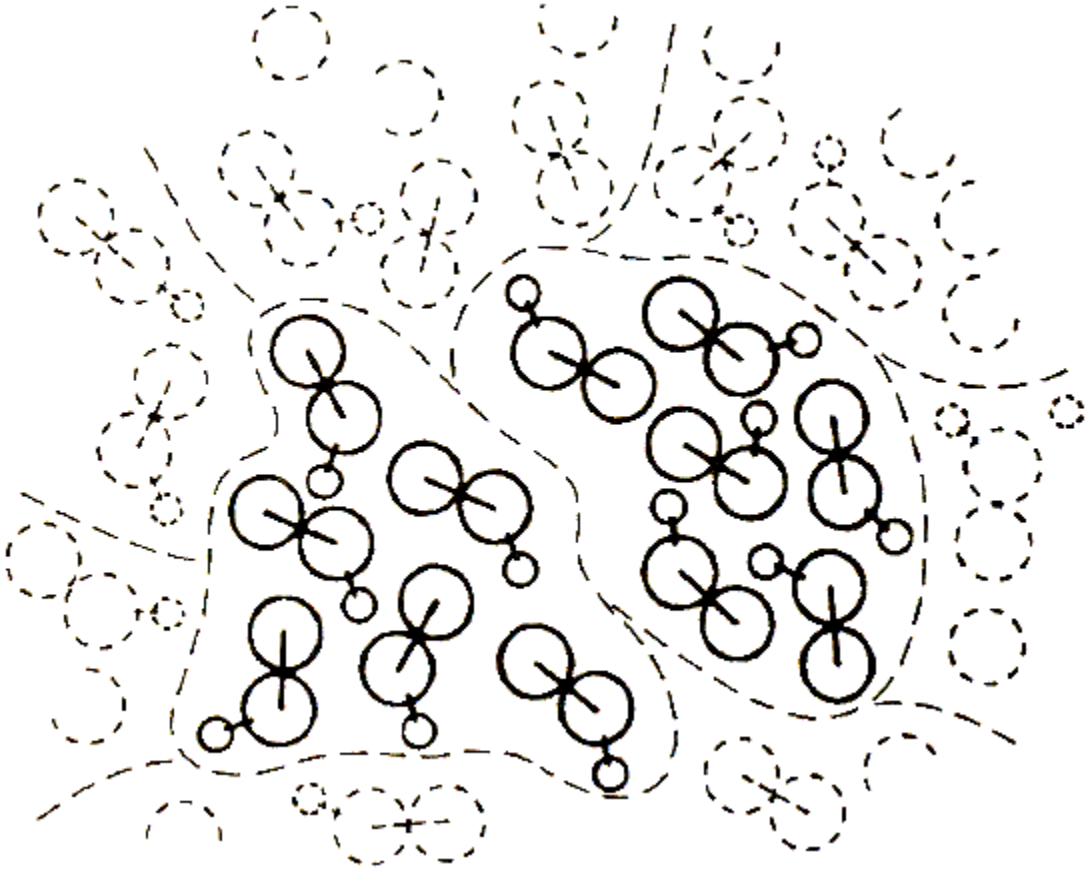

Figure 2.25: Illustration of cooperative domain sizes where z = 6[38]

One measure of cooperativity is the extent of non-linearity in the transition region. Polymeric materials show a departure from Arrhenius behavior in the glass transition

region. Angell has described this non-linearity as fragility, where materials can be classified as "strong" or "fragile" based on the extent of deviation from Arrhenius behavior.[41] Strong liquids show behavior very close to Arrhenius, and are named "strong" as a result of "the evident resistance of their short-and intermediate-range order to thermal degradation."[41] The phrase "thermal degradation" in this case refers only to the loss of local order, independent of chemical stability.[42] On the other hand, fragile liquids deviate most strongly from Arrhenius behavior. Fragility is a measure of the temperature dependence of the most probable segmental relaxation time near T_g, where more fragile liquids are more temperature dependent.[42] Connolly and Karasz suggested that "fragile" materials, which exhibit greater temperature sensitivity, should have a greater degree of intermolecular cooperativity.[36] Plots of the time-temperature shift factor versus the T_g normalized temperature (T_g/T), called fragility plots, are used to quantify the fragility. These plots have also been referred to as "cooperativity" plots.[43] Fragility (*m*) is the slope of the line at $T = T_g$ (equation 2.6). This parameter *m* is proportional to the apparent activation energies normalized by the T_g (equation 2.7).[39] A higher *m* value indicates a more fragile material.

$$m = d\log\langle\tau\rangle/d(T_g/T) \text{ at } T = T_g \quad (2.6)$$

$$m = \Delta E/2.303RT_g \quad (2.7)$$

Another measure of cooperativity is the degree of non-exponentiality of the relaxation behavior in the transition regions. The non-exponentiality can be described by the Kolrausch-Williams-Watts (KWW) equation (equation 2.8). In the KWW equation τ is the most probable relaxation time and β is related to the distribution of relaxation times.[39] In the limit where $\beta = 1$ there is only 1 relaxation time that governs relaxation behavior, called a Debye-type relaxation.[36] A decrease in β from 1 represents a broader distribution of relaxation times. This broadening in the relaxation time spectrum occurs because the relaxation times (activation energies) of larger domains have a greater temperature dependence than those of the smaller domains.[37] The coupling parameter n can be determined from the KWW exponent β ($\beta = 1-n$). This coupling parameter indicates the strength of intermolecular cooperative rearrangements.[36] The higher the coupling parameter the broader the relaxation spectrum.

$$\phi(t) = \exp[-(t/\tau)^{\beta}] \qquad (2.8)$$

In a study on poly(vinylethylene) [96 % poly(1,2-butadiene)] networks Roland has shown the relationship between crosslink density and intermolecular cooperativity. In isolated chains, skeletal bond rotation is only dependent on the cooperative rotation of neighboring segments on the same chain. However, in a dense phase the segmental motion can be dependent on interactions with non-bonded neighboring segments of different chains. Roland[44] noticed a broadening in the transition associated with segmental relaxation with an increase in crosslink density. This broadening is most likely the result of the segments close to the crosslink points having more retarded motion. This phenomenon has been called inhomogeneous broadening. The effects of crosslink density on intermolecular cooperativity were investigated through both cooperativity (fragility) plots and determination of the coupling parameter (n) from the KWW equation (β = 1-n). Networks with higher crosslink densities showed higher temperature sensitivities, or fragilities, which were determined from a semi-log plot of the relaxation time versus the T_g normalized temperature. This suggests that segmental relaxation in more highly crosslinked systems "is associated with stronger intermolecular coupling."[44] These results were confirmed by the increase in both the T_g and the coupling parameter, n, with an increase in crosslink density. The increase in n represents a broader distribution of relaxation times.[44]

In a study of the fragility of different liquids Angell noted "some peculiarities associated with hydrogen bonding liquids."[45] Although their heat capacity changes at T_g were higher than that of fragile liquids, monomeric alcohols have intermediate fragilities. The normal trend for glass forming liquids is that materials with the largest changes in heat capacity at T_g are also the most fragile. Angell suggested that the very large jump in heat capacities was a result of the additional energy required to rupture one or more hydrogen bonds between molecular units.[45] In a study of a series of disubstituted benzenes with varied potential for hydrogen bonding, Angell noted that the most strongly hydrogen bonded liquids were the most fragile, although the differences were small.[46] This same trend was noted by Bohmer et al..[47] He stated that fragile glass formers tended to have non-directional interatomic/intermolecular bonds, whereas the strong liquids were

typically the non-hydrogen bonded networks. These authors demonstrated that polymers such as polyethylene and polytetrahydrofuran that had very weak intermolecular interactions had very small *m* values corresponding to low fragilities. Additionally, Roland and Ngai[43] stated that less polar polymers tended to have lower fragilities. Therefore, based on these results it can be concluded that secondary bonding can increase the fragility of polymers.

Bohmer et al. have extensively shown correlations between fragility (the departure from Arrhenius behavior), and the KWW exponent β (indicating the departure from exponential relaxation), although these are determined from different methods and represent different properties. They presented data on fragilities and non-exponentialities from more than 70 glass formers over a broad range of T_g's from 3.6 to 1500K. A clear linear inverse relation between *m* and β is evident. The correlation is strongest when comparing somewhat similar materials such as only polymers, as opposed to comparing polymers to low molecular weight glass formers (Figure 2.26). This figure is based on the data presented by Bohmer et al. giving *m* and β for many polymers. The correlation weakens when the polymers are compared with simple or complex small molecules. [47]

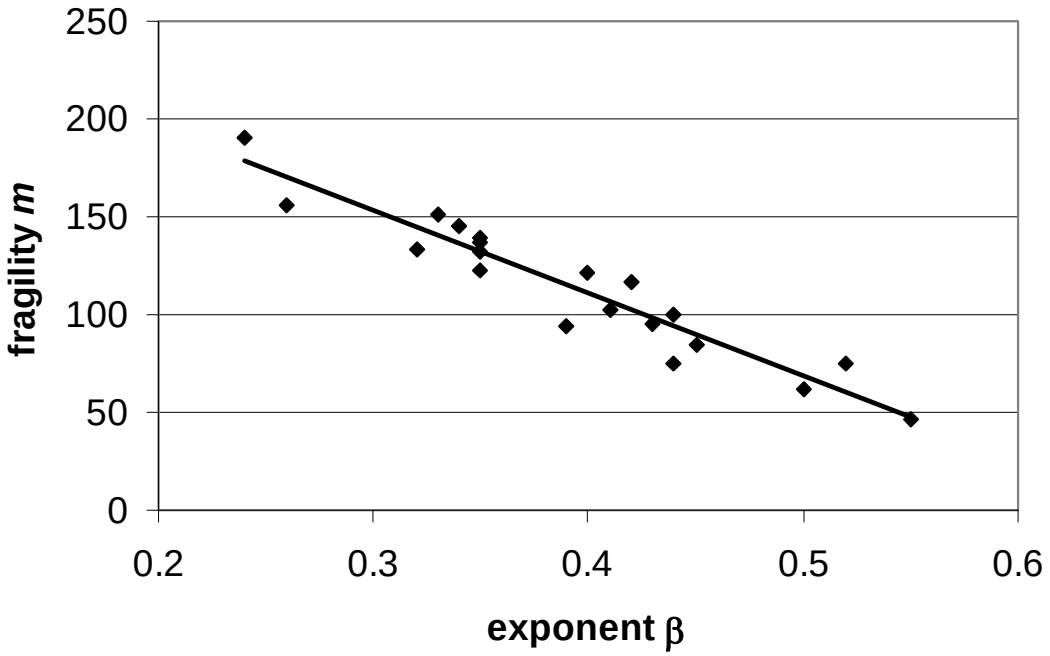

Figure 2.26: Correlation of *m* and β of different glass forming polymers.

2.3.4 Cone Calorimetry

The cone calorimeter is an instrument for fire testing for which the data correlates well with large scale fire testing. The heat release rates of materials can be determined in order to suggest their potential contributions to a room fire. Along with the heat release rates, the cone calorimeter is capable of measuring ignitability, total heat released, effective heat of combustion, specific extinction area (a measure of the smoke production), soot yield, mass loss rate, and the evolution of carbon monoxide, carbon dioxide, and other combustion products. The results obtained from the cone calorimeter can be used to correlate or predict the behavior of materials in a full-scale fire. Development of the cone calorimeter was based on the oxygen consumption principle where the total mass flow of oxygen in the combustion products is compared to the initial inflow (equation 2.9).[48]

$$q = (\Delta h_c / r_o)(m_{O2,\infty} - m_{O2}) \quad (2.9)$$

q = heat rate (kW)

Δh_c = net heat of combustion (kJ/kg)

r_0 = stoichiometric oxygen to fuel mass ratio

$m_{O2,\infty}$ = initial mass flow of oxygen(kg/s)

m_{O2} = total mass flow of oxygen in combustion products (kg/s)

For most organic materials the heat of combustion per unit mass oxygen consumed is assumed to be relatively constant at ~13.1 MJ/kg.[2] One primary advantage of this principle is that the instrument does not need to be thermally insulated, allowing for design of an accurate yet simple instrument (Figure 2.27). Samples can be tested in a horizontal or vertical orientation and can be irradiated with a heat flux up to 100 kW/m^2 with good uniformity.[48] The only limitations besides the size and shape requirements are that the sample should not swell sufficiently to interfere with the spark plug operation or the heater, and the specimens should not show explosive spalling or delamination. Samples that melt and flow upon heating must be tested in the horizontal orientation.[48]

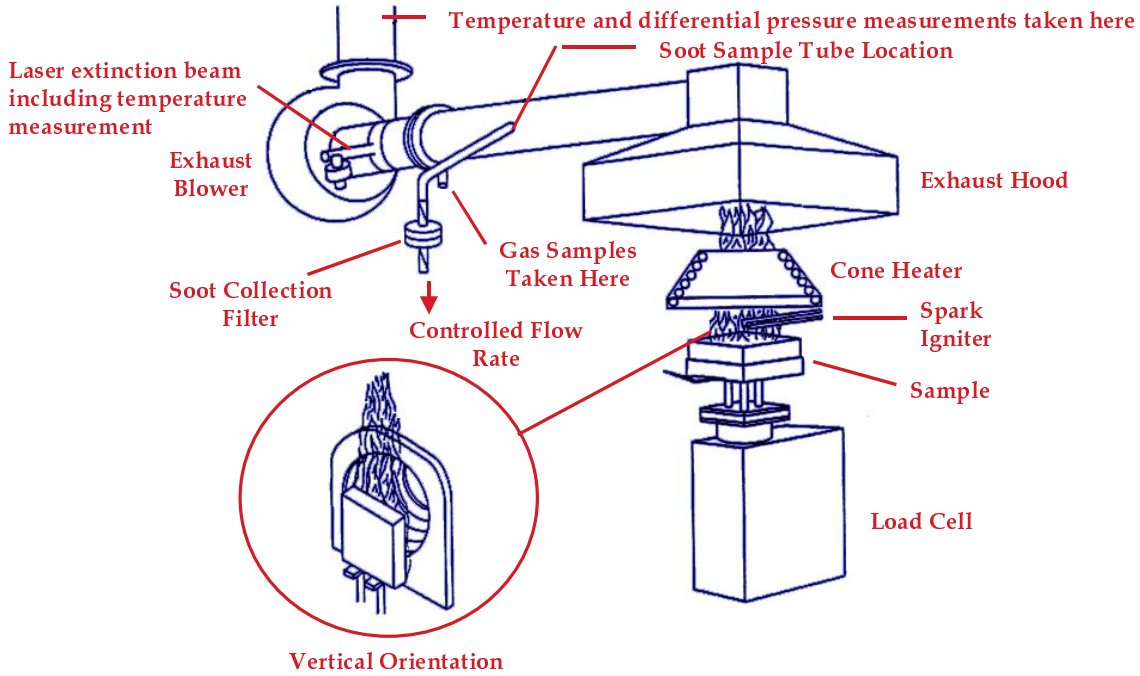

Figure 2.27: Schematic of a cone calorimeter

One of the most useful measurements obtained from cone calorimetry is the heat release rate of the burning materials.[2] Most materials show a single maximum in the heat release rate curves that is denoted the peak heat release rate (PHRR). However, in some char forming materials more than one peak is evident. There may be an initial peak then a decrease in heat release rate followed by a second peak (Figure 2.28). Babrauskas suggested that after the first peak, the rate of heat release drops due to the formation of an insulating char layer. He further suggested that the second peak results from the specimen being "heated through to the rear face and no longer behaves as if thermally thick."[48] The majority of heat is released during the second peak stage. Although they do not have evidence to prove that the two peaks are a result of a protective char layer being formed, this seems like a reasonable explanation for their results. However, another possibility is that this initial peak, or spike, in the heat release rate may be a result of the rapid burning of volatiles that build up prior to ignition. However, since this peak is usually only seen for the char forming materials, it is possible that both of these factors are important. In non-char forming materials the initial spike from burning of volatiles may be masked by the intense burning of the combustible material.

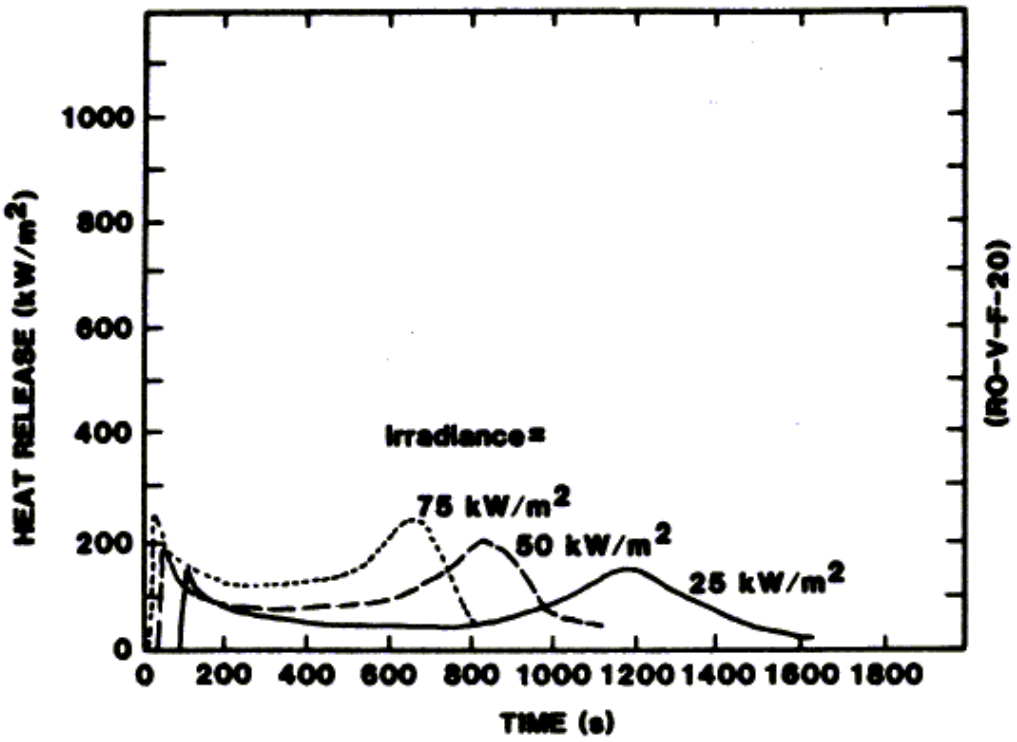

Figure 2.28: HRR curves of char forming materials[48]

Goff[49] investigated the behavior of different types of polymers with cone calorimetry. After testing several different types of polymers including poly(ether imide) (PEI), poly(ether sulfone) (PES), polyvinylchloride (PVC), polycarbonate (PC), polybutylene terephthalate (PBT), polyphenylene oxide (PPO), polystyrene (PS), polyethylene (PE), polypropylene (PP), and high impact polystyrene (HIPS), properties such as ignition delay times, critical heat flux, heat release and mass were analyzed. Ignition time was dependent on the production of fuel that was determined by the chemical composition and the degradation mechanisms of the polymer. The trend of ignition delay times for a series of polymers tested at 30kW/m^2 was as follows: PEI and PES > PVC > PC > PBT > PPO and HIPS.[49] Polymers with a high aromatic content showed longer ignition delay times (IDT's) possibly due to their ability to form a protective char layer. Polymers which were more susceptible to chain cleavage (degradation) showed shorter IDT's, and

polymers capable of depolymerization had the shortest IDT's. These ignition studies were consistent with the results of heat release rates and mass retention. Materials that crosslinked further with heat or with high aromatic contents had lower peak heat release rates and higher mass retentions, or char yields).[49] It seems likely that the formation of a protective char layer greatly increases the flame retardance. However, the only evidence of this protective char layer is the high mass retention and the two peaks in the heat release rate curves.

The main criticism of the cone calorimeter has been that the oxygen level is not representative of a true fire in the later stages of burning.[50] Christy et al. suggests that "the cone simultaneously simulates the heat scenario of a fully developed fire while resembling the oxygen availability of an early stage, developing fire."[50] In order to solve this problem a controlled atmosphere cone calorimeter was developed which is capable of varying both the oxygen concentration and the rate of ventilation during the burning to more accurately simulate fully developed fires.

Christy et al. used the controlled atmosphere cone calorimeter to investigate the burning of three different materials, a polymethylmethacrylate and two polyisocyanurate rigid foams formed by different methods.[50] The results indicated that the peak rate of heat release and the ratio CO_2/CO decreased with decreasing oxygen concentration. The maximum smoke production was observed at 18% oxygen, and there was no correlation between the effective heat of combustion on the oxygen concentration. In addition, for the PMMA (a material with very low char), the mass loss rate decreased linearly with oxygen concentration in the combustion gas. Similarly, for the polyisocyanurate foams (char forming materials), the char yields increased with decreasing oxygen levels.[50] Based on these results Christy et al. concluded that the controlled atmosphere cone calorimeter "can model well ventilated, fully developed fires, which the standard cone calorimeter cannot."[50]

2.4 Polymeric Composites

2.4.1 Introduction

Fiber reinforced polymeric composites are typically lightweight, stiff materials which may be effective alternatives to steel and concrete. The aerospace industry has shown interest in advanced composites for their high strength to weight ratios.[51] These composites typically have three main components, fiber, matrix resin, and usually a sizing material on the fiber (Figure 2.29). The role of the matrix resin is to transfer load to the fibers as well as to protect the brittle fibers.[52] The matrix resin can be a tough, ductile thermoplastic polymer, or a more brittle thermoset. Some typical thermoplastic matrix materials are poly(ether ether ketone) (PEEK), poly(ethylene terephthalate), LaRC TPI™, and poly(phenylene sulfide) (PPS).[52] Thermoplastics typically require high temperatures or solvents for processing. Some common thermosetting matrix materials are epoxies, phenolics, unsaturated polyesters and vinyl esters. These materials can usually be processed from low viscosity oligomers at reasonable temperatures in the melt. Their networks are brittle due to the high crosslink density. However, they provide dimensional stability at high temperatures. The fibers impart high modulus and stiffness to the composite. Carbon fibers can be derived from pyrolysis of poly(acrylonitrile). Other common fibers include ceramics, E-glass, aramids such as Kevlar and high molecular weight polyethylene (Spectra™).[52] A third component is the fiber sizing. Fiber sizings are typically used to hold the fiber tows together to allow for processing without significant fraying of the toe. Some authors have shown that the correct choice of sizing agent may also improve the composite properties by improving the fiber matrix adhesion. In cases were there is a poor interface between the fibers and the matrix resin a sizing can be employed to improve this interface region. The effects of the sizing and interface on the composite properties will be discussed in the following paragraphs.

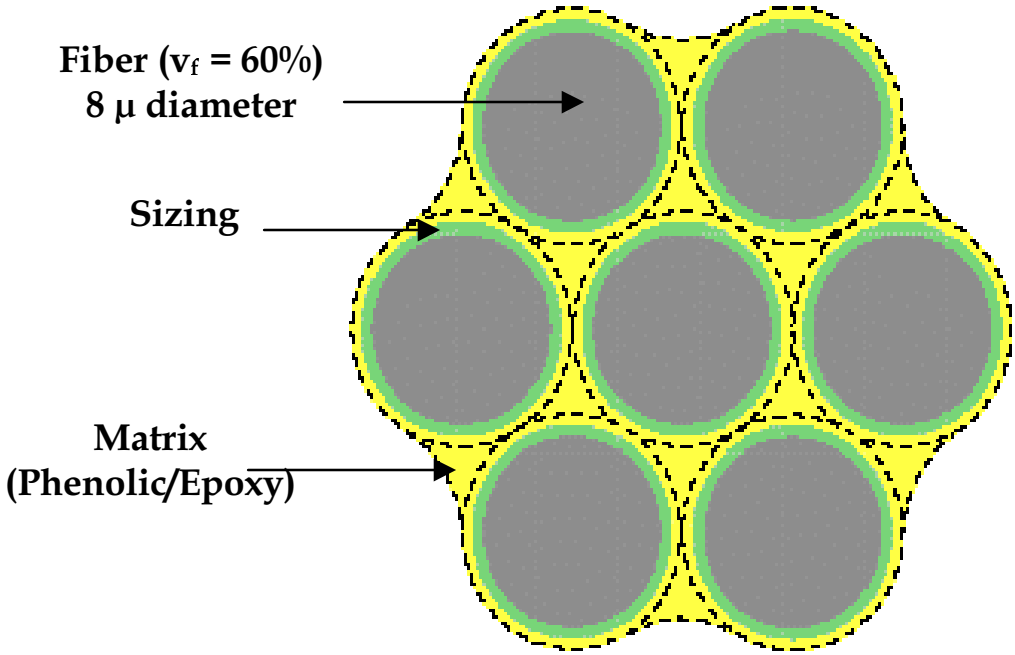

Figure 2.29: **Depiction of a carbon fiber composite with hexagonal packing (the interphase region is assumed to be 0.5μ in thickness).**

2.4.2 Fiber sizings

In 1985, Lehmann et al. investigated the effects of carbon fiber surface treatments on composite performance.[53] They discovered that improved composite properties could be achieved when there was a compromise between the fiber dominated and the resin dominated properties. Lehmann et al. found that composite properties such as flexural strength and short beam shear strength were dependent on the surface treatment. Composites prepared from fibers with no surface treatment showed the lowest strengths. A maximum in strength occurred at one times the normal amount of the proprietary surface treatment and a slight decrease was evident with significantly higher levels of surface treatment on the fiber. SEM results indicated that the fiber surface treatments could increase fiber matrix adhesion. They also found that the desirable surface treatment levels were dependent on the type of matrix resin, and that adhesion was dependent on both the type of matrix resin and the type of sizing.[53]

The effect of the interphase region was further investigated by Lesko et al. in 1994.[54] They investigated the effects of two types of sizing materials, poly(N-vinylpyrrolidone) (PVP) and Bisphenol-A based epoxy, on the interphase regions and composite mechanical properties while maintaining identical fiber, matrix, and processing conditions. SEM micrographs, enhanced by a permanganate etchant, illustrated differences in the interphase region between the two types of sizings (Figure 2.30).[54] The PVP sizing showed a distinct polymer layer surrounding the fiber of about 0.2 μm, illustrated by the gap where the sizing had been removed by the etchant. In addition, the morphology around the gap suggested diffusion of the sizing into the matrix resin, with a thickness of 0.3 μm. These distinct regions were not as evident in the SEM of the fibers with the epoxy sizing (Figure 2.30). Meso-indentation tests showed no significant difference in the interphase strength between the two sizing materials. However, the PVP sizing yielded a more ductile interface. In addition, the 90° flexural strength was not statistically different between the two materials. However, both the static compressive strength and strain to failure were higher for the composite with the PVP sizing material. In addition the fatigue life of the composite with the PVP sizing was two orders of magnitude higher than that of the composite with the epoxy sizing.[54] From further studies with these same systems it was shown that the composite with the PVP sizing showed higher tensile strengths and strains to failure.[51] Therefore, it was concluded that the type of sizing agent and resultant interphase morphology affected some composite mechanical properties.

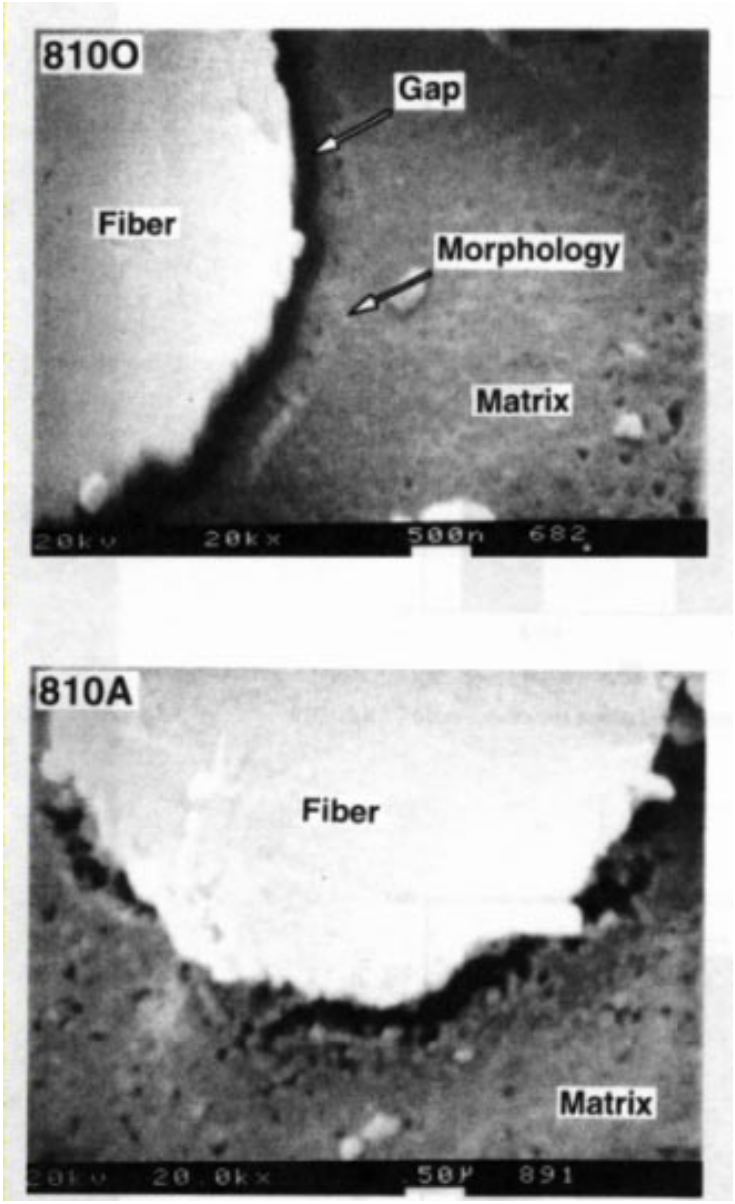

Figure 2.30: Effects of sizing on morphology of interphase regions[54]

Based on these interphase studies it was of interest to develop a method to better control the application of the sizing materials to the carbon fibers. In the earlier work the fibers were obtained with a pre-determined sizing already on the fiber. Broyles et al. developed a sizing apparatus to coat carbon fibers with a controlled amount of sizing material from aqueous water-dispersible polymeric sizing materials (Figure 2.31).[52] Using this apparatus, the amount of deposited polymer could be controlled over a range of 0.1 to 1.4

wt %, by controlling the concentration of the sizing bath. The weight percent sizing was a linear function of the bath concentration of PVP with a slope of 2/3.[52] Therefore, the amount of sizing on the fiber could be controlled using this process to allow for a more accurate study of the effects of sizing agents on composite properties.

Later Broyles et al. investigated the interphases in carbon fiber-vinyl ester composites using the above sizing process.[55] This allowed for depositing a controlled amount of sizing on the fiber and controlling drying/heating conditions to achieve a good sizing. Pyrolysis was used to determine the weight percent sizing on the fiber. Sizing solutions of 1.0 wt % were employed to achieve sizing levels of 0.6-0.7 wt % on the fiber depending on the type of sizing. Vinylester composites of these sized fibers were processed using resin-film infusion (RFI). Mechanical properties of composites with two different types of sizing materials, poly(vinylpyrrolidone) and a polyhydroxyether of bisphenol A, were compared to the properties of composites from unsized fibers. Broyles et al. found no significant effect of the sizing on shear strength or flexural strength of the composites. However, the flexural moduli of the composites containing the sized fibers were significantly higher than those of the composites from the unsized fibers.[55] The authors suggested that the increased flexural moduli using sized fibers were a result of improved fiber/matrix adhesion. Investigation of the fatigue limits of the different composites showed a dependence on the presence and type of sizing material. Composites from both types of sized fibers had improved fatigue limits over composites from the unsized fiber. In addition, the tough thermoplastic polyhydroxyether sizing resulted in composites with significantly higher fatigue limits than the brittle PVP sizing.[55]

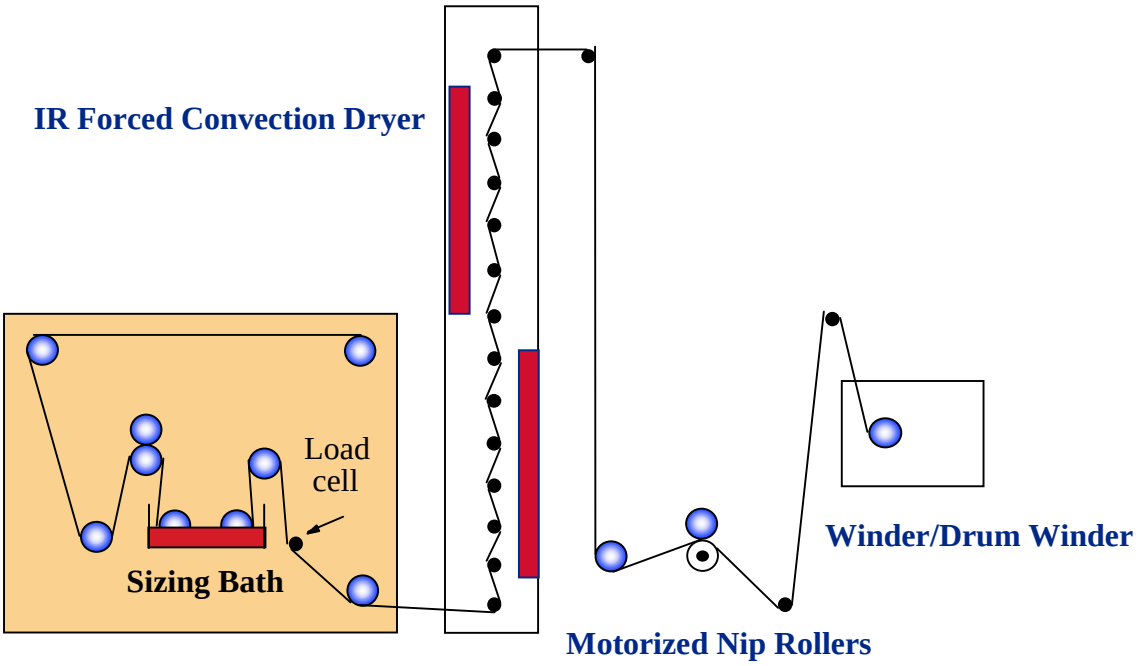

Figure 2.31: Schematic of the sizing process[52]

2.4.3 Composite Toughness

Interlaminar fracture toughness in unidirectional carbon fiber composites provides a measure of the properties of the matrix resin, fiber matrix adhesion, and interphase effects. Mode I interlaminar fracture toughness can be measured using double cantilevered beam (DCB) specimens with a sharp crack at the interlaminar surface (Figure 2.32).[56] According to the ASTM standard there are three methods of calculating the mode I interlaminar fracture toughness (G_{1c}): A modified beam theory, a compliance calibration method, and a modified compliance calibration method.[57] There is very little variation in the results between calculations from the three different methods. However, the modified beam theory is recommended because it yields the most conservative results. This method includes a correction factor for the crack length to account for any rotation at the delamination front if the beam is not perfectly built in. If the correction factor is ignored the calculations will usually overestimate G_1. This modified beam theory method employs the following equation:

$$G_1 = 3P\delta/[2b(a+\Delta) \qquad (2.10)$$

where P is the load, δ is the load point displacement, b is the specimen width, a is the delamination length, and Δ is the correction factor for the delamination length.[57] Mode II toughness is typically measured using end notched flexure specimens (ENF) in a three point bend loading geometry (Figure 2.33).[56] Several different methods have been proposed to calculate the mode II toughness from the ENF test. Detailed explanations of these can be found in the protocol for a joint round robin (EFG/ASTM/JIS) by P. Davis.[58]

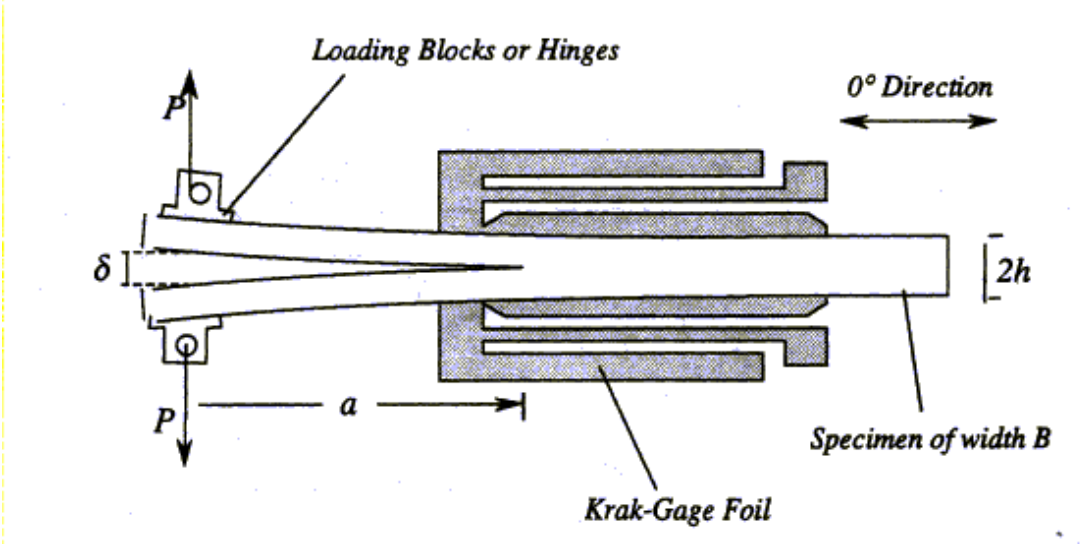

Figure 2.32: Double-cantilever beam configruation[56]

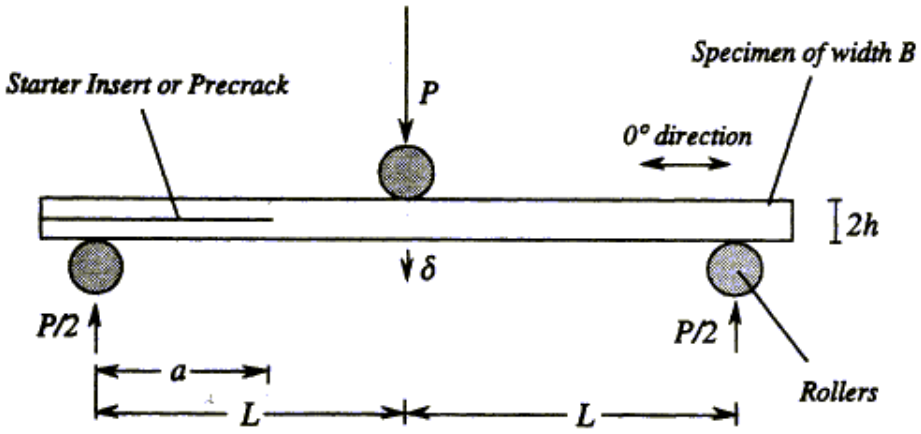

Figure 2.33: End-notched flexural configuration[56]

Fracture toughness of carbon fiber reinforced epoxy composites, both toughened and untoughened has been investigated previously. The highest numbers found in the literature for mode I and II toughness of carbon fiber epoxy composites are 390 +/- 30 J/m^2 and 1150 +/- 130 J/m^2 respectively.[59] These results are for a composite with AS-4c sized fibers with Epon 828 (a bisphenol-A based epoxy from Shell chemical) cured with m-phenylene diamine as the epoxy component.[59] Several other authors have reported significantly lower toughness for carbon fiber/epoxy composites. Asp measured the mode I and II toughness of carbon fiber/ epoxy composites from prepreg obtained from Ciba-Geigy (toughened HTA/6376c carbon/epoxy prepreg).[60] The mode I toughness was 219 +/- 30 J/m^2 and the Mode II toughness was 883 +/- 117 J/m^2 tested at 20°C.[60] Truss et al. measured mode I toughness of similar carbon fiber epoxy composites (HTA fibers with 913 resin - prepreg was obtained from Ciba Geigy).[61] Their results of mode I toughness were consistent with Asp's results, G_{1c} = ~250 J/m^2.[61] Woo and Mao studied the effect of adding interlaminar toughening agents, applied as powders, in the interlaminar regions between the 8^{th} and 9^{th} plies, on the mode I and II interlaminar fracture toughness.[62] They used prepreg obtained from Fiberite (HYE-1076), which contained T300 carbon fibers with epoxy resin from tetraglycidyl-4,4'-diaminodiphenylmethane (TGDDM) with diaminodiphenyl sulfone (DDS) as the amine hardener. The mode I and II toughness values were 165 and 290 J/m^2 respectively. Significant toughening was obtained using polyetherimide (PEI) and polyhydroxyether (phenoxy) toughening agents in the interlaminar region. The PEI toughened composites had mode I and II toughness values of 420 and 910 J/m^2, and the phenoxy toughened composites had mode I and II toughness values of 440 and 640 J/m^2 respectively. However, the addition of polycarbonate (PC) at the interlaminar region showed a decrease in mode I and II toughness. Woo and Mao suggested that the decrease in toughness may be a result of crystallinity in the PC particulate.[62] These results indicate that addition of a tough, ductile, non-crystalline thermoplastic polymer in the interlaminar region can greatly increase the interlaminar fracture toughness.

3 Structure-Property Relationships

3.1 Introduction

One objective in developing a tough, void-free flame retardant matrix material for composite applications was to gain a thorough understanding of the structure property relationships of these networks. The two main variables in this system are the ratio of phenolic component to epoxy, and the structure of the epoxy. The goal was to control the ratio of phenol to epoxy to obtain networks, which possessed both toughness and flame retardance. By increasing the phenolic component and decreasing the epoxy, the crosslink density was decreased significantly. Therefore by controlling the molar ratio of phenol to epoxy the crosslink density could be controlled to improve mechanical properties. In addition, increasing the phenolic component increased the flame retardance due to its high aromatic content.[63,64,65]

The effects of crosslink density were investigated by determining the molecular weights between crosslinks of a series of phenolic-epoxy networks with different ratios of phenol to epoxy. Relaxation tests were performed to understand the effects of the phenolic/epoxy ratio on the moduli in the temperature range from well below the T_g to well above the T_g. Cooperativity analysis was performed on three networks with different phenolic/epoxy ratios in order to gain an understanding of the behavior of these networks through the transition region, and possibly gain a better understanding of the non-equilibrium glassy state. Fracture toughness, T_g's, flame retardance and moisture uptake were also investigated as a function of the crosslink density. One would expect an increase in toughness, moisture uptake and flame retardance, and a decrease in Tg, with decreased crosslink densities of these networks. The increased moisture uptake is expected because as the crosslink density is decreased there remains a higher concentration of unreacted phenolic hydroxyl groups which can promote increased hydrogen bonding. Increased flame retardance with increased phenolic content was expected due to the excellent flame retardance of the pure phenolic networks.

In addition to varying the crosslink densities, a series of difunctional epoxies with different structures were investigated in order to achieve networks with desirable

properties. The structure of the epoxy component could be varied depending on what properties were desirable such as: increased flame retardance, increased T_g, decreased moisture uptake, decreased melt viscosity, etc.. A brominated bisphenol-A based epoxy was investigated because it is known to have improved flame retardance. A siloxane epoxy was investigated in hopes of increasing flame retardance and lowering viscosity. A fluorinated epoxy was investigated in hopes of obtaining networks with decreased moisture uptake. A stilbene epoxy was investigated with hopes of creating networks with an increased T_g. This work describes the effects of both changing the ratio of phenol to epoxy and changing the structure of the epoxy on the properties of these networks.

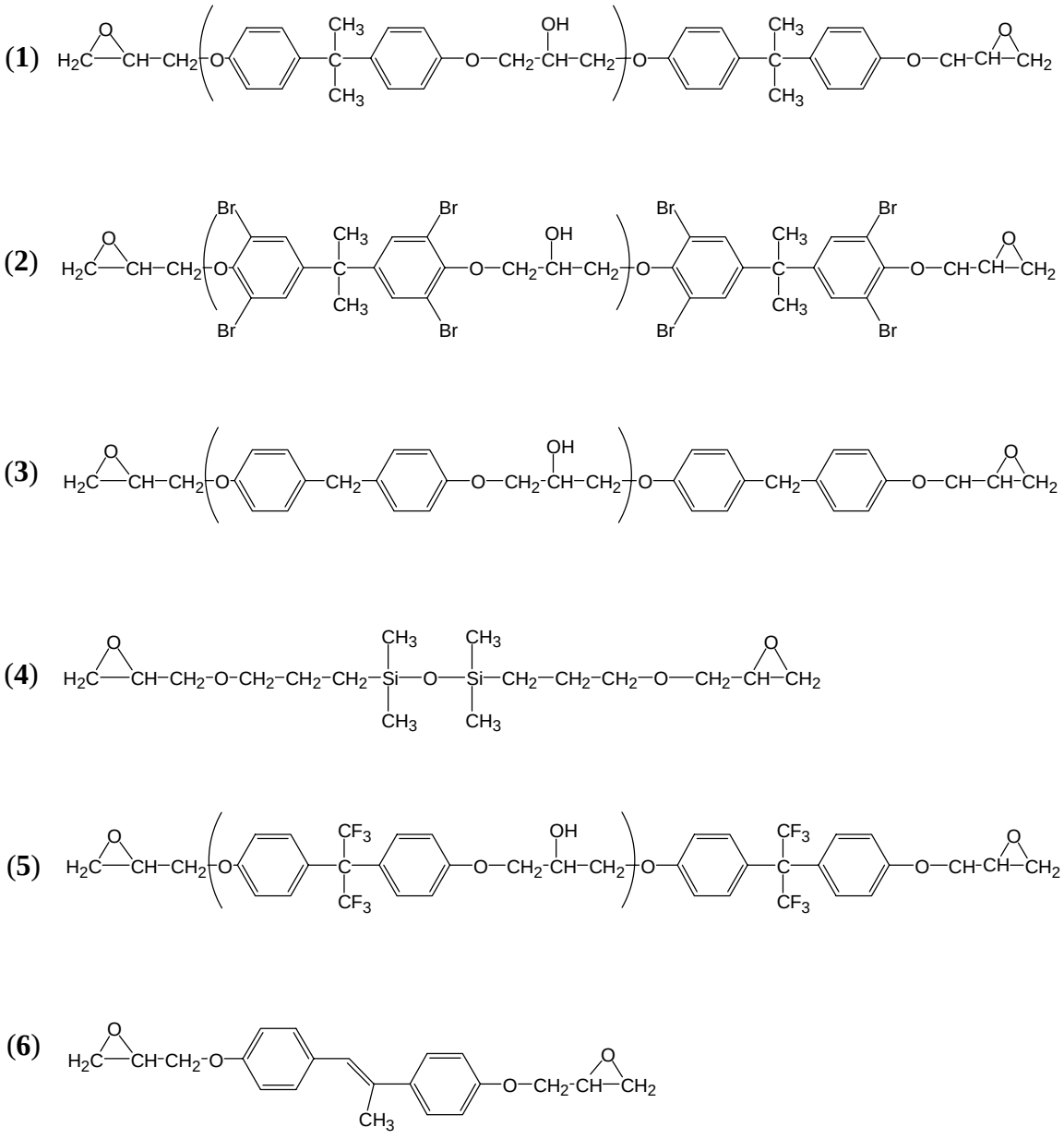

Figure 3.1: **Epoxy resin structures (bisphenol-A based epoxy (1), brominated bisphenol-A based epoxy (2), bisphenol-F based epoxy (3), siloxane epoxy (4), hexafluorobisphenol-A based epoxy (5) and stilbene epoxy (6)).**

3.2 Experimental

3.2.1 Materials

Commercial phenolic resins were provided by Georgia-Pacific (Product # GP-2073). The phenolic resin had a molecular weight of ~741g/mol. Epon 828 epoxy resin (**1**) was obtained from Shell Chemical. XUR-1544-55284-35 epoxy (**2**), DER 354 epoxy (**3**), and XUR-YM-1999-25711 epoxy (**6**) were obtained from Dow Chemical Co. (Figure 3.1). Triphenylphosphine (TPP) was obtained from Aldrich and used as received. 1,1,3,3-Tetramethyldisiloxane was obtained from United Chemical Technologies, Inc. and used as received. Allyl glycidyl ether, epichlorohydrin and hydrogen hexachloroplatinate(IV) hydrate were obtained from Aldrich and used as received. Hexafluorobisphenol-A was obtained from Riedel-dettaen and used as received. Potassium hydroxide (KOH) was obtained from Mallinckrodt and used as received.

3.2.2 Synthesis and Sample Preparation

3.2.2.1 *Synthesis of 1,3-Bis(3-glycidoxypropyl)tetramethyldisiloxane (4)*[66]

To a 250 ml 3-neck flask equipped with a dropping funnel, nitrogen inlet, thermocouple, and magnetic stirrer, was added allyl glycidyl ether (87.56 g) and hydrogen hexachloroplatinate(IV) hydrate (0.0083 g). This solution was stirred at 25°C for 45 minutes to activate the catalyst. Tetramethyldisiloxane (39.58 g) was added to the dropping funnel. After 45 minutes a few drops were added to the allyl glycidyl ether/catalyst solution. This was stirred at 25-30°C until a temperature increase of ~ 5°C due to the reaction exotherm was observed. At this point the tetramethyldisiloxane was added dropwise in order to control the exotherm to less than 45°C. After all the siloxane was added, the solution was allowed to cool to room temperature. The remaining allyl glycidyl ether was vacuum stripped at 60°C and 2 torr pressure. The epoxy was then vacuum distilled at 200°C and 2 torr pressure.(Figure 3.2)

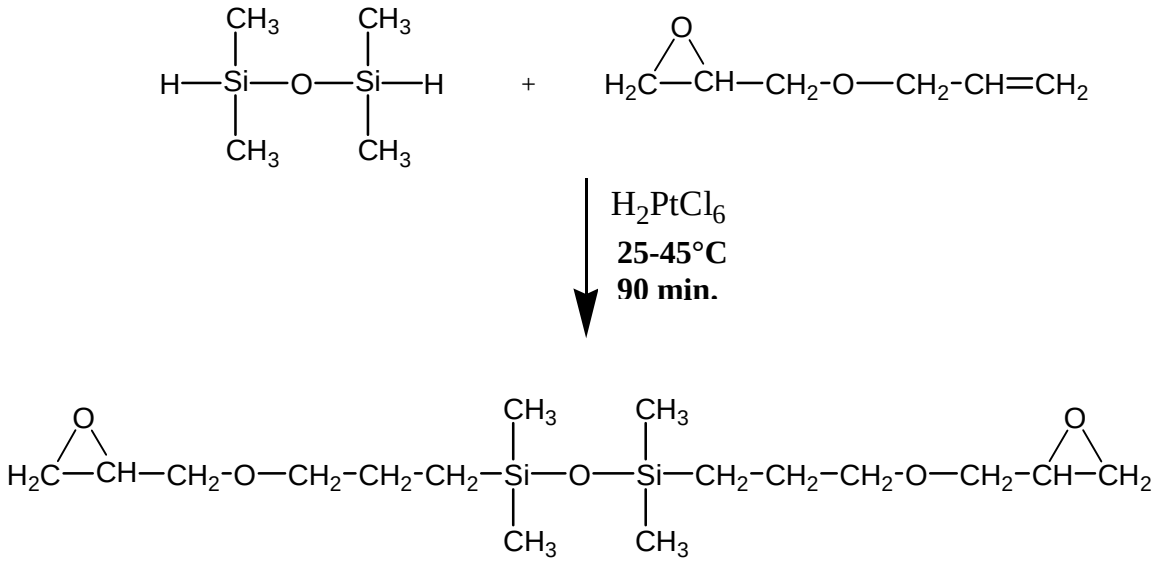

Figure 3.2: Synthesis of a siloxane based epoxy (4)

3.2.2.2 Synthesis of a Tetrafunctional Siloxane Epoxy

To a 250 ml 3-neck flask equipped with a dropping funnel, nitrogen inlet, thermocouple, and magnetic stirrer, was added allyl glycidyl ether (25.0 g) and platinum-divinyltetramethyldisiloxane (0.0656 g). This solution was stirred at 25-30°C for 20 minutes to activate the catalyst. After 20 minutes, 5 wt % of the tetrakisdimethylsiloxy silane (0.5 g) was added to the 28°C solution, and an aliquot was removed for infrared (IR) analysis to observe the Si-H absorbance. The reaction was then heated to 40°C and stirred for 35 minutes and a sample was removed for IR. There was no Si-H absorbance in the IR spectrum at this point indicating that the reaction had started. The remaining tetrakisdimethylsiloxy silane was added dropwize to control the exotherm to < 55°C. After all the siloxane was added and the exotherm stopped the solution was allowed to cool to room temperature. IR was run on the solution and indicated that all the Si-H groups had been reacted. The remaining allyglycidyl ether was vacuum distilled at ~80 °C and 2 torr pressure. The epoxy was heated to 260°C in an oil bath to degrade the catalyst, then diluted with acetone. The solution was stirred with charcoal and filtered, then run through a celite column to remove the platinum. The purified sample was a bright yellow color. (Figure 3.3)

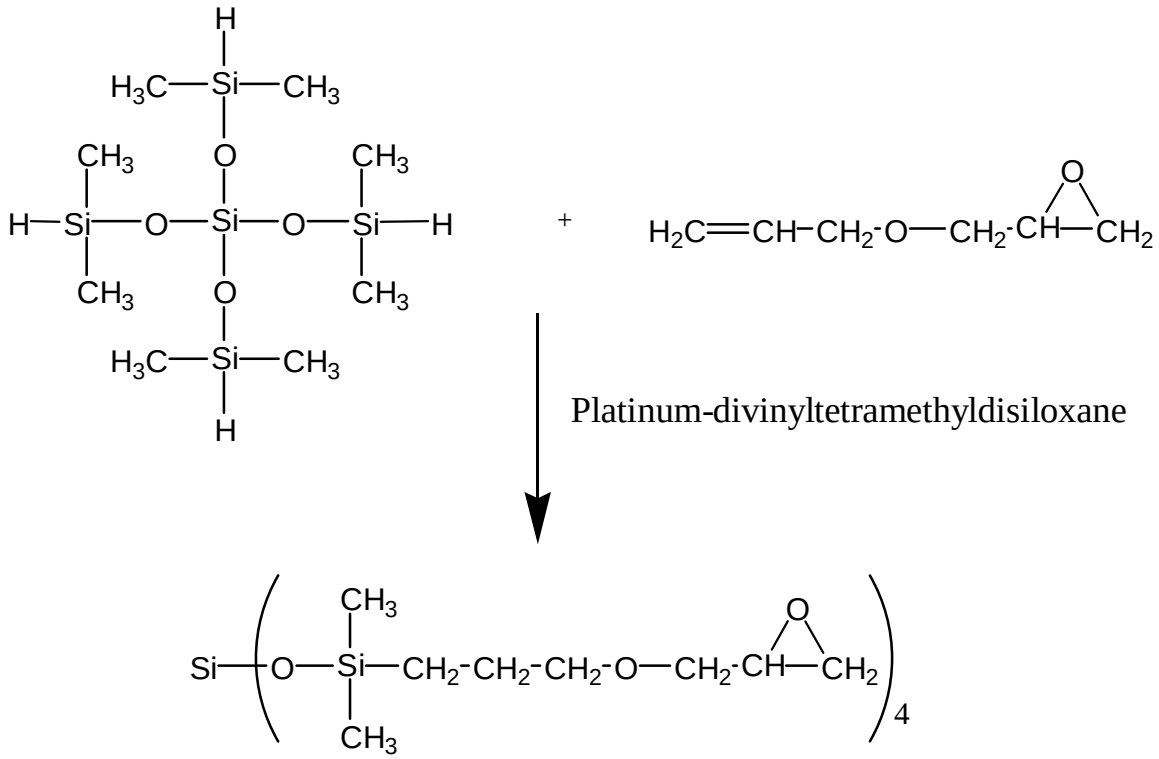

Figure 3.3: Synthesis of a tetrafunctional siloxane epoxy.

3.2.2.3 Synthesis of the Diglycidyl Ether of Hexafluorobisphenol-A (5)

To a 3000 ml 3 neck round bottom flask adapted with a dropping funnel, stir bar, and thermocouple was added hexafluorobisphenol-A (211 g, 0.63 mol), Epichlorohydrin (580 g, 6.3 mol), isopropanol (300 ml), and water (50 ml). The solution was heated to 70°C in an oil bath. A 20 % solution of KOH in water (228 ml) was added to the dropping funnel. Once the temperature inside the flask reached 70°C, the base solution was added dropwise over a period of 45 minutes, then the solution was allowed to stir for another 30 minutes. The solution was then cooled and placed in a seperatory funnel to remove the water layer. The organic layer was then poured back into the reaction flask and heated to 70°C. At this point the remaining KOH solution (114 ml) was added to the dropping funnel. The base was added dropwise over a period of about 45 minutes, then the solution was allowed to stir for and additional 30 minutes. The solution was then cooled, poured into a separatory funnel, and washed with water 4 times. The organic layer was

vacuum distilled at 115°C for about 2 hours to remove the solvent. The product was analyzed by ^{1}H NMR (Figure 3.5). Based on the calculations from ^{1}H NMR the product contained 15% chain extension.

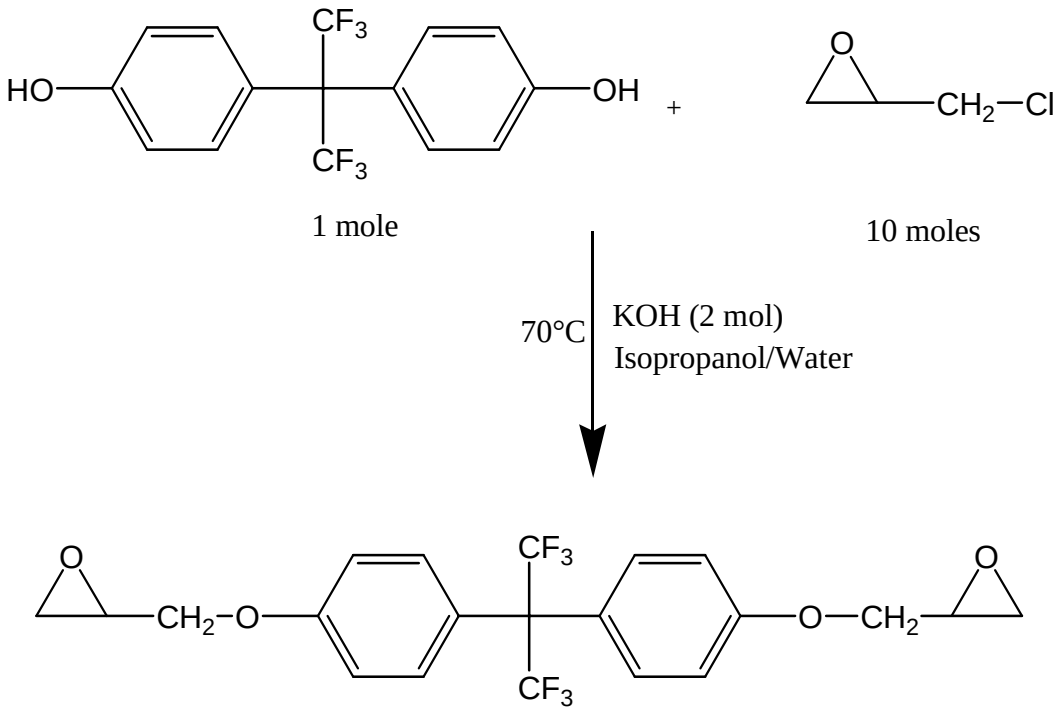

Figure 3.4: Synthesis of the diglycidylether of hexafluorobisphenol-A (5).

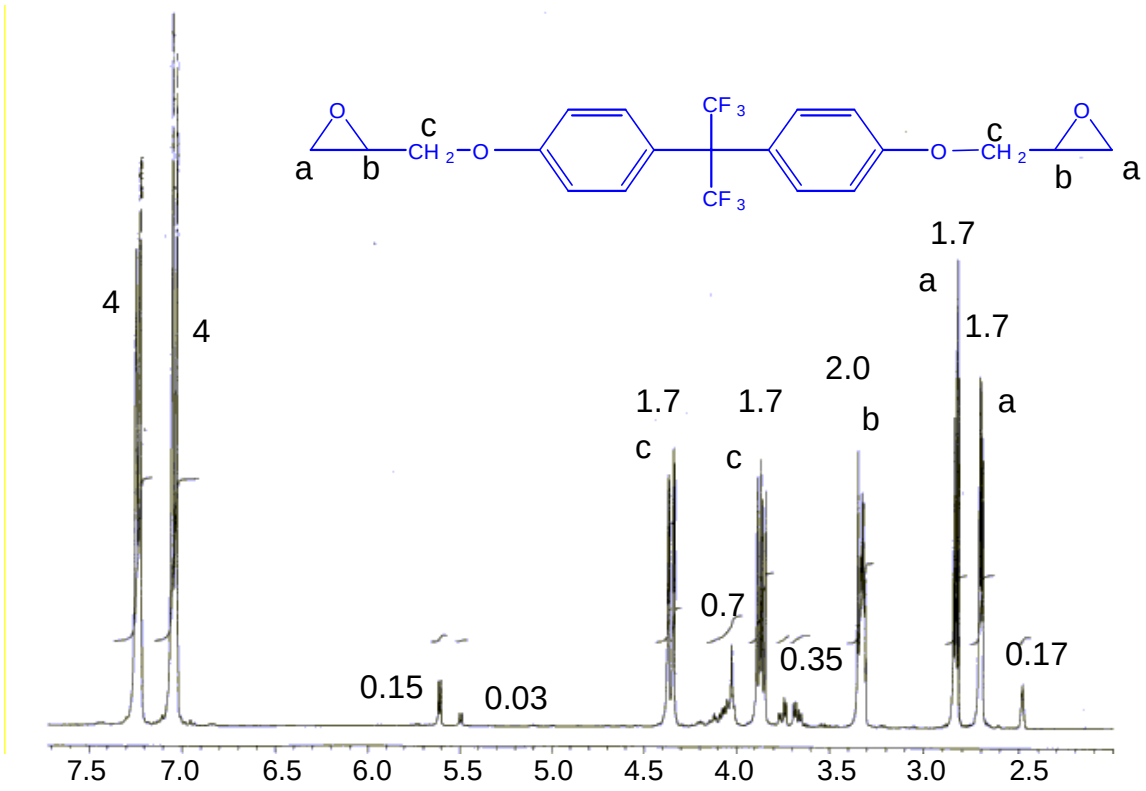

Figure 3.5: **^{1}H NMR of the hexafluorobisphenol-A based epoxy.**

3.2.2.4 Preparation of Control Epoxy Panels

Bisphenol-A based epoxy (250 g) was placed in a three neck round bottom flask equipped with a vacuum adapter and a mechanical stirrer. To this was added diaminodiphenyl sulfone as the crosslinking reagent. The mixture was stirred under vacuum at 140°C until all DDS had dissolved (~20 min). The melt was then poured into a mold and cured for 2 hours at 180°C and 2 hours at 220°C.

3.2.2.5 Preparation of a Phenolic Control[67]

"The co-resols were prepared using a total phenol-to-formaldehyde mole ratio of 1:2.5. The mole ratio of phenol to the monohydroxydiphenylalkanes and monohydroxybenzyl PAHs was 3:1 to ensure that a reasonably high degree of crosslinking was achieved in the initial resols. Sodium hydroxide was used as catalyst in the condensation reaction at a mole ratio of 0.1 with respect to phenol. Phenol, the monohydroxydiphenylalkane or mono-hydroxybenzyl PAHs, and formalin (37% v/v

formaldehyde) were mixed in a 250 cm^3 three-neck round-bottom flask and stirred until all the phenol was in solution. The mixture was then cooled in an ice-bath for about 10 minutes before sodium hydroxide (0.006 mol, 20M) was added dropwise to the reaction mixture. This was then refluxed at 70°C for 30 minutes and acidified with 85% lactic acid to a pH of 4-5 (indicated by universal indicator paper) before excess water was removed by vacuum distillation. The thick, resinous material was poured into a capped container for curing in an oven purged with nitrogen that was initially set at 70°C for 4 days. The oven temperature was then raised to 130 and 200°C for additional 24-h periods."[67]

3.2.2.6 *Solution Mixing of Epoxy and Phenolic Components with TPP*

The epoxy component (**1**, **2**, **3**, or **4**), Novolac, and triphenylphosphine (TPP) were weighed into a round bottom flask, then stirred in acetone (1/10 wt/wt polymer/solvent) until dissolved. The solvent was evaporated under nitrogen, and the sample was placed in a vacuum oven at room temperature for 24 hours. The sample was then heated above T_g at ~ 60°C for 2-3 hours. Samples prepared in this manner were used for melt viscosity measurements.

3.2.2.7 Preparation of Networks with Epoxies 1, 3, 4, 5, and 6

To a three neck round bottom flask equipped with a vacuum tight mechanical stirrer and a vacuum adapter was added phenolic Novolac and ~75% of the required epoxy. The flask was heated in an oil bath to 170°C. When the Novolac began to melt at 170°C, mechanical stirring was begun. The vacuum was applied incrementally to prevent the material from swelling into the vacuum line. Once final vacuum was achieved (2-5 Torr) the solution was stirred for about 20 minutes to degas the blend. During this time the remaining epoxy, with the initiator (0.1 to 0.5 wt % based on the total weight of epoxy) dissolved in it, was degassed in a vacuum oven at ~80°C. The stirring solution was cooled to between 130 and 150°C, depending on the viscosity of the blend being prepared, and the vacuum was temporarily released to add the remaining epoxy with initiator. This was stirred for about 4 minutes to fully degas the samples. The melt was then poured into a mold (which had been preheated to the initial cure temperature of the

material) in a preheated oven and covered with mold release cloth and a heavy metal plate. The samples with epoxy **1** and 0.1 wt % triphenylphosphine based on the weight of the epoxy were cured at 180°C for 1 hour and then 200°C for 1 hour. The samples with epoxy **3** and 0.1 wt % TPP (based on the weight of epoxy) were cured at 180°C for 1 hour, 200°C for 1 hour, and 220°C for 1 1/2 hours. The samples with epoxy **4** and 0.25 wt % TPP (based on the weight of epoxy) were cured at 200°C for 1 1/2 hours and 220°C for 2 hours. Samples with epoxies **5** and **6** were prepared with no initiator and cured for 1 hour at 200 and 4 hours at 220. The cure schedules were determined by isothermal differential scanning calorimetry (DSC) measurements of uncured samples as well as dynamic mechanical analysis (DMA) to determine T_g's of the cured samples. The samples cured by the indicated cure cycles showed no change in T_g with additional heating, indicating that the samples were fully cured. Each phenolic/epoxy system required different initiator concentrations and cure cycles based on the resin viscosities and the cure rate of the material.

3.2.2.8 *Preparation of Networks with Epoxy 2*

After samples were mixed by the solution method and dried in a vacuum oven, the solid blends were crushed to powder. The powders of each composition were placed in molds and heated to ~110°C for about 10 minutes in a vacuum oven to melt and degas the samples. The molds consisted of the appropriate shape grooves of 3.18 mm x 6.35 mm x 38.1 mm for fracture toughness bars and 10 cm x 10 cm x 6.3 mm for fire test panels; in addition, an extra 1 cm border was added around the perimeter of each mold to prevent the samples from bubbling out of the molds during the degassing process. The molds were then removed from the vacuum oven and placed in a preheated oven to cure the samples. The samples were heated at 180°C for 1 hour and 200°C for 1 hour. This method produced void free samples for fracture toughness and fire testing.

3.2.2.9 Hot-Melt Prepregging and Composite Fabrication

A lab scale Model 30 prepregger manufactured by Research Tools Corporation, Ovid, Michigan was used in composite preparation (Figure 3.6). In this apparatus, a 36K sized AS-4 carbon fiber tow was passed through a wedge-slit die at the bottom of a heated resin pot containing the matrix resin. The wetted tow was then passed between a pair of

flattening pins and around a guide roller before being wound on a drum. The flattening pins and the guide rollers were independently heated. Unidirectional carbon fiber prepregs were prepared with various phenolic/epoxy resin compositions with no initiator using the hot-melt technique. The set-point temperatures of the resin pot, flattening pin, and roller were determined by viscosity data. The set-point temperature was 120°C for the 50/50 wt/wt phenolic/epoxy and 140°C for the 70/30 wt/wt and 80/20 wt/wt phenolic/epoxy resins. These high temperatures were necessary to give a low enough melt viscosity to process the materials. Low melt viscosities of the resins were critical to permit good wet-out of the reinforcing fiber tows and yield uniform resin content. The prepregs were then cut and placed in a metal mold and cured with a thermal cycle of 230°C for 4 hours to make composite panels. This cure cycle was determined by DMA to give the highest Tg, comparable to that of the initiated materials, indicating that it was sufficient to promote complete cure of the uninitiated systems. The weight percent of fibers in the composites was 74 - 77 % fiber for the glass fabric and 74 - 79 % fiber for the carbon fiber. The fiber weight fraction of the glass fabric composites was determined by dividing the weight of the fabric by the weight of the composite. The Glass fabric had 28 yarns/inch in the warp direction, and 16 yarns/inch in the weft direction. The panels for mechanical testing were 12 ply and 6” x 6”. The fiber weight fraction of the carbon fiber composites was calculated from the measured composite densities and the densities of the fiber and cured neat networks.

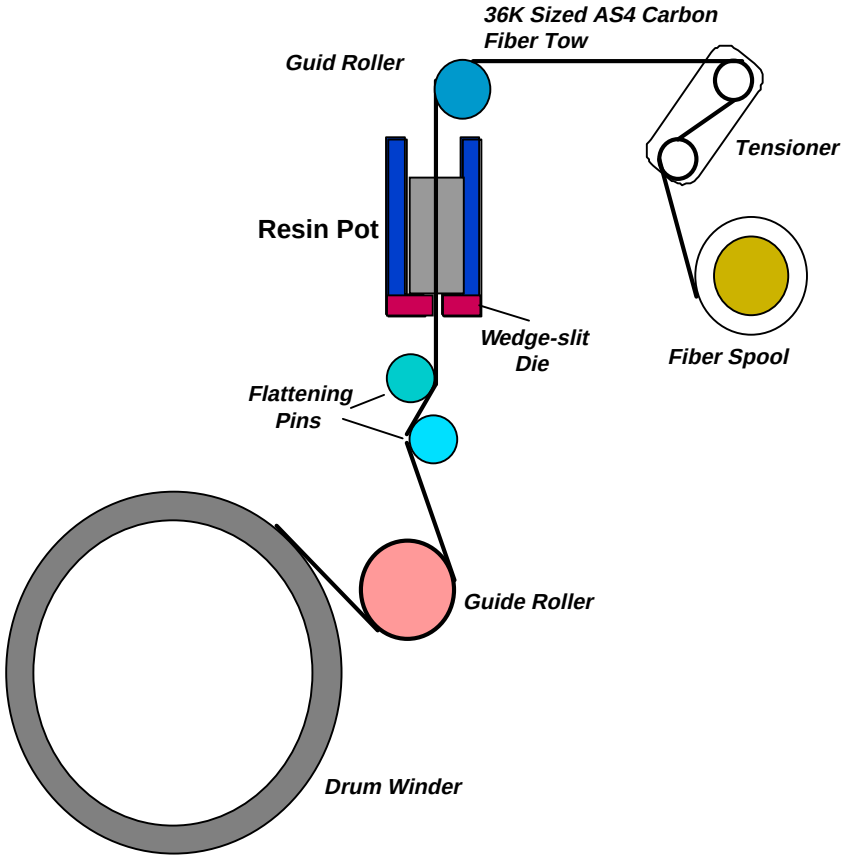

Figure 3.6: The hot melt prepregging process.

3.2.3 Measurements

3.2.3.1 Nuclear Magnetic Resonance Spectroscopy

^{1}H NMR spectra were obtained on a Varian Unity 400 spectrometer operating at 399.95 MHz. ^{1}H NMR was used to characterize the phenolic novolac obtained from Georgia Pacific, as well as the diglycidylether of hexafluorobisphenol-A.

3.2.3.2 Gel Permeation Chromatography

Gel permeation chromatography (GPC) was performed on a Waters 150-CALC/GPC chromatograph equipped with a refractive index detector and a Viscotek Model 100 differential viscometer. The mobile phase was NMP + 0.02 M P_2O_5 with a flow rate of 1 ml/min at 60°C. The columns were styragel HT with pore sizes of 10^3 and 10^4 A. The injection volume was 100 ml with a sample concentration on 6 mg/ml.

3.2.3.3 Differential Scanning Calorimetry

Differential scanning calorimetry measurements were carried out using a Perkin-Elmer differential scanning calorimeter, model DSC-7. Samples of about 10-15 mg were placed in hermetically sealed pans and cured using a dynamic temperature scan from 30 to 260°C with a heating rate of 5°C/minute. The peaks in the reaction exotherms were used to determine network cure temperatures and rates. Activation energies were obtained following ASTM E 698, with a correction for the influence of heating rate on temperature. The correction was calculated by the deviation in the melting point of indium from the accepted value of 156.60°C. The temperature calibration was performed using indium and zinc as standards.

3.2.3.4 Thermogravimetric Analysis

Thermogravimetric analyses were carried out using a Perkin-Elmer Thermogravimetric Analyzer model TGA-7. Samples of about 5 mg were placed in an aluminum pan, and heated at 10°C/min from 30°C to 600°C under nitrogen.

3.2.3.5 Dynamic Mechanical Analysis

Dynamic mechanical analyses were used to determine the glass transition temperatures. These measurements were performed using a Perkin-Elmer dynamic mechanical analyzer, model DMA-7. The T_g's were calculated from the peaks in the tan delta curves. The analyses were conducted using a 3-point bend set-up with rectangular specimens. The tests were run with tension control set at 110% using amplitude control adjusted to set the initial moduli to 1×10^9 Pa. Fully cured samples were heated at 5°C/minute from 25 to 200°C. Coefficient of thermal expansion (CTE) measurements were performed in TMA mode using the large quartz parallel plate measuring device. The static force was set at 15 mN and the samples were heated from 50 to 250°C at 10°C per minute. The CTE's below and above T_g were determined from the linear regions of the curves below and above T_g.

3.2.3.6 Creep and Relaxation Tests

Relaxation tests to determine storage moduli versus time were performed using a Dynastat calibrated using digital calipers accurate to 0.01 mm.[68] The Dynastat was

designed for materials testing: performing creep, relaxation, and dynamic tests. The oven temperature is controlled automatically, with a range of -150 to 250°C. Prior to testing, all samples were heated to 30°C above Tg for 30 minutes in the same oven at the same time, then cooled to room temperature in the oven to normalize the thermal history.

The test specimens, with dimensions of height b (3.18 mm), width w (6.35 mm), and length l (38.1 mm), were placed on two flat supports with a span of 2.54 cm, in the three point bend setup. Samples were heated to 70°C below their T_g (determined from the peak in the tan delta curve obtained by DMA). At this temperature, a constant displacement of 0.1 mm was applied to the sample (0.1 mm displacement was reached in less than 1 second). The load was recorded over a period of 1000 seconds. At this point the displacement was removed and the sample was allowed to recover for 2000 seconds (~ 35 min.). The temperature was then increased by 5°C and the cycle was repeated until the temperature had reached 35°C above the Tg. The displacement at each temperature increment was slightly greater due to the thermal expansion of the sample and the instrument. The thermal expansion of both the instrument and sample were used to calculate the corrected displacement (instrument expansion = 0.0033 mm/°C, sample = ~0.0005 mm/°C in the glassy state and ~0.00015 mm/°C in the rubbery state). The moduli were calculated from the measured load and displacement values by equation 3.1.

$$E = g(P/\Delta)(L^3/48I) \tag{3.1}$$

P/Δ = Slope of load versus displacement data

g = gravitational constant = 9.81 m/s^2

L = Length between supports = 2.54 cm

$I = (1/12)wb^3$

Creep tests, using a Dynastat, were performed to determine the rubbery moduli at 60°C above the glass transition temperatures. The samples were heated to 60°C above T_g, a small load (0.01 kg) was placed on the samples and the displacements at equilibrium were measured. Equilibrium was obtained in less than 3 seconds, indicating that the material was in the rubbery plateau region at the testing temperature of T_g + 60°C. The load was increased by increments of 0.01 kg up to about 0.08 kg and at each load the equilibrium displacement was recorded. From this data, load versus

displacement curves were generated and linear regression analysis was used to determine the slopes of the lines**.** These slopes were used to determine the moduli according to equation 3.1. The displacement values measured from the Dynastat are accurate to within 0.05 mm.

3.2.3.7 Densities and Molecular Weights Between Crosslinks

Room temperature density measurements were conducted using a Mettler-Toledo AG204 balance adapted with a Mettler-Toledo density determination kit for AT/AG and PG/PR balances. Rectangular samples with dimensions of approximately 19 mm x 6.35 mm x 3.18 mm were sanded, then polished, to prevent any trapping of air bubbles. Deionized water was degassed in the vacuum oven at 23°C for about 30 minutes prior to use. Using this setup, the weight of the solid in air (A) and the weight of the solid in water (B) were measured. The temperature of the water was recorded to within 0.1°C and the density of distilled water at that temperature was obtained from a density table. Room temperature densities were calculated according to equation 3.2 (Table 3.1).

$$\rho = \{A/(A-B)\}\rho(H_2O) \tag{3.2}$$

The densities at 60°C above T_g were calculated using the coefficients of thermal expansion below T_g and above T_g, measured by Thermal Mechanical Analysis (equation 3.3), Where α_1 is the coefficient of thermal expansion below T_g, and α_2 is the coefficient of thermal expansion above T_g.

$$\rho_{\text{room temp.}} = 1/V_1$$

$$\Delta V_1 = \alpha_1(V_1)(T_g - T_{room})$$

$$V_2 = V_1 + \Delta V_1$$

$$\Delta V_2 = \alpha_2(V_2)(T - T_g)$$

$$V_f = V_2 + \Delta V_2$$

$$\rho_{Tg\ +60°C} = 1/V_f \tag{3.3}$$

Using these densities and the rubbery elastic moduli (determined from Dynastat measurements) the molecular weights between crosslinks (M_c) were calculated by equation 3.4, where E is the rubbery moduli, R is the gas constant, T is the absolute temperature at T_g + 60°C, and ρ is the density at T_g + 60°C.

$$M_c = 3RT\rho/E' \tag{3.4}$$

Table 3.1: Densities and coefficients of thermal expansion of phenolic/epoxy networks with epoxies 1-4.

Epoxy	Phenolic / Epoxy (wt/wt)	Density (R. T.)	CTE x 3 (below Tg)	CTE x 3 (above Tg)	Density (Tg + 60°C)
1	50/50	1.215	1.48×10^{-4}	5.04×10^{-4}	1.163
1	65/35	1.230	1.78×10^{-4}	5.07×10^{-4}	1.178
1	80/20	1.240	1.73×10^{-4}	7.60×10^{-4}	1.167
2	50/50	1.490	1.40×10^{-4}	5.32×10^{-4}	1.419
2	65/35	1.411	1.36×10^{-4}	5.49×10^{-4}	1.346
3	65/35	1.247	1.68×10^{-4}	2.75×10^{-4}	1.211
3	80/20	1.249	1.10×10^{-4}	6.95×10^{-4}	1.188
4	65/35	1.183	1.51×10^{-4}	1.05×10^{-3}	1.102
4	80/20	1.213	4.53×10^{-5}	1.23×10^{-3}	1.126

3.2.3.8 Sol-Fraction Determination

Soxhlet extractions with methyl ethyl ketone (MEK) as the solvent were used to determine the sol fractions of the networks. Cellulose thimbles were soaked in MEK for 24 hours then dried in the vacuum oven at room temperature for 24 hours. They were subsequently heated to 140°C for about 12 hours. After the samples were allowed to cool to room temperature in the vacuum oven, they were weighed within 30 seconds of releasing the vacuum and the weight was recorded. Samples were extracted for 72 hours, placed in the vacuum oven at room temperature for 24 hours, then heated to 140°C under vacuum for about 12 hours and allowed to cool to room temperature under vacuum. After being removed from the vacuum oven, the thimbles containing sample were weighed within 30 seconds to prevent any significant weight gain due to moisture absorption.

3.2.3.9 *Cone Calorimetry*

Flame retardance was directly measured using cone calorimetry on void free neat panels (no fiber), as well as carbon and glass fiber composites, in a horizontal orientation. Panels with a surface area of ~0.01 m^2 and 6.35 mm thick were used with an incident radiant heat flux of 50.0 kW/m^2 for the neat resins, and 75 kW/m^2 for the composite panels.

3.2.3.10 Fracture Toughness Testing

Three point bend tests were utilized to characterize the toughness of the phenolic-epoxy networks in terms of the critical stress intensity factor K_{1c}, according to ASTM standard D 5045-91.[69] The specimens had thicknesses b (3.12 mm) and widths w (6.28 mm) for the phenolic/epoxy networks and the epoxy control. The samples to determine K_{1c} of the phenolic control were larger to help compensate for their extremely brittle nature. These samples had thickness b (6 mm) and widths w (12.5 mm). The single edge notch bending method was used. First, a sharp notch was created in the sample by sawing. A natural crack was initiated by inserting a cold razor blade (which had been immersed in liquid nitrogen) into the notch and tapping with a rubber hammer. The depth of the natural crack (a) was between 40 and 60 percent of the width (w). For the more brittle samples that were difficult to crack, a vise with two small pin rollers (Figure 3.7) was used to hold the sample during precracking with the razor blade. The vise created compression on the bottom half of the sample, while creating tension on the top half. This allowed accurate natural crack generation even for very brittle samples. The pre-cracked notched specimen was loaded crack down, into a three point bend fixture and tested using an Instron model 4204 instrument. The single edged notched bending rig had moving rollers to avoid excess plastic indentation. The three point bend fixture was set up so that the line of action of applied load passed midway between the support roll centers within 1% of the distance between these centers. The crosshead speed was 1.27 mm/minute, and the testing was conducted at room temperature.

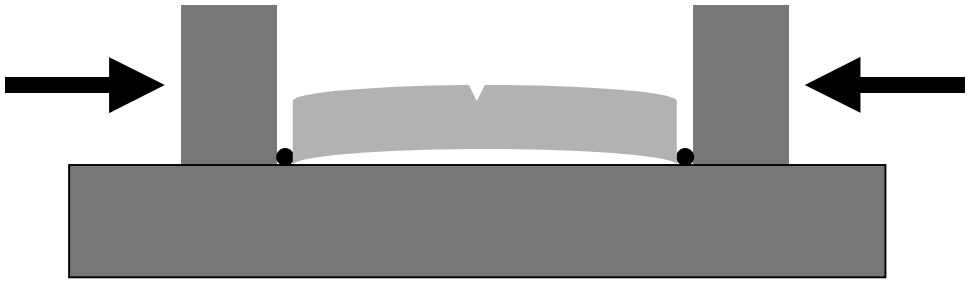

Figure 3.7: **Vice for pre-cracking brittle samples for fracture toughness testing.**

3.2.3.11 Moisture Uptake

Room temperature water absorption was determined for phenolic/epoxy (**1**) networks cured with 0.1 wt % TPP based on the weight of epoxy and compared to an epoxy control cured with diaminodiphenylsulfone at 180°C for 2 hours and 220°C for 2 hours. Rectangular samples with dimensions of approximately 13 mm x 6.4 mm x 1 mm were sanded and polished to remove any flaws which might affect the results. The samples were dried in a vacuum oven at ~ 140°C overnight then allowed to cool in the vacuum oven. Two samples of each composition were accurately weighed then placed in vials filled with water at room temperature. The samples were periodically removed from the water, dried with a Kimwipe, then weighed in order to measure the moisture uptake. The sample weight and the amount of time elapsed from the start of the experiment were recorded. The time was normalized for the varied thickness by dividing by the sample thickness. For each composition, the average moisture uptake of the two samples was recorded and plotted vs. the square root of the time in hours divided by the thickness. Data was collected until the curves leveled off. After the completion of the test the samples were dried in the vacuum oven for 48 hours at 60°C and 24 hours at 140°C, then allowed to cool to room temperature in the vacuum oven and weighed. The final weights were equivalent to the original dry weights indicating that no extractables were removed during the test. The same procedure was followed for determining moisture uptake at 60°C.

3.2.3.12 Viscosity determination

Rheology experiments were carried out on a Bohlin VOR Rheometer in continuous oscillation mode with a frequency of 1 Hz. Temperature control was accomplished with a Bohlin HTC. The auto-strain was set to control the torque to 25% of the maximum torque allowed. The maximum strain for the instrument was 0.25. Samples of about 0.7 g of dry powder were pressed into a pellet then placed between the preheated 25 mm diameter parallel plates of the rheometer. The gap was closed to ~1 mm and the sides were scraped to remove excess sample before the run was started. The samples used in these test were prepared by solvent mixing.

3.2.4 Composite Panel Characterization

The composite panels were C-scanned for overall quality using a sonix model HF 1000 instrument by a pulse-echo arrangement using a 15 MHz transducer with a focal length of 38.1 mm. Scanning electron photomicrographs, obtained from an ISI SX-40 SEM, were used to establish the void free nature of the composites and to confirm good resin distribution and fiber wet-out. Transverse and longitudinal flexural tests following ASTM standard D-790 were used to evaluate a systematically varied series of phenolic/epoxy compositions.

3.3 Results and Discussion

3.3.1 Introduction

A phenolic Novolac resin with an average functionality of 7.3 phenolic hydroxy groups was cured with six different epoxy resins, **1** (bisphenol-A based epoxy), **2** (brominated bisphenol-A based epoxy), **3** (bisphenol-F based epoxy), **4** (1,3-bis(3-glycidoxypropyl)tetramethyldisiloxane), **5** (fluorinated bisphenol-A based epoxy), and **6** (stilbene epoxy) to investigate the effects of epoxy structure on network properties (Figure 3.1). For each chemical structure of the epoxy component, systematically varied compositions were studied ranging from 50 to 80 wt % phenolic Novolac. Structural and compositional effects on network toughness, transition temperatures, and flame retardance were investigated.

3.3.2 Materials Investigated

The phenolic Novolac was analyzed by ^{1}H NMR to determine the average molecular weight of the phenolic chains. The average molecular weight was determined by taking the ratio of aromatic protons to aliphatic protons, determined from ^{1}H NMR, according to the following equation where n is the number of repeat units (Figure 3.8):

$$\text{Aromatic Protons/ Aliphatic Protons} = (3n+8)/(2n+2) \qquad (3.5)$$

Based on this equation, the molecular weight of the Novolac was determined by ^{1}H NMR to be 760 g/mol, which indicates, and average functionality of 7.31. The functionality of 7.31 was used in the predictions for the molecular weights between crosslinks of the networks. Gel permeation chromatography confirmed that the phenolic novolac had a broad distribution of molecular weights (Figure 3.9).

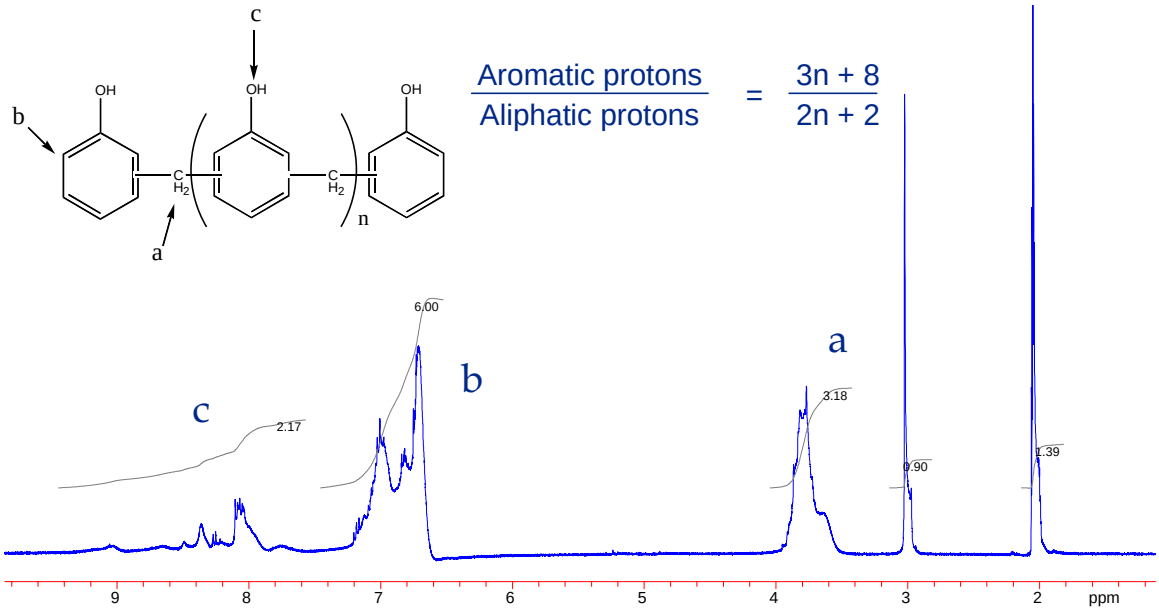

Figure 3.8: **^{1}H NMR of phenolic novolac and molecular weight calculation.**

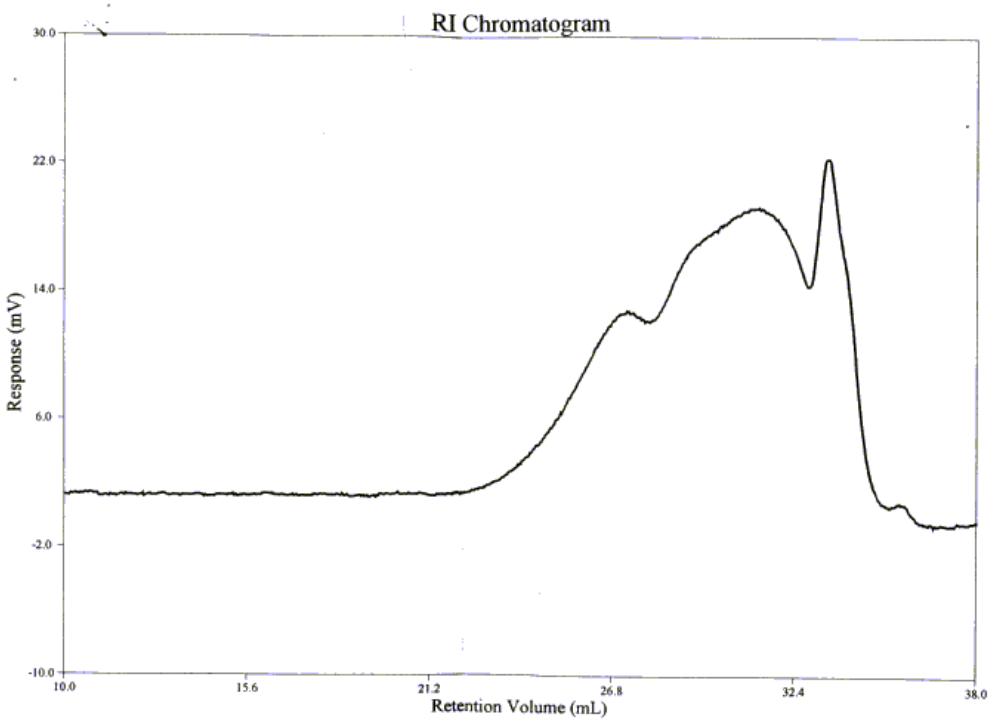

Figure 3.9: **GPC of commercial phenolic novolac.**

Six epoxies with slightly different structures were employed to investigate the effects of the epoxy structure on the network properties. The majority of the structure-property relationships were performed on networks using the bisphenol-A based epoxy; however, glass transition temperatures, fracture toughness, and flame retardance were determined for networks from all six epoxies. Of the six epoxies used 4 were obtained from Dow Chemical and 2 required synthesis. The siloxane epoxy was prepared by a hydrosilation reaction between allyl glycidyl ether and tetramethyldisiloxane. It was then purified by vacuum distillation. The fluorinated epoxy was prepared by reacting hexafluoro-bisphenol-A with epichlorohydrin in the presence of a base, and was analyzed by ^{1}H NMR. The percent chain extension calculated by ^{1}H NMR was 15 % (Figure 3.5). In addition to varying the type of epoxy the ratio of phenolic novolac to epoxy was varied to vary the crosslink density of the networks.

In addition to the six diepoxides, two tetrafunctional epoxies were investigated in an attempt to decrease the amount of the epoxy component necessary for optimal mechanical properties. A higher functionality should allow the use of less epoxy to produce the same network densities as with a difunctional epoxy. Decreasing the epoxy component by incorporating a higher functionality epoxy should improve flame retardance of the networks. The two tetrafunctional epoxies investigated were MT 0613 obtained from Dow, and a tetrafunctional siloxane epoxy prepared from a hydrosilation of allyl glycidylether with tetrakisdimethylsiloxylilane catalyzed by platinum-divinyltetramethyl disiloxane. The tetrafunctional siloxane could not be purified by distillation due to its high boiling point, so the platinum catalyst was degraded with heat then removed by washing with charcoal.

During melt mixing and degassing of each of these tetrafunctional epoxies with the phenolic novolac, gelation was reached in 10-30 minutes at 160°C with no initiator. This made processing of these materials very difficult. These materials were not further investigated because their fast uninitiated gel times would make commercial processing much more difficult than with the difunctional epoxies. In reacting the phenolic novolac with an average functionality of 7.31 with a difunctional epoxy at a ratio of 3 moles of phenol to one mole of epoxy, the calculated gel point occurs at ~ 69 % conversion of the epoxy (Equation 3.6). However, the calculated gel point for reaction of the phenolic

novolac with a tetrafunctional epoxy at the same equivalent ratio occurs at 39 % conversion of the epoxy. These results explain the decreased processing window in the melt.

$$p_c = 1/\{r(f_{epoxy} - 1)(f_{novolac} - 1)\}^{1/2} \quad (3.6)$$

r = ratio of epoxy to phenol(1/3)

f_{epoxy} = the average functionality of the epoxy

$f_{novolac}$ = the average functionality of the novolac

3.3.3 Modulus and M_c

In general, network toughness would be expected to increase with the average molecular weight between crosslinks (increase in ratio of phenols to epoxies) up to some point where the amount of unconnected phenolic chains begins to dominate properties. Likewise, glass transition temperatures of fully cured networks should decrease as the distance between crosslinks increases. Thus, it was of interest to predict and measure network densities and correlate these chemical structures to physical properties of the networks. "Theoretical" average distances between crosslinks were predicted by considering the stoichiometries and assuming a linear phenolic chain with a functionality of 7.31(Table 3.2). In considering the chemical structures of these networks, it was predicted that the crosslink densities should decrease as the stoichiometric offset (excess of phenols) was increased. These predicted values were then compared to experimental measurements of crosslink densities derived from rubbery moduli and elasticity theories. The following assumptions were made in order to calculate the predicted molecular weights between crosslinks: (1) all chains were of equal length (the effect of molecular weight distribution was not considered) (2) a segment was defined by any chain connected by two junction points (3) a junction point was defined as a point were at least three segments intersect. The number of segments for each system was calculated based on the stoichiometric ratio of epoxy to phenol and the average functionality of the phenolic chains (f = 7.31). The calculation for M_c's involves dividing the total molecular weights of all chains considered by the total number of segments. This method should correlate well to measured values for cases where very few "dangling ends" (i.e., elastically inactive segments) exist. The number of so-called "dangling ends" would be

minimized when the phenolic chains were either very long or for cases where the crosslink density was very high. On the other hand, since this method for calculating M_c includes the total weights of all the chains considered (including the weights of the "dangling ends") and it did not count those chain ends as segments, then the theoretical values should be higher than those measured from moduli data. In addition, the distribution of molecular weights of the phenolic chain, which affects the functionality, may also cause deviations between the theoretical and measured molecular weights between crosslinks.

According to rubber elasticity theory, the rubbery moduli of these networks should be proportional to the crosslink densities. Absolute values for the moduli in the rubbery plateau regions were determined from creep tests at 60°C above T_g using a Dynastat. The slopes of the load vs. displacement curves were used to calculate moduli according to equation 3.1, and the molecular weights between crosslinks were calculated from the elastic moduli and the densities at 60°C above T_g (equation 3.4) (Tables 3.1 and 3.2). Equation 3.4 was derived to apply to elastically active network chains only (not dangling ends or unconnected chains)[30] and depends on the following four basic assumptions (1) the chains have gaussian statistics (2) the material deforms affinely (3) the internal energy of the system is independent of the conformations of the individual chains and (4) the chains are treated as phantom networks (there is no excluded volume).[30] Therefore, the networks with the highest number of dangling ends would be expected to deviate most significantly from the theoretical predictions.[30] The experimental trend in M_c values followed the expected increase with stoichiometric offset (higher ratios of phenols to epoxy groups) in all cases (Table 3.2). However, the experimental M_c values were lower than those predicted from stoichiometry for the materials with the lower network densities (Table 3.2). This difference can be partially attributed to the distribution of molecular weights of the phenolic oligomers, which was not considered in the theoretical predictions, and the fact that as the ratio of phenols to epoxies was increased, the number of chains which did not contribute to networking increased (i.e., the number of dangling ends increased). Therefore as the offset increased, the molecular weight between

crosslinks increased significantly due to the large increase in the number of phenolic hydroxyls unreacted (in the network) and the increased fraction of dangling ends.

Table 3.2: Glass transition temperatures, moduli and molecular weights between crosslinks of phenolic/epoxy networks with epoxies 1-4.

Epoxy	Phenolic / Epoxy (wt/wt)	Phenolic / Epoxy (eq/eq)	T_g (°C)	Modulus at T_g + 60°C (Pa)	M_c (measured)	M_c (theoretical)
1	50/50	1.8/1	151	2.09×10^7	643	492
1	65/35	3.3/1	127	9.35×10^6	1413	3564
1	80/20	7.2/1	114	2.87×10^6	4539	∞
2	50/50	3.1/1	148	1.10×10^7	1554	2179
2	65/35	5.8/1	130	4.43×10^6	3511	∞
3	65/35	3/1	118	1.53×10^7	872	1768
3	80/20	6.4/1	109	4.99×10^6	2622	∞
4	65/35	3.3/1	87	1.12×10^7	1030	3518
4	80/20	7.2/1	96	2.97×10^6	4051	∞

3.3.4 Glass Transition Temperature

Dynamic mechanical analyses were used to determine the glass transition temperatures (T_g's) of the networks. The T_g's were calculated from the peaks in the Tan delta curves (Table 3.2). Results of these DMA analyses showed that as the stoichiometric offset (excess of phenols) was increased, the T_g's decreased. This was the expected trend due to the expected decrease in network density in going from 2/1 (phenol/epoxy) to 7/1 (phenol/epoxy). The Tg's of networks with similar molar ratios of phenolic to epoxy varied between epoxies. Networks from the brominated epoxies had slightly higher Tg's than networks from the bisphenol-A based epoxy. Lower Tg's were observed with networks from both the Bisphenol-F based epoxy and the siloxane epoxy due to decreased stiffness of the epoxy backbone. Networks from the fluorinated and

stilbene epoxies had equivalent Tg's to networks of the same equivalence ratios using the bisphenol-A based epoxies.

3.3.5 Cooperativity

For the system under study, it should be noted that crosslink density was not the only factor affecting the physical properties of the networks. As the compositions were varied from 2/1 to 7/1 phenol/epoxy equivalence ratios, the network densities decreased, but at the same time the glassy intermolecular forces increased along this series, probably due to an increase in hydrogen bonding from the larger numbers of unreacted phenols. Therefore, the composition with the lowest network density had the highest amount of unreacted phenols, and highest hydrogen bonding capability. This caused the glassy moduli of the materials having the lower network densities to be unusually high. This is illustrated in the ten-second storage moduli versus temperature curves that were generated from the relaxation data for each composition (Figure 3.10). It is evident from these curves that the rubbery moduli follow the trends expected based on crosslink densities, e.g., as crosslink density decreases the rubbery modulus decreases. On the other hand, the glassy moduli seem to run in the opposite direction. The glassy moduli can be affected by thermal history; however, the thermal history of these samples tested was identical. Therefore, the increase in glassy moduli of the samples with similar thermal histories suggested that increased intermolecular forces in the glassy region were causing the increase in the glassy moduli. These curves suggested that by optimizing the network density both toughness (decreased rubbery moduli) and stiffness (increased glassy moduli) could be optimized. These results were further investigated using a cooperativity analysis. Cooperativity describes the temperature dependence of segmental relaxations through the transition region. This type of analysis was used to gain an understanding of the behavior of these networks as they relaxed through the transition region, and to gain a better understanding of the non-equilibrium glassy state.

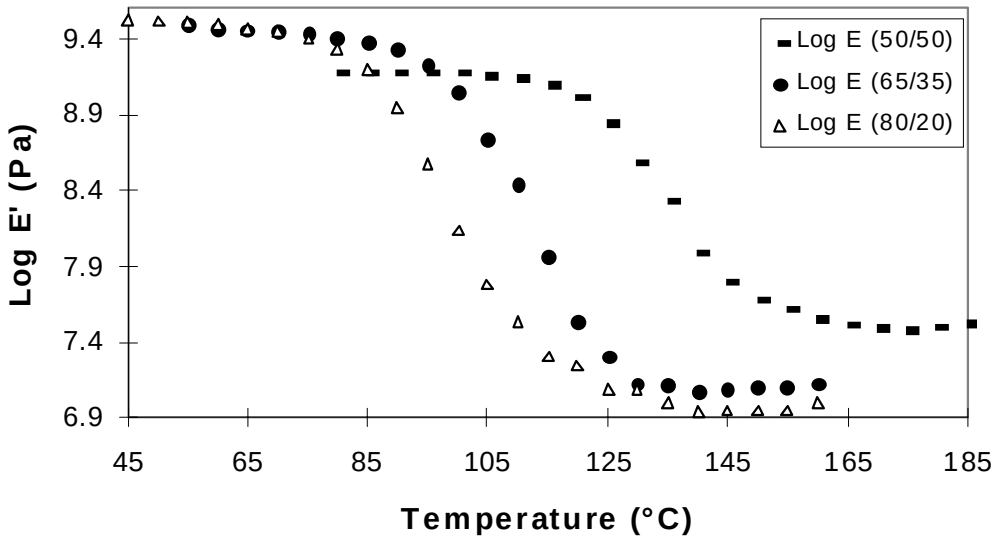

Figure 3.10: **Ten second relaxation moduli vs. temperature for phenolic/epoxy (1) networks.**

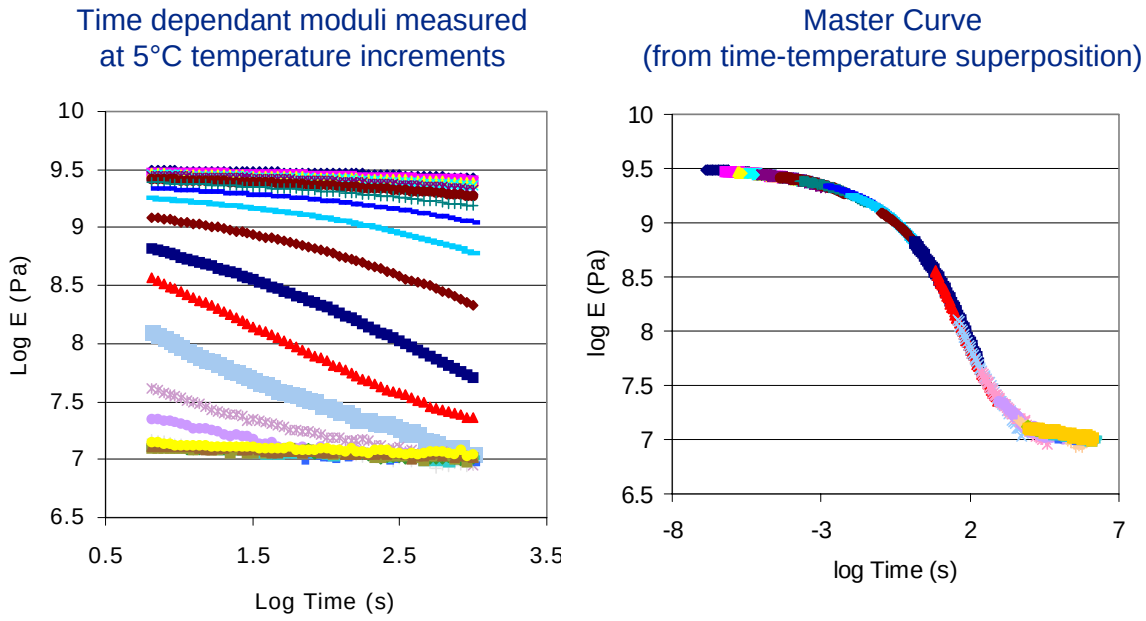

Figure 3.11: **Generation of a log modulus versus log time master curve from relaxation tests using the time-temperature superposition principle.**

The influence of network structure on the behavior of these networks through the transition region was probed by analyzing relaxation moduli. Relaxation modulus versus time curves were generated at 5°C temperature increments from the glassy to the rubbery regions. From these curves, a master curve was generated for each composition based on the time-temperature superposition principle, with no vertical shifting (Figure 3.11). The shift factors (log a_T) used in generating the master curves were plotted as a function of the temperature ($T-T_g$) (Figure 3.12). Both the master curve and the shift factor plots were uniform indicating that the time-temperature superposition principle was valid for these networks. The WLF equation did not show a good fit to the data at higher temperatures and therefore was not used in any calculations for cooperativity. Cooperativity plots of the shift factors (log a_T) as a function of the T_g normalized temperature (T_g/T) were generated for three compositions (Figure 3.13). The indicated range was limited in temperature resulting in the somewhat linear appearance of the curves. Slopes of the curves in the linear region, at $T = T_g$, were determined by fitting each curve to a third and fourth order polynomial and calculation the derivative at $T = T_g$ ($T_g/T = 1$). The average from the two polynomials was used to determine the fragility (*m*) (Table 3.3). From these cooperativity plots a quantitative measure of cooperativity called fragility was determined. The slope of the lines at $T = T_g$ gives the fragility (*m*) of the networks (equation 3.7).

$$m = [d\log(a_T)/d(Tg/T)] \text{ at } T = Tg \qquad (3.7)$$

Fragility, *m*, describes the increase in the most probable segmental relaxation time with a decrease in temperature, in close proximity to the glass transition region. Therefore, a large *m* implies that the rate at which the degree of cooperativity changes with decreasing temperature is higher. This would correspond to a higher cooperativity because materials that are more cooperativity at lower temperatures would have a larger range for the degree of cooperativity to decrease as the temperature was increased. An increase in fragility (*m*) has been previously correlated to an increase in crosslink density[44]. Likewise, an increase in fragility (*m*) has been associated with an increase in secondary

bonding[43,46,47]. In this phenolic/epoxy network series, the expected direction of *m* was interesting (but difficult to predict) due to the two competing effects, crosslink density and hydrogen bonding. Based on the molecular weights between crosslinks, a decrease in *m* was expected as the offset in stoichiometry was increased from 1.8/1 to 7.2/1, with the highest fragility (*m*) for the tightest network (50/50 wt/wt phenolic/epoxy). However, this was not observed, the composition with the tightest network, lowest M_c, exhibited the lowest fragility (Table 3.3). Both the 65/35 and 80/20 wt/wt phenolic/epoxy networks exhibited higher fragilities than the 50/50 wt/wt phenolic epoxy. These same compositions with the higher fragilities also exhibited the highest glassy moduli. The fragility, calculated from the T_g normalized Arrhenius plot at $T = T_g$, suggested that both the crosslink density and hydrogen bonding were important factors affecting the glass formation processes for these networks (Table 3). As the molecular weight between crosslinks increased the amount of unreacted phenolic hydroxyls per phenolic chain increased (Table 3.3). Therefore, the cooperativity did not follow the trend expected based on crosslink densities, in contrast the compositions with the highest cooperativities where those which showed the highest glassy moduli. This suggested that hydrogen bonding was an important factor in the relaxations of these materials through the transition region and in the glassy state properties.

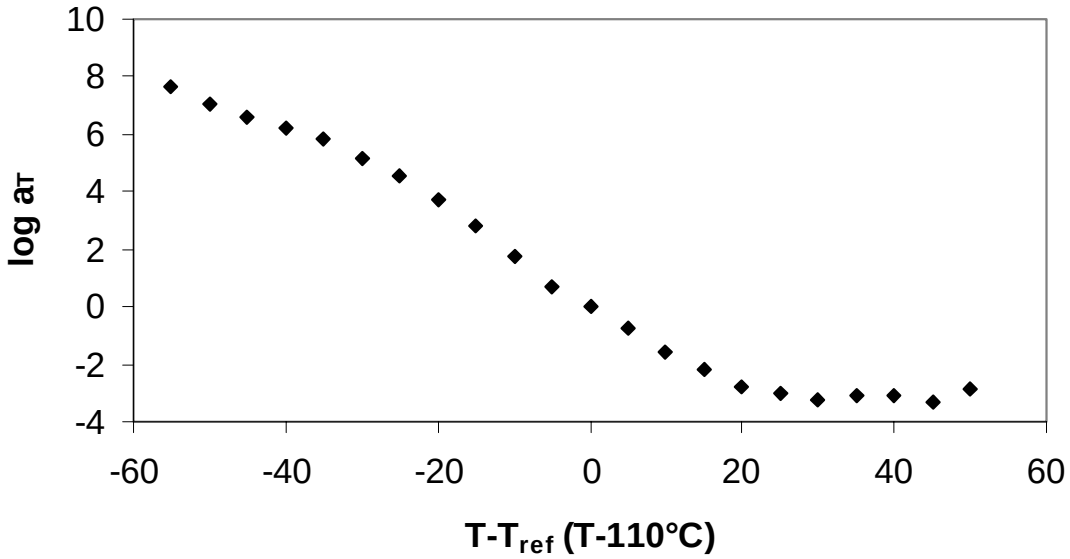

Figure 3.12: Example of a shift factor plot generated from the time-temperature superposition principle.

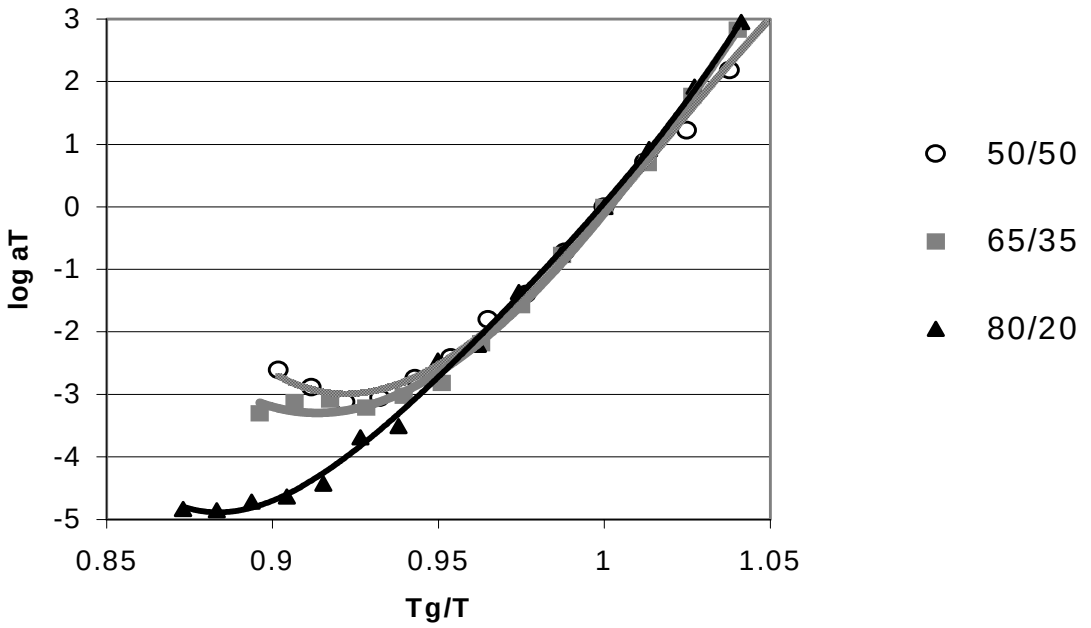

Figure 3.13: Cooperativity plots to determine the fragility (*m*)

Table 3.3: Cooperativity parameters

Phenolic/ Epoxy (wt/wt)	Phenolic/ Epoxy (eq/eq)	M_c (measured)	Unreacted-OH /Phenolic Chain	Fragility (m) $d(\log a_T)/ d(Tg/T)_{T=Tg}$	Coupling Parameter (n)
50/50	1.8/1	644	3.3	58	0.742
65/35	3.3/1	1413	5.2	67	0.797
80/20	7.2/1	4539	6.4	62	0.782

In addition, the master curves were fit with the KWW equation (Equation 3.8) to solve for the coupling parameter (n) for each composition (Table 3.3). These coupling parameters have been shown to have some correlation with fragility, *m*, for many glass-forming materials, although the two have different physical meanings and are derived from different concepts[47]. The coupling parameter (n) is a measure of the breadth of the

distribution of segmental relaxation times. Therefore a larger value for n suggests a broader distribution of relaxation times that relates to a more cooperative system[70]. It has been shown previously that a decrease in M_c correlates with an increase in the coupling parameter n and therefore a broader relaxation response[70]. Just as with the fragility measurements, the data for these phenolic/epoxy networks does not follow this trend, probably as a result of the higher intermolecular forces for the systems with the lower network density. The material with the highest network densities has the lowest cooperativity indicated by the lower n value.

$$\phi(t) = \exp[-(t/\tau)]^{1-n} \tag{3.8}$$

For the phenolic/epoxy networks under study, there was a reasonable correlation between fragility (*m)* and the coupling parameter (n) (Figure 3.14). The increasing trend in *m* as the coupling parameter increased was consistent with the trends found by Bohmer et al..[47] Therefore, the interpretation of relaxation response using the relaxation time breadth parameter (n) suggested a consistent measure of cooperativity in comparison to that determined by the fragility approach. This correlation between fragility and the coupling parameter was important in determining the validity of these measures of cooperativity, due to the very small changes in cooperativity between the three samples.

It is still somewhat unclear what conclusions can be made about the glassy state properties from cooperativity analyses. However, Shan et al. has shown a correlation between fracture toughness and cooperativity normalized by crosslink density.[71] Their results suggested that increased cooperativity in the transition region correlates with increased fracture toughness for materials with similar network densities. It is interesting to note that for the networks analyzed, the compositions with the higher cooperativity also showed higher fracture toughness of the compositions investigated.

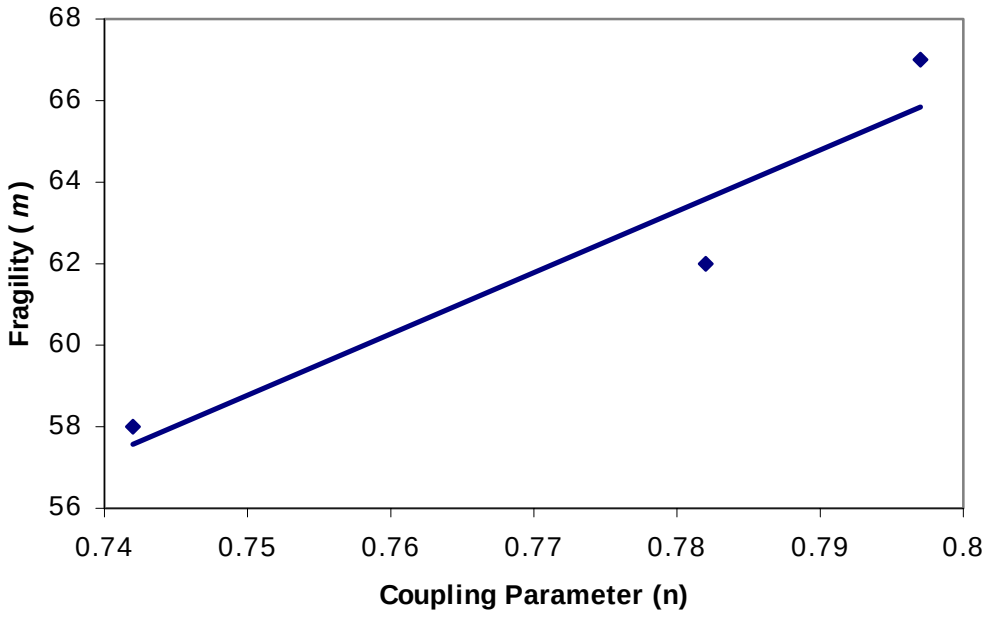

Figure 3.14: **Correlation between the fragility (*m*) and the coupling parameter (n).**

3.3.6 Fracture Toughness

Fracture toughness of the networks was measured by determining the plane-strain stress intensity factors, K_{1c}. Higher values of K_{1c} indicated improved resistance to crack propagation, i.e., increased toughness. Toughness increased with the increased offset in stoichiometry to a maximum of 1.03 $MPa \cdot m^{1/2}$ for the 5/1 phenol/epoxy **1** networks (Table 3.4). This is consistent with the drop in moduli and decrease in network density. The toughness decreased slightly when the stoichiometric offset became too large (7/1 phenol/epoxy). This was undoubtedly related to the increase in dangling ends and unconnected phenolic chains at these very high phenol to epoxy ratios. This was evident from the large increase in soluble fraction from the 3/1 network to the 7/1 network (Table 3.5). Most of the materials with a Phenolic content of 50 wt % or greater had significantly higher toughness than the epoxy control (epoxy **1** stoichiometrically cured with p,p'-diaminodiphenylsulfone). This was considered a breakthrough because the commercially cured phenolic resins were much more brittle than epoxies, with a K_{1c} of

less than 0.20 MPa•$m^{1/2}$. The low toughness of the phenolic resol may be a result of it's porous nature and high crosslink density. The K_{1c} values for the 65/35 (wt/wt) networks using epoxies **2-6** were also relatively high (Table 3.4). In general the fracture toughness was not significantly affected by changing the structure of the epoxy component for the same equivalent ratio of phenol to epoxy. Thus, it can be reasoned that phenolic-epoxy mechanical properties using this particular phenolic oligomer can be optimized by controlling stoichiometry at between 3/1 and 5/1 phenol to epoxy. Lower ratios lead to increased brittleness associated with higher network densities, and higher ratios resulted in too many dangling ends and unconnected chains for optimum mechanical properties. An additional limiting factor in increasing the phenolic content above the 65 wt % phenolic/35 wt % epoxy (3/1 for epoxy **1**) was the viscosity of these melts. Employing a higher functionality phenolic oligomer should improve the properties of the networks with higher ratio's of phenol to epoxy by decreasing the number of dangling ends. However, increasing the molecular weight (functionality) of the phenolic chain resulted in an significant increase in the viscosity of the blends. It would be of interest to investigate the use of controlled molecular weight linear novolacs where the novolac functionality could be increased without a significant increase in the melt viscosity.

Table 3.4: Fracture toughness of phenolic/epoxy networks from epoxies 1-6.

Epoxy	Phenolic/Epoxy (eq/eq)	Phenolic/Epoxy (wt/wt)	K_{1c} (MPa-$m^{1/2}$)
1	Control (Epoxy 1 cured w/DDS)	-----	0.62
Phenolic control[1]	Control (Phenolic Resol[1])	-----	0.16
1	1/1	36/64	0.57
1	2/1	53/47	0.64
1	3/1	63/37	0.87
1	5/1	74/26	1.03
1	7/1	80/20	0.70
2	3.1/1	50/50	0.84
2	5.8/1	65/35	0.74
3	3/1	65/35	0.87
3	6.4/1	80/20	0.41
4	3.3/1	65/35	0.77
4	7.2/1	80/20	0.62
5	4.6/1	65/35	1.05
6	3/1	65/35	0.91

Table 3.5 : Sol fraction of phenolic/epoxy networks from epoxy 1.

Phenolic/Epoxy 1 (eq/eq)	Phenolic/Epoxy 1 (wt/wt)	Sol Fraction
1/1	36/64	2.6
2/1	53/47	3.4
3/1	63/37	12.5
7/1	80/20	24.5

3.3.7 Viscosity

One challenge in processing these phenolic/epoxy networks is overcoming the high viscosity of the phenolic component. Increased viscosity of the melts resulted in higher temperatures required for processing into the desired geometry. However, there was a limit on how high these resins could be heated before they began to cure and the viscosity increased rapidly. For these resins the viscosity increased significantly as the ratio of phenol to epoxy was increased. For the composition with 65 wt % phenolic and 35 wt % epoxy **1** the resin had to be heated to above 130°C to reach 2 Pa-s (a reasonable viscosity for melt processing) (Figure 3.15). However, at about 150°C the viscosity increased significantly. With no initiator the resin could be heated to about 170°C without a significant increase in viscosity during the time scale of the experiment (Figure 3.15). The structure of the epoxy component does have some effect on the viscosity of the blend as would be expected. The networks from the bisphenol-F based epoxy (**3**) had slightly lower viscosities than the bisphenol-A based epoxy (**1**) (Figure 3.16). The siloxane epoxy (**4**) resulted in melts with the lowest viscosities, allowing much easier processing. Due to the low viscosity of the siloxane epoxy (4), blends with 65 wt % phenolic and 35 wt % epoxy (**4**) with 0.07 mol % TPP initiator had a processing window of greater than 2 hours at 100°C (Figure 3.17). The lower melt viscosites, of blends with the siloxane epoxy, allowed for lower processing temperatures that resulted in longer processing windows. Networks from the brominated epoxy (**2**) had significantly higher viscosities, preventing preparation of networks with greater than 65 wt % phenolic. In addition due to the high viscosities of the melts with the brominated epoxy (**2**) these materials required a unique processing method to form the void free networks required for structure-

property relationships. Isothermal viscosity was investigated to determine the temperature at which the processing window (time below 2 Pa-s) was the largest. If the temperature was too low the melt never reached this low viscosity; however, if the temperature was too high the viscosity increased too rapidly. For the primary composition studied (65 wt % phenolic/35 wt % epoxy **3** with 0.07 mol % initiator) the temperature that gave the longest processing window was 145°C (Figure 3.18). These results were used in determination of the optimum temperature for composite melt processing.

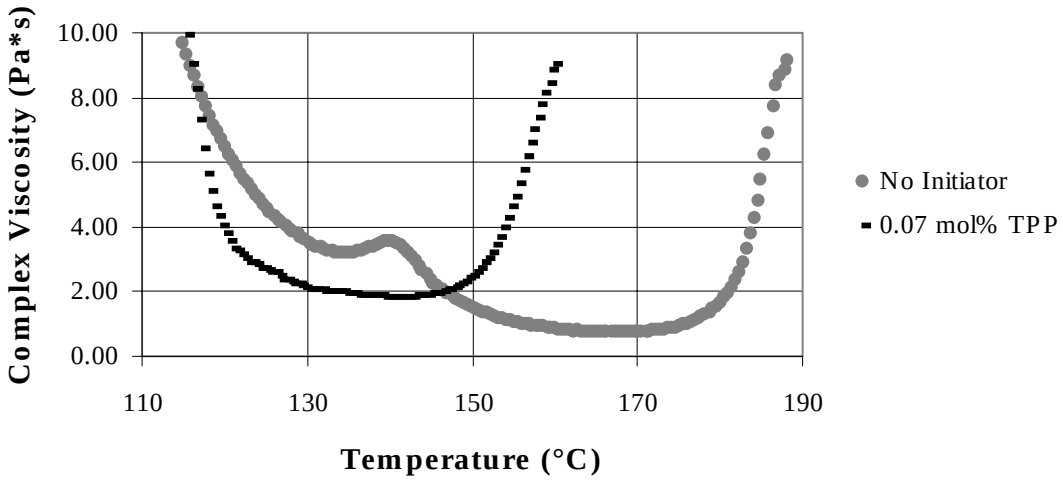

Figure 3.15: Complex viscosity versus temperature for 65/35 wt/wt phenolic/epoxy 1.

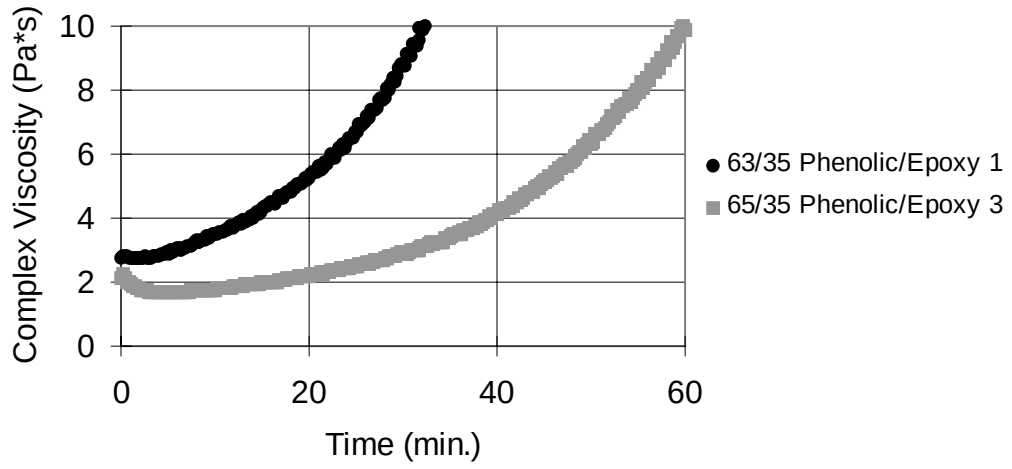

Figure 3.16: **Complex viscosity versus time at T = 130°C of 65/35 wt/wt phenolic/ epoxy 1 and 3 with 0.07 mole % TPP based on moles of epoxy.**

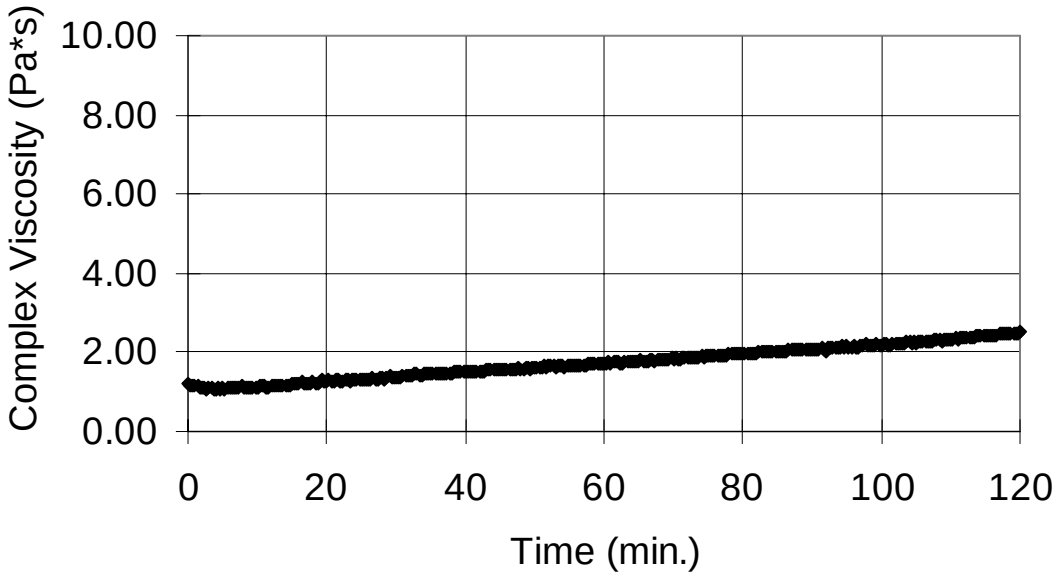

Figure 3.17: **Complex viscosity versus time at T = 100°C of 65/35 wt/wt phenolic/epoxy 4 with 0.07 mole % TPP initiator based on moles of epoxy.**

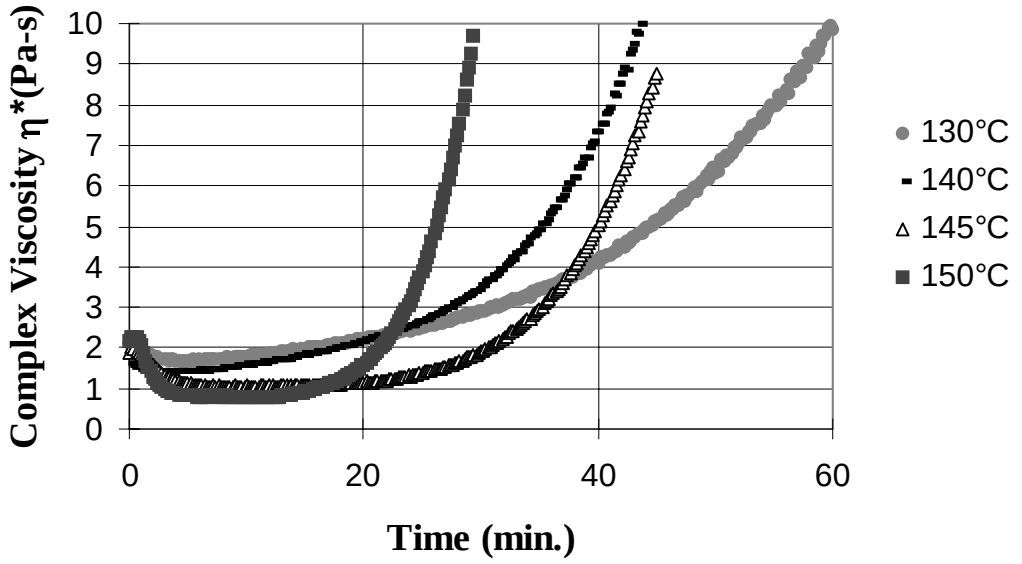

Figure 3.18: **Complex viscosity versus time at different temperatures for 65/35 wt/wt phenolic/epoxy 3 with 0.07 mole % TPP based on moles of epoxy.**

3.3.8 Flame Retardance

The flame retardance of neat panels of the phenolic/epoxy networks was measured using a cone calorimeter with a heat flux of 50 kW/m^2 and 20.9% O_2 (atmospheric oxygen). The heat release rate curves from the phenolic/epoxy networks showed a much lower peak heat release rate and lower total heat released than the epoxy control (Figure 3.19). The heat release rate of the 80/20 wt/wt phenolic/epoxy **1** network never reached 300 kW/m^2; whereas, the epoxy control had a maximum heat release rate of about 1200 kW/m^2 (Table 3.6). In addition to the different maximum heat release rate values another notable difference was evident from the heat release rate curves (Figure 3.19). It can be speculated that the initial spike in the heat release rate curve of the phenolic/epoxy networks was the result of ignition followed by immediate production of a protective char layer which resulted in a reduction in the heat release rate. It is also possible that the initial spike resulted from the ignition of volatiles produced prior to ignition. It is likely that this initial spike was not seen in the control epoxy because this was not a char

forming material, and the heat release rate was so high that it may have masked this effect. The Heat Release rate curves of the phenolic control also showed two peaks indicative of a char forming material. However, the first peak was lower in intensity and more rounded than with the phenolic/epoxy networks. It is likely that the less intense initial burning and the longer time to sustained ignition of the phenolic control resulted from the lack of the flammable epoxy component (Figure 3.20).

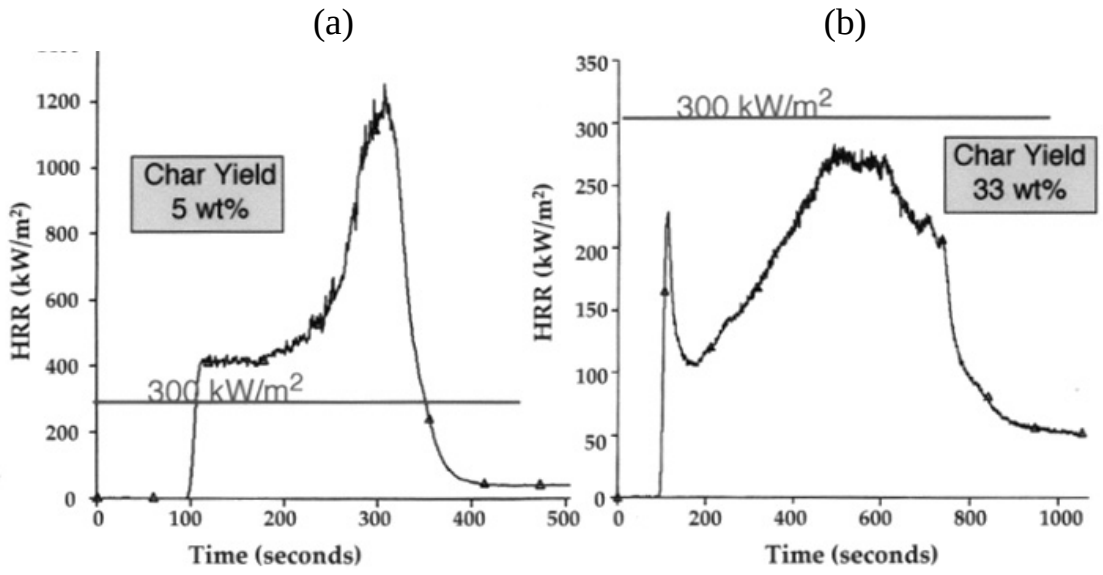

Figure 3.19: Heat release rate curves of (a) epoxy 1 cured w/DDS and (b) 80/20 wt/wt phenolic/ epoxy 1 network.

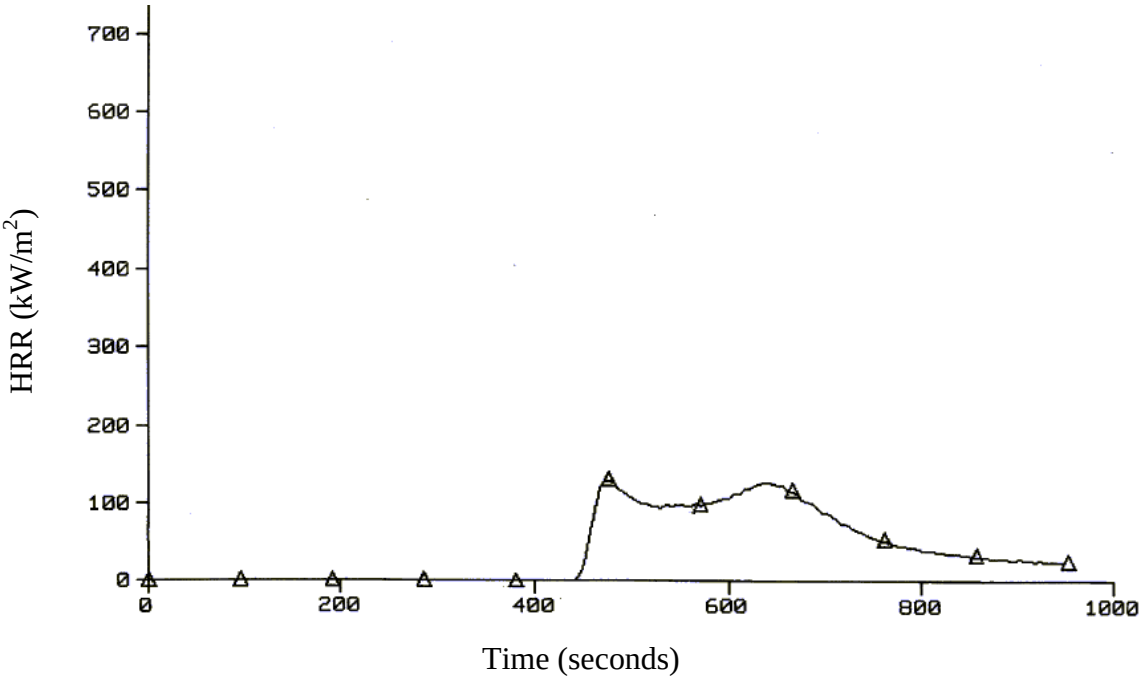

Figure 3.20: Heat release rate curve of the phenolic control.

Changing the structure of the epoxy component did appear to have some effect on the flame retardance as would be expected. Networks with the brominated epoxy **2** had the lowest heat release rates, but the smoke produced had a much higher toxicity. In addition, this measure of toxicity only considers the ratio of carbon monoxide to carbon dioxide. In the networks from the brominated epoxy there was most likely a significant amount of HBr being given off along with the carbon monoxide. On the other hand, networks with the siloxane epoxy **4** had a low heat release rate as well as very low smoke toxicity (Table 3.6). Therefore, networks from the siloxane epoxy appear to be very important in view of their flame retardance as well as low viscosity; however due to the more detailed synthesis reaction of the siloxane epoxy, the commercially available bisphenol-A based epoxy was used for the composite analysis. As would be expected the phenolic resol had the lowest peak heat release rate and smoke toxicity and the highest char yield, but the phenolic/epoxy networks with high phenolic content approached these values.

Table 3.6: Flame retardance of phenolic/epoxy networks.

Epoxy	Phenolic/Epoxy (wt/wt)	Peak Heat Release Rate (kW/m^2)	Char Yield (wt%)	Smoke Toxicity (CO yield / CO_2 yield) ($x10^{-3}$)
None	Phenolic Control (Resol*)	116	65	11
1	Control Epoxy (Epon 828/DDS)	1230	5	44
1	35/65	477	17	45
1	50/50	382	23	36
1	65/35	357	29	34
1	80/20	260	33	27
2	50/50	158	9	175
2	65/35	165	8	189
3	65/35	397	17	76
3	80/20	266	26	53
4	65/35	325	22	24
4	80/20	226	35	15
5	65/35	353	-----	-----
6	65/35	407	-----	-----

From the cone calorimetry data we know that the networks have a high degree of flame retardance, but we do not fully understand what the factors involved in the flame retardance are. One possibility is that the free phenolic groups on the Novolac may act as free radical traps to retard degradation at the burning front. It was reasoned that such behavior might result in the feed of volatiles to the flame being reduced. Another

possibility is that the high aromatic content of the Phenolic resin leads to a high char yield at the burning surface. The char would not burn readily, and might also shield heat transfer from the flame to the substrate. The initial spike in the heat release rate curves of the phenolic/epoxy networks suggests the production of a protective char layer. In addition, higher char yields for the networks high in phenolic content were observed by thermogravimetric analyses. These thermograms showed that materials with a higher content of phenolic material in the network have higher char yields (Figure 3.21).

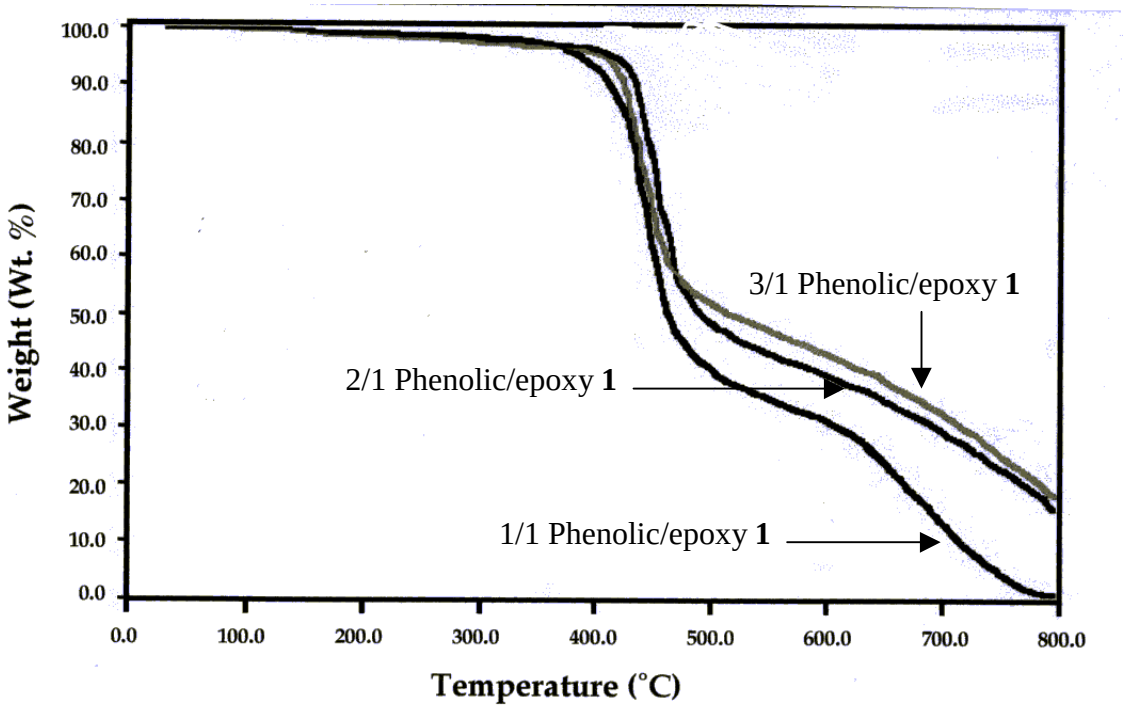

Figure 3.21: **Thermogravimetric analysis of phenolic/epoxy 1 networks in nitrogen.**

3.3.9 Moisture Uptake

Moisture uptake of a series of materials with varied stoichiometries was measured for the phenolic/epoxy **1** networks and compared to an epoxy control. These samples were immersed in water at room temperature for several months until equilibrium was achieved (Figure 3.22). The phenolic/epoxy showed significantly increased moisture uptake when compared with the control epoxy. In addition, the moisture uptake

increased significantly as the phenolic content increased, as a result of the higher concentration of hydroxyl groups. These results can be explained by increased hydrogen bonding of phenolic/epoxy networks as the phenolic concentration was increased. The phenolic/epoxy material with the highest network density and correspondingly the lowest concentration of hydroxyl groups (including both aliphatic hydroxyls and phenols), 50/50 wt/wt phenolic/epoxy **1**, was closest to the epoxy control as was expected. The moisture uptake at 60°C followed the same trends, but the values were slightly higher (Figure 3.23). The network prepared from the fluorinated epoxy **5** was investigated in hopes that it would exhibit decreased moisture uptake due to the hydrophobic 6F groups. However, at this composition of 5 moles phenolic to 1 mole epoxy the hexafluoro group did not appear to have any effect on the moisture uptake. The 5/1 phenolic/epoxy **5** fell directly between the 3/1 phenolic/epoxy **1** and 7/1 phenolic/epoxy **1.**

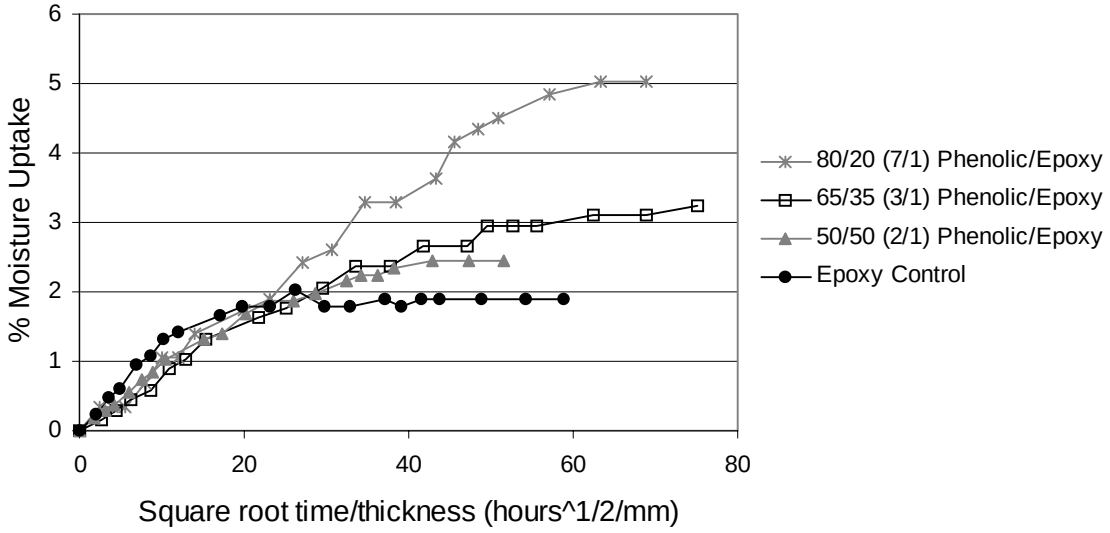

Figure 3.22: Room temperature moisture uptake for phenolic/epoxy 1 networks.

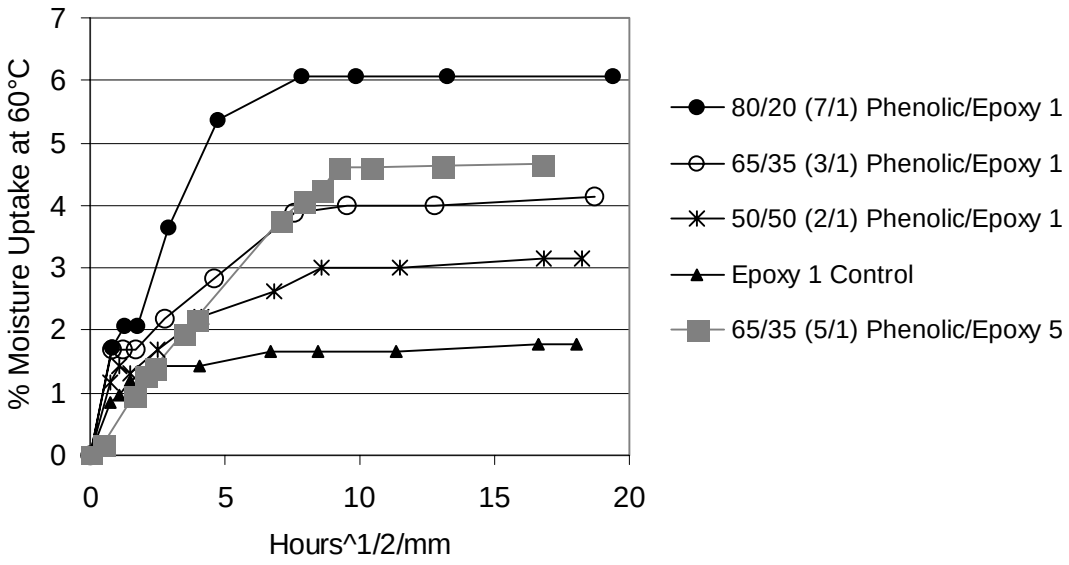

Figure 3.23: Moisture uptake of a phenolic/epoxy 5 network compared to phenolic/epoxy 1 networks at 60°C.

3.3.10 Composite Properties

3.3.10.1 Scanning Electron Microscopy

Scanning electron microscopy (SEM) was used to confirm the void-free nature of the composites. Images of composite cross-sections prepared with a commercial phenolic matrix (from a resol resin), and one of the phenolic/epoxy matrices described herein are depicted in figure 3.24. It is evident that the void content is greatly reduced in the phenolic/epoxy system. No voids are evident in the representative region scanned. This is consistent with the volatile-free cure reaction of the phenolic/epoxy networks.

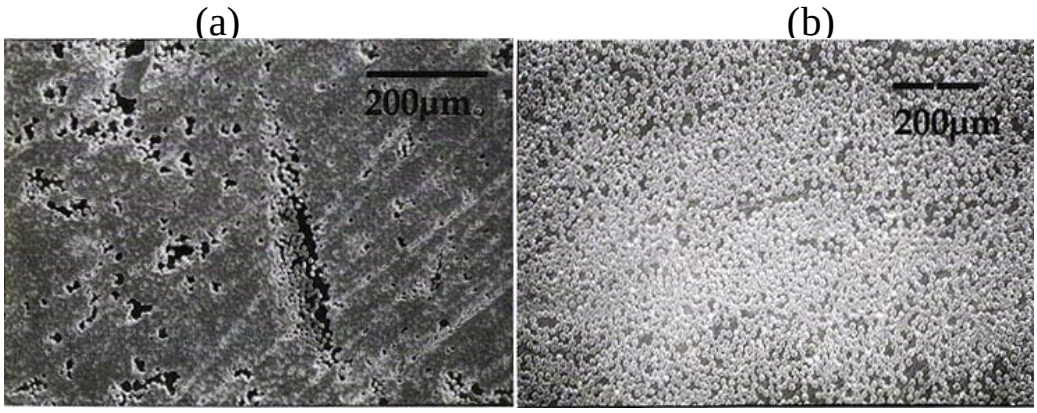

Figure 3.24: **SEM micrographs of unidirectional carbon fiber reinforced composite cross-sections: a) commercial phenolic resol matrix and b) phenolic/epoxy 1 networks.**

3.3.10.2 Transverse and Longitudinal Flexural Strengths and Moduli

Unidirectional carbon fiber reinforced composites made with the phenolic/epoxy resins exhibited superior transverse and longitudinal flexural strengths and moduli compared to the epoxy control (Table 3.7). The panels prepared from the 50/50 and 70/30 wt/wt phenolic/epoxy compositions exhibited the highest values, consistent with the superior toughness of these materials, which was measured for the neat networks. The excellent transverse flexural properties of the phenolic/epoxy compositions may also reflect improved fiber/matrix adhesion. This might be expected due to the unusually high potential for hydrogen bonding inherent in the chemical backbone structure for the phenolic material. Glass fabric reinforced composites prepared from the 70/30 wt/wt phenolic/epoxy resin exhibited superior warp and weft flexural strength, exceeding the epoxy control as well as the other phenolic/epoxy ratios (Table 3.8). This is also consistent with the fracture toughness of the neat networks.

Table 3.7: Longitudinal (0°) and transverse (90°) flexural strengths and moduli of carbon fiber reinforced phenolic/epoxy 1 and epoxy control composites.

Novolac/Epoxy (wt./wt.)	0° Flexural Strength (MPa)	90° Flexural Strength (MPa)	0° Flexural Modulus (GPa)	90° Flexural Modulus (GPa)
Control Epoxy (Epoxy 1/DDS)	1389	29	159	8.9
50/50	2051	63	156	12.1
70/30	2020	66	162	11.3
80/20	1808	39	174	11.1

Table 3.8: Flexural strengths of glass fabric reinforced phenolic/epoxy 1 and epoxy control composites.

Novolac/Epoxy (wt./wt.)	Warp Flexural Strength (MPa) (28 strands/inch)	Weft Flexural Strength (MPa) (16 strands/inch)
Control Epoxy (Epoxy/DDS)	442	367
50/50	436	351
70/30	567	372
80/20	379	261

3.3.10.3 Cone Calorimetry

Cone calorimetry measurements were performed on carbon and glass fiber composites of both the epoxy control, and the 80/20 wt/wt phenolic/epoxy network. The weight percents matrix in the composites were 24 % for the carbon and 25 % for the glass. This was important in that only about 20% of the total weight was lost in the flammability experiments with an incident heat flux of 75 kW/m^2. This resulted in a smaller change in properties between samples as compared to the analogous data on neat networks. In spite of this, as expected, both the carbon and glass fiber composites with the phenolic/epoxy system showed reduced heat release rates, mass loss rates, and specific extinction areas relative to the epoxy controls (Table 3.9).

Table 3.9: Cone calorimetry of carbon fiber and class fabric reinforced phenolic/epoxy 1 and control epoxy composites.

Property	Phenolic/ Epoxy (Carbon)	Epoxy control (Carbon)	Phenolic/ Epoxy (Glass)	Epoxy Control (Glass)
% Consumed	19.2	22.9	15.9	21.7
Avg. HRR (kW/m^2)	72	105	81	93
Total Heat Released (MJ/m^2)	38.7	57.5	44.8	54.8
CO/CO_2	0.0262	0.0378	0	0
Avg. Mass Loss Rate ($g/s*m^2$)	4.2	9.0	6.6	9.0
Avg. SEA (m^2/kg) (Specific Extinction Area)	672	1060	874	1052

3.4 Conclusions

Relationships between the chemical network structures and the physical and flame performance properties of new phenolic-epoxy materials have been elucidated. Network densities have been explored by measuring the moduli in the rubbery regions and these experimental values were compared with those predicted from stoichiometry. At least trends in experimental results followed predictions. It was shown that the T_g's decreased and toughness increased, as the phenolic Novolac content in the network was increased up to the point where the concentration of unreacted phenolic chains and dangling ends dominated properties. Both results could be correlated to the decrease in network densities along this series. Cooperativity studies suggested correlations between the parameters *m* and n, and suggested a crossover in properties from the two competing factors, network density and intermolecular forces. The increase in hydrogen bonding was also evident in the moisture uptake where increased phenolic content lead to increased moisture uptake. In addition, the composition with the highest cooperativity also exhibited the highest toughness of the three compositions analyzed, suggesting a correlation between the degree of intermolecular cooperativity and the non-equilibrium glassy state. Toughness values exceeded those of typical untoughened epoxy networks and far exceeded existing commercial phenolic resins. In addition, an increase in Novolac content improved the flame retardance rather dramatically. The maximum flame retardance was achieved for networks with 80 wt % of the phenolic component, and these networks had significantly better flame retardance than the epoxy control. Networks containing 80 wt % phenolic Novolac and 20 wt % siloxane epoxy yielded both very low heat release rates and the lowest smoke toxicity. Thus, by increasing the Novolac content up to a phenol to epoxy ratio of about 3 and by varying the structure of the diepoxide, both mechanical properties and flame retardance could be maximized.

4 Latent Initiators and Composite Properties

4.1 Introduction

Based on the structure property relationships, the optimum ratio of phenol to epoxy is 65/35 wt/wt.[68],[72] This composition gives networks with both good flame retardance and fracture toughness while maintaining a low enough viscosity to allow melt mixing and degassing of the uninitiated blends. However, due to high viscosities of the phenolic-epoxy resins, melt composite fabrication is challenging. The resin must be heated to ~140-145°C to achieve sufficiently low viscosity (~ 5 Pa*s) for efficient fiber preform impregnation in melt processes, and the resin viscosity must remain stable at those temperatures for an extended period. In addition, it is desirable for the resin to react rapidly at cure temperatures of about 180-200°C to prepare composite components within a few minutes. Embedding the cure initiators in the fiber sizing allows both of these seemingly paradoxical requirements to be met.[73],[74] Since the initiator is not in contact with the resin in the processing "resin pre-bath," stable viscosity can be maintained during this stage. Also, relatively high initiator concentrations can be placed in the fiber sizings to achieve rapid matrix cure at elevated temperatures.

This work focuses on an investigation of the kinetics of the phenolic-epoxy curing reaction with different types of initiators as well as the effects of placing the initiators within the fiber sizings. Several initiators were investigated to determine the effects of initiator structure on the cure rates at elevated temperatures.

The following properties were considered in the investigation of initiators. First of all, it was desirable to have an initiator that could be encapsulated into a water dispersible sizing material, and would initiate the phenolic/epoxy matrix at a very high rate. Therefore, several water dispersible initiators were prepared and their catalytic ability was analyzed. In addition, since the initiator was in a sizing material it was also important that the initiator remain on the fiber during processing through the resin pot, then diffuse rapidly through the matrix resin. Therefore, the T_g of the initiator/sizing was also important. In addition, the effects of the initiator/sizing on the interface between the fiber and matrix, as well as on the mechanical properties of the composite were

important. To assess the effects of the initiator on the interface region and composite properties, composite panels were prepared by melt prepregging the sized fibers, followed by curing in a press for the appropriate cure cycles (determined by kinetic analyses). Composite properties were investigated as a function of sizing material to investigate these effects of the sizing on the interface region as well as the bulk composite properties.

4.2 Experimental

4.2.1 Materials

AS-4 unsized but surface treated 12K tow fibers and G' (Hexcel's proprietary sizing) sized 12K tow fibers, were obtained from Hexcel. Tetrahydrofuran (EM Sciences) was refluxed over sodium with a small amount of benzophenone as an indicator for dryness and distilled immediately prior to use. The poly(hydroxyether) and the "commercially modified poly(hydroxyether) sizing" were donated by Phenoxy Associates, Rock Hill, SC. Phthalic anhydride was obtained from Aldrich and sublimed prior to use. Succinic anhydride was obtained from Aldrich, and stored under nitrogen prior to use. Dimethylaminopyridine (DMAP) was obtained from Aldrich and used as received. 2,2'-Bis[4-(3,4-dicarboxyphenoxy)phenyl]propane dianhydride (bisphenol A dianhydride), obtained from General Electric, was recrystallized from toluene and acetic anhydride four times, then washed with toluene and n-heptane. The purified bisphenol A dianhydride was dried in the vacuum oven at 140°C overnight immediately prior to use. 6F dianhydride was obtained from Clariant Fine Chemicals and dried in the vacuum oven at 180°C overnight immediately prior to use. Meta-phenylene diamine (Aldrich) was sublimed using an 80°C oil bath prior to use. Tripropylamine was obtained from Aldrich and used as received. The commercial phenol-formaldehyde novolac resin was provided by the Georgia Pacific Corp., Decatur, GA (Product #GP-2073). The molecular weight by proton NMR was 760 g/mole. Epon 828 epoxy resin was obtained from Shell Chemical. Triphenylphosphine (TPP) and tris (2,4,6-trimethoxyphenyl)phosphine (TMOPP) were obtained from Aldrich and used as received. Sodium acetate, rubidium

acetate and cesium acetate were obtained from Aldrich and used as received. Acetic acid was obtained from Aldrich and used as received.

4.2.2 Sample Preparation

4.2.2.1 Resin Preparation by Melt Mixing

To a three neck round bottom flask equipped with a vacuum tight mechanical stirrer and a vacuum adapter was added phenolic novolac (65 wt %). The flask was heated in an oil bath to 170°C. When the novolac began to liquefy at 170°C, mechanical stirring was initiated, and a heat gun was used to facilitate the process. Once all the novolac was liquefied, a slight vacuum was applied for about 3 minutes to partially degas the novolac. The epoxy crosslinking component (35 wt %), which had been degassed in a vacuum oven at ~60°C, was then added to the novolac. The flask was sealed and a vacuum was applied incrementally to prevent the material from swelling into the vacuum line. Once full vacuum was achieved (2-5 Torr) the solution was stirred for 2 minutes to degas the blend. The hot melt was then poured into aluminum pans and cooled in a dry ice/isopropanol bath. The resin was stored at room temperature prior to use.

4.2.2.2 Solvent Mixing for Rheology Measurements

To a 100 ml round bottom flask was added ~2-3 grams epoxy resin (35 wt. %), novolac (65 wt. %) and initiator (triphenylphosphine or TMOPP). The solids were dissolved in acetone (~ 30 % by wt.) with stirring. The solvent was evaporated first by a Rotovap and then in a vacuum oven at room temperature for 2-3 days until all the acetone had been removed. Samples were stored at ambient temperature and pressure until used.

4.2.2.3 Sample Preparation for DSC

The novolac and epoxy were melt mixed as described above with no added initiator, then ground to a powder. The initiator was crushed to a powder and mixed with the novolac-epoxy powder. When necessary the initiator was cooled with liquid nitrogen while grinding to allow powder formation of tougher polymeric initiators. For the kinetic comparisons between initiators, 2.0 mol % initiator was used based on the equivalents of epoxy in the resin. For determination of composite cure cycles, the initiator

concentration was determined by the calculated weight percent sizing in the composites, to model the kinetic behavior of the composite panels.

4.2.3 Synthesis of Latent Initiators

4.2.3.1 Synthesis of Ultem™ Type Poly(amic acid) (Figure 4.1)

Bisphenol A dianhydride (51.3032 g, 0.0986 mol) was weighed into a dry 500 ml round bottom flask with a stir bar. The flask was then sealed with a rubber septum and purged with nitrogen. Dry THF (250 ml) was added to the flask by cannula. Phthalic anhydride (0.7524 g, 0.0051 mol) and m-phenylene diamine (10.9313 g, 0.1011 mol) were added to a 100 ml round bottom flask. The stoichiometry was controlled by the Courther's equation to achieve controlled molecular weight poly(amic acids). This flask was also sealed with a rubber septum and purged with nitrogen. Dry THF (50 ml) was added to the 100 ml flask by cannula and the mixture was stirred for about 10 minutes, until all monomers had dissolved. The solution was then added to the heterogeneous bisphenol-A dianhydride/THF mixture by cannula. The 100 ml flask was rinsed twice with ~ 25 ml of dry THF, and the wash solution was added to the reaction flask by cannula. After 24 hours the polymer solution was poured into a Teflon dish, placed inside a covered glass container equipped with a nitrogen sweep, and was exposed to a brisk nitrogen flow at room temperature for about 48 hours to evaporate the solvent. The poly(amic acid) was then placed in a vacuum oven at 20°C to remove more of the solvent. The weight percent THF remaining in the poly(amic acid) was determined, by proton NMR, to be about 20 % for all samples. This was used to obtain an accurate weight of the poly(amic acid) for poly(amic acid) salt formation. The number average molecular weight ($<M_n>$) determined by GPC of the polyimide was 22,000 g/mol.

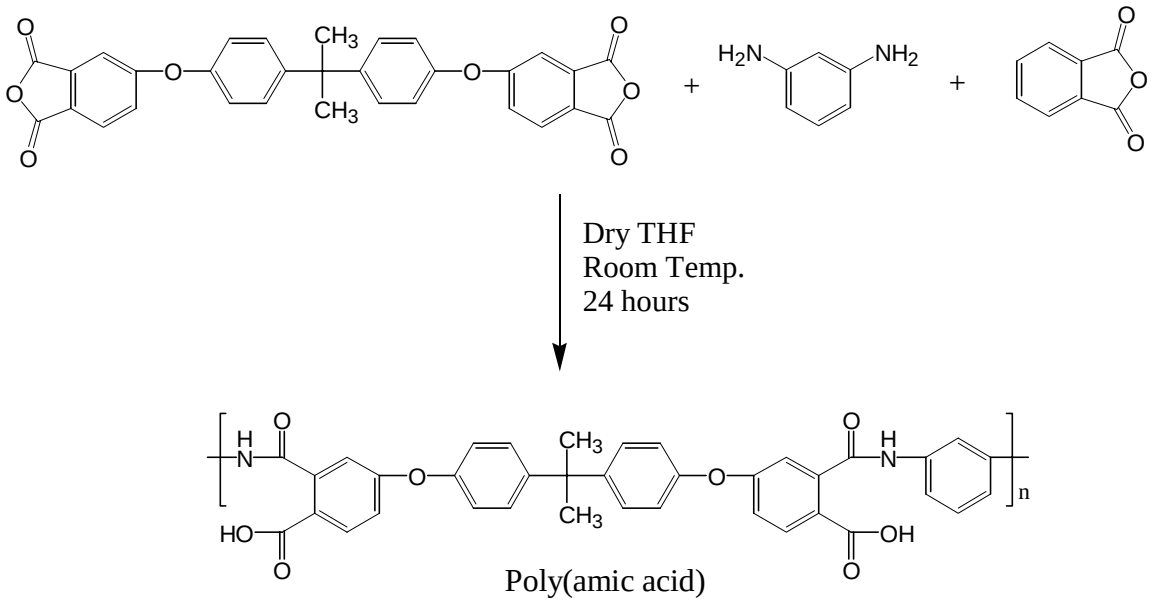

Figure 4.1: Synthesis of Ultem™ type poly(amic acid).[75]

4.2.3.2 Synthesis of Ultem™ Type Poly(amic acid) Salt with TPP

To a 1000 ml beaker was added methanol (600 ml) and tripropylamine (11.65 ml). A 10 mol % excess of base was added relative to carboxylic acid groups to assure 100 % conversion to the poly(amic acid) salt. To this solution was added Ultem™ type poly(amic acid) and stirring was initiated. The beaker was covered with parafilm and the mixture was stirred until all poly(amic acid) had dissolved (about 5 hours), indicating formation of the salt. The solution was then poured into a Teflon boat and the solvent was evaporated.

4.2.3.3 Synthesis of Ultem™ Type Poly(amic acid) Salt with TMOPP

To a 2000 ml beaker with a magnetic stir bar was added THF (1000 ml), methanol (500 ml), and TMOPP (52.300 g, 0.0982 mol), a 10 % excess relative to carboxylic acid groups. Once the TMOPP had dissolved, poly(amic acid) (28.062 g, 0.0893 mol) was added. The solution was stirred for about 6 hours (all poly(amic acid) had dissolved within 5 hours), then poured into a Teflon boat to evaporate the solvent.

4.2.3.4 Synthesis of Hexafluorinated Poly(amic acid) (Figure 4.2)

Hexafluorodianhydride (36.773 g, 0.0828 mol) was weighed into a dry 500 ml round bottom flask with a stir bar. The flask was then sealed with a rubber septum and purged with nitrogen. Dry THF (~300 ml) was added to the flask by cannula and the mixture was stirred for 10 minutes to allow most of the monomer to dissolve. *m*-Phenylene diamine (8.9518 g, 0.0828 mol) was added to a 100 ml round bottom flask. This flask was also sealed with a rubber septum and purged with nitrogen. Dry THF (60 ml) was added to the 100 ml flask by cannula and the mixture was stirred for about 10 minutes, until all monomers had dissolved. The solution of *m*-phenylene diamine in THF was then transferred to the 500 ml reaction flask by cannula. The 100 ml flask was rinsed twice with ~ 25 ml of dry THF, and the wash solution was added to the reaction flask by cannula. After 24 hours the polymer solution was poured into a Teflon dish, placed inside a covered glass container equipped with a nitrogen sweep, and was exposed to a brisk nitrogen flow at room temperature for about 48 hours to evaporate the solvent. The poly(amic acid) was then placed in a vacuum oven at 20°C to remove more of the solvent. For preparation of the target 10,000 g/mol poly(amic acid) the molecular weight was controlled by adding the phthalic anhydride as the endcapper and controlling the stoichiometry according to the Courther's equation. The weight percent THF remaining in the poly(amic acid) was determined, by proton NMR, to be about 26 % for all samples. This was used to obtain an accurate weight of the poly(amic acid) for poly(amic acid) salt formation.

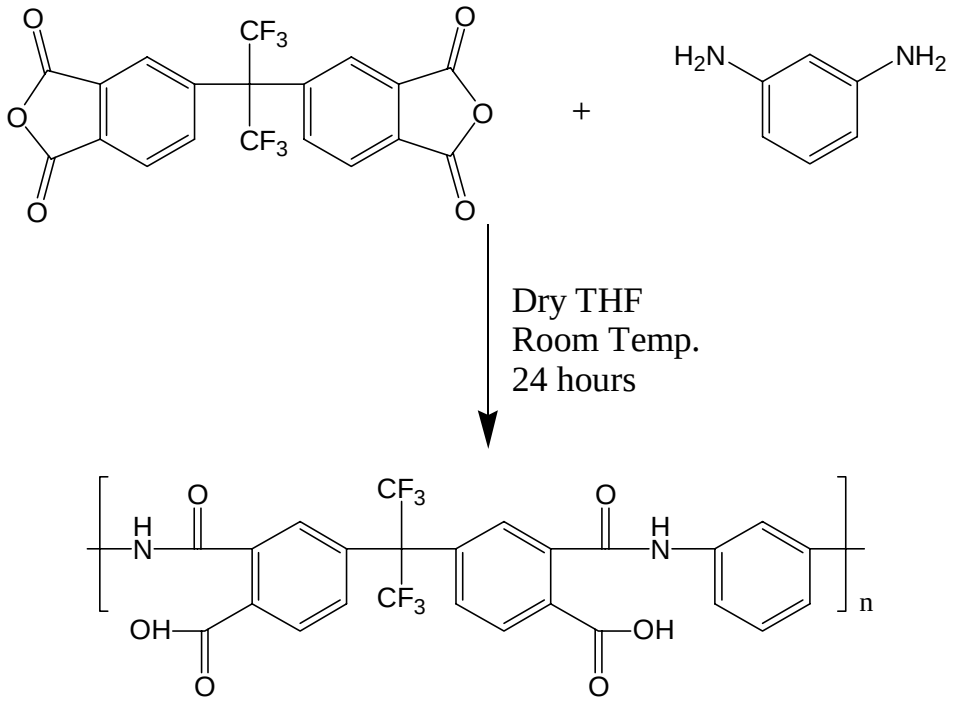

Figure 4.2: Synthesis of a hexafluorinated poly(amic acid).

4.2.3.5 Synthesis of Hexafluorinated Poly(amic acid) Salt with TPP

To a 1000 ml beaker with a magnetic stir bar was added THF (150 ml), methanol (450 ml), and triphenylphosphine (TPP) (24.36 g, 0.0929 mol), a 5 % excess relative to carboxylic acid groups. Once the TPP had dissolved, poly(amic acid) (24.400 g, 0.0884 mol) was added. The solution was stirred for about 6 hours [all poly(amic acid) had dissolved within 5 hours], then poured into a Teflon boat to evaporate the solvent.

4.2.3.6 Modification of the Commercial Polyhydroxyether (Figure 4.3)

4.2.3.6.1 With Phthalic Anhydride

To a 500 ml round bottom flask was added polyhydroxyether (15.21g, 0.0535 mol), phthalic anhydride (8.318 g, .05616 mol), and dry tetrahydrofuran (300 ml). A 5 mol % excess of phthalic anhydride, based on hydroxyl groups, was used to promote high conversion. The mixture was stirred until all particles had dissolved (about 3 hours), then a catalytic amount of dimethylaminopyridine (DMAP) (0.327 g, 0.00267 mol) was added. The solution was refluxed under nitrogen for 18 hours. The modification reaction

was monitored by infrared and nuclear magnetic resonance spectroscopies to determine the percent conversion of hydroxyl groups to pendant acid groups. The solution was then poured into a Teflon boat and the solvent was evaporated. After 24 hours, the modified polyhydroxyether was placed in a vacuum oven at room temperature for 24 hours, then 60°C for 24 hours to remove most of the remaining solvent. After drying, about 7 % by weight THF remained in the sample, determined by NMR. The conversion was calculated by NMR to be 82 %.

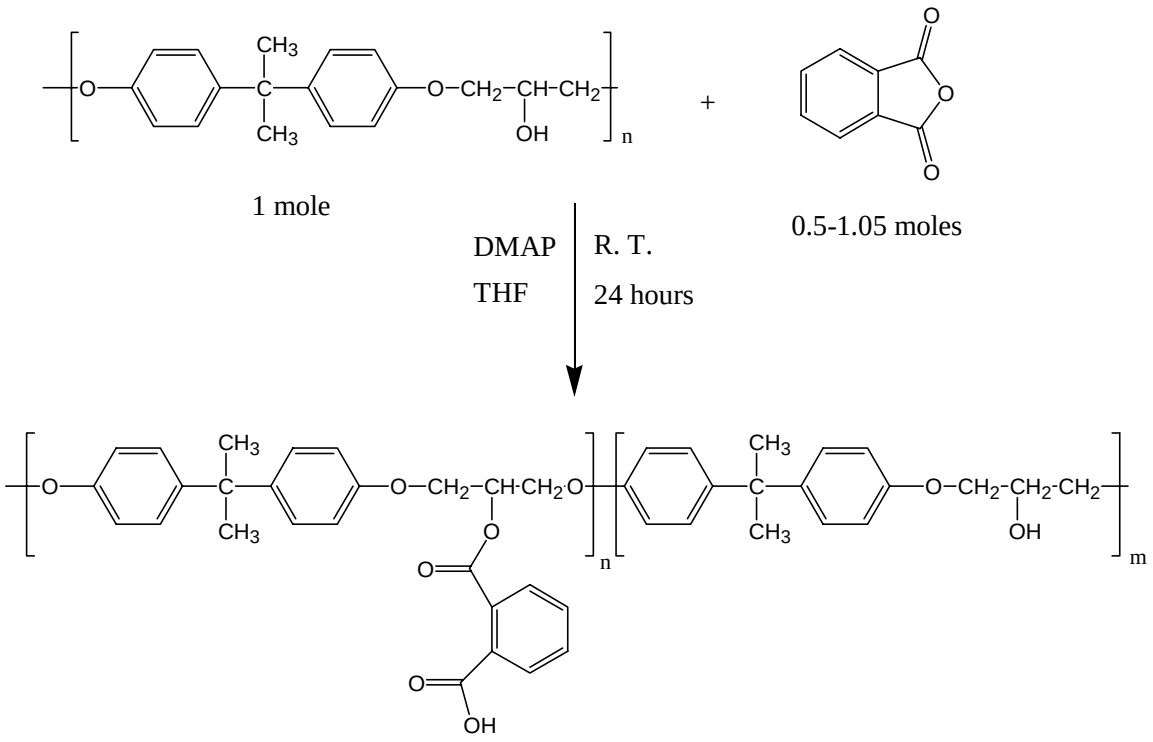

Figure 4.3: Modification of polyhydroxyether with phthalic anhydride.

4.2.3.6.2 With Succinic Anhydride

To a 500 ml round bottom flask was added polyhydroxyether (40.353g, 0.1419 mol), succinic anhydride (11.363 g, 0.1135 mol), and dry THF (250 ml). The mixture was stirred under nitrogen until all particles had dissolved (about 3 hours), then a catalytic amount of DMAP (0.869 g, 0.0071 mol) was added. The reaction was monitored by NMR to achieve the desired 50 % conversion. After stirring at room temperature under nitrogen for 20 hours the reaction was quenched by adding a few drops of water to

convert the remaining anhydride to acid. The polymer solution was precipitated into a 50/50 acetone/water solution to remove unreacted succinic acid, then dried in a vacuum oven at room temperature for ~72 hours. After drying, ~11 % by weight THF remained in the sample, determined by NMR. The conversion was calculated by NMR to be 63 %.

4.2.3.7 Synthesis of the Polyhydroxyether Salt of TMOPP

4.2.3.7.1 From Phthalic Anhydride (82 % Modification*)*

To a 500 ml beaker was added modified polyhydroxyether containing some unreacted phthalic acid from the modification reaction (7.546 g, 0.0205 eq. acid) and TMOPP (12.000 g, 0.0226 mol). A 10 % molar excess of the TMOPP was added to promote full conversion of the acid to the salt. THF (250 ml) and methanol (250 ml) were added to the beaker, and the solution was stirred for 3 hours, then poured into a Teflon boat and the solvent was evaporated. The film was placed in a vacuum oven and dried at room temperature for 24 hours then 60°C for 24 hours. The resulting material was soluble in methanol, indicating conversion to the salt.

4.2.3.7.2 From Succinic Anhydride (63% Modification)

To a 500 ml beaker was added the modified polyhydroxyether (4.439 g, 0.0072 eq acid) and TMOPP (4.022 g, 0.0076 mol). A 5 % molar excess of TMOPP was added to promote full conversion of the acid groups to the salt. THF (200 ml) was added to the beaker, and the solution was stirred for 3 hours, then poured into a Teflon boat and the solvent was evaporated. The film was placed in a vacuum oven and dried at room temperature for 48 hours then heated to 60°C for 24 hours. The resulting material was soluble in methanol, indicating conversion to the salt.

4.2.3.8 Preparation of Na^+ Phenolate Salts of Novolac

To a 100 ml beaker was added novolac (5.5234 g, 0.0531 eq phenolic hydroxyl), sodium hydroxide (1.0622 g, 0.0266 mol), and methanol (50 ml). The mixture was stirred for about 4 hours then poured into a Teflon boat to evaporate the solvent. All particles had dissolved within one hour and a dark red color appeared. The phenolate was then dried in a vacuum oven at 60°C for 24 hours.

4.2.4 Sizing Materials

4.2.4.1 Introduction

Seven different fiber sizings were investigated, two control sizings with no initiator and five latent initiator sizing materials (Figure 4.4). Sizing (1) was a commercial G' sizing obtained from Hexcel. Sizing solution (2) was prepared by dissolving a 2 wt % solution of the poly(amic acid) salt from tripropylamine in methanol. Sizing solution (3) was prepared by dissolving a 2 wt % solution of the poly(amic acid) salt from TMOPP in methanol. Sizing solution (4) was prepared by dissolving a 2 wt % solution of the fluorinated poly(amic acid) salt from TPP in methanol. Both sizings (3) and (4) were also analyzed from a dispersion of 20% methanol/80% water. Sizing solution (5) consisted of a 1.5 wt % aqueous solution of the potassium salt of a novolac with 50 % conversion of the phenolic hydroxyl groups to the salt. The sizing solution was prepared by adding the novolac (15.000 g, 0.1442 eq phenolic hydroxyl) to 1000 ml of water containing potassium hydroxide (4.046 g, 0.0721 mol). A small amount of acetone (80 ml) was added to dissolve the novolac, then evaporated before the sizing process. Sizing solution (6) consisted of a 2 wt % dispersion of the modified polyhydroxyether (from phthalic anhydride) in a 50/50 NMP/water solution. This was prepared by dissolving the modified polyhydroxyether in NMP, then slowly adding the water to the solution. Initially the solution appeared soluble but after several hours became cloudy. The dispersion was stable with stirring for 2 weeks. Sizing solution (7) consisted of a 2 wt % dispersion of a commercially modified polyhydroxyether in water.

4.2.4.2 Sizing Procedure for Sizing(2-4)

Fiber tow was sized on a custom made small scale sizing line from 2 wt. % solutions in methanol. The tows were dried by passing through a vented tower at room temperature, then wound onto a spool. The tow was then passed back through the vented tower heated to 260°C at a speed that produced a total of 3 minutes in the heated "drying" tower on the sizing line. This allowed for rapid on-line imidization of the poly(amic acid) salt sizing.

4.2.4.3 Sizing Procedure for Sizing (5)

Fiber tow was sized on a custom made small scale sizing line from the 1.5 wt % solution in water. The tow was dried by passing through a vented tower at about 180°C, then wound onto a spool.

2

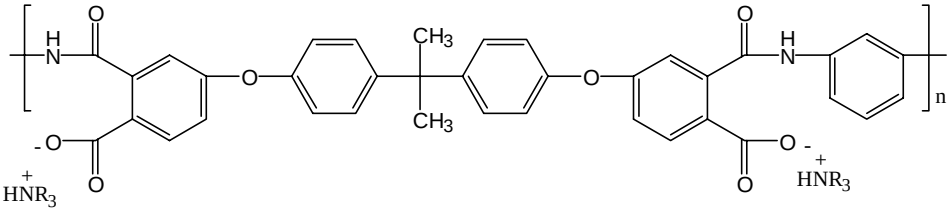

3

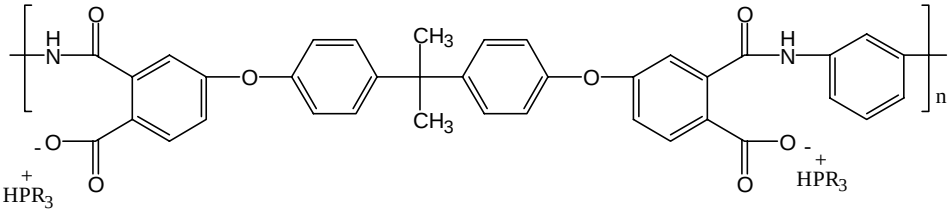

4

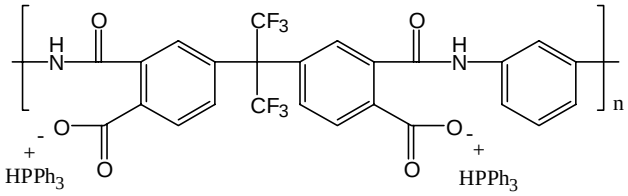

5

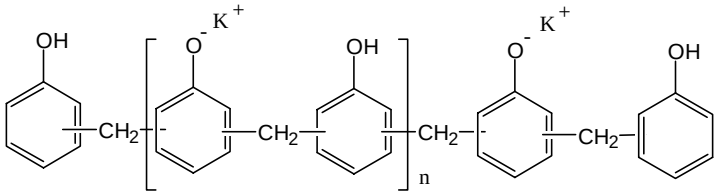

6

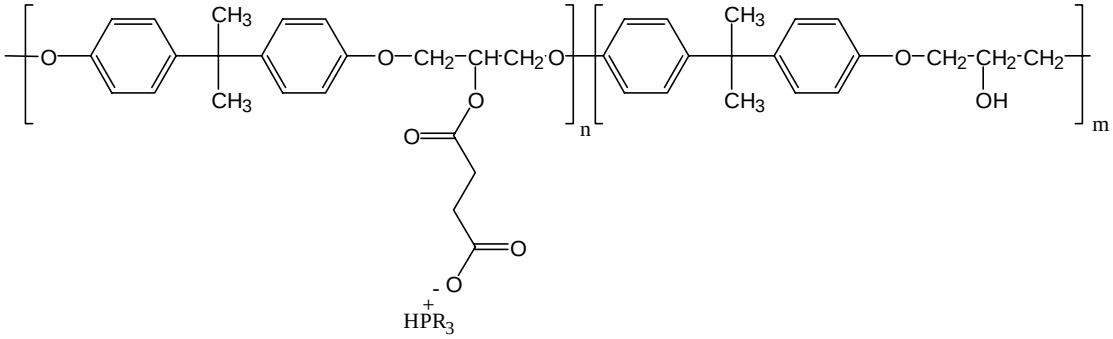

Figure 4.4: **Poly(amic acid) control (2) and latent initiator (3-6) sizing materials.**

4.2.4.4 Sizing Procedure for Sizings (6 & 7)

Fiber tow was sized on a custom made small scale sizing line from the 2 wt % solution in NMP/water for sizing (6) and a 2 wt % solution in water for sizing (7). The tow was dried by passing through the vented tower heated to 230°C at a speed that produced a total of 5 minutes in the tower, then wound onto a spool. This pretreatment results in light crosslinking of the polyhydroxyether sizings.

4.2.5 Measurements

4.2.5.1 Viscosity

Rheological experiments were carried out on a Bohlin VOR rheometer in continuous oscillation mode with a frequency of 1 Hz. Temperature control was accomplished with a Bohlin HTC. The auto-strain was set to control the torque to 25% of the maximum torque allowed. The maximum strain for the instrument was 0.25. Samples of about 0.7 g of dry powder were pressed into pellets then placed between the preheated 25 mm diameter parallel plates of the rheometer. The gap was closed to ~1 mm and the sides were scraped to remove excess sample before the run was begun. The samples used in these tests were prepared by solvent mixing.

4.2.5.2 Determination of Weight % Sizing on Fiber

In order to determine the weight percent sizing on the fiber for sizing solutions 2, 3 and 5, the sized fiber (before imidization in the case of sizings 2 and 3) was cut into sections, placed in 3 separate aluminum pans and weighed. The fibers were washed five times with methanol by soaking for about 20 minutes with agitation then pouring off the methanol to remove all sizing material. The aluminum pans containing the fiber were dried in a vacuum oven at ~80°C for 3 hours then re-weighed. The weight percent sizing in the composite, and the mole percent initiator based on epoxy content, were calculated based on a predicted fiber volume fraction of 60 % and the densities of the resin (1.23

g/ml) and fiber (1.80 g/ml) (equation 4.1). These calculations were used to determine the cure times needed to achieve 100% conversion.

Wt. % sizing in composite = wt. of fiber * wt.% sizing on fiber/wt. of composite (4.1)

In order to determine the weight percent sizing on the fiber for sizing solutions 6 and 7, the fibers were weighed, then heated to 600°C for 30 minutes under nitrogen. The fibers were then re-weighed to determine the weight loss. In addition a small sample of sizing was analyzed by TGA under the same conditions (600°C for 30 min under nitrogen) to determine the percent weight loss of the sizing under these conditions. From this analysis a corrected weight percent sizing on the fiber was determined (equation 4.2).

wt.% sizing = wt. of sizing burnt off * % wt. loss of sizing in TGA/initial fiber wt. (4.2)

4.2.5.3 Differential Scanning Calorimetry

A Perkin-Elmer DSC-7 was used for differential scanning calorimetry measurements. The DSC was calibrated with indium and zinc standards, and ice water was used as the coolant. Samples of ~15-20 mg were sealed hermetically in aluminum pans. Isothermal analyses were conducted by loading the samples at room temperature and heating to the load temperature at 300°C/min. The area of the exotherm was integrated to determine percent conversions from partial areas. Dynamic scans were performed at systematically varied heating rates (5°C/min to 20°C/min) from 50 to 270°C. Activation energies were obtained following ASTM E 698, with correction for the influence of heating rate on temperature. The correction was calculated by the deviation in the melting point of indium from the accepted value of 156.6°C. Half-life analyses according to the ASTM standard were conducted to determine the validity of the kinetic parameters. For the samples in which the half-life analysis proved the kinetic parameters to be invalid, rate constants were determined from isothermal scans. For half-life analyses, the samples were heated isothermally in the DSC at a time and temperature that was calculated, using the kinetic parameters, to promote 50 % conversion. Temperature scans were then performed on both the isothermally aged sample and uncured sample at 10°C/min from 50 to 270°C. The peak heights divided by the sample weights of the partially cured samples were compared to those of the uncured samples, in order to confirm or refute the validity of the apparent activation energies.

In order to determine the glass transition temperatures of the polyimides, samples were scanned from 50 to 300°C at 10°C/min then cooled rapidly (200°C/min), and scanned a second time from 50 to 300°C at 10°C/min. The glass transition temperatures were measured from the second heating scans.

4.2.5.4 Transmission Electron Microscopy

Single aramid fiber strands were coated with a 20-30 wt % solution of the sizing material to give a very thick film on the fiber. The fibers were then suspended in uncured phenolic/epoxy matrix material in a silicone mold. The mold was placed in the oven at 180°C for 1 hour and 220°C for 3 hours to fully cure the matrix resin. Cross-sections of single sized aramid fibers embedded in the phenolic-epoxy matrix material were microtomed at room temperature using a Reichert-Jung Ultracut-E ultramicrotome. The resulting sections were approximately 500-700 angstroms thick. The sections were collected on 300 mesh copper grids and analyzed using transmission electron microscopy (TEM). The TEM was performed using a Philips 420T TEM at 100 kV. Transmission Electron Microscopy was used to investigate the interaction of the fiber sizing with the matrix resin.

4.2.5.5 Hot-Melt Prepregging and Composite Fabrication

4.2.5.6 Composite Fabrication

A lab scale Model 30 prepregger manufactured by Research Tools Corporation, Ovid, Michigan was used for composite preparation. In this apparatus, a 12K sized AS-4 carbon fiber tow was passed through a wedge-slit die at the bottom of a heated resin pot containing the matrix resin. The wetted tow was then passed between a pair of flattening pins and around a guide roller before being wound on a drum. The flattening pins and the guide rollers were independently heated. Unidirectional carbon fiber prepregs were prepared with 65/35 wt/wt phenolic-epoxy resin (without added initiator in the resin), with the series of sizing materials, using the hot-melt technique. The set-point temperature of 140°C for the resin pot, flattening pin, and roller was determined by viscosity data. This high temperature was necessary to achieve a low enough melt viscosity to process the materials. Low melt viscosity of the resins was critical to permit

good wet-out of the reinforcing fiber tows and yield uniform resin content. The prepregs were then cut and placed in a metal mold and cured under pressure using a thermal cycle determined by the kinetic parameters.

4.2.5.7 Composite Fabrication for Transverse Flexural Strength

Panels for G_{1c} and G_{2c} tests were prepared by aligning 10-14 plies unidirectionally. The samples were then cured in a metal mold with a thermal cycle determined by the kinetic parameters. The 15.2 x 15.2 cm (6" x 6") panels were cut to ten 12.7 x 1.27 cm (5" x 0.50") specimens. The weight fraction of fibers in the composites ranged from 0.72 - 0.78.

4.2.5.8 Composite Fabrication for G_{1c} and G_{2c} Tests

Panels for G_{1c} and G_{2c} tests were prepared by aligning 10-14 plies unidirectionally with a 0.05 mm Teflon delamination tab placed midway through the laminate, with a length of 50.8 mm (2 in.) from the outside of the panel. The number of plies was determined based on the ply thickness after prepregging to achieve a specimen thickness close to 3.18 mm. The samples were then cured in a metal mold with a thermal cycle determined by the kinetic parameters. The 15.2 x 15.2 cm (6" x 6") panels were cut to six 12.7 x 2.0 cm (5" x 0.79") specimens. Prior to testing, an initial crack was generated about 1 mm past the Teflon delamination tab through the resin rich region. This crack was generated by placing the sample in a vise with the sample clamped approximately 1-2 mm below the end of the Teflon. A thin wedge was then placed in the crack and tapped lightly with a hammer until the crack propagated through the resin rich region (evidenced by a soft cracking noise). For the G_{1c} samples, piano stock hinges were adhered to the samples to facilitate loading. The piano hinges allowed free rotation and minimal stiffening of the specimens. The weight fraction of fibers in the composites ranged from 0.72 - 0.78.

4.2.5.9 Composite Fabrication for Fatigue Testing

Panels for quasi-static compression and fatigue tests were prepared by orienting 7 plies in a $(0°/90°)_{7s}$ lay-up with sizings (1) and (7). The samples were cured in the metal mold with a thermal cycle determined by the kinetic parameters. The 15.2 x 15.2 cm (6"

x 6") panels were then cut to five 15.2 x 2.54 (6" x 1") specimens with a 6.35 mm (0.25 in.) diameter hole in the center. Prior to testing, aluminum tabs with a spacing of exactly 2.54 cm (1 in.) were adhered to the samples to allow for attachment of the extensiometer. The weight fraction of fibers in the composites ranged from 0.65 - 0.70.

4.2.6 Composite Panel Characterization

4.2.6.1 C-Scan and SEM

The composite panels were C-scanned for overall quality using a Sonix model HF 1000 by a pulse-echo arrangement using a 15 MHz transducer with a focal length of 38.1 mm. Scanning electron photomicrographs, obtained from an ISI SX-40 SEM, were used to establish the void free nature of the composites and to confirm good resin distribution and fiber wet-out. SEM was also used to investigate the morphology of the sizing on the fiber prior to melt prepregging.

4.2.6.2 Dynamic Mechanical Analysis

Dynamic mechanical analyses were used to determine the glass transition temperatures of the cured composite panels. These measurements were performed using a Perkin-Elmer dynamic mechanical analyzer, model DMA-7. The T_g's were measured from the peaks in the tan δ curves. The tests were conducted using a 3-point bend set-up with rectangular specimens. The tests were run with tension control set at 120% using an amplitude of 9 μm. Samples were heated at 5°C/minute from 25 to 200°C. Two samples of each material were tested and averaged.

4.2.6.3 G_{1c} Testing

A double cantilever beam set-up with piano hinge tabs was used to measure G_{1c} of the composite panels according to ASTM D 5528-94a.[57] The specimens were placed in the grips of the Instron with a 1000 lb. load cell. Prior to loading, the sides of the specimens were painted white to facilitate analysis of the crack as it progressed along the length of the specimen. The specimens were then loaded at a crosshead rate of 0.5 mm/minute to allow crack propagation to be followed and recorded easily (Figure 4.5). The crack tip was marked and recorded as a function of the load and displacement. The crack length

was measured using a lighted magnifying glass and marked with a pencil. The crack propagation was recorded in ~2 mm increments for the first 15 mm, followed by ~5 mm increments until the crack had propagated at least 60-65 mm from the starter film. The samples were then unloaded at 5 mm/min.

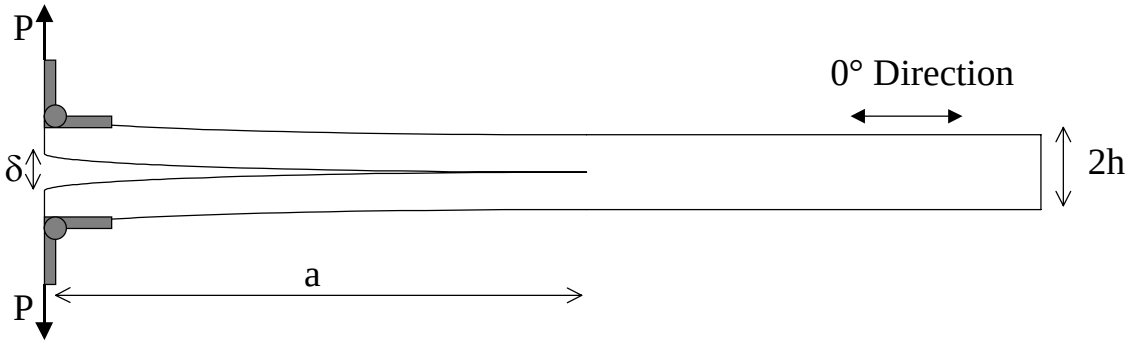

Figure 4.5: Loading geometry for mode I toughness.

4.2.6.4 G_{2c} Testing

G_{2c} tests were conducted with the end notched flexural specimen geometry in three-point bend loading according to the protocol for interlaminar fracture testing by the European group on fracture.[58] Initially the uncracked portion of each sample was tested using the three-point bend setup to determine the compliance (Figure 4.6a). For the initial compliance test of the uncracked length, a span of 75.8 mm was used with a testing rate of 0.5 mm/minute. The load/deflection data was obtained up to 0.25 kN to determine the compliance and this value was used in the calculation of bending stiffness for each specimen. Following the initial compliance measurement, the span was changed to 101.1 mm and the sample was positioned to give a/l = 0.5, where (a) was the pre-crack length and (l) was half the span. The sample was then loaded at 0.5 mm/minute until the crack propagated to the center of the sample (Figure 4.6b).

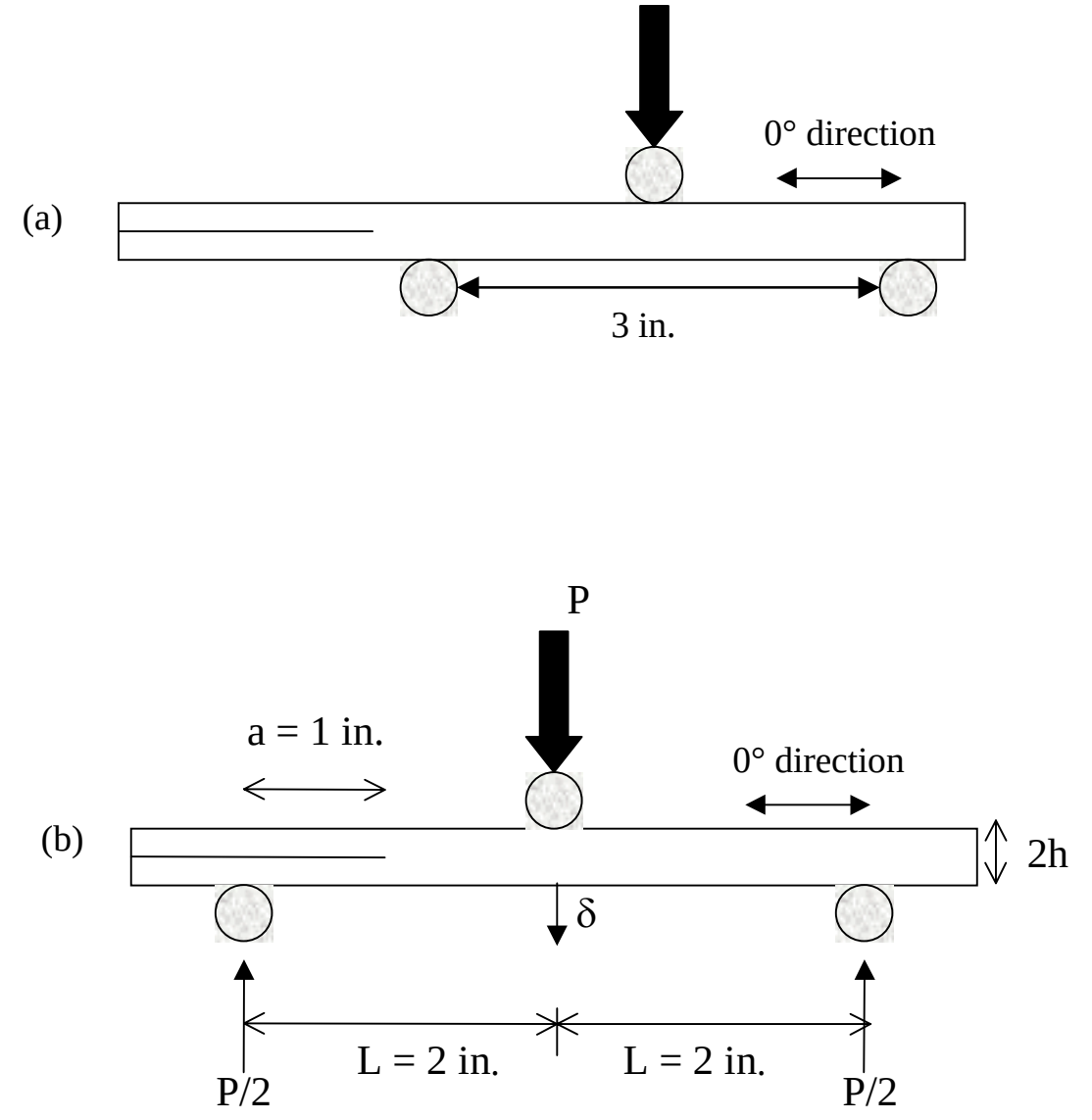

Figure 4.6: **Loading geometry for mode II toughness (a) initial compliance measurement and (b) loading to failure.**

4.2.6.5 Quasi-static Compression and Fatigue Testing

Quasi-static compression and fatigue tests were conducted on notched cross-ply specimens using an MTS test frame to assess composite strength and durability. Quasi-static compression tests were conducted with a loading rate of 200 pounds per second. Fatigue tests were conducted using a sinusoidal mode in fully reversed tension-compression (R = -1) at a frequency of 10 Hz. A 5.08 cm (2 in.) test gauge length was

used to ensure that buckling would not influence failure. The specimens were loaded into the grips at a grip pressure ranging from 1300 – 1700 psi depending on the composite thickness. Specimen alignment was ensured with a spirit level. Emory cloth (100 grit) was wrapped around the grip sections of the specimens to prevent slip and protect the sample. An MTS Model 632 extensiometer with a gauge length of 12.7 mm (0.5 in.) and a maximum strain limit of 4 % was used to monitor strain. Aluminum extensiometer tabs were used to hold the extensiometer's knife edges and the signal from the extensiometer was amplified using a 2310 Vishay Measurements Group amplifier. Lab View™ was used to acquire data on load, stroke, strain, and number of cycles.

4.2.6.6 Composite Moisture Uptake

Thin composite panels with sizings 1, 4, and 7 were prepared by melt prepregging followed by curing in a hot press. The thickness was controlled to close to 1.5 mm by preparing panels from 5 prepreg plys. The cured composites were cut to approximately 30 mm x 15 mm x 1.5 mm using a diamond saw. Moisture Uptake at 60°C was determined for these fiber reinforced composites with varied sizing. The samples were dried in a vacuum oven at ~ 140°C overnight then allowed to cool to room temperature in the vacuum oven. Two samples of each composition were accurately weighed then placed in vials filled with water at 60°C. The samples were periodically removed from the water, dried with a Kimwipe, then weighed in order to measure the moisture uptake. The sample weight and the amount of time elapsed from the start of the experiment were recorded. The time was normalized for the varied thickness by dividing by the sample thickness. For each composition, the average moisture uptake of the two samples was recorded and plotted vs. the square root of the time in hours divided by the thickness. Data was collected until the curves leveled off.

4.3 Results and Discussion

4.3.1 Introduction

Previous work has demonstrated that phenolic-epoxy networks with a ratio of three equivalents phenol to one equivalent epoxy (65 wt. % novolac-35 wt. % epoxy) have excellent mechanical properties. Because of the void free nature of these materials combined with tailored crosslink densities, these thermosets have toughness comparable to or exceeding untoughened aerospace epoxies (bisphenol-A based epoxy cured with diaminodiphenylsulfone) and much higher than commercial phenolic resol networks, while maintaining flame retardant properties approaching those of the pure phenolic materials. Therefore, the processing of these materials by commercial means such as prepregging and pultrusion was of great interest. Although solution processing from acetone was achievable, due to the high viscosity of the resin and the tendency toward premature curing in the processing step, a latent initiator was required for melt processing.

Melt processing requires the resin to have a viscosity of less than ~5 Pa*s to achieve good wet-out of the reinforcing fiber tows and yield uniform resin content. The temperature necessary to reach this low viscosity, determined by complex viscosity measurements, was 140-145°C. At these high temperatures, the resin cures quickly even with only small amounts of initiator (Figure 4.7). For example, the time below 5 Pa*s was only about 10 minutes with a triphenylphosphine concentration of 0.07 mol % (based on moles of epoxy). In addition, this amount of initiator required a cure time of about 2 hours at 180°C to achieve 100 % conversion. On the other hand, the resin without added initiator had a much longer processing window, greater than 1 hour (Figure 4.7), but required very long cure times at high temperatures to achieve complete cure (220°C for 4 hours).

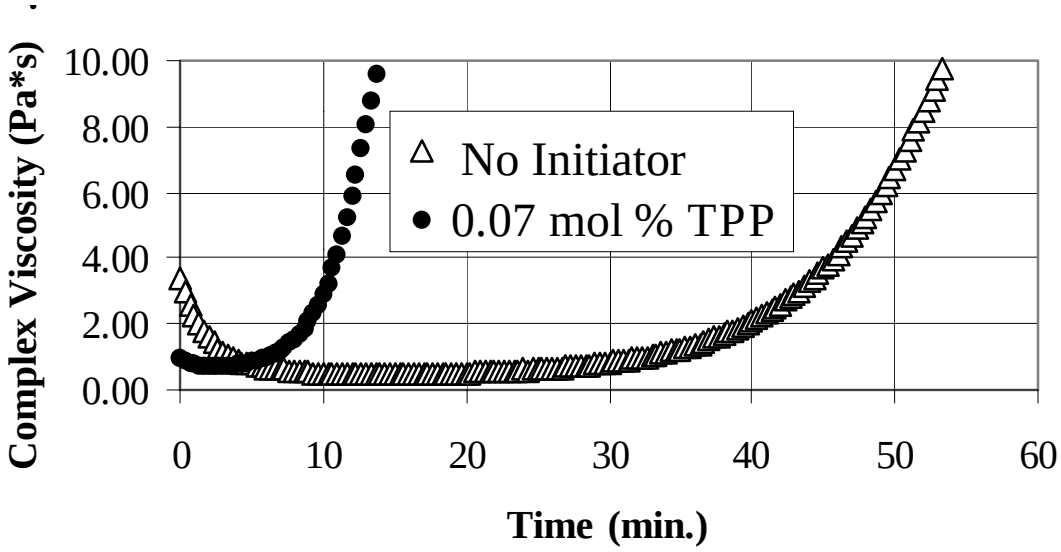

Figure 4.7: **Isothermal rheology at 145°C of an initiated versus uninitiated 65/35 wt/wt phenolic/epoxy reaction.**

In order to prevent premature curing during the processing stage, followed by rapid reaction during the curing stage, several latent initiators have been investigated. These initiators were designed to either be encapsulated into a fiber sizing in relatively high concentrations or grafted onto a polymer that was then sized onto the fiber. During melt prepregging, the hot resin was in contact with the fibers for less than 5 seconds before it was cooled. Therefore, initiators embedded in the fiber sizings did not cure the resin significantly during this processing stage, and thus, high concentrations of initiator could be used. This lead to rapid reaction during the cure cycle. This method may also be sufficient for other melt processes such as pultrusion.

4.3.2 Preparation of Latent Initiators

Three types of latent initiators to be introduced as fiber sizings have been investigated to assess the feasibility of melt processing phenolic-epoxy matrix resins. The first type of latent initiator was a polymeric sizing material with a sequestered monomeric phosphine initiator. The first of this type of latent initiator had tris(2,4,6-trimethoxyphenyl)phosphine (TMOPP) dispersed in a 22,000 g/mol $<M_n>$ Ultem™ type polyimide. In order to use the polyimide as a sizing material, it had to be sized by way of a soluble precursor, since polyimides are highly insoluble. In order to achieve a soluble

precursors, Ultem™ type poly(amic acid) was synthesized in tetrahydrofuran (THF) at room temperature then dried by removing the solvent. One disadvantage of the poly(amic acid) is it is hydrolytically unstable, and must be stored under dry conditions. The molecular weight drops significantly with exposure to moisture in the air or water. However, the poly(amic acid) can be reacted with a base to form a water soluble hydrolytically stable material.[76] Water solubility was achieved with tripropylamine as the base, but only water dispersibility could be achieved with larger more hydrophobic bases. Therefore, the material can be sized onto the fiber from a solution or dispersion depending on the type of base used. It can then be imidized in the drying tower to produce the polyimide sizing. A second advantage of sizing from the salt form is that rapid imidization in less than three minutes at 220-250°C can be achieved, whereas imidization of the poly(amic acid) is somewhat slower.[77,78]

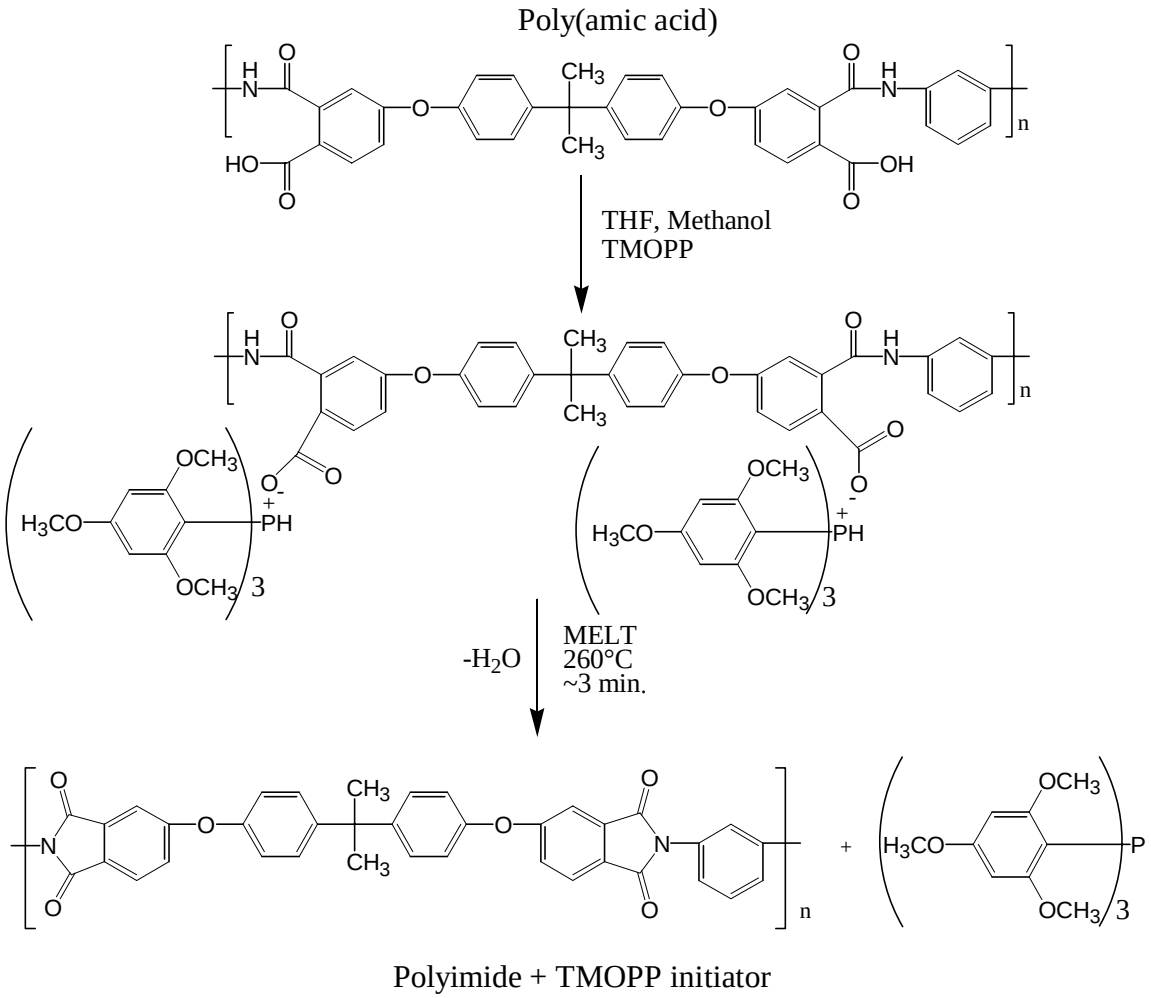

Figure 4.8: Formation of a polyimide sequestered latent initiator.

To prepare the latent initiator sizing, TMOPP was reacted with an Ultem™ type poly(amic acid) to form a poly(amic acid) salt (Figure 4.8). The salt was soluble in methanol and dispersible in a 15/85 wt/wt NMP/water mixture and thus the sizing operation could be conducted with either of these solvents. TMOPP was chosen as the base due to it's sufficiently strong basicity to quantitatively form the poly(amic acid) salt and also because of its high vaporization temperature. It was important that the phosphine remain in the polyimide and not volatilize at the imidization temperature. Attempts to form the poly(amic acid) salt using TPP as the base were unsuccessful due to the pK_a of the poly(amic acid). The poly(amic acid) salt eliminated the phosphine and cyclized to the corresponding polyimide when heated at 260°C for 3 minutes. Therefore the phosphine initiator became sequestered in the high molecular weight polyimide sizing material (Figure 4.8). Complete encapsulation is probably not important, because the initiator has minimal contact with the resin prior to the curing stage.

A control polyimide sizing with no initiator was also prepared to allow for accurate determination of the effects of initiator on the properties of the composites. The control polyimide sizing was prepared by synthesizing the Ultem poly(amic acid) salt with tripropylamine as the base. During imidization in the tower all of the tripropylamine should volatilize, leaving a polyimide sizing with no initiator. In addition, the amount of initiator in the sizing can be controlled by using a combination of TMOPP and tripropylamine as the base. Since all the tripropylamine will volatilize during imidization only the TMOPP will remain to initiate the phenolic/epoxy reaction.

Due to the reduced availability and high cost of the tris(2,4,6-trimethoxyphenyl)phosphine (TMOPP), it was of interest to develop a similar polymeric initiator with sequestered triphenylphosphine (TPP). In order to achieve this goal a fluorinated poly(amic acid) was synthesized. The electron withdrawing 6F group decreased the pK_a of the carboxylic acid to promote reaction with triphenylphosphine. This type of initiator exhibited comparable kinetics to the Ultem™ type polyimide with TMOPP. This fluorinated polyimide sizing may also have an effect on moisture uptake at the interface due to it's hydrophobic nature.

The second type of latent initiator was a polyhydroxyether with carboxylate grafts. This type of material is used as a commercial sizing material to improve processability and fiber matrix adhesion in some composites.[79] Carboxylate grafts have been added commercially to promote dispersibility in water. These same grafts that aided in water dispersibility acted as initiators for the phenolic/epoxy reaction, enabling use of this sizing as an initiator. This type of polymeric sizing would have multiple initiators on one chain. The polymer that was investigated was the TMOPP salt of a commercial bisphenol-A based polyhydroxyether modified with carboxylic acid grafts (Figure 4.9). TMOPP was chosen as the counter ion because it was a strong enough base to react with the acid groups, but a weak enough nucleophile that it did not attack the ester functionality and cleave the grafted carboxylic acid. Triphenylphosphine was not a strong enough base to react with the acid groups, and bases such as NaOH and KOH resulted in cleavage of the ester group. The initiator concentration in the polymer can be controlled by controlling the amount of carboxylate grafts added to the polyhydroxyether. This was controlled by the amount of anhydride added, as well as the time and temperature of the reaction. The percent conversion was monitored by NMR during the reaction to achieve the desired amount of carboxylic acid grafts (Figure 4.9). The amount of hydroxyl groups that have been reacted with the anhydride to generate carboxylic acid grafts was determined by taking the ratio of peak b to peak a in the ^{1}H NMR spectra (Figure 4.9). The polyhydroxyether salt prepared as a latent initiator was soluble in methanol and dispersible in a 50/50 NMP/water mixture. This particular material had about 82 % conversion of hydroxy groups to carboxylate grafts. The solubility in water could be improved by increasing concentration of carboxylate grafts, or by using a smaller, less hydrophobic counter ion. This sizing/initiator combination was of particular interest since similar polyhydroxyether sizing materials have been shown to improve composite properties in other systems.[79]

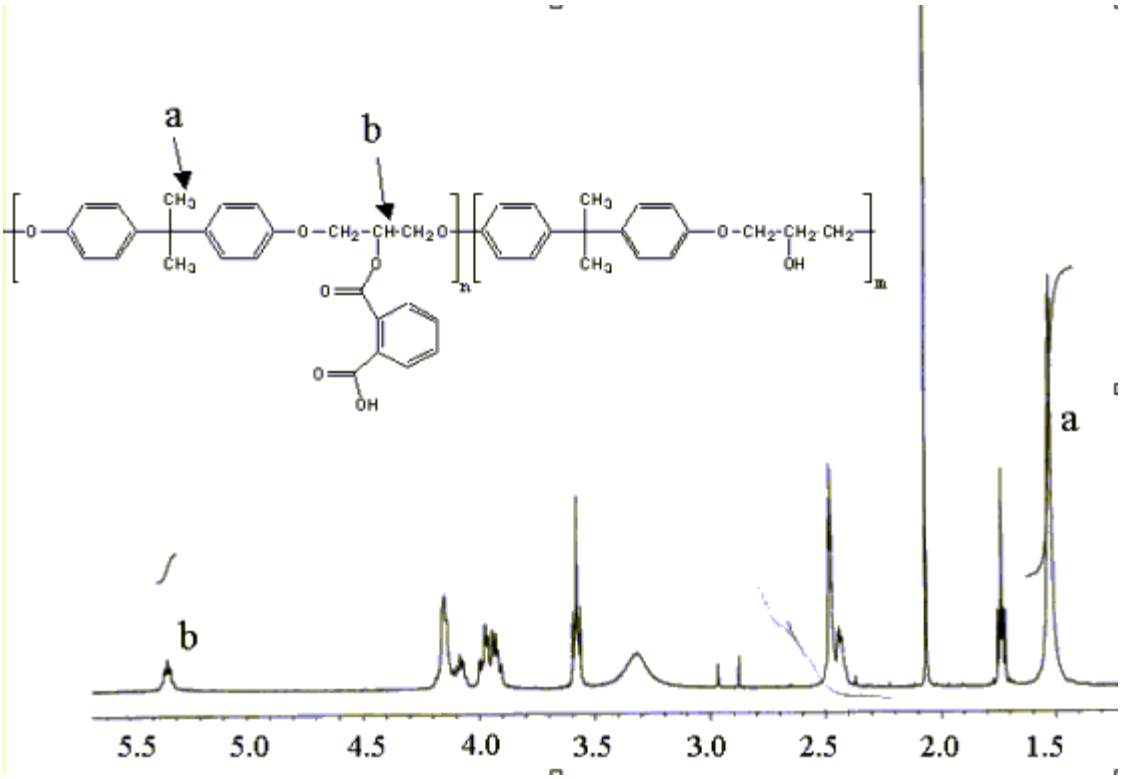

Figure 4.9: NMR of polyhydroxyether modified with phthalic anhydride.

The third type of latent initiator investigated was a phenolate salt of novolac (Mn ~ 760 g/mol) resin. This material was cost effective and did not require co-solvents or high temperatures during the sizing process. The novolac phenolate with 1 phenolate/1 phenol was soluble in water and therefore was sized from an aqueous solution. The phenolate salt can be formed by reacting the phenolic groups with a strong base such as NaOH, or KOH. This produced a phenolate initiator with a small inorganic counter ion. Attempts to form the TMOPP salt of the phenolic novolac were unsuccessful. It was evident that TMOPP was not a strong enough base to form the phenolate.

4.3.3 Kinetics

It was necessary to study kinetic parameters of the phenolic-epoxy network forming reactions to relate effects of initiator structure to the rate of reaction. A detailed understanding of the kinetics with different initiator systems was important for the design

of latent initiators as well as for determining appropriate cure cycles for the composite panels cured with the latent initiators.

Kinetic parameters were calculated from dynamic DSC data using the procedure outlined in ASTM E 698.[80] The standard is based on a method developed by Ozawa[81] for determining apparent activation energies, and relates the heating rate (B) to the temperature of maximum reaction rate (T_{max}). For each sample several heating rates were used and the peaks shifted accordingly (Figure 4.10). Activation energies were calculated at the appropriate initiator concentrations using equation 4.3 where d(log B)/d(T_{max}) was determined from linear regression, D is determined from the standard based on the value of E_a/RT, B is the heating rate, and T_{max} is the temperature at maximum reaction rate. The activation energies were refined until self-consistent using a process outlined in the ASTM standard. Pre-exponential factors (A) where calculated based on the ASTM standard (Equation 4.4).

$$E_a = -2.303\ R/D^*\ d(\log B)/d(T_{max}) \quad (4.3)$$

$$A = BE_a/RT_{max}^2(\exp(-E_a/RT_{max})) \quad (4.4)$$

With these kinetic parameters, rate constants were calculated utilizing the temperature dependence of k'(Equation 4.5).

$$k' = A\ \exp(E_a/RT) \quad (4.5)$$

The percent reaction conversion versus time was predicted over a range of temperatures based on the kinetic parameters for each initiator. For higher initiator concentration these percent conversion versus time predictions were comparable to conversion versus time determined by isothermal differential scanning calorimetry using a partial areas calculation (Figure 4.11).

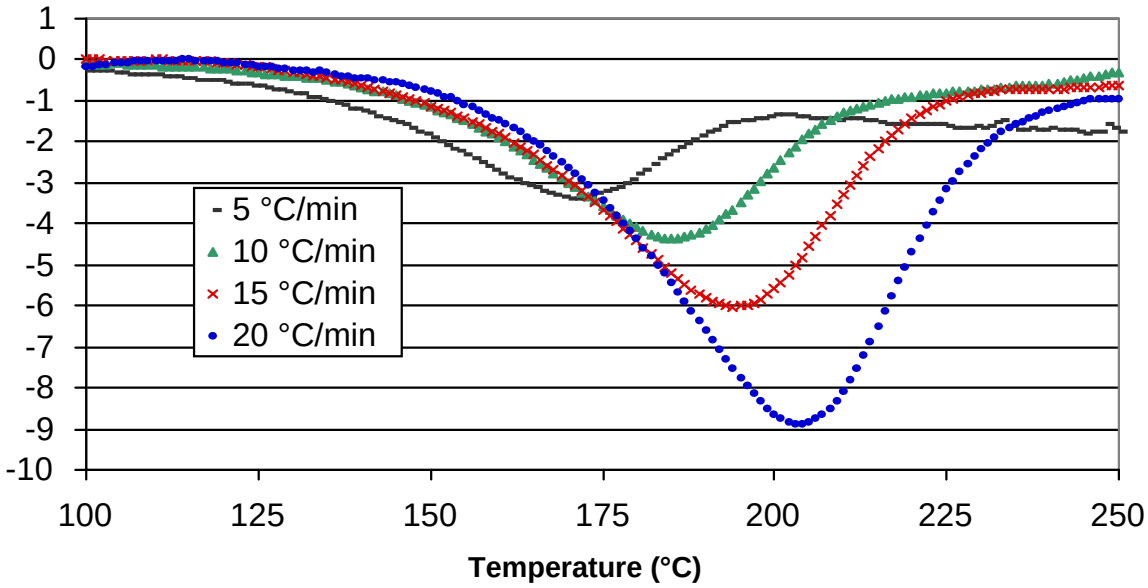

Figure 4.10: **Sample DSC curves used in activation energy calculations.**

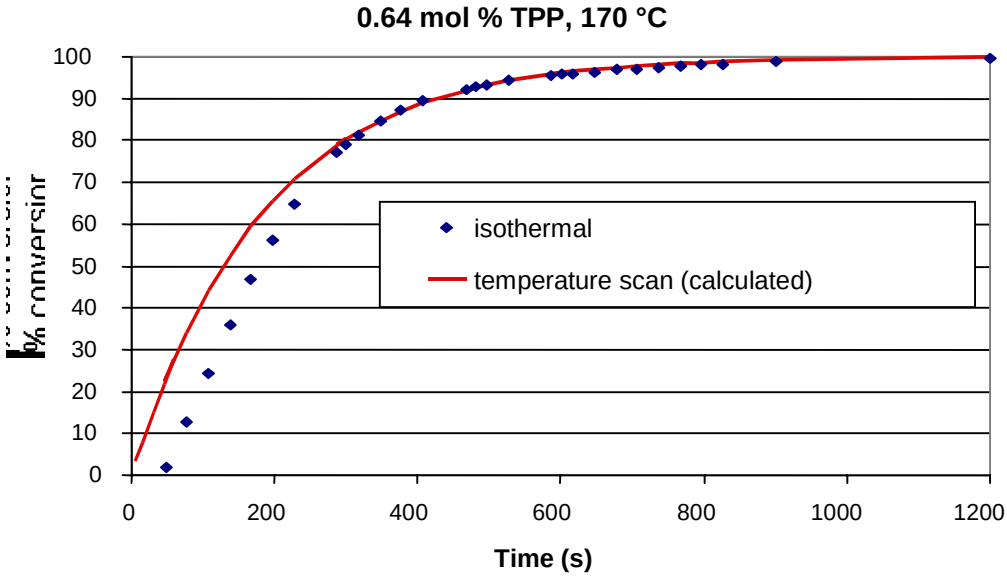

Figure 4.11: **Percent conversion of epoxy versus time for 0.65 mole % of TPP based on epoxy (comparison of results from isothermal DSC vs. those predicted from kinetic parameters).**

The validity of the kinetic parameters (E_a and A) for each type of initiator was established by half-life analyses according to the ASTM standard. Samples were reacted isothermally to a predicted 50 % conversion at a temperature at which the reaction rate was relatively slow to allow good control of the reaction. The times and temperatures needed to achieve 50 % conversion were determined from the rate constants, which were calculated from the activation energies and pre-exponential factors. According to the standard, samples achieving within 10 % of the desired 50 % conversion based on peak heights, are considered to have valid kinetic parameters (Table 4.1). For the samples in which the E_a and A were determined to be invalid, isothermal differential scanning calorimetry was used to determine the rate constants and reaction conversion versus time.

Table 4.1: Half-life analysis of phenolic/epoxy melts (65 wt. % phenolic novolac / 35 wt. % epoxy) with latent nucleophilic initiators.

Latent Nucleophilic initiators	**Initiator Type**	**Percent Conversion (with target 50 %)**	**Validity of Kinetic Parameters**
Triphenylphosphine	Monomer	52	Valid
Polyimide encapsulated TMOTPP	Encapsulated Monomer	48	Valid
Acetic acid salt (Na+)	Monomer	48	Valid
Acetic acid salt (TMOTPP)	Monomer	56	Valid
Modified polyhydroxyether salt (TMOTPP)	Polymer	63	Not Valid
Phenolate (Na+)	Monomer	48	Valid
Novolac Phenolate (Na+)	Oligomer	38	Not Valid

The reaction mechanism of a phenolic novolac with epoxy in the melt initiated by triphenylphosphine has been investigated previously for electronic applications.[14] In this reaction the triphenylphosphine can ring open the epoxy generating a zwitterion. In the

presence of phenol groups, a rapid proton transfer from the phenol to the secondary hydroxyl occurs, generating a phenolate ion (Figure 4.12a). This phenolate ion can then either react with the electrophilic carbon to regenerate the triphenylphosphine or react with another epoxy group (Figure 4.13).[14] The phenolate nucleophile is the propagating species of the reaction, and it's concentration is assumed to be constant once all the initiator has reacted. It is reasonable to expect TMOPP to react by a similar mechanism as the triphenylphosphine. Another type of initiator for the phenolic-epoxy reaction is the salt of a carboxylic acid. The carboxylate can ring open the epoxy creating a zwitterion, then rapid proton transfer from a phenolic group to the secondary hydroxyl will generate the phenolate nucleophile (Figure 4.12b).

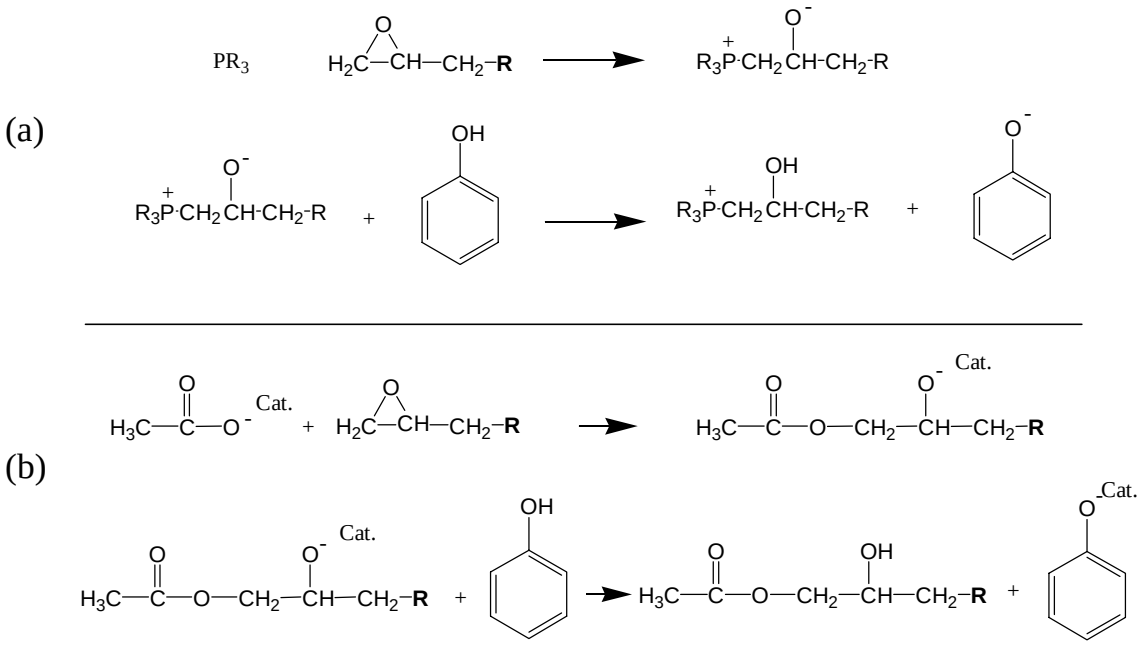

Figure 4.12: Phenolic/epoxy reaction initiation (a) initiated by a phosphine and (b) initiated by a carboxylate anion.

Mechanism 1

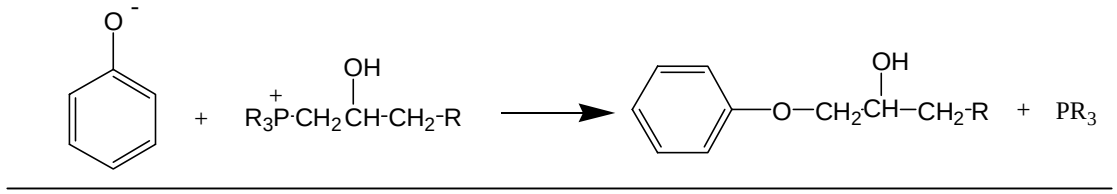

Mechanism 2

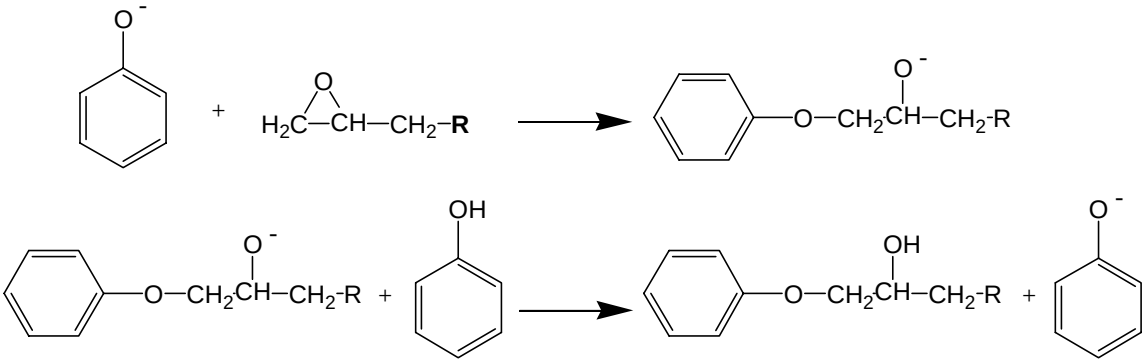

Figure 4.13: Phenolic/epoxy reaction propagation

The kinetics of the latent initiators were strongly dependent on the initiator structure. Both the counter ion type and the number of initiation sites per chain affected the kinetics of the phenolic epoxy reaction. These two effects were analyzed by studying a series of different initiators.

A series of four similar initiators with different counter ions were used to investigate the effect of counter ion size and type on the kinetics. These included the acetate salts of sodium, rubidium, cesium, and TMOPP-H. There was no apparent effect of the counter ion size on the activation energies or rate constants within the series of inorganic counter ions investigated (Table 4.2). On the other hand, the rate constants were significantly higher with the phosphonium counter ion, although the activation energies were similar. This suggested a weaker ion pair once the phenolate propagating species is formed, which could be a result of the very large increase in counter ion size or a difference in charge distribution.

Table 4.2: Kinetic parameters for phenolic/epoxy melts (65 wt.% phenolic novolac / 35 wt.% epoxy) containing 2.0 mole % initiator based on moles of epoxy (effect of counter ion structure on rate of reaction).

Initiators	E_a (KJ/mol)	k (s^{-1}) at T =180°C	Time to 99% Conversion at T = 180°C (min)
Acetate salt (Na+)	66	5.3×10^{-3}	15
Acetate salt (Rb+)	63	4.9×10^{-3}	16
Acetate salt (Cs+)	68	5.4×10^{-3}	14
Acetate salt (TMOPP-H)	66	1.1×10^{-2}	7

Several types of latent initiators were investigated for the phenolic-epoxy matrix composites, ranging from partially encapsulated small molecules (e.g., encapsulated TMOPP) to oligomeric (e.g., novolac phenolate) and polymeric (e.g., succinic acid modified polyhydroxyether) species. Reaction kinetics with the oligomeric and polymeric initiators, which also had multiple initiator sites on the same chain, were directly compared with monomeric analogues. In addition, effects of encapsulation were probed by comparing rates with TMOPP embedded in polyimides versus free TMOPP (Table 4.3).

Table 4.3: Kinetic parameters for phenolic/epoxy melts (65 wt.% phenolic novolac / 35 wt.% epoxy) containing 2.0 mole % initiator based on moles of epoxy (effects of initiator type on kinetic parameters).

Initiators	E_a (KJ/mol)	k (s^{-1}) at T =180°C	Time to 99% Conversion at T = 180°C (min)
TMOTPP	70	2.0×10^{-2}	4
Polyimide encapsulated TMOTPP	69	8.3×10^{-3}	9
Acetic acid salt (TMOTPP)	66	1.1×10^{-2}	7
Modified polyhydroxyether salt (TMOTPP)	------	2.5×10^{-3}	31
Phenolate (Na+)	63	6.6×10^{-3}	12
Novolac Phenolate (Na+)	------	3.2×10^{-3}	24

A comparison of the rate of reaction at 180°C with the sodium salt of novolac versus the sodium salt of phenol indicated that the reaction rate was slower for the oligomeric material at the same anion concentration (Figure 4.14). With 2.0 mol % initiator, the material initiated by the sodium salt of phenol reached 99 % conversion in 12 minutes, whereas it took 24 minutes for the material initiated by the sodium salt of novolac to reach 99 % conversion. In addition, doubling the concentration of the oligomeric initiator showed a slight rate increase, but the rate did not double as would be expected for a monomeric initiator. A similar comparison between the TMOPP-H salt of the carboxylate modified polyhydroxyether and the TMOPP-H salt of acetate indicated that the reaction rate was also much slower with the polymeric initiator (Figure 4.15). With 2.0 mol % initiator the material initiated by the TMOPP-H salt of acetate reached 99 % conversion in 7 minutes, whereas the material initiated by the TMOPP-H salt of the modified polyhydroxyether required 31 minutes to reach 99 % conversion.

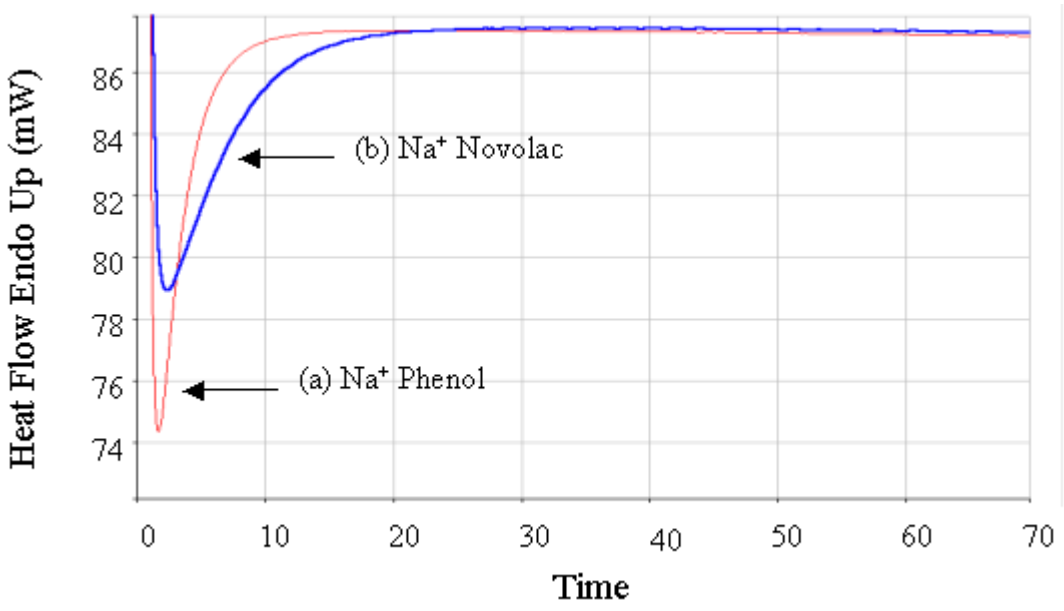

Figure 4.14: **Isothermal DSC kinetics of the phenolic epoxy reaction initiated by 2.0 mol % of (a) the sodium salt of phenol and (b) the sodium salt of novolac.**

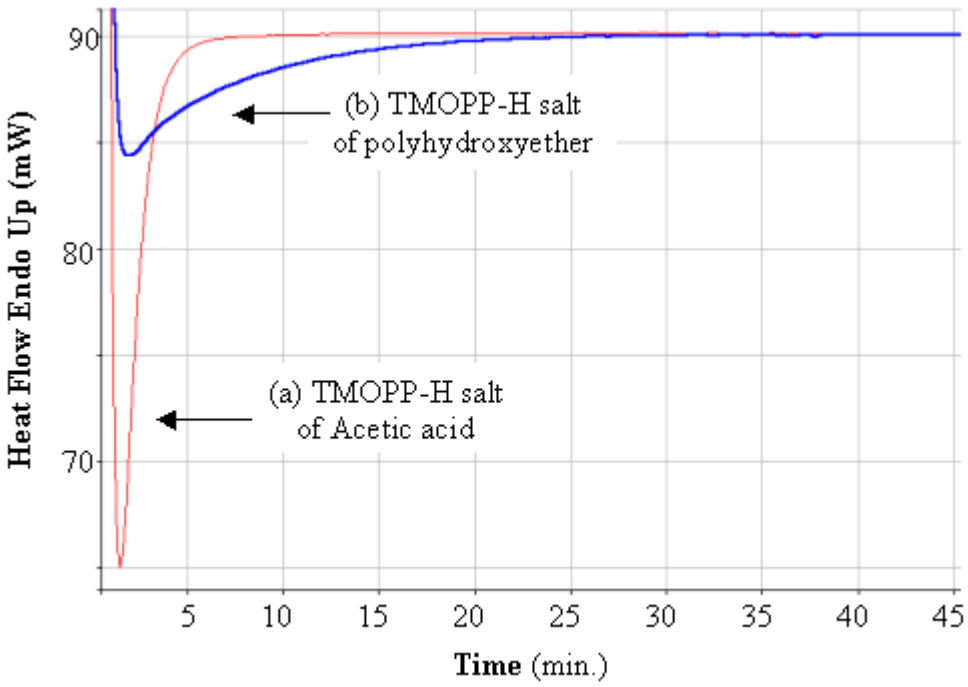

Figure 4.15: **Isothermal DSC kinetics of the phenolic epoxy reaction initiated by 2.0 mol % of (a) the TMOPP-H salt of acetate versus (b) the TMOPP-H salt of modified polyhydroxyether.**

It should also be noted that kinetic parameters (determined from the ASTM method previously described) were "invalid" with the oligomeric and polymeric initiators (Table 4.1). This also indicated that there was some effect on the kinetics when a polymeric initiator was used as opposed to a monomeric initiator of the same type and concentration. For this reason, kinetics with the polymeric initiators were investigated by isothermal DSC analysis as opposed to the dynamic method.

The comparison between the polyimide encapsulated TMOPP and the free TMOPP indicated some drop in the rate due to encapsulation in the polyimide, but no significant change in the activation energy (Table 4.3). This was probably a result of the low T_g of the polyimide blended with high initiator concentrations. The T_g of the polyimide (22,000 g/mol) with 1 mole of TMOPP per imide group was plasticized from 213°C to 98°C. This should allow significant diffusion of the TMOPP at the 180-200°C cure temperatures of the phenolic epoxy networks.

4.3.4 Diffusion

Some important consideration in understanding effects of embedding the matrix cure initiators in the fiber sizing are diffusion issues. The time required for an initiator to diffuse from its initial location at the fiber surface throughout the matrix resin at the cure temperature becomes a critical parameter. The DSC cure kinetics described above were conducted on mixtures of initiator and resin powders. During the kinetic measurements, these heterogeneous powder mixtures were heated (without shear mixing) to afford homogeneous melts. The kinetic analyses with the polyimide encapsulated monomeric TMOPP initiator suggested that this initiator rapidly diffused into the matrix resin at 180°C. This was evident by the fact that the rate constants with the *encapsulated* TMOPP were only slightly lower than with the *free* TMOPP and the activation energy was equivalent (Table 4.3).

Diffusion rates of both a monomeric initiator (TMOPP) and a polymeric initiator (the TMOPP-H salt of modified polyhydroxyether) were estimated from the Lusis-Ratcliffe equation (Equation 4.6).[82] The total time for diffusion over the predicted distance between fibers (assuming 8 micron diameter fibers, 60 volume % fiber in the composite and 5 microns between fibers) was estimated to be 5 seconds for the monomeric initiator and 41 seconds for the polymeric initiator at a cure temperature of 180°C. This suggests that initiators may effectively diffuse throughout the resin during composite processing at early stages of the cure cycle.

$$D^{\circ}_{AB} = \frac{(8.52 \times 10^{-8}\ T)}{\eta_B\, V_B^{1/3}} \left[1.4 \left(\frac{V_B}{V_A} \right)^{1/3} + \frac{V_B}{V_A} \right] \qquad (4.6)$$

Resin parameters for a 65/35 wt/wt novolac/epoxy composition were assumed as follows. The average molecular weights of the epoxy and novolac components were 374 and 750 g/mole respectively, resulting in an average molecular weight of (0.65)(750) + (0.35)(374) = 618 g/mole. Assuming the density of the resin (uncured) was 1.1 g/cm^3, the molar volume (V_B) of the resin is (618 g/mole)/(1.1 g/cm^3) = 562 cm^3/g. Tris(2,4,6-trimethoxyphenyl)phosphine has a molecular weight of 540 g/mole and the density was

assumed to be 1 g/cm^3. This affords a molar volume of TMOPP (V_A) of (540 g/mole)/(1 g/cm^3) = 540 cm^3/g. The resin viscosity at 453 K (η_B) was assumed as 1000 cps and the cure temperature (T) considered was 453 K. This results in estimation of the diffusion coefficient ($D°_{AB}$) for the TMOPP through the resin at this temperature to be 1.15 x 10^{-8} cm^2/sec. The following parameter were used to estimate a diffusion time for a carboxylate modified polyhydroxyether through the novolac/epoxy resin. The modified polyhydroxyether molecular weight was assumed to be 49,000 g/mol. and the polymer density was estimated at 1 g/cm^3. The molar volume (V_A) was then calculated as (49,000 g/mole)/(1 g/cm^3) = 49,000 cm^3/g. The viscosity of the resin at 453 K (η_B) was assumed as 1000 cps and the cure temperature (T) of 453 K was used to estimate the diffusion coefficient ($D°_{AB}$) of 1.53 x 10^{-9} cm^2/sec.

In an idealized model of a fiber reinforced composite with 60 vol. % fiber and a fiber diameter of 8μ, there is about 5 μ between fibers. If one assumes that an initiator has to travel half the distance between fibers at the widest point, then it has to travel 2.5 μ. Diffusion time (t_{diff}) = (distance)^2/($D°_{AB}$) so the predicted required time for the initiator to diffuse over this distance is: (TMOPP) t_{diff} = (2.5 x 10^{-4} cm)^2/1.15 x 10^{-8} cm^2/sec = 5.4 sec and (carboxylate modified polyhydroxyether) t_{diff} = (2.5 x 10^{-4} cm)^2/1.53 x 10^{-9} cm^2/sec = 41 sec. One assumption is that the fiber volume fraction before curing is close to that after curing. This is true if only minimal amounts of resin are squeezed out during the cure.

These calculations suggested that the slower curing rates of the phenolic-epoxy network with polymeric initiators were not a result of slow diffusion of the initiators. The polymer should be dispersed throughout the resin within 41 seconds. Therefore the slower rate may have been a result of a localized initiation around the polymer, as opposed to random initiation throughout the resin.

Diffusion of the sizing material into the matrix resin was also analyzed by transmission electron microscopy (TEM) of sized single aramid fibers imbedded in the phenolic epoxy matrix resin. Aramid fibers were used instead of carbon fibers because the carbon fibers were very brittle and tended to shatter during microtoming. The single fibers were coated with a very thick coating of sizing material in order to see the sizing, with a thin coating no sizing was observed. Both the polyimide and the

polyhydroxyether sizings were investigated. The polyimide sizing with the TMOPP initiator was compared to the polyimide with no initiator. In both samples an interface between the fiber and the matrix was observed as long as a thick film of sizing was coated on the fiber (Figure 4.16). This interface appeared similar for the two samples indicating that addition of the initiator to the sizing did not have a significant effect on the interface morphology compared to the polyimide sizing with no initiator. The white region in the TEM of the sample with no initiator was a result of the fiber falling out of the sample due to the very thin slicing. The modified polyhydroxy ether sizing was also investigated. Due to the crosslinking reaction of the polyhydroxy ether at high temperatures the diffusion of the polyhydroxyether sizing away from the fiber was dependent on the time and temperature at which the polyhydroxyether was pretreated. The polyhydroxyether pretreated for 8 minutes at 200°C was compared to the polyhydroxyether pretreated for 30 minutes at 180°C (Figure 4.17). The interface in the TEM micrograph of the material pretreated for only 8 minutes at 200°C was evident but very difficult to see; whereas, the interface of the polyhydroxyether pretreated for 30 minutes at 180°C was much clearer. Therefore, the time and temperature that the polyhydroxy ether was pretreated affected the interfacial morphology of the composites. This was considered in preparation of latent initiator sizing materials for phenolic/epoxy composites. A pretreatment of 5 minutes at 250°C was used to achieve light crosslink of the sizing material. More than 5 minutes was not considered because it would drastically slow the on-line sizing process.

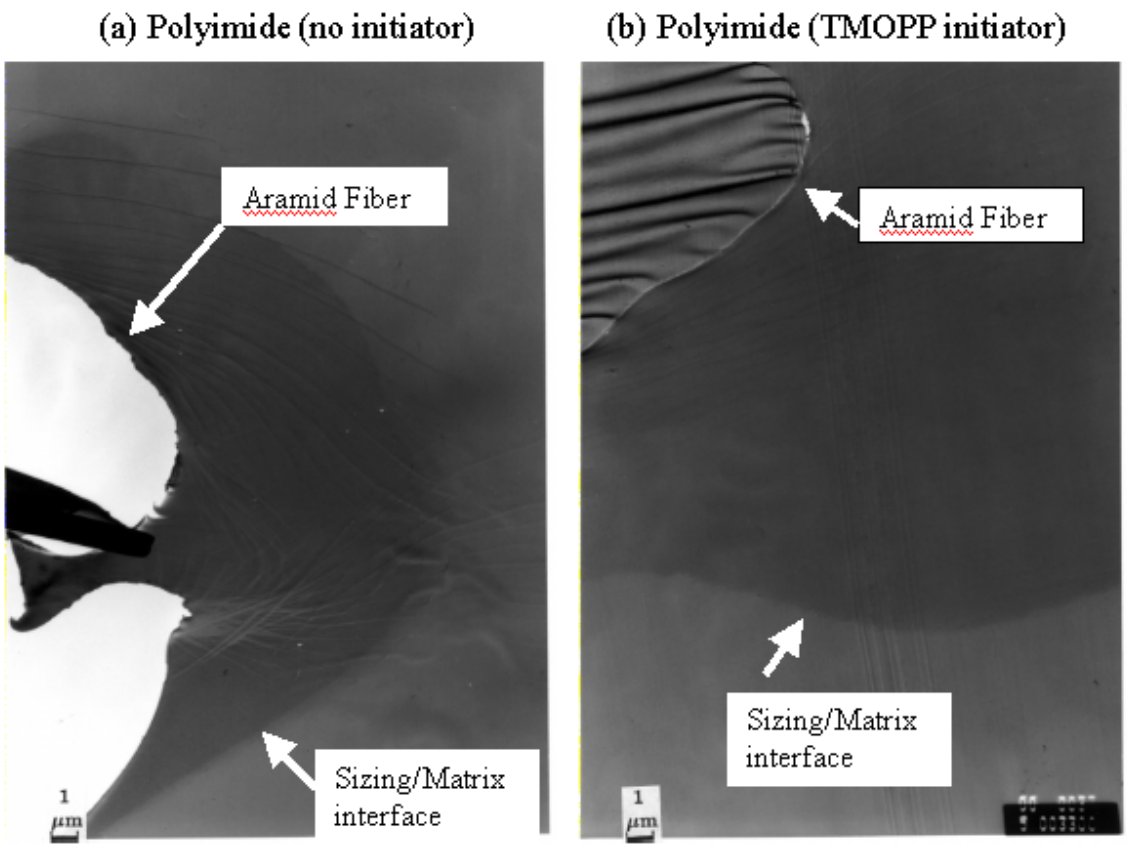

Figure 4.16: **TEM images of a single aramid fiber coated with a polyimide sizing embedded in phenolic/epoxy matrix material (a) polyimide with no initiator and (b) polyimide with TMOPP initiator.**

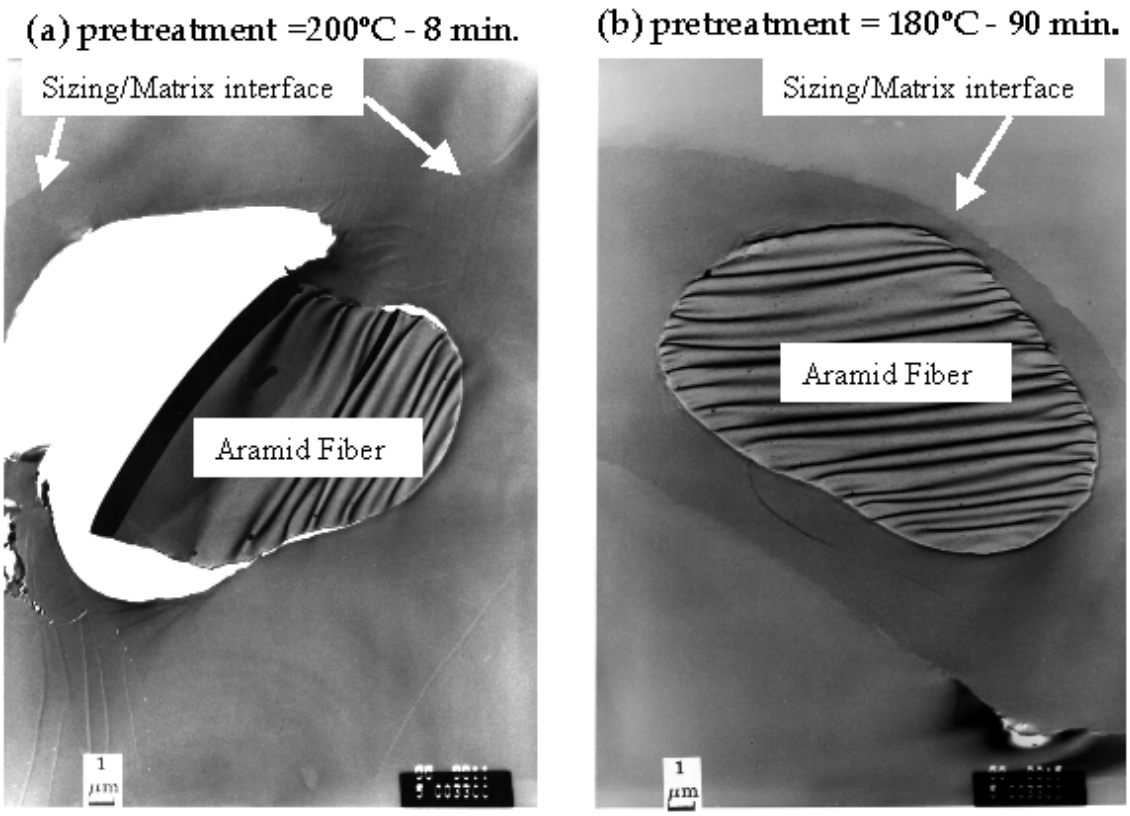

Figure 4.17: **TEM images of a single aramid fiber coated with a polyhydroxyether sizing embedded in phenolic/epoxy matrix material (a) pretreated for 8 min at 200°C (b) pretreated for 30 min at 180°C.**

4.3.5 Sizings

Control panels were fabricated from 12 K G' commercially sized fiber from Hexcel. All sizing solutions were sized onto 12 K AS-4 unsized carbon fibers from Hexcel. Composite panels were fabricated with six different sizing materials to study the effects of the latent initiators on the thermal and mechanical properties of the composites. The following sizing materials were used in composite fabrication: a commercial G' sizing material (1), a 22,000 g/mol polyimide with no initiator (2), a 22,000 g/mol polyimide with 3.2 mol % TMOPP initiator (3), a fluorinated polyimide with ~3.2 mol % TPP initiator(4), a potassium salt of phenolic novolac with 5.2 mol % initiator (5), a modified polyhydroxyether with 1.5 mol % initiator (6), and a commercially modified polyhydroxyether with an unknown initiator concentration (7) (Figure 4.4).

Sizing materials are commonly used in composite preparation. Two goals of commercial sizing materials are to improve ease of processing of the fiber bundles and to improve the fiber-matrix interface. Unsized 12 K carbon fiber tows are composed of a bundle of ~12,000 very thin (~ 5 μm diameter) fibers. During processing, these fiber bundles can begin to fray making processing very difficult. During the melt prepregging process, if the fibers begin to fray, they can become balled up in the dye and create enough tension to break the toe, which would halt the prepregging process. Therefore, a sizing material can be coated onto the fiber to help hold the fiber bundles together during processing. Another possible use of the sizing material would be to improve the fiber-matrix adhesion. This is most important for composites with a poor interface region. Therefore, in developing sizing materials to act as latent initiators it was important to consider how well the sizing holds the fiber together, the fiber matrix interface, and the kinetics of the initiator in the sizing.

For these latent initiator sizing materials several variables were important in creating a sizing that would sufficiently hold the fiber bundles together: such as coating the fiber from a solution vs. a dispersion, the temperature of the drying tower, and the T_g of the sizing. Poor sizings resulted from coating the fiber from a dispersion with no heating or heating only slightly above the T_g of the resin. However, good stiff fiber bundle were produced either when the sizing was coated from a solution, or if it was coated onto the fiber from a dispersion then heated well above the T_g of the sizing. Scanning electron microscopy was employed to investigate the morphology of the sizing on the fiber. The sized fiber bundles that frayed easily and did not hold together well, appeared to have particles on the fiber (not a uniform coating) (Figures 4.18a and 4.19a). However, the fibers that appeared to be stiff and held together well appeared to have a uniform film coating on the fiber (Figures 4.18b and 4.19b). These results suggested that a good sizing should form a uniform film coating on the fiber as opposed to particles on the fiber. Based on these results the appropriate sizing conditions were used to give a uniform film coating of sizing material. Sizings were either coated from a solution or heated well above their T_g if coated from a dispersion.

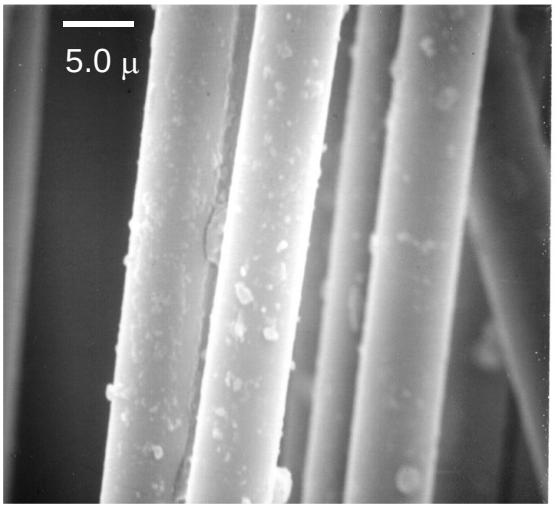

6F Poly(amic acid) salt sized from a methanol/water Dispersion

(a)

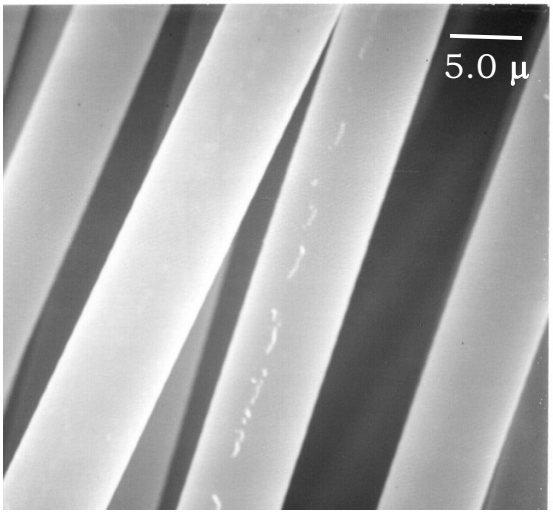

6F-Poly(amic acid) salt sized from a solution in Methanol

(b)

Figure 4.18: **SEM of sized carbon fibers (effect of sizing from a dispersion (a) versus a solution (b) on sizing morphology).**

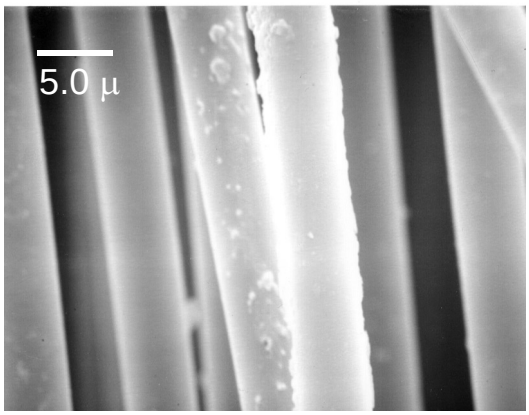

6F polyimide from Dispersion imidized at ~250°C

T_g ~ 150°C

(a)

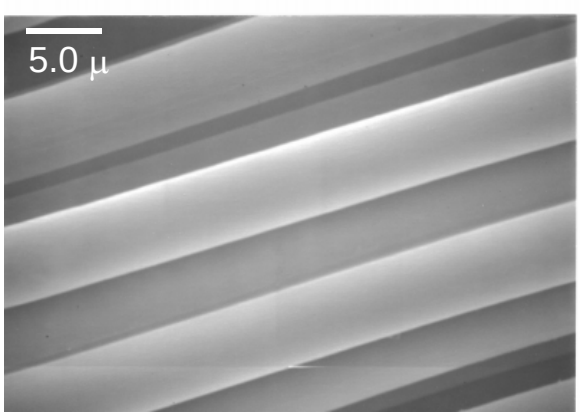

Ultem polyimide from Dispersion imidized at ~250°C

T_g = 98°C

(b)

Figure 4.19: **SEM of sized carbon fibers (effect of the T_g of the sizing and the drying temperature on sizing morphology)**

4.3.6 Panel Preparation

The cure cycles for panels from each type of sized fiber were determined by kinetic analysis based on the initiator concentration (Table 4.4). The T_g's of the cured panels were measured to confirm that the panels were fully cured with the designated cure cycles (Table 4.5). All of the panels with the latent initiator sizings were fully cured with significantly shorter cure times than the control uninitiated panel. With no initiator, a cure cycle of 1 hour at 200°C and 3 hours at 220°C was required to reach full conversion. Panels with no initiator cured for only 3 hours showed a significantly lower T_g than both the panels with initiator, and those without initiator cured for cured for 4 hours. There was no significant change in the T_g's of initiated panels when post cured for an additional 1 hour at 200°C, indicating that all composites were fully cured.

Table 4.4: Kinetic predictions for composites based on the calculated mole % initiator in the composite.

Sizing	Sizing Soln. (Wt %)	Wt % Sizing on Fiber	Mol % Initiator in Composite	Time to 99% conversion (T = 180°C)
3	2.0	1.62	3.2	5 min.
4	1.5	0.63	5.2	15 min.
5	2.0	0.74	1.5	41 min.
6	2.0	1.38	-----	43 min.

Table 4.5: Cure cycles and glass transition temperatures of composites with varied sizing materials.

Sizing	Mol % Initiator	Cure Cycle	Tg (°C)
None	None	200°C (1 hr.) 220°C (3 hr.)	124
1	None	200°C (1 hr.) 220°C (3 hr.)	132
2	None	200°C (1 hr.) 220°C (3 hr.)	132
3	3.2	180°C (20 min.) 200°C (10 min.)	130
4	5.2	180°C (30 min.) 200°C (30 min.)	135
5	1.5	180°C (20 min.) 200°C (20 min.)	135
6	-----	180°C (1 hr.) 200°C (1 hr.)	128

In comparing mechanical properties of fiber reinforced composites it was important that the fiber volume fractions of the composites being compared are similar. For the unidirectional composites tested the fiber volume fraction ranged from 0.64-0.71 (0.72-0.78 weight fraction fiber). Cross-ply composites analyzed for compression strength and fatigue had fiber volume fractions ranging from 0.56-0.61 (0.65-0.70 fiber weight fraction). The cross-ply composites exhibit lower fiber volume fractions because the fiber could not pack as tightly as in the unidirectional composites. Mechanical Properties of composites prepared from sizings **5** and **6** could not be tested due to their low fiber volume fraction. This low fiber volume fraction was a result of premature curing in the press. For our lab scale composite preparation the prepregged ply's were placed in a metal mold in a hot press to cure. One requirement of this set-up is that a significant amount of resin must be squeezed out of the mold during curing in order to generate the appropriate fiber volume fraction, because the prepreg had an excess of resin. Therefore the mold had to be heated to a temperature at which the resin had a low enough viscosity to be squeezed out of the mold under pressure, without reaching the gel point of the network. In addition, the mold used required about 45 minutes to heat to the desired

temperature for the resin to be squeezed out. Therefore, preventing premature curing became a challenge because there were very high concentrations of initiator in the composite at this point. During this heating stage premature curing would be expected for the time period that the temperature was above the T_g of the sizing. It appeared that sizing materials with higher T_g's or lower initiator concentrations (sizings 1, 2, 3, 4 and 7) could be processed successfully. However, sizings with both a high initiator concentration and low T_g (sizings 5 and 6) cured prematurely in the mold, preventing the desired fiber volume fraction. It is likely that this problem could be overcome by developing a prepregging process in which the amount of resin placed on the fiber could be better controlled, or a mold that could be preheated before placing the prepregged plys in it.

4.3.7 Composite Properties

4.3.7.1 Transverse Flexural Strength

Transverse flexural Strength of Composites from unsized fibers as well as with sizings (1) and (3) were measured. The flexural strength of the composite from the unsized fibers was significantly lower than the other two composites. This can be understood by the fact that the unsized fibers tended to fray and ball up during processing resulting in numerous defects in the composites. In addition, as evident by the T_g, the composite with the unsized fibers , which was only cured for 3 hours, was not fully cured. There appeared to be no effect of the type of sizing on the transverse flexural strength of the composite from the commercial G1 sizing (1) compared to that of the composite with the Poly(amic acid)/TMOPP latent initiator sizing (3). Therefore the cure time could be reduced from 4 hours to less than 30 minutes while maintaining equivalent flexural strength (Table 4.6).

Table 4.6: Transverse flexural strengths of unidirectional AS-4 carbon fiber reinforced phenolic/epoxy composites from unsized fibers and sizings 1 and 3.

Sizing	Mol % Initiator	Cure Cycle	Transverse Flex. Strength (MPa)
None	None	200°C (1 hr.) 220°C (3 hr.)	83 +/- 5
1	None	200°C (1 hr.) 220°C (3 hr.)	100 +/- 8
3	3.2	180°C (20 min.) 200°C (10 min.)	102 +/- 9

4.3.7.2 Mode I Toughness

Mode I fracture toughness of the composite panels with sizings (1), (2), and (3), were analyzed (Table 4.7). The corrected crack length (a + Δ), for each sample, was determined from a plot of the cube root of compliance versus the measured crack length, based on the corrected beam theory. G_{1c} values were calculated for the entire range of crack lengths by equation 4.7 according to ASTM D5528-94a.[57] The values reported were

$$G_{1c} = 3P\delta/2b(a+\Delta) \quad (4.7)$$

P = applied load

δ = displacement

b = specimen width

a = crack length

Δ = correction factor for the crack length

taken from the region of stable crack growth of each sample indicated by the plateau in the plot of G_{1c} versus corrected crack length.

Table 4.7: Mode I composite toughness of unidirectional AS-4 carbon fiber reinforced phenolic/epoxy composites from sizings 1, 2 and 3.

Sizing	Mol % Initiator	Cure cycle	Fiber vol. Fraction	G_{1c} (J/m^2)
1	None	200°C (1 hr.) 220°C (3 hr.)	67.6%	573 +/- 46
2	None	200°C (1 hr.) 220°C (3 hr.)	71.1%	695 +/- 83
3	3.2	180°C (20 min.) 200°C (10 min.)	64.2%	542 +/- 92

Mode I toughness of the phenolic-epoxy panels, both with and without initiators, was significantly higher than for untoughened epoxy/carbon fiber composites and equivalent to toughened epoxy/carbon fiber composites[59,60,61,62]. The slight differences in the values between the 3 panels may be the result of small differences in fiber volume fractions. There were no significant differences in toughness between the uninitiated panels from sizings (1) and in the panel from the polyimide encapsulated TMOPP sizing (3). This demonstrated that the desired properties of the novolac/epoxy resin system can be retained with much shorter cure times (30 minutes instead of 4 hours) and lower cure temperatures (180-200°C as opposed to 200-220°C).

4.3.7.3 Mode II Toughness

Mode II fracture toughness using end-notched flexural (ENF) geometry on unidirectional composites with the same three sizing materials was measured. Before testing each sample, the compliance was measured from the region of the sample with no crack, using three-point bend testing with a span of 7.62 cm (3 in.). This compliance was used to determine the flexural modulus (Equation 4.8). The flexural moduli were later used in calculations for the corrected crack lengths. Each sample was loaded in three-

point bend geometry with a span of 10.16 cm (4 in.) and a crack length of 2.54 cm (1 in.). This was necessary to meet the requirement that a = 1/2 L. The corrected crack length was calculated by equation (4.9) then used in the calculation for G_{2c} (Equation 4.10).

$$E_{flex} = L^3/4bC'h^3 \quad (4.8)$$

L = half the span

b = specimen width

C' = compliance of the sample with no pre-crack

h = half the specimen height

$$a_{corr} = [8E_{flex}Cbh^3/3]^{1/3} \quad (4.9)$$

C = compliance of the pre-cracked sample

$$G_{2c} = 9\Delta a_{corr}^2 P/2b(2L^3 + 3a_{corr}^3) \quad (4.10)$$

Δ = displacement at failure

P = load at failure

Trends in the mode II composite toughness, for the composites with the three different sizing materials, were similar to the mode I results. There was no significant difference in toughness between panels prepared with initiators embedded in the fiber sizings and those prepared at higher temperatures and in longer cure cycles without any added initiator (Table 4.8). All of these phenolic-epoxy composites had relatively high mode II toughness, equaling the values of toughened epoxies[59,62] and exceeding the toughness of untoughened carbon fiber/epoxy composites.[59,60] In addition, the G_{2c} values were close to twice the G_{1c} values, as would be expected.

Table 4.8: Mode II composite toughness of unidirectional AS-4 carbon fiber reinforced phenolic/epoxy composites from sizings 1, 2 and 3.

Sizing	Mol % Initiator	Cure cycle	Fiber vol. Fraction	G_{2c} (J/m^2)
1	None	200°C (1 hr.) 220°C (3 hr.)	66.4%	1410 +/- 302
2	None	200°C (1 hr.) 220°C (3 hr.)	70.4%	1254 +/- 64
3	3.2	180°C (20 min.) 200°C (10 min.)	69.0%	1224 +/- 250

4.3.7.4 Fatigue, Compression Strength, and Interface Properties

Composite panels $(0°/90°)_{7s}$ prepared from sizings (1) and (7) were tested in fully reversed (R = -1) notched fatigue to determine the effects of the fiber-matrix interphase material on the composite fatigue performance. Robertson et al.[79] have previously shown the composite fatigue results to be particularly sensitive to changes in the fiber-matrix interface. Improved fatigue performance is noted by a decrease in the slope of the S-N curve and an increase in the stress level that defines the fatigue limit, i.e. the stress level at which the material survives 10^6 cycles. The number of cycles before failure was plotted versus the applied stress (Figure 4.20). This stress is not normalized for the differences in compression strength. In addition the number of cycles data was plotted versus the stress normalized by the compression strength of the panels (Figure 4.21). The second method allowed for a more accurate comparison of the fatigue limit of materials with different compression strengths. In both plots there was no significant difference in the fatigue limits of composite panels prepared from sizing (1) and (7) (Figures 4.20 and 4.21). These materials also had similar compression strengths. This demonstrated that the performance of the composite panel was not dependent on whether the sizing material contained initiator. Therefore, good fatigue performance can be achieved with lower cure times and temperatures using these latent initiator sizings.

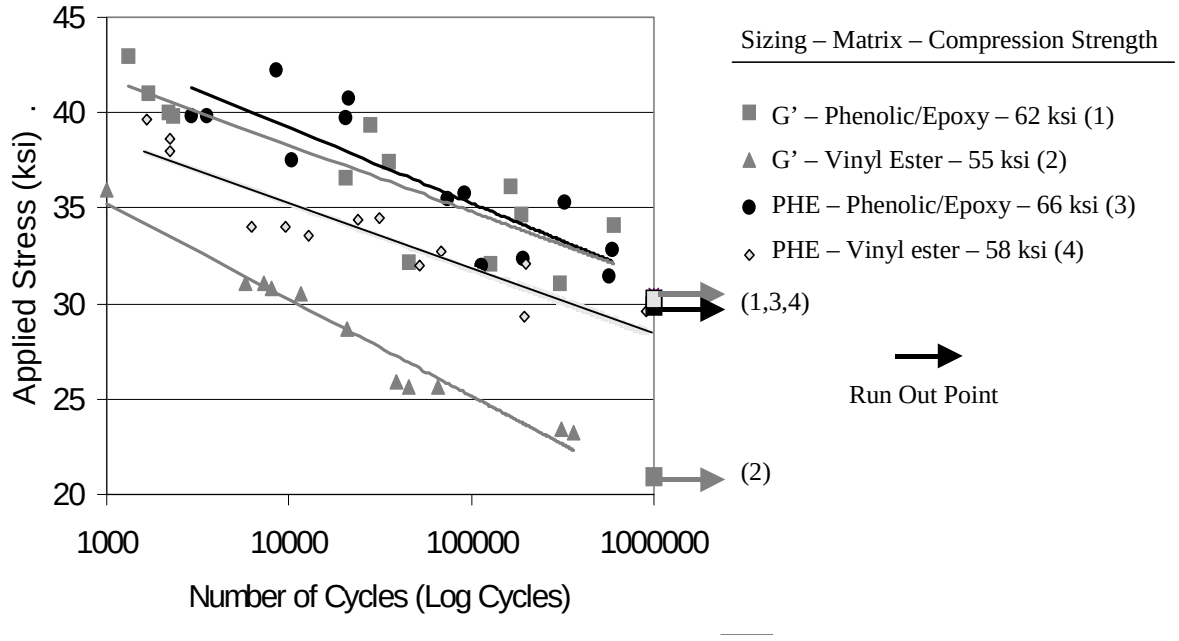

Figure 4.20: **Applied stress versus number of cycles of phenolic/epoxy composites from sizings 1 (G') and 7 (PHE) compared with vinyl ester composites.**

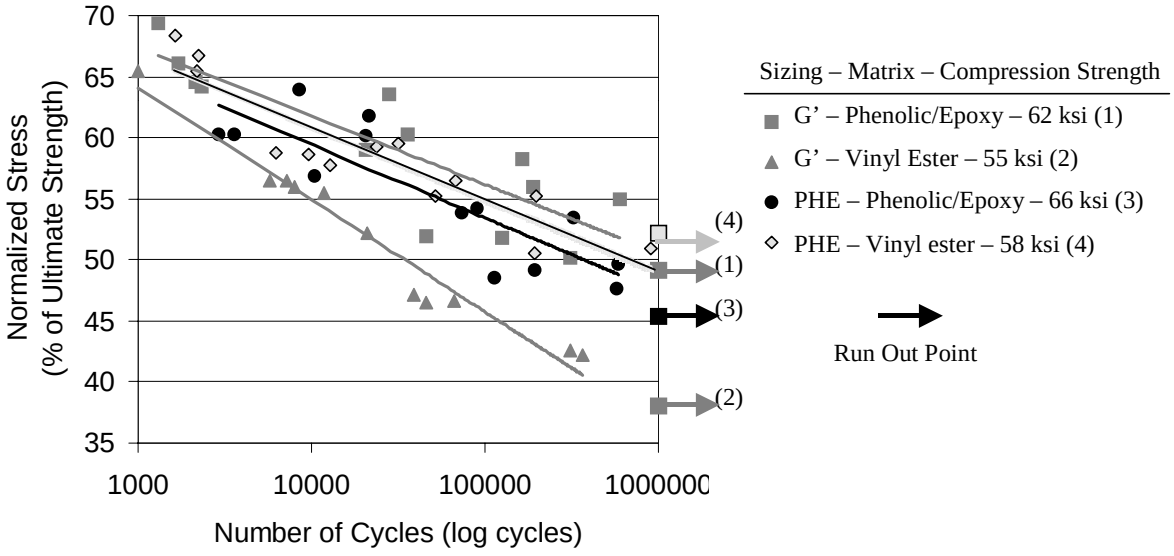

Figure 4.21: **Normalized stress versus number of cycles of phenolic/epoxy composites from sizings 1(G') and 7 (PHE) compared with vinyl ester composites.**

Fatigue properties of these phenolic/epoxy panels were also compared to similar panels with vinyl ester matrices, since vinyl ester matrices are well established in the composite industry. Both vinyl ester panels prepared with the G' sizing (1) and vinyl ester panels with an improved interface (Polyhydroxyether (PHE) sizing) (7) were investigated.[79] The vinyl ester network composition was derived from 70 wt. % of a methacrylate terminated vinyl ester oligomer (M_n = 700 g/mol) co-cured with 30 wt. % styrene, and the fibers were stitched prior to composite fabrication by resin film infusion.[79] The phenolic/epoxy composites studied herein had improved fatigue limits and compression strengths relative to the vinyl ester composites with the commercially sized (G') fibers and equivalent fatigue limits relative to the vinyl ester composites with the improved interface (Figures 4.20 and 4.21). This probably reflects properties of both the matrix resins and also their interactions with the interphase materials (between fiber and matrix). Comparison between the applied stress versus normalized stress S-N curves of the two vinyl ester composites suggested that interface changes affect both the compression strengths and the fatigue limits. The vinyl ester material showed a significant increase in both the fatigue limit and the compression strength in changing from the G' sizing to the phenoxy sizing. This suggested an improvement in the interface region, since only the sizing was changed. On the other hand, there was no difference in the fatigue limit of the phenolic-epoxy composites when using these same two sizings, the G' sizing (1) and the commercial polyhydroxyether sizing (7). This would suggest that there was a good interface between the phenolic-epoxy matrix resin and the fiber with both sizing materials.

4.3.7.5 Composite Moisture Uptake and Interface properties

Another method to analyze the interface region of the fiber and matrix is by measuring the moisture uptake of composites prepared with different sizing materials and comparing these values to neat resin moisture uptake. For the same vinyl ester illustrated in the fatigue curves, it has been shown that changing the sizing from the G' sizing to the polyhydroxyether sizing significantly reduced composite moisture uptake from 1.12% to 0.24%.[83] These results were consistent with the fatigue results, which suggested an improved interface for the vinyl ester from the polyhydroxyether sized fibers.

Composite moisture uptake at 60°C for phenolic/epoxy composites from sizings 1, 4, and 7 were investigated. The fluorinated polyimide/TPP sizing (4), was a hydrophobic sizing material, which was expected to prevent diffusion of water at the interface. If the interface between the fiber and matrix was poor, allowing moisture uptake at the interface, one would expect the composite with the fluorinated sizing to have the lowest moisture uptake and the composite with the G' sizing to have the highest moisture uptake. However, there was no significant difference in moisture uptake between the composites from the three different sizing materials (Figure 4.22). The composite moisture uptake could also be predicted from the neat resin moisture uptake based on the fiber weight fraction in the composites, assuming no additional moisture uptake at the fiber matrix interface. The fiber weight fraction of the composites studied ranged from 0.65 to 0.73 and the moisture uptake of the neat resin at 60°C was 4.0%. By multiplying the neat resin moisture uptake by the weight fraction of resin in the composites the moisture uptake was predicted to be 1.1 to 1.4%, for composites with an ideal interface. Therefore, the composite moisture uptake of 1.4% suggested that there was no significant moisture uptake due to the interface. This was consistent with the fatigue results, which suggested a good interface between the phenolic/epoxy matrix and the carbon fiber for all three sizing materials.

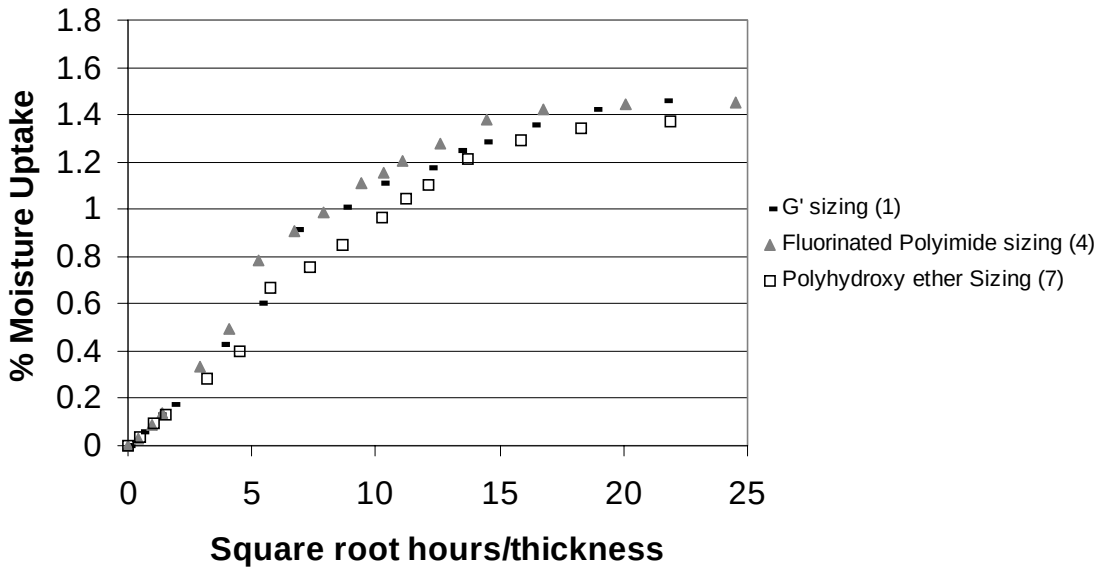

Figure 4.22: Moisture uptake of unidirectional phenolic/epoxy composites from sizings 1,4 and 7.

4.4 Conclusions

Phenolic/epoxy composites with high phenolic compositions (65 wt. % phenolic/35 wt. % epoxy) are difficult to process in the melt due to the high viscosities of the resins. Temperatures at which the viscosities were in a processable range caused premature curing with even very small initiator concentrations. However high initiator concentrations were required for rapid cure at elevated temperatures. The approach of embedding the initiator in a fiber sizing allowed for high initiator loadings, which resulted in rapid cure in the cure stage (99% conversion in less than 5 minutes) with minimal premature curing during the processing step. The kinetic analyses indicated that sizing materials containing monomeric organic initiators (such as TMOPP) encapsulated into polymeric sizings allow for the fastest cure times of the initiators investigated. Both initiators with inorganic cations and polymeric initiators resulted in slower cure rates and therefore were not as desirable for use as sizing encapsulated initiators.

Composite toughness, compression strength, and fatigue were investigated both to determine the effects of the sizings on these properties and to determine the feasibility of phenolic/epoxy composites for infrastructure applications. The properties of the composite panels prepared from sizing materials with and without initiator were equivalent, indicating that embedding the initiator in the fiber sizing does not diminish the composite properties. In addition, the phenolic/epoxy composites had equivalent toughness when compared to toughened epoxies, and equivalent fatigue when compared to a vinyl ester composite with an improved interface. The fact that changing the sizing did not have a significant effect on composite properties or moisture uptake indicated that the interface between the carbon fiber and the matrix was ideal. These composite properties were important since flame retardant phenolic composites are typically extremely brittle.

5 Conclusions

Void-free, flame retardant, tough networks can be produced from the reaction of a phenolic novolac with a difunctional epoxy where phenolic is the major component. The ratio of phenol to epoxy was adjusted to control the network densities and molecular weights between crosslinks (M_c). The M_c's were determined from the moduli in the rubbery region well above the glass transition temperature. As the phenolic content was increased from 2 phenols per epoxy to 7 phenols per epoxy, the rubbery moduli decreased indicating an increase in molecular weight between crosslinks (M_c). In contrast to the trends in the rubbery moduli, as the phenolic content was increased the glassy moduli increased. It is likely that the increase in glassy moduli was a result of increased hydrogen bonding in the networks with increased phenolic content. These networks with the increased glassy moduli also exhibited higher cooperativities, indicating that hydrogen bonding affected the relaxation of these materials through their transition regions.

As the molecular weight between crosslinks increased the glass transition temperatures decreased, as would be expected based on network density. Fracture toughness increased with molecular weight between crosslinks until the networks became unconnected at very high phenolic contents. Fracture toughness of the networks with between 3 and 5 phenols per epoxy exceeded that of commercial untoughened aerospace epoxies and far exceeded that of phenolic resols. The peak heat release rate (PHRR) and smoke toxicity of these networks, measured from cone calorimetry, decreased as the phenolic content in the networks was increased. Flame retardance for all phenolic epoxy networks was significantly improved over the epoxy control, and flame retardance of the networks with high phenolic content approached that of the phenolic control. Moisture uptake for the phenolic/epoxies increased with increasing phenolic content due to increased hydrogen bonding in the networks with more unreacted phenolic hydroxyls. The composition with 3 phenols per epoxy had a moisture uptake of about twice the epoxy control.

Viscosities of these blends were high due to hydrogen bonding of the novolac. The viscosity increased significantly as the ratio of phenol to epoxy was increased because there was less of the epoxy diluent. The 65/35 wt/wt phenolic/bisphenol-A epoxy networks reached a processable viscosity of 2 Pa*s (2000cp) at ~140°C. At this temperature premature curing occurred even with only small initiator concentrations making processing in the melt challenging. However, the same composition of phenolic crosslinked with a siloxane epoxy had a much lower melt viscosity. The 65/35 phenolic/siloxane epoxy reached 2 Pa*s at 100°C. At this temperature, even with a small amount of initiator, the processing window (or time below 2 Pa*s) was greater than 2 hours. However, these siloxane epoxies had lower glass transitions than networks with the bisphenol-A based epoxy.

To allow melt processing of the phenolic/bisphenol-A based epoxy compositions latent nucleophilic initiators were developed. The method was to encapsulate these initiators onto the fiber as a fiber sizing. This method prevented premature curing during processing because the initiator did not come in contact with the resin until the cure cycle. In addition, this method enabled high initiator loadings to promote rapid cure during the cure cycle. Several types of latent initiators were investigated and their kinetics were studied to determine the factors important for latent initiators for phenolic/epoxy composites. Investigations into the kinetics of these latent initiators indicated that monomeric phosphine initiators resulted in fast cures. Both polymeric initiators and initiators with inorganic counterions had significantly reduced cure rates when compared to monomeric initiators with phosphine counterions. The polyimide with sequestered TMOPP sized onto the fiber from a 2 wt % solution in methanol produced 99 % conversion in 5 minutes. Using these latent initiators cure times were reduced from 4 hours to less than 30 minutes. Mode I and II composite toughness values were independent of the sizing material and in all cases were significantly higher than the epoxy control. Composite fatigue limits and compression strengths were higher than both a commercially available vinyl ester and a vinyl ester with an improved interface. Incorporation of different sizings with and without initiator had no effect on the fatigue limit of the phenolic/epoxy composites. This indicated a good interface between the fiber and the matrix for the phenolic/epoxy composites independent of the type of sizing or the

presence of initiator. Moisture uptake of the composites confirmed that there was a good interface between the fiber and matrix.

Therefore, both neat resin and composite mechanical and flame retardant properties indicated that the goal of developing a processable material, which possessed both flame retardance and toughness for use in infrastructure applications, has been achieved. The toughness of these materials far exceeded the toughness of commercial phenolics and the flame retardance was drastically better than a commercial aerospace epoxy.

6 Future Work

These phenolic/epoxy networks have many excellent properties and have a broad range of applications. More knowledge of the phenolic novolac structure, including the molecular weight distribution and the concentration of short chains would be beneficial. In addition the development of a phenolic novolac with a more controlled molecular weight distribution may allow the formation of networks with fewer dangling ends and unconnected chains. This may have some effect on the mechanical properties of these networks. In addition, infrared characterization of the networks may give more insight into the importance of hydrogen bonding.

Flame retardance of these networks should be further characterized by performing different types of flame tests such as the UL-94 and limiting oxygen index tests and comparing these results with results from cone calorimetry. In addition, investigations into the addition of flame-retardants may result in networks with even better flame retardance. One method may be to incorporate phosphorous or nitrogen into the networks.

For microelectronics applications it would be of interest to develop networks with higher glass transitions and decreased moisture uptake. Higher glass transitions may be achieved by incorporation of epoxies capable of hydrogen bonding such as epoxies with phosphine oxide or sulfone functionalities. However, these may increase the moisture uptake. Decreased moisture uptake may be achieved by functionalizing the phenolic hydroxyls to reduce hydrogen bonding. However, this may affect the flame retardance as well. It may be possible to functionalize the hydroxyls with phosphate, which should decrease hydrogen bonding, but at the same time improve flame retardance. Another possibility may be to functionalize the phenolic hydroxyls with a char forming thermally labile component which would decrease moisture uptake in the networks yet allow these phenolics to act as free radical traps during burning.

In order to further improve the processability of these materials it may be of interest to investigate methods to inhibit the reaction, in the absence of initiator, to increase melt stability. In addition, the latent initiators should be investigated further. It is likely that

the polyhydroxyether initiator may cure at a faster rate if shorter polymeric or oligomeric chains were incorporated. It is possible that commercial epoxy sizings could be easily functionalized to produce a latent initiator, to promote a rapid cure reaction between the phenolic and epoxy. In addition, other polyimide latent initiators could be developed containing electron withdrawing groups in order to promote reaction of the acid with triphenylphosphine.

7 References

[1] 1A. Knop and L. A. Pilato, *Phenolic Resins, Chemistry, Applications and Performance, Future Directions*, Springer-Verlag, New York, 1985.

[2] F. Y. Hshieh and H. D. Beeson,"Flammability Testing of Flame-Retarded Epoxy Composites and Phenolic Composites," *Fire and Materials*, **21**, 41-49, 1997.

[3] N. B. Sunshine, *Flame retardancy of Phenolic materials*, Chapter 4: Flame Retardancy of Phenolic Resins and Urea- and Melamine-Formaldehyde Resins, W. C. Kuryla and A. J. Papa Eds., Vol. 2, Marcel Dekker, Inc. New York, 1973.

[4] D. H. E. Kunz, *Macromol. Chem., Macromol. Symp.*, "Flame Retarding Materials for Advanced Composites," **74**, 155-164, 1993.

[5] F. Hshieh and H. D. Beeson,"Cone Calorimeter Testing of Epoxy/Fiberglass and Brominated Epoxy/Fiberglass Composites in Normal Oxygen and Oxygen-Enriched Environments," *ASTM Spec.Tech. Publ.*, **STP 1267**, 152-167, 1995.

[6] A. Hale, C. Macosko, and H. E. Bair, "DSC and 13C NMR Studies of the Imidazole-Accelerated Reaction Between Epoxides and Phenols," *Journal of Applied Polymer Science*, **38**, 1253-1269, 1989.

[7] M. Ogata, N. Kinjo, T. Kawata,"Effects of Crosslinking on Physical Properties of Phenol-Formaldehyde Novolac Cured Epoxy Resins," *Journal of Applied Polymer Science*, **48**, 583-601, 1993.

[8] Mark; Bakales; Overberger; and Menges *Encyclopedia of Polymer Science and Engineering*, **Vol. 11**, John Wiely & Sons, New York, 1988, Chapt. Phenolic Resins.

[9] S. L. Madorsky, *Thermal Degradation of Organic Polymers, Chapter XVI Phenolic Resin*, Interscience Publishers, New York, pp. 288-292, 1964.

[10] R. T. Conley and J. F. Bieron,"A Study of the Oxidative Degredation of Phenol-Formaldehyde Polycondensates Using Infrared Spectroscopy" *Journal of Applied Polymer Science*, **7**, 103-117, 1963.

[11] H. W. Lochte, E. L. Strauss, and R. T. Conley,"The Thermo-Oxidative Degredation of Phenol-Formaldehyde Polycondensates: Thermogravimetric and Elemental Composition Studies of Char Formation," *Journal of Applied Polymer Science*, **9**, 2799-2810, 1965.

[12] W. M. Jackson and R. T. Conley,"High Temperature Oxidative Degratation of Phenol-Formaldehyde Polycondensates," *Journal of Applied Polymer Science*, **8**, 2163-2193, 1964.

[13] S. G. Kuzak, J. A. Hiltz, and P. A. Waitkus, "Impact Performance of Phenolic Composites Following Thermal Exposure," *Journal of Applied Polymer Science*, **67**, 349-361, 1998.

[14] R. W. Biernath, D. S. Soane,"Cure Kinetics of Epoxy Cresol Novolac Encapsulants for Microelectronics Packaging" *Contemporary Topics in Polymer Science*, J. C. Salamone and J. S. Riffle Eds., **7**, 130-159 (1992)

[15] A. K. Banthia and J. E. McGrath,"Catalysis of Bisphenol-Diglycidyl Ether Linear Step-Growth Polymerization," *Polymer preprints*, **20(2)**, 629-633, 1979.

[16] W. A. Romanchick, J. E. Sohn, and J. F. Geibel,"Synthesis, Morphology, and Thermal Stability of Elastomer-Modified Epoxy Resins," *In ACS Symposium Series 221 – Epoxy Resin Chemistry II*, R. S. Bauer, Ed. American Chemical Society: Washington D. C., 85-118, 1982.

[17] D. Gagnebien, P. J. Madec, and E. Marechal,"Synthesis of Poly(Sulphone-b-Siloxane)s - I Model Study of the Epoxy-Phenol Reaction in the Melt" *Eur. Polym. J.*, **21(3),** 273-287, 1985.

[18] S. Han, W. G. Kim, H. G. Yoon, and T. J, Moon,"Kinetic Study of the Effect of Catalysts on the Curing of Biphenyl Epoxy Resin," *Journal of Applied Polymer Science*, **68**, 1125-1137, 1998.

[19] S. Han, W. G. Kim, H. G. Yoon, and T. J,"Curing Reaction of Biphenyl Epoxy Resin with Different Phenolic Functional Hardners," Moon *Journal of Polymer Science:Part A Polymer Chemistry*, **36**, 773-783 (1998).

[20] S. Han, H. G. Yoon, K. S. Suh, W. G. Kim, and T. J, Moon,"Cure Kinetics of Biphenyl Epoxy-Phenol Novolac Resin System using Triphenylphosphine as Catalyst," *Journal of Polymer Science:Part A Polymer Chemistry*, **37**, 713-720 (1999).

[21] J. D. B. Smith,"Metal Acetylacetonates as Latent Accelerators for Anhydride-Cured Epoxy Resins," *Journal of Applied Polymer Science*, **26**, 979-986, 1981.

[22] A. J. Landua, "BF_3 Catalyzed Reactions of Epoxy Compounds," *American Chemical Society, Division of Organic Coatings Plastics Chemical Preprints*, **24(2),** 299-308, 1964.

[23] J. B. D. Smith, "Novel Epoxy-Anhydride VPI Resins Containing Chromium Latent Accelerators," *Proceedings of the Electrical/Electronic Insulating Conference*, **18th**, 262-268, 1987.

[24] J. D. B. Smith, "Organotin Amine Complexes as Latent Catalysts for Epoxy Resins" *Proceedings of the Electrical/Electronic Insulating Conference*,**23rd**, 239-244, 1997.

[25] S. C. Lin and R. A. Andrejak, "Phosphines as Latent Epoxy Curing Accelerators," *Polymeric Materials Science and Engineering*, **52**, 350-354, 1985.

[26] V. Razafindrakoto, B. Bonnetot, C. Pautet, and H. Mongeot, "Study of Adducts of Tertiary Amines with Halo or Isothiocyanato Boranes as Latent Catalysts of Epoxide-Amine Compositions," Polymer Bulleton, 40(4-5), 439-446, 1998.

[27] S. P. Pappas, V. D. Kuntz, and B. C. Pappas, "Latent Amine Catalysts for Epoxy-Carboxy Hybrid Powder Coatings. Investigations of Phase Change Control of Reactivity," *Journal of Coatings Technology*, **63(796**), 39-46, 1991.

[28] M. Kobayashi, F. Sanda, and T. Endo, "Application of Phosphonium Ylides to Latent Catalysts for Polyaddition of Bisphenol A Diglycidyl Ether with Bisphenol A: Model System of Epoxy Novolac Resin," *Macromolecules*, **32(15),** 4751-4756, 1999.

[29] L. E. Nielsen,"Cross-Linking - Effect on Physical Properties of Polymers," Journal of Macromolecular Science-Reviews Macromolecular Chemistry, C3(1), 69-103, 1969.

[30] J. J. Aklonis and W. J. MacKnight, Introduction to Polymer Viscoelasticity, second edition, John Wiley and Sons, New York, p. 111, 1983.

[31] J. D. Lemay, B. J. Swetlin, and F. N. Kelley,"Structure and Fracture of Highly Cross-linked Networks," in Characterization on Highly Crosslinked Polymers, S. Labana and R. Dickie eds., ACS Symposium Series No. 234, American Chemical Society, Washington DC, 165-183, 1984.

[32] H. L. Bos and J. J. H. Nusselder,"Toughness of Model Polymeric Networks in the Glassy State: Effect of Crosslink Density," *Polymer*, **35(13),** 2793-2799, 1994.

[33] J. J. H. Nusselder and H. L. Bos,"Toughness of Polymeric Networks: The Limited Importance of Crosslink Density" *Macromolecular Symposium*, **93**, 17-25, 1995.

[34] E. Espuche, J. Galy, F. F. Gerard, J. P. Pascault, and H. Sautereau,"Influence of Crosslink Density and Chain Flexibility on Mechanical Properties of Model Epoxy Networks," *Macromolecular symposia*, **93**, 107-115, 1995.

[35] J. P. Bell, Mechanical Properties of a Glassy Epoxide Polymer: Effects of Molecular Weight between Crosslinks," *Journal of Applied Polymer Science*, **14**, 1901-1906, 1970.

[36] M. Connolly and F. Karasz,"Viscoelastic and Dielectric Relaxation Behavior of Substituted Poly(p-phenylenes)," *Macromolecules*, **28**, 1872-1881, 1995.

[37] S. Matsuoka and X. Quan,"A model for Intermolecular Cooperativity in Conformational Relaxations near the Glass Transition," *Macromolecules*, **24**, 2770-2779, 1991.

[38] S. Matsuoka, *Relaxation Phenomena in Polymers*, Hanser Publishers, Munich, 1992.

[39] C.G. Robertson and G. L. Wilkes, "Correlation between Physical Aging Rates and Glass Transition cooperativity (Fragility): Part 1. Experimental Results," *Macromolecules*, in press.

[40] I. M. Hodge,"Adam-Gibbs Formulation of Nonlinear Enthalpy Relaxation," *Structure, Relaxation, And Physical Aging of Glassy Polymers*, R. J. Roe and J. M. O'Reilly Eds., Materials research Society, Pittsburgh, Pennsylvania, 1991.

[41] C. A. Angell, L. Monnerie, and L. M. Torell,"Strong and Fragile Behavior in Liquid Polymers," *Structure, Relaxation, And Physical Aging of Glassy Polymers*, R. J. Roe and J. M. O'Reilly Eds., Materials research Society, Pittsburgh, Pennsylvania, 1991.

[42] C. M. Roland and K. L. Ngai," Normalization of the Temperature Dependence of Segmental Relaxation Times," *Macromolecules*, **25(21),** 5765-5768, 1992

[43] C. M. Roland and K. L. Ngai," Constraint Dynamics and Chemical Structure" *Journal of Non-crystalline Solids*, **172-174**, 868-875, 1994.

[44] C. M. Roland,"Constraints on Local Segmental Motion in Poly(vinylethylene) Networks," *Macromolecules*, **27**, 4242-4247, 1994.

[45] C. A. Angell,"Relaxation in Liquids, Polymers, and Plastic Crystals - Strong/Fragile Patterns and Problems," Journal of Non-Crystalline Solids, **131-133**, 13-31, 1991.

[46] C. A. Angell, "Transport Processes, Relaxation, and Glass Formation in Hydrogen-Bonded Liquids," in Hydrogen Bonded Liquids, J. C. Dore and J. Teixeira, eds., **Vol. 329**, 59-79, 1991.

[47] R. Bohmer, K. L. Ngai, C. A. Angel, and D. J. Plazek, "Nonexponential Relaxations in Strong and Fragile Glass Formers," *Journal of Chemistry and Physics*, **99(5)**,4201-4209, 1993.

[48] V. Babrauskas, "Development of the Cone Calorimeter - A Bench-Scale Heat Release Rate Apparatus Based on Oxygen Consumption," *Fire and Materials*, **8(2),** 81-95, 1984.

[49] L. J. Goff,"Testing of Polymeric Materials via the Cone Calorimeter" *Annual Technical Conference - Society of Plastics Engineering*, **49th**, 1630-1632, 1991.

[50] M. R. Christy, R. V. Petrella, and J. J. Penkala, "Controlled-Atmosphere Cone Calorimeter," *Fire and Polymers II*, G. L. Nelson ed., 498-517, 1995.

[51] S. Subramanian, J. J. Lesko, K. L. Reifsnider, and W. W. Stinchcomb, "Characterization of the Fiber-Matrix Interphase and Its Influence on Mechanical Properties of Unidirectional Composites," *Journal of Composite Materials*, **30(3),** 309-332, 1996.

[52] N. S. Broyles, R. Chan, R. M. Davis, J. J. Lesko, and J. S. Riffle, "Sizing of carbon fibres with aqueous solutions of poly(vinyl pyrollidone)," *Polymer*, **39(12),** 2607-2613, 1998.

[53] S. Lehmann, C. Megerdigian, and R. Papalia, "Carbon Fiber/Resin Matrix Interphase: Effect of Carbon Fiber Surface Treatment on Composite Performance," *National SAMPE symposium*, **30th**, 290-301, 1985.

[54] J. J. lesko, R. E. Swain, J. M. Cartwright, J. W. Chin, K. L. Reifsnider, D. A. Dillard, and J. P. Wightman, "Interphases Developed from Fiber Sizings and their chemical-Structural Relationship to Composite Compressive Performance," *Journal of Adhesion*, **45**, 43-57, 1994.

[55] N. S. Broyles, K. E. Verghese, S. V. Davis, H. Li, R. M. Davis, J. J. Lesko, and J. S. Riffle, "Fatigue performance of carbon fibre/vinyl ester composites: the effect of two dissimilar polymeric sizing agents," *Polymer*, **39(15),** 3417-3424, 1998.

[56] K. D. Cowley and P. W. R. Beaumont, "The Interlaminar and Intralaminar Fracture Toughness of Carbon-Fibre/Polymer Composites: The Effect of Temperature," *Composite Science and Technology*, **57**, 1433-1444, 1997

[57] ASTM standard "Standard Test Method for Mode I Interlaminar Fracture Toughness of Unidirectional Fiber-Reinforced Polymer Matrix Composites,"Annual Book of ASTM Standards, vol 14.02, designation: D5528-94a.

[58] P. Davies, "Interlaminar Fracture Testing of Composites, Protocol for joint round robin," European Group of Fracture, polymers and composites task group, April 1990.

[59] M. S. Madhakar and L. T. Drzal, "Fiber-Matrix Adhesion and its Effect on Composite Mechanical Properties: IV. Mode I and Mode II Fracture Toughness of Graphite/Epoxy Composites," *Journal of Composite Materials,* **26(7),** 936-968, 1992.

[60] L. E. Asp, "The Effects of Moisture and Temperature on the Interlaminar Delamination Toughness of a Carbon/Epoxy Composite," *Composites Science and Technology*, **58**, 967-977, 1998.

[61] R. W. Truss, P. J. Hine, and R. A. Duckett, "Interlaminar and intralaminar fracture toughenss of uniaxial continuous and discontinuous carbon fibre/epoxy composites," *Composites Part A*, **28a**, 627-636, 1997.

[62] E. M. Woo, and K. L. Mao, "Interlaminar morphology effects on fracture resistance of amorphous polymer-modified epoxy/carbon fibre composites," *Composites Part A***, 27a**, 625-631, 1996.

[63] Ghassemi, H., Shoba, H. K., Sankarapandian, M., Shultz, A., Sensenich, C. L., Riffle, J. S., Lesko, J. J., and McGrath, J. E. "Volatile-Free Phenolic Networks for Infrastructure" in Fiber Composites in Infrastructure, Saasatamanesh, H. and Ehsani, M. R. editors, 1, 14-22 (1998)

[64] Tyberg , C. S., Bergeron, K., Sankarapandian, M., Shih, P., McGrath, J. E. and Riffle, J. S. "Tough, Void Free, Flame Retardant Phenolic Networks" International Composites Conference (ICE'99) Technomic Publishing Co., Lancaster, PA, May, 1999

[65] Sankarapandian, M., Shoba, H. K., Sensenich, C., Shih, P., Riffle, J. S., Loos, A. C., McGrath, J. E., Sorathia, U. "Void-Free Phenolic Networks," Materials and Process Affordability : Keys to the Future, Vol. 2, SAMPE, 1550-1559, Spring, 1998.

[66] U.S. Pat.. 4,689,383 to J. S. Riffle and I. Yilgor, Thoratec Laboratories Corp., "Hydroxyl-Functional Disiloxanes and Polysiloxane Oligomers,"8/25/87.

[67] O. Sirkecioglu, J. M. Andresen, C. McRae, C. E. Snape, "Synthesis and Structural Characteristics of Polycyclic Aromatic Hydrocarbon-Containing Phenol Formaldehyde Resites," Journal of Applied Polymer Science, 66, 663-671, 1997.

[68] C. S. Tyberg, M. Sankarapandian, K. Bears, P. Shih, A. C. Loos, D. Dillard, J. E. McGrath, and J. S. Riffle, "Tough, Void-Free, Flame Retardant Phenolic Matrix Materials" *Construction and Building Materials*, **13**, 343-353, 1999.

[69] Standard test methods for Plain-Strain Fracture Toughness and Strain energy Release Rate of Plastic Materials, Designation : d 5045 - 91.

[70] K. L. Ngai and C. M. Roland, "Junction Dynamics and the Elasticity of Networks," *Macromolecules***, 27**, 2454-2459, 1994.

[71] L. Shan, C. G. Robertson, K. N. E. Verghese, E. Burts, J. S. Riffle, T. C. Ward, and K. L. Reifsnider," Influence of vinyl ester network structure on mechanical response," Journal of Applied Polymer Science, submitted.

[72] Tyberg, C. S., Bergeron, K., Sankarapandian, M., Shih, P., Loos, A. C., Dillard, D. A., McGrath, J. E. and Riffle, J. S. "Structure-Property Relationships of Void-Free Phenolic-Epoxy Matrix Materials" *Polymer*, In press.

[73] Tyberg, C. S., Shih, P., Verghese, K. N. E., Loos, A. C., Lesko, J. J., and Riffle, J. S. "Latent Nucleophilic Initiators for Melt Processing Phenolic-Epoxy Matrix Composites" Polymer, In press.

[74] Tyberg, C. S., Lin, S. L., Bergeron, K., Sankarapandian, M., Shih, P., Loos, A. C., McGrath, J. E. and Riffle, J. S. "Tough, Void-Free Flame Retardant Phenolic Composites: Processability and Properties," Evolving and Revolutionary Technologies For the New Millennium, Vol. 1, SAMPE, 1206-1216, Spring, 1999.

[75] Facinelli, J. V., Gardner, S. L., Dong, L., Sensenich, C. L., Davis, R. M., and Riffle, J. S. "Preparation of Controlled Molecular Weight Polyimides from Poly(Amic Acid) Salt Precursors," Macromolecules, 29, 7342-7350 (1996)

[76] Sensenich, C. L., Bowens, A. D., Ji, Q., McCartney, S. R., Robertson, M. A. F., and Riffle, J. S. "Waterborne Polyimides and Poly(Imide-Siloxane)s," in Fiber Composites in Infrastructure, Saasatamanesh, H. and Ehsani, M. R. editors, 1, 14-22 (1998)

[77] J. F. Facinelli, "The Preparation of High Performance Polymers for Composites and Blends: a) Thermally Stable Ion Containing Polymers and b) Epoxy and Hydroxy Functional Polyolefin Macromers, Ph. D. Dissertation, Virginia Tech, 1996.

[78] Sensenich, C. L., Facinelli, J. V., Dong, L., Gardner, S. L., Davis, R. M., and Riffle, J. S. "Preparation of Polyimides from Poly(Amic Acid) Salts," Polymer Preprints, 37(2), 400-401 (1996)

[79] M. A. F. Robertson, M. B. Bump, K. E. Verghese, S. R. McCartney, J. J. Lesko, J. S. Riffle, I. -C. Kim, and T. -H. Yoon, "Designed Interphase Regions in Carbon Fiber Reinforced Vinyl Ester Matrix Composites," *Journal of Adhesion*, **71**, 395-416, 1999.

[80] Standard Test Method for Arrhenius Kinetic Constants for Thermally Unstable Materials, Designation : E 698 -79

[81] T. Ozawa, "Kinetic Analysis of Derivative Curves in Thermal Analysis," *Journal of Thermal Analysis*, **2**, 301-324, 1970.

[82] R. C. Reid, J. M. Prausnitz, and T. K. Sherwood, *The Properties of Gasses and Liquids*, McGraw-Hill, N. Y., p. 572, 1977.

[83] K.N.E. Verghese, N. S. Broyles, J. J. Lesko, R. M. Davis, and J. S. Riffle, "Pultruded Carbon Fiber/Vinyl Ester Composites Processed with Different Fiber Sizing Agents, Part II: Enviro-Mechanical Durability," Journal of Materials in Civil Engineering [ASCE Journal], submitted.